A provisional basin analysis of the Karoo Supergroup, Springbok Flats Basin, South Africa

Camille Kraak

04296494

A thesis submitted in fulfilment of the requirements for the degree of

MASTERS IN SCIENCE

in

GEOLOGY

In the

FACULTY OF NATURAL AND AGRICULTURAL SCIENCES

of the

UNIVERSITY OF PRETORIA

Supervisors: Prof PG Eriksson, Prof AJ Bumby

August 2014

Abstract

The Springbok Flats (SBF) Basin is one of the smaller basins associated with the Karoo basins of the Late Carboniferous–Middle Jurassic age interval. The preserved SBF basin is a topographically flat area with very few outcrops. It has a NE-SW orientation and is approximately 205 km long and 30 km wide. This study is based on borehole log data captured by the Council for Geoscience, which has been collected from various exploration companies throughout the history of the investigation of the SBF Basin area.

The purpose of this study is to identify an evolutionary history of the basin by utilising methods of basin analysis and literature search, and to establish how the basin relates to other Karoo Supergroup basins in southern Africa. The postulated genetic model of a retro-arc fore-bulge rift basin was compared to the inferred depositional environments.

The geophysical interpretations and structural contour maps of the various strata indicate the presence of the major Zebedelia Fault, which is part of the Thabazimbi Murchison Lineament (TML) relay system. This fault runs along the northern boundary of the basin and has caused the strata of the SBF Basin to be down-faulted by 800 to 1000 metres. The isopachs of the identified Karoo successions do not indicate thickening towards this lineament, which suggests that the faulting along this lineament post-dates the Karoo sedimentation.

The Thabazimbi Murchison Lineament played a significant role during the later stages of the SBF sedimentation. Once the depocentre became more centrally located in the depository, it began to migrate towards the TML. Although the major faulting was yet to occur, the weakness in the craton was apparent. During the breakup of Gondwana, the Zebedelia Fault shifted the strata down and allowed the extrusion of the Letaba Basalt, along with the multi-intrusion of dykes throughout the strata.

The onset of the deposition of the Karoo Stratigraphy in the SBF was due to uplift resulting from the mid-carboniferous assembly of Pangea. During the Lower Karoo deposition, lithospheric subsidence was facilitated by crustal-scale faults, resulting in the deposition of the glacial Dwyka and Lower Ecca sediments. Flexural subsidence was occurring in the forebulge due to the relaxing of the initial compression of the Cape Fold Belt (CFB). The later Ecca succession was characterized by large subsidence with little accompanying brittle deformation. The lower Beaufort was a deltaic basin and was terminated towards the end of the Permian period, identified by a significant loss of fauna and flora. There was a ± 3km uplift, known as the Namaqua Uplift and erosion north of the fold belt. This marked the structural inversion during deposition of the Beaufort Group and Early Molteno Formation. These uplift events resulted in uplift in the foredeep which resulted in the compression of the forebulge during the deposition of the Molteno Formation. Once these events subsided, the forebulge relaxed and underwent subsidence and extension. Elliot Formation formed during this unloading of structural relief and relaxation of basin-forming stresses. The upper Elliot and Clarens formations and Letaba Basalts exhibit the transition from sinistral strain of the late Karoo Basin to the dextral tectonics of the Gondwana breakup that terminated the basin deposition.

The Karoo sediments in the SBF Basin clearly represent the broad spectrum of the same set of palaeoenvironments that are recognised in the Main Karoo Basin rocks. These reflect the progressive infilling of the Karoo Basins, the changing tectonic framework as well as the migration of Gondwana from polar to tropical latitudes. However, due to the development of the SBF basin on the forebulge, the compression of the CFB had the opposite effect, where it resulted in uplift of the fore-bulge and subsidence of the foredeep. This subsequently resulted in the SBF correlated Karoo sedimentary successions being markedly thinner than those of the Main Karoo Basin, and in some cases, certain strata are completely absent.

An extensional basin formed by reactivation of older structures, such as the TML, as a result of displacement on the principle shear zones. This resulted in the preservation of the SBF strata in the basin today.

This study is a baseline and preliminary investigation into the SBF Basin, and may act as a canvas to which more in-depth investigations may be added. Various questions have been identified that require further understanding and are listed under recommendations. Many of the questions put forth may be answered with a thorough Quality Assurance-Quality Control (QAQC) of the database.

Contents

List of Figures

List of Tables

Abbreviations

mamsl	metres above mean sea level
BC	Bushveld Complex
CFB	Cape Fold Belt
CV	Calorific Value
Ga	Billion years ago
Km	Kilometres
Ma	Million years ago
mbs	Metres below surface
SBF	Springbok Flats
TML	Thabazimbi Murchison Lineament

1 Introduction

The Karoo Supergroup is one of the most extensive groups of rocks that are found on the Earth today. Many basins of these similarly aged and stratigraphically comparable rocks cover large parts of South America, Africa, Madagascar, Australia, India and various islands in between. This supergroup consists of a series of rocks that depict a change in climate during deposition as the continents making up Gondwana drifted over the South Pole and towards the palaeo-equator. This change in latitudes resulted in palaeoenvironments ranging from glaciated, to fluvial, to arid settings, ending with widespread flood basalts, associated with the break-up of Gondwana. Also depicted in the Karoo succession, is a continuous record of over 100 million years of mainly continental sedimentation which represents a variety of tectonically controlled depositories (Smith, 1990), the Springbok Flats (SBF) Basin being one of them, situated in northern South Africa, and forming the focus of this study (Figure 1-1).

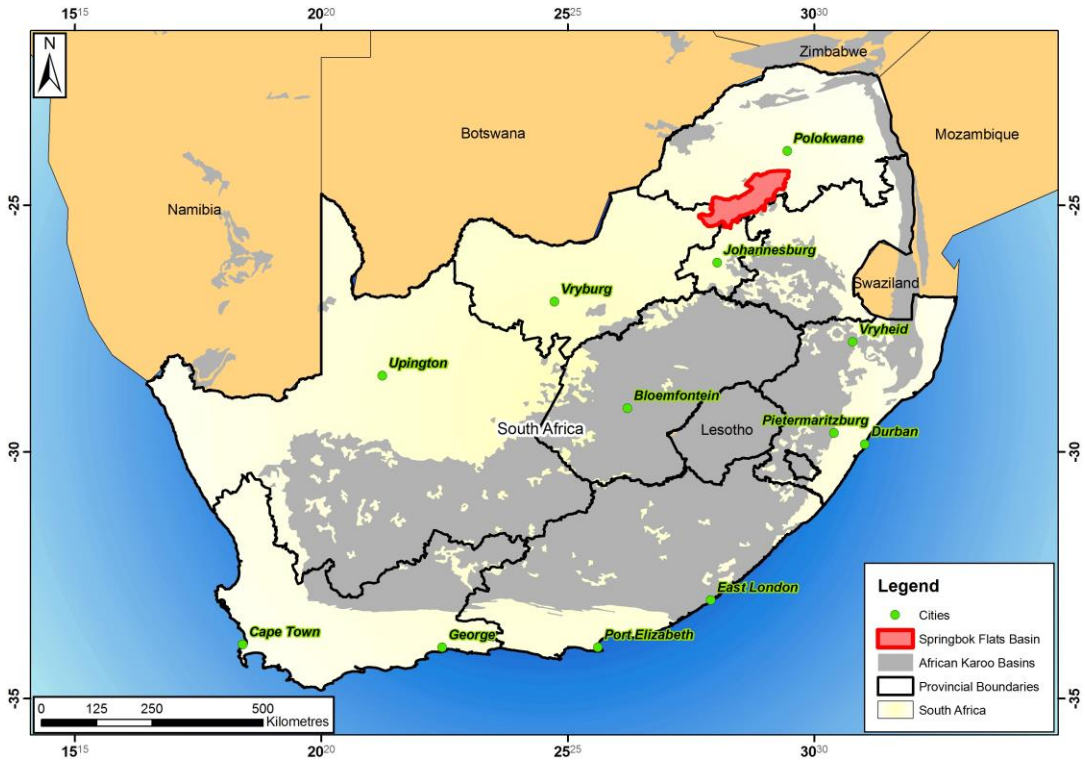

Figure 1-1: Location of study area

1.1 Objectives of this Study

This study is aimed at identifying an evolutionary history of the SBF Basin by utilising methods of basin analysis and literature search, and to establish how the basin relates to other Karoo Supergroup basins in southern Africa. The genetic model is to be compared to the inferred depositional environments, to either validate them or to suggest alternatives as well as to contribute to the understanding of the geodynamics of the SBF.

1.2 Study Area Location

The SBF basin is one of the smaller basins associated with the Karoo depositories of the Late Carboniferous–Middle Jurassic age interval. The preserved SBF basin (Figure 1-1) is a topographically flat area with very few outcrops (Hemming, 2009) (Figure 1.2). It has a NE-SW orientation (Hemming, 2009), and is approximately 205 km long and 30 km wide. It extends from northeast of Pretoria to the town of Zebediela in the Limpopo Province with a total surface area of roughly 8770 square kilometres. The basin is associated with subsidiary extensions to the south which are now preserved as outliers north and south of Pretoria, and to the west as far as Pilanesberg, while its north-western side is marked by a post-Karoo fault (Haughton, 1969).

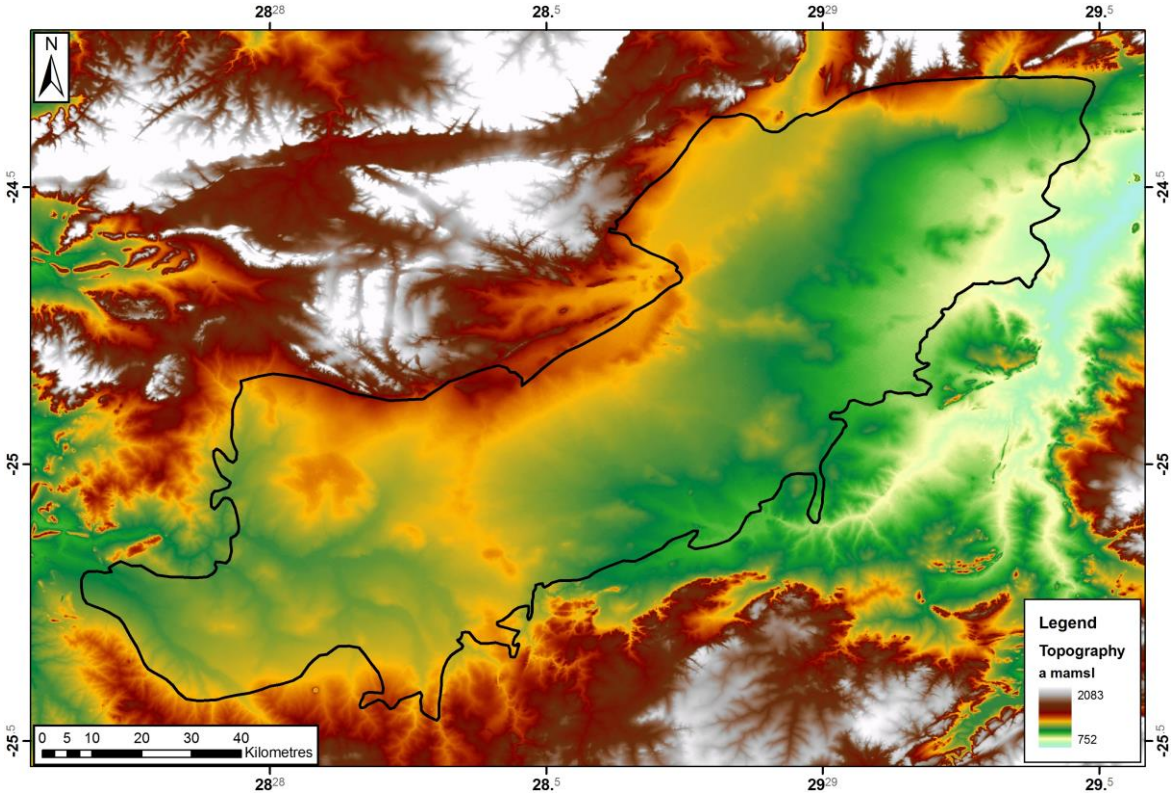

Figure 1-2: Regional topography of the SBF basin (black line) and surrounds, using Shuttle Radar Topography Mission (SRTM) data.

2 Geological Setting

The SBF Basin is related to the Main Karoo retro-arc foreland basin and formed within the forebulge depozone, in an intracontinental, cratonic to marginal cratonic setting (Rust, 1975; Catuneanu, 2004).

The forebulge depozone represents the sediment that is deposited between the forebulge and the backbulge (Figure 2-1). A key characteristic of these forebulge sub-basins within flexural foreland basin systems is that isopach patterns indicate regional closure around a central thick zone, which suggests that sediment accommodation may involve some component of flexural subsidence cratonward of the foredeep. Stratigraphic units in

the forebulge and backbulge depozone are much thinner than those in the foredeep due to the relatively low rates of subsidence (DeCelles and Giles, 1996). Depositional systems in these depozones are predominantly shallow marine and non-marine, and the sediment is generally fine-grained due of the large distance from its principal source in the proximal orogenic belt (Figure 2-1). Local deposits of coarser-grained sediment may be present on the flank of the uplifted forebulge area (Giles and Dickinson, 1995).

The limit between the forebulge and the back-bulge depozone in the Main Karoo retroarc foreland basin in South Africa was controlled by the contact between the Bushveld and the Pietersburg blocks of the Kaapvaal Craton, which was reactivated during the evolution of the foreland basin system (Catuneanu, 2004).

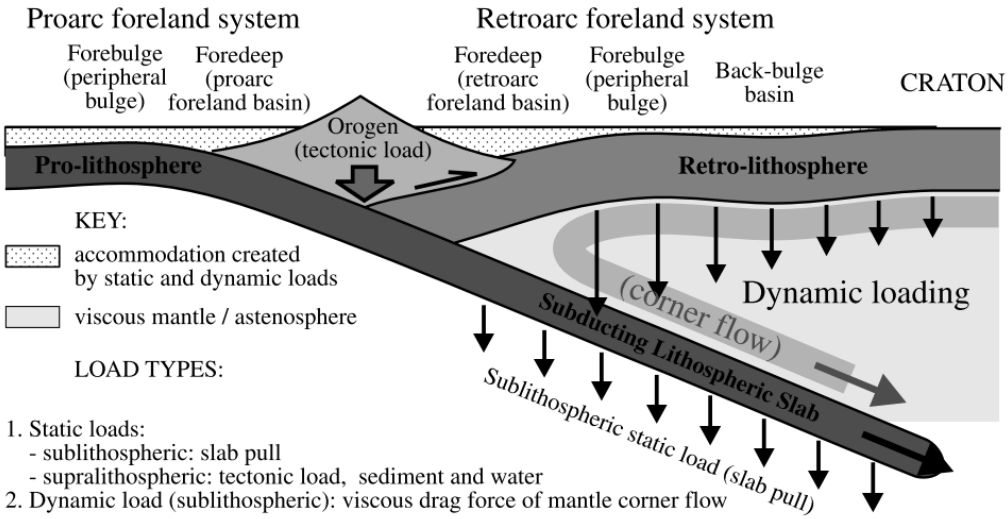

Figure 2-1: Proarc and retroarc foreland systems' tectonic setting and controls on accommodation (modified from Catuneanu et al., 1997a).

3 Regional Geology

The SBF basin lies within the limbs of the Proterozoic aged Bushveld Complex, which is preserved to the east and west of the basin. The Main Waterberg and Soutpansberg Basins lie to the north, and the Main Karoo Basin to the South; the latter is separated from the SBF basin by rocks of the Transvaal Supergroup, Bushveld Complex and locally, the Middelburg Waterberg Basin, all of Proterozoic age. As mentioned in Section 1.2, the SBF is a topographically flat area, and since this area is located in a region with a relatively dry climate, lateritic soils are not very deep. Due to the lack of outcrops, the geology of this area has been previously determined with the use of geological boreholes.

The onset of the Karoo Stratigraphy in the SBF was due to uplift resulting from the mid-carboniferous assembly of Pangea (Veevers *et al.,* 1994). The Karoo succession in South Africa ranges in age from Late Carboniferous to Middle Jurassic. Many different stratigraphic nomenclatures have been used over time to describe the SBF basin-fill geology (Figure 3-1), and are indicated in Table 3-1. For the purpose of this study, the geological

description of the stratigraphy will be based on the Main Karoo basin for the general geological reference and on Johnson et al. (2006) for the SBF Basin stratigraphy specifically.

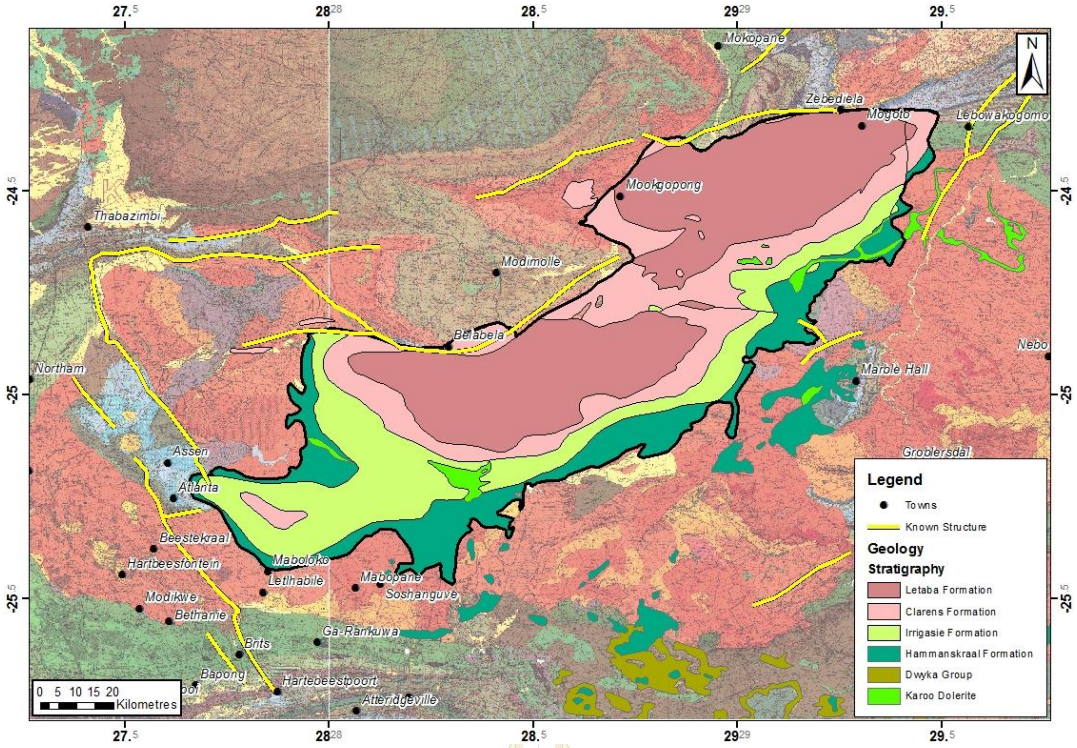

Figure 3-1: Geological map of the SBF Basin (Geological survey, 1:250 000 geological series maps).

Table 3-1: Different nomenclature used to describe the SBF's stratigraphy over the years.

Age	Du Toit (1954); Haughton (1969)		S.A.C.S. (1980)	De Jager, (1983); Mc Rae, (1988)	Johnson *et al*. (2006)
End of Early Jurassic	Stormberg Series	Bushveld Amygdaloid	Letaba Formation	Letaba Formation	Letaba Formation
Late Triassic - Early Jurassic		Bushveld Sandstone	Clarens Sandstone Formation	Clarens Sandstone Formation	Clarens Formation
Late Triassic		Bushveld Mudstone	Irrigasie Formation	Elliot Formation	Irrigasie Formation
End Middle Triassic				Molteno Formation	
Late Permian - Middle Triassic	Ecca Series	Upper Ecca Shale Stage	Ecca Group (formations not named)	Beaufort Group	
Early Permian		Middle Ecca Coal Measures Stage		Vryheid Formation	Hammanskraal Formation
		Lower Ecca Shale Stage		Pietermaritzburg Shale Formation	
Late Carboniferous - Early Permian	Dwyka Series		Not Named	Dwyka Group	Dwyka Group

3.1 Evolution of the Karoo Supergroup

In the Main Karoo Basin, the thickness of the cumulative Karoo strata extends to approximately 12 km in the south and thins out towards the north. The Karoo Supergroup succession in this basin accumulated in a flexural retro-arc foreland basin, which formed

when the palaeo-Pacific plate was subducted below the Gondwana supercontinent (Catuneanu et al., 2005 and references therein). As the supercontinent drifted over the South Pole, the first unit, the Dwyka Group, was deposited. This group is the result of glaciation, with an ice cap inferred over the highlands to the north, and an extensive floating ice sheet postulated to the south. With the continued drifting past the South Pole, the glaciation of the supercontinent came to an end. In its place was a widespread shallow epicontinental sea in the Main Basin which was fed by large volumes of melt-water (Catuneanu et al., 2005 and references therein; Johnson *et al.*, 2006).

The black mudrocks of the lower Ecca Group were deposited in the south (in the foredeep sub-basin of the foreland system) under cool climate conditions. To the south, the Cape Mountain range, derived from the Cape Fold Belt orogeny, was undergoing erosion and this sediment was being deposited in large deltas. High-lying areas to the north, east and west of the basin were also being subjected to erosion, and the deltas formed subsequent to this were beginning to encroach into the Ecca Sea (Catuneanu et al., 2005 and references therein; Johnson *et al.*, 2006).

These deltas began to fill the Ecca basin with sediment (both continental and shallow marine), which subsequently lead to a predominantly meandering fluvial environment in which the Beaufort Group was deposited. The Cape Fold Belt activity created pulses of uplift in the main source area, causing coarse-grained debris fans to intermittently prograde into the central parts of the basin. The climate by this stage had become semi-arid with highly seasonal rainfall, and along with two pulses of uplift to the south-east, two major wedges of coarser clastics were deposited, the Katberg Member, Beaufort Group and succeeding Molteno Formation (Catuneanu et al., 2005 and references therein; Johnson *et al.*, 2006; Turner *et al.,* 1975, 1983).

To follow this, the Elliot Formation was deposited under progressive aridification with a predominantly playa-lake and loessic type environment, which finally gave way to a fully arid dune sand dominated system, the Clarens Formation (Catuneanu et al., 2005 and references therein; Johnson *et al.*, 2006; Turner and Thomson, 2005).

The end of the Karoo deposition occurred during the middle Mesozoic Era, when basin-wide volcanic activity deposited the Drakensberg Group, forming the upper-most deposits of the Karoo Supergroup. These eruptions are associated with the Gondwana supercontinent breakup and the lavas were fed by the Karoo dolerites, now preserved as numerous dykes and sills (Catuneanu et al., 2005 and references therein; Johnson *et al.*, 2006).

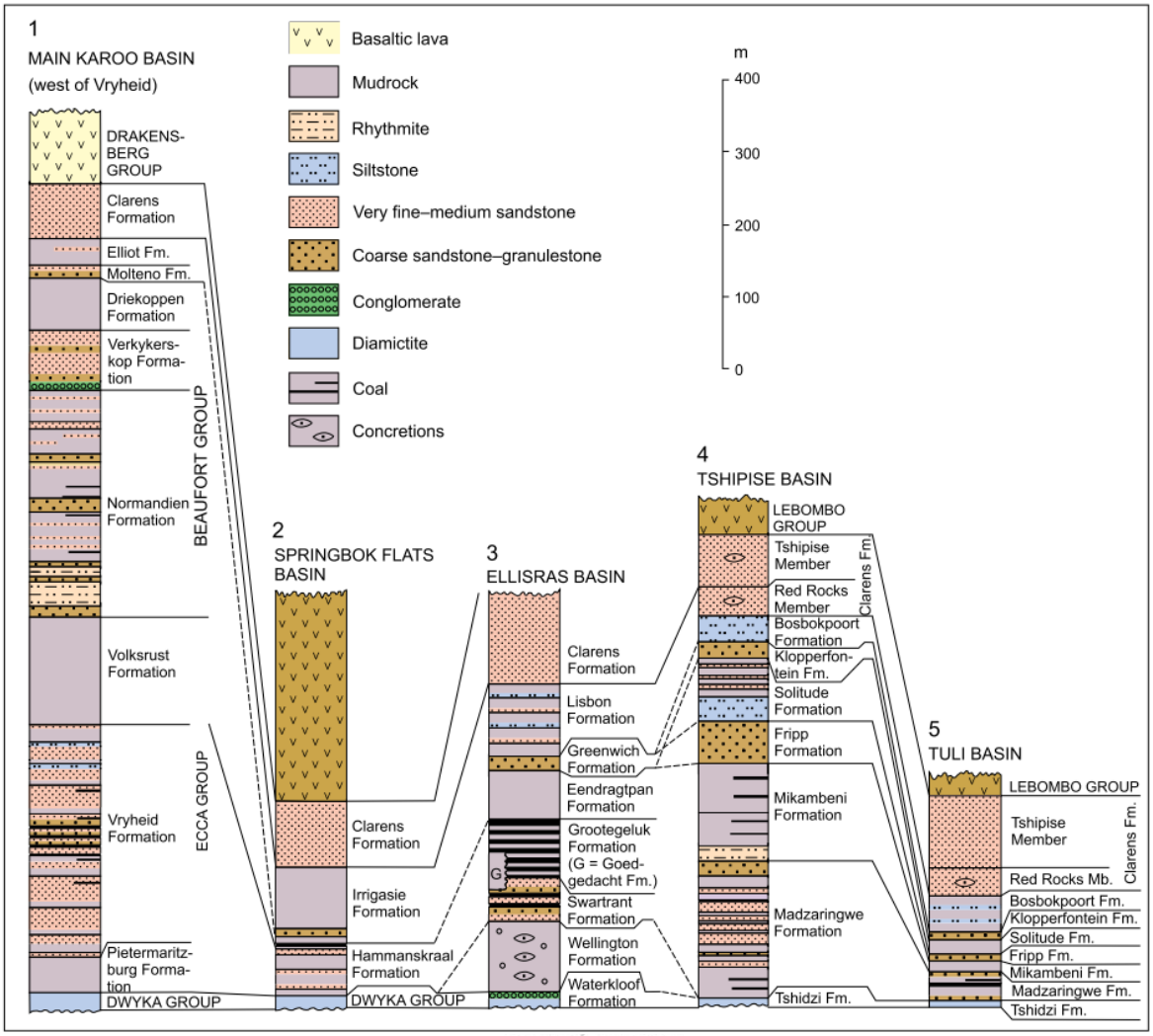

Figure 3-2: South–north trending cross-sections showing correlation of the Karoo lithostratigraphic units from the Main basin to the smaller, northerly basins (Johnson *et al*., 1996).

The extent of the Karoo sedimentation can be tracked across Africa from the Main Karoo basin in the south all the way to Somalia, western Sudan and Gabon to the north, and ranges in tectonic regime from a retro-arc foreland system to extensional rifted basins (e.g. Catuneanu et al., 2005). In the South African examples, the predominant tectonic setting was that of a flexural retro-arc foreland basin, where the foredeep lies in the southern regions (Main basin) and the forebulge to the north, which hosts the SBF depository, and which is flanked further north by backbulge sub-basins of the Waterberg and Soutpansberg Karoo Basins. Only the foredeep and forebulge facies zones of this larger system will be described for the purpose of this study.

Although the SBF basin has a much thinner total succession than the Main Karoo Basin (Figure 3-2), there is a clear link between the two basins. The Dwyka Group correlates directly, whereas the Hammanskraal Formation is correlated with the Ecca Group, comprising of the Vryheid, Pietermaritzburg and Volkrust Formations in the NE of the Main basin. The Irrigasie Formation then follows in the SBF basin, and is equivalent to the

Beaufort Group, and the Molteno and Elliot Formations. The Clarens Formation has a significant presence in the SBF basin, and can be correlated directly with its namesake in the Main Karoo basin. The Drakensberg Lavas, signifying the end of the Karoo deposition, are known in the SBF basin as the Letaba Formation (Johnson *et al.*, 2006).

3.2 End-Permian Mass Extinction

Towards the end of the Permian Era and the Beaufort Group deposition, the P-Tr (Permian-Triassic) mass extinction is recorded, where 54% of latest Permian marine families, 67% of genera, and about 92% of all species did not survive (Knoll *et al.*, 2007). Radiometric data on sedimentary rocks from that time suggest that the event was rapid in geological terms, occurring over less than ca. 0.5 million years. Although the event was rapid, studies indicate that the recovery took some 4-5 million years after the event (Knoll *et al.*, 2007).

There are many studies and theories that have been put forward to explain the mass extinction event and some of them are briefly discussed below. For more information, please see Knoll *et al.*, 2007.

3.2.1 Bolide Impact

A bolide impact is one of the most common theories used to explain any extinction event recorded. Some evidence for a bolide impact being the source of extinction is that fullerenes containing extra-terrestrial gases have been identified, along with shocked quartz crystals, metallic particles with meteoritic elemental abundances and monophase iron oxides. The impact site off the north western coast of Australia has been proposed to be the site of this P-Tr bolide impact event (Knoll *et al.*, 2007).

Little research has been dedicated towards this theory, as the survivorship patterns of the P-Tr event do not reflect this type of event. Research has been done into the shocked quartz crystals, and the concluding comments are that these optically visible deformation features are not shock-induced planar deformation lamellae, but decorated sub-grain walls (Langenhorst *et al.*, 2005).

3.2.2 Siberian Trap Volcanism

The Siberian Trap volcanism is the world's largest known flood basalt event, and coincides with the P-Tr Event. The resulting global atmospheric and oceanographic changes that occurred were facilitated by the trap-associated volatiles; therefore this event is commonly proposed to account for the biological catastrophe (Knoll *et al.*, 2007).

The suspected basalt volumes that were erupted during this event are roughly 10^6 km^3, which released an estimated range of CO_2 of 10^{17} to10^{19} mol CO_2. It is inferred that this major influx of volatiles resulted in acid rain (CO_2 and SO_2), poisoning from halogen and halide gases, hypercapnia, and immediate but transient global cooling (increased particle and SO_2 flux) followed by global warming (CH_4 and CO_2). There would inevitably be oceanographic consequences due to the global change, which would result in various

catastrophes, one being the lowering of the water's ability to absorb O_2 and facilitate the expansion of anoxia in oxygen-minimum zones (Knoll *et al.*, 2007).

3.2.2.1 Shallow Water Anoxia

The interest in anoxia as a source event was prompted with the identification of wide spread distribution of black shales in the lowermost Triassic sediments, as well as biomarker lipids diagnostic of anoxygenic photosynthetic bacteria (Knoll *et al.*, 2007).

Global increase in sea surface temperature induced by CO_2 influx into the ocean and atmosphere triggered the expansion of shallow water anoxia. Once anoxia is in place, anoxic waters would develop increasing abundances of CO_2 and sulphide. The consequences of anoxia are regional asphyxia, global hypercapnia, H_2S poisoning and sulphide driven loss of stratospheric ozone (Knoll *et al.*, 2007).

3.2.2.2 Catastrophic Methane Release

Methane release provides an alternative explanation for the P-Tr event, and is backed up by the depletion of biogenic methane by approximately -60% in ^{13}C. Recent studies indicate that during the P-Tr transition and into the Early Triassic, there were multiple C-isotope fluctuations. Additionally, the intrusion of the Siberian Trap sills into the Tungusskaya coals would have ignited these coals and resulted in massive outpouring of methane (Knoll *et al.*, 2007).

Short term global warming would have occurred and resulted in similar effects to that of increased CO_2 levels in the atmosphere, as methane would oxidise to CO_2 in the atmosphere. From this, the resulting consequences would have been global warming, hypercapnia stress and the development of marine anoxia (Knoll *et al.*, 2007).

3.3 SBF Basin Geology

The basin is a half-graben structure, with a normal fault being the northern-most boundary of the basin (Roberts, 1992). This major feature caused the strata to dip towards this normal fault by approximately 1°-5°, in a northerly direction. This fault is the result of the normal faulting of the earlier strike-slip Zebedelia Fault and is indicated in Figure 3-2, along with the known structures in and around the SBF basin. The Zebedelia Fault is known to be a relay structure of the Thabazimbi-Murchison Lineament (TML) which extends for more than 500 km in an ENE-WSW direction across the Kaapvaal Craton (Figure 3-3), and has been considered as a major structural weakness in this craton (Good and De Wit, 2013).

This lineament has a reactivation history that dates back to 2.96 Ga when the TML may have originated within the boundary of the Archaean granite/greenstone terrains. The TML exhibits normal, strike-slip and reverse faulting that varies from a ductile-dominated to a brittle-dominated regime from east to west. The final major reactivation of the TML occurred during the eruption of the Mesozoic Karoo basalts and sediments forming the SBF basin (Good and De Wit, 2013).

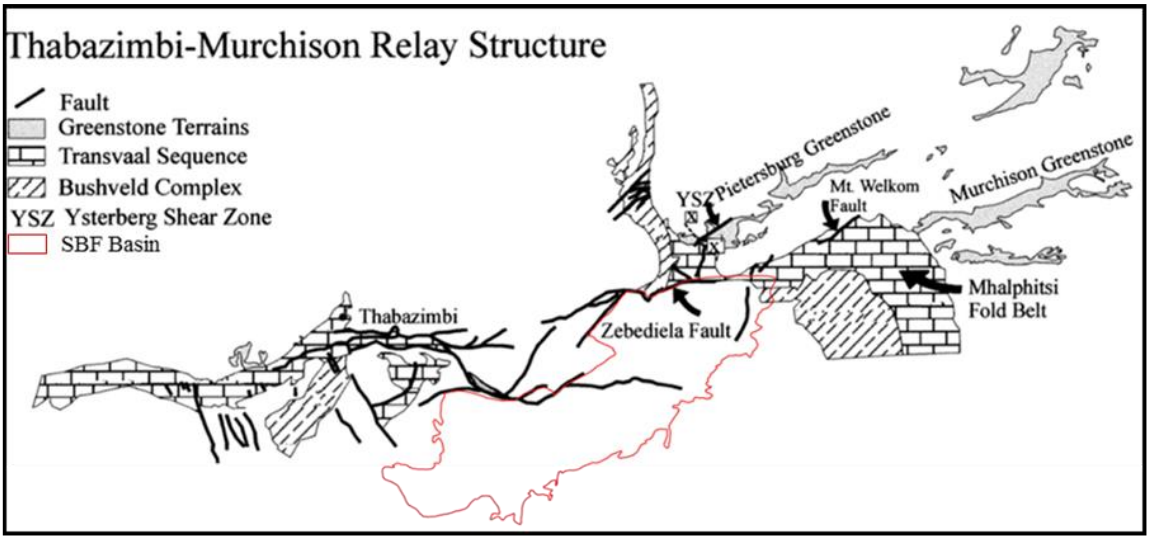

Figure 3-3: The Thabazimbi-Murchison relay structure in relation to the SBF (adapted from Good and De Wit, 2013).

The Karoo sediments were deposited in two shallow north-east trending elongated basins or synclinal flexures, connected by a broad flat anticlinal flexure (Visser and van der Merwe, 1959). Several normal faults following the north-easterly strike occur in the connecting anticlinal flexure.

At depth, the basin appears to be subdivided into two smaller sub-basins, one in the north-eastern area, and the other in the south-western area. The north-eastern basin is the smaller of the two sub-basins, and has an estimated basin-fill thickness of 700m. The larger south-western sub-basin has a maximum fill thickness of 1000 m (Viljoen *et al.,* 2010).

3.3.1 Pre-SBF Karoo Rocks

With the use of borehole data and outcrop mapping, Roberts (1992) determined that the SBF Basin lies unconformably on the Bushveld Complex, the Transvaal Supergroup, the Lower Waterberg Group strata and the Rooiberg Group.

The Bushveld Complex (BC) is the largest preserved layered mafic intrusion in the world and is host to the largest platinum group elements, chromium and vanadium ore deposits (Cawthorn *et al.*, 2006). Rocks from the BC were identified to be the dominant basement rocks of the SBF Karoo strata, and comprise of granites, felsites and minor granophyres. These rocks are dominant in the northern region of the basin, with varying lithologies to the south. Roberts (1992) also identified mafic BC rocks which comprise of gabbros and norites. The mafic rocks that outcrop in the north disappear beneath the Karoo strata and their extent could not be accurately determined.

The rocks of the Transvaal Supergroup form a major anticlinal structure to the northwest of the SBF basin, which extends beneath the Karoo strata. Similar to the BC rocks, the extent of this anticline and the distribution of the Transvaal rocks beneath the SBF could not be determined due to lack of data (Roberts, 1992).

The basement of the highland between the two sub-basins of the SBF is dominated by rocks of the lower Waterberg strata, which overlie granitic lithologies. The southern region of the SBF also hosts Waterberg strata as the basement.

Roberts (1992) identified alkaline complex rocks comprising of syenites, natites and breccias in the southern region of the southern sub-basin.

There was a lengthy period of no deposition in this region of the craton, which resulted in extensive erosion prior to Karoo sedimentation. Due to the different characteristics of the basement lithology, an undulating palaeotopography was created.

3.3.2 Dwyka Group

This group was deposited during the Late Carboniferous to Early Permian (300 – 290 Ma interval) and is found on all Gondwana continents. The Karoo Supergroup of the SBF basin was deposited on an undulating pre-Karoo surface. Towards palaeohighs, the lower stratigraphic subdivisions of the Karoo Supergroup pinch out or have been eroded. The Dwyka group lies unconformably on preceding Palaeozoic to Precambrian rocks in the Main Karoo basin and in the SBF Basin (Smith *et al*., 1993; Roberts, 1992).

There is quite significant lateral facies change evident in the Dwyka Group of the Main basin. To the south, the rocks fall under a foredeep facies regime and reflect primarily sediments derived from floating ice (Smith *et al*., 1993). Further north are the remnants of the distal shoreline of this Dwyka Sea, which was associated with the boundary between the foredeep and forebulge facies (Fig. 2.1). This area was uplifted above the base level, which led to continental ice sheets. The thickness of the succession in this region is highly variable, ranging from 1 to several metres in thickness and is generally comprised of supraglacial tills and basal lodgement. These deposits are generally massive with simple horizontal bedding towards the top. There appears to be a high variation in lateral deposition in this region, which suggests that there were local developments of grounded ice lobes separated by ponds and outwash fans (Catuneanu et al., 2005).

The Dwyka Formation equivalent in the SBF basin correlates weakly with the northerly Dwyka Group deposits in the Main Karoo basin, and only extends to a maximum thickness of about 30 m. The Dwyka appears as lithologies with apparent dropstones, and as diamictites, polymictic conglomerates, boulder beds and the occasional tillite with intercalated argillaceous layers (Visser and van der Merwe, 1959). The coarse material is matrix-supported by an argillaceous or arenaceous matrix and in certain areas these deposits are stratified and accompanied by rhythmites. The pebbles in the diamictite are comprised of fragments of angular felsite, granite and quartzite that originated from pre-Karoo rocks in the vicinity (Smith, 1990).

3.3.3 Hammanskraal Formation (Ecca Group)

The Ecca Group in the Main basin, formed during the Permian, and occurs between the Late Carboniferous Dwyka Group and the Late Permian-Middle Triassic Beaufort Group. The Ecca Group equivalent in the SBF Basin is the Hammanskraal Formation, and this was

deposited unconformably on an uneven pre-Karoo or Dwyka Formation surface. Visser and van der Merwe (1959) divided this formation into the Upper Ecca Stage (UES) and Middle Ecca Stage (MES). The lower portion of the UES is comprised of grit, sandstone, sandy shale and carbonaceous shales which are possibly comparable to the Vryheid Formation of the Main Karoo Basin, and the UES ranges in thickness from 0 to 40m. It is in this UES sequence that local developments of coal are found (Upper Coal Seam); however, it is of low quality in the north-eastern portion of the basin (Visser and Van Der Merwe, 1959; McDonald, 2007).

The MES grades into the upper portion of this formation and is comprised of grey sandy shale, shaley sandstone with cross-bedding and minor layers of white sandstone and poorly bedded grey shale. This sequence can possibly be correlated to the Volkrust Formation of the Main Karoo Basin. The contact between the UES and the MES is in some cases marked by different stratigraphy, and has therefore resulted in confusion as to what sequences are found in the SBF basin that correlate to the Main Karoo basin (Visser and van der Merwe, 1959). The coal zone consists of interbedded black shale and coal in local basins at the top of the formation (top of the UES).

The overall lithostratigraphy of the Hammanskraal Formation begins with the Lower Coal Zone lying directly above the Dwyka Formation, which forms part of a thin arkosic conglomerate. It is a sporadically developed coal seam (recorded maximum thickness of 7m) with a medium grained sandstone roof which comprises of quartz, quartzite and feldspar grains in a grey argillaceous matrix, and is of no economic interest (Visser and van der Merwe, 1959; McDonald and Waldeck, 2008). Conformably overlying the Lower Coal Zone is approximately 20 metres of upward-coarsening rocks with grey shale at the base. The shale is often carbonaceous with disseminated pyrite and with well-developed laterally continuous horizontal lamination. The grey shale grades into a heterogeneous assemblage of silty shales, siltstones and very fine grained sandstone (Visser and van der Merwe, 1959; McDonald, 2007).

The top portion of this upward coarsening sequence (cf., the UES) comprises medium to fine grained, micaceous sandstone which is characterised by sedimentary structures such as ripple cross-bedding, lamination and intense bioturbation. Minor upward-fining cycles occur in the sandstone. Interlaminated coal occurs in the top portion of the sandstone directly underlying the Upper Coal Zone (Visser and van der Merwe, 1959; McDonald, 2007). The Upper Coal Zone varies in thickness from approximately 9m in the deeper parts of the basin to where it pinches out and was eroded by the overlying Molteno sandstones on the flanks of palaeohighs (Visser and van der Merwe, 1959).

3.3.4 Irrigasie Formation

The Irrigasie formation in the SBF Basin hosts correlative strata to that of the Beaufort Group, Molteno and Elliot Formations in the Main Karoo Basin. For the purpose of comparing these strata, the three separate successions will be discussed below.

3.3.4.1 Beaufort Group

This fluvial derived succession is of Permo-Triassic age and is composed of alternating mudstone and sandstone, characterised by upward fining-textures. By this time in the evolution of the SBF basin, the palaeoclimate had warmed sufficiently to become semi-arid with seasonal rainfall and sediment was accumulated on vast semi-arid alluvial plains. This is evident from the desiccation cracks, palaeo-pedonogenic carbonate horizons, red and purple coloured sediment and vertebrate fossils (Smith *et al.,* 1993). The strata consist predominantly of mudstones and siltstones with subordinate lenticular and tabular sandstones deposited by a variety of fluvial systems, mainly by floodplain aggradation (McDonald and Waldeck, 2008).

Lower Beaufort Group sediments were derived from different margins of the SBF Basin, resulting in pebbly sandstones being deposited in the north and fine-grained sandstones elsewhere. These sandstone sequences relate to north easterly, north-north westerly and east-south easterly directed fluvial transport systems. There is an overall fining-upward trend of the lower Irrigasie succession and this is interpreted in terms of decreasing palaeoslope, channel gradients and sediment supply (McDonald and Waldeck, 2008)).

The middle part of the Beaufort Group is represented by a mudrock-dominated succession consisting of a shallow lacustrine facies at the base, overlain by vertically stacked upward-fining sequences (Johnson, 1976). The latter sequences comprise erosive-based sandstone, siltstone and mudstones deposited by delta distributary and meandering river channels, flanked by crevasse splays and extensive areas of mud-dominated floodplain (McDonald and Waldeck, 2008).

The Upper Beaufort Group comprises fining-upward sandstone-dominated sequences deposited by a network of low sinuosity streams (Turner, 1978). Within this succession are subordinate laterally-accreted sandstone bodies that form sandstone-rich intervals. In the eastern part of the basin, the overlying succession consists of a sequence of lacustrine mudstones, shales, rhythmites and sandstones with wave ripple structures, which becomes more sandy and redder in colour towards the top (McDonald and Waldeck, 2008).

A sudden change in depositional conditions is thought to have occurred at the Palaeozoic-Mesozoic boundary in the Main Karoo Basin due to episodic, but pronounced tectonic uplift of the south easterly source area, as well as rapid climatic warming initiated by the end-Permian extinction event and this resulted in aridification (Smith and Ward, 2001).

In the SBF Basin the Irrigasie succession is very similar to the correlative strata in the Waterberg and Soutpansberg Karoo basins. The Beaufort Group sedimentary strata in the northern part of the SBF basin are much coarser-grained and have a ‘‘coal measures’’ character not unlike the older Vryheid Formation, and consist of two coarsening-upward deltaic cycles. It is characterised overall by red, brown and grey mudstone and shale with sporadic sandy layers. In some instances, the shale is ferruginous, well-bedded and brownish yellow in colour. The thickness of the Beaufort Group ranges from approximately 9 to 45 m (Johnson et al., 2005).

3.3.4.2 Molteno Formation

The Molteno Formation in the SBF Basin is known as the Cordington Member (Roberts, 1992 and Johnson et al., 1996). However, for the purpose of this study it will be referred to as the Molteno Formation (following Johnson et al., 2006). This unit is easily confused with analogous upper Beaufort Group (Permo-Triassic) fluvial deposits. However, it is common that the base of the Molteno unconformity oversteps older, underlying Karoo units onto basement rocks, thus making it distinguishable (McDonald and Waldeck, 2008).

Only thin (10–25m), erosive-based, fluvial sandstones are known from SBF and are subdivided into two clearly distinctive lithological units. These subdivisions are based on changes in properties arising from different depositional environments. Sedimentary structures are mainly absent, though cross-bedding and horizontal bedding occur in the distal parts of the deposit (McDonald and Waldeck, 2008).

A wedge-shaped deposit, characterised by units of poorly sorted conglomerates and granular to coarse grained sandstones, alternating in poorly defined upward-fining cycles, is located in the lower part of the Molteno Formation. This deposit is restricted to areas adjacent to pre-Karoo palaeohighs (McDonald and Waldeck, 2008).

The lower part of the Molteno Formation shows rapid lateral and vertical facies changes. The deposit can be distinguished from the upper part of the Molteno Formation by the predominance of conglomerates and coarse-grained sandstones with subordinate, mostly silty mudstones (McDonald and Waldeck, 2008).

The upper part of the formation is characterized by well-defined upward-fining cycles, comprising thick basal conglomerates, medium to fine grained light coloured sandstones and massive purple mudstones. Tuffaceous mudstones, in a fine argillaceous matrix are sporadically developed at the top, comprised of angular to subangular quartz, feldspar, mica and opaque minerals (McDonald and Waldeck, 2008; cf. Turner *et al.,* 1975, 1983).

The Molteno deposit in the SBF Basin is highly porous and has a high sandstone:shale ratio. The conglomerates comprise subrounded to subangular quartz, quartzite, felsite and perthite pebbles in a brown to grey arenaceous matrix. The individual pebbles are poorly cemented and can easily be removed by hand from the beds. These pebbles reveal a weak fabric with the long axes of the pebbles parallel to one another. The sandstones are mainly granular to coarse-grained and are notably better sorted than the conglomerates. A red iron oxide matrix is characteristic of the sandstones (McDonald and Waldeck, 2008).

Towards the top of the upper part of the formation, a gradual increase in argillaceous sedimentary rocks occurs. This gradational transition makes it difficult to discern the exact contact between the Molteno and overlying Elliot Formation. The thickness of the Molteno Formation varies from 40m to a few centimetres. The maximum development occurs adjacent to the basin-marginal palaeohighs and rapidly thins out away from these palaeohighs towards the deeper parts of the basin (McDonald and Waldeck, 2008).

3.3.4.3 Elliot Formation

The Elliot Formation comprises both arenaceous and argillaceous sedimentary rocks and can be subdivided into three distinct units, lower, middle and upper parts (McDonald and Waldeck, 2008).

The lower part of the formation is characterised by massively bedded mudstone, varying from red to purple and more rarely to blue grey and green in colour (Bordy *et al.,* 2004). These mudstones, particularly in the lower portion, enclose thin layers of siltstone and sandy mudstones. Subordinate thin cherty layers are developed locally (McDonald and Waldeck, 2008).

The middle part of the formation comprises well defined upward-fining cycles. These cycles are essentially graded, with clay pebble conglomerate basal units, laminated and cross-laminated medial units, and very thinly laminated and/or dark-brown mudstone upper units (Bordy *et al.,* 2004). Clay pebble conglomerate beds are best developed in the lower-most cycles, where they contain abundant fossil bone fragments. These conglomerates are regionally developed and can be considered as a marker horizon (McDonald and Waldeck, 2008).

The upper part of the formation has the same character as the overlying Clarens Formation. However, a decrease in grain size and a change in colour from light coloured (Clarens) to reddish brown (Elliot) is a distinguishing feature. Furthermore, the absence of bioturbation in the Clarens Formation distinguishes those sedimentary rocks from these of the Elliot Formation (McDonald and Waldeck, 2008).

In the areas where the Molteno Formation is not developed, no distinct lithological differences exist between the lower part of the Elliot Formation and the Beaufort Group. In these areas it is difficult to discern the contact between these two stratigraphic units (McDonald and Waldeck, 2008).

The thickness of the Elliot Formation is fairly constant and seldom exceeds 125m. In certain areas however, especially towards the southern rims of the two SBF sub-basins it thins out to where a minimum thickness of 5m was recorded (McDonald and Waldeck, 2008).

3.3.5 Clarens Formation

The lower portion of the Clarens Formation is associated with wet desert (fan and wadi, playa lakes) sub-environments which suggest that the transition from the Elliot Formation to the Clarens Formation was very gradational. The appearance of the first bioturbated horizon in the transitional succession has been taken as the contact between the two formations, with the Clarens being above this. Sedimentary structures are rarely developed in the Clarens Formation. In areas where sedimentary structures are present, mainly medium-scale cross bedding and horizontal bedding are developed (Catuneanu et al., 2005).

The Clarens Formation consists of fine grained, light coloured pinkish, even–textured (well sorted) sandstone. The thickness of this formation remains fairly constant over the entire SBF basin and seldom exceeds 125m (McDonald and Waldeck, 2008).

The sandstone comprises mainly sub-angular to rounded quartz grains (0.04 – 0.30mm) accompanied by subordinate potassic feldspar and plagioclase grains. The heavy minerals comprise zircon, epidote, tourmaline and magnetite. The sandstone is typically free of pebbles and granular particles (Wagner et al., 1927).

The upper 10m of the formation has well-defined upward-fining cycles and is tuffaceous, fine-grained, green to grey in colour. Sedimentary structures are typically stratification, and cross-lamination. Minor plant imprints and minor coal bands do occur. The upper contact with the lavas suggests synchronous desert sedimentation and early volcanism (McDonald and Waldeck, 2008).

3.3.6 Drakensberg Group (Letaba Formation)

The Karoo sedimentation was terminated by the outpouring of the basaltic lavas in the late Triassic, which originally covered much of southern Africa (Du Toit, 1954), but today is generally preserved in smaller parts of the various Karoo basins. The extrusion of these basalts continued until the early Cretaceous.

The tholeiitic lavas comprise of alternating, finely crystalline dark-grey to green massive and amygdaloidal units, in which distinctive flows can be recognised. In the lower parts of the Letaba Formation, sandstones are intercalated with the lavas (McDonald and Waldeck, 2008). Such intercalations are commonly developed towards the central part of the preserved SBF basin. These resemble the sandstone of the Clarens Formation and differ from it only in being better stratified and composed of exceptionally well rounded quartz grains (Wagner et al., 1927, pg. 78). The contact of the Letaba Formation with the underlying Clarens Formation is sporadically marked by thin agglomerate.

3.3.7 Karoo Dolerite Suite

The intrusive dolerite suites occur as an interconnected network of dykes, sills and saucer-shaped sheets (Chevallier and Woodford, 1999). These intrusions are the shallow feeder system to the flood basalt eruptions (Walker and Poldervaart, 1949).

In the SBF basin a prominent dolerite sill, approximately 30 to 50m thick, transgresses the coal seams around the south-western quadrant of the basin (Figure 3-1 Karoo Dolerite – bright green). Numerous smaller dolerite sills tend to follow the floor of the basin and are probably of the same generation. In some parts of the basin, such as the central area, no dolerite is present.

Where dolerite sills intersect the coal zones, complete burning of the Upper Coal Zone has occurred while where the dolerite over- or underlies the coal zones in close proximity, de-volatilization is prominent.

4 Economic Potential of the SBF

4.1 Coal

The *in situ* bituminous coal resource in the SBF Basin is estimated to be 3.3 Gt., and the remaining recoverable reserves of coal in the basin are 1.7 Gt. as stated in Bredell (1987) and Snyman (1998). The coal in the SBF Basin is underexploited primarily due to the nature and depth of the Coal Zone. About 15% (1 210 Mt) of the coal occurs in the open-castable range of 0 – 75m, and in small resource blocks around the edges of the basin (Jeffrey, 2005). The quality of the raw coal makes it suitable for steam coal that is used in industrial boilers, electricity generation, etc., and a beneficiated product of coking coal may be used in the steel industry (Figure 4-1).

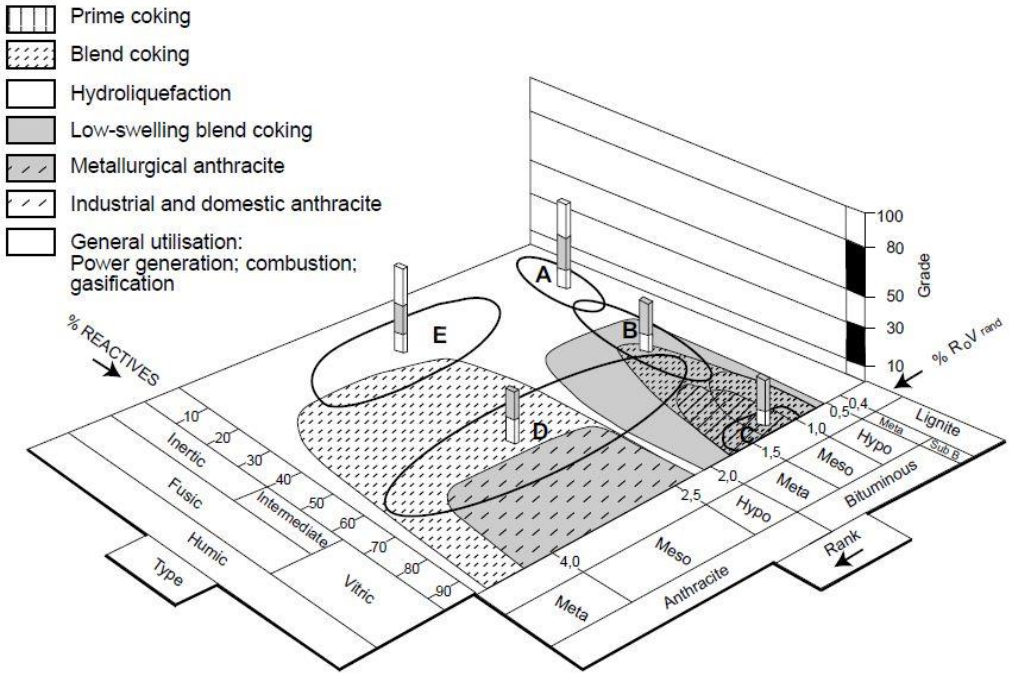

Figure 4-1: Alpern Diagram, illustrating variability in grade, type and rank of South African coals. Coal fields: A: Free State, Vereeniging/Sasolburg, South Rand; B: Witbank, Highveld, Ermelo; C: Ellisras, Tuli, Mopane, Tshipise, Pafuri, SBF; D: Klip River, Utrecht, Vryheid, Nongoma, Kangwane; E: Molteno/Indwe (Snyman, 1998).

The factors that have, and are, inhibiting exploitation of the SBF are water supply, transport infrastructure, as well as underground mining currently not being an option due to difficult conditions at depths of over 250m. The coals are, however, amenable to significant upgrading through dense-medium beneficiation methods, creating yields of around 50%, from a float at a relative density of 1.65, on run-of the mine (Jeffrey, 2005).

The coal zones fall in the Hammanskraal Formation, with correlation to Main Basin equivalent units encompassing the Vryheid Formation (SFB Lower Coal Seam, LCS) and the Volkrust Formation (SFB Upper Coal Seam, UCS). During the time of deposition, the palaeoenvironment was fluvial in nature. The LCS has poor lateral development and an average thickness of 2 to 4m (Christie, 1989). The UCS is laterally persistent with a

thickness of 5 to 8m, and is the zone of potential economic interest. In the west of the basin, the majority of the coal had been devolatilized by numerous doleritic intrusions near the Warmbad-Pienaarsrivier area (Jeffrey, 2005). Analysis of the coal qualities has found that the coal has sulphur content, in raw coal, of 2-4% and averages ±1.5% in the beneficiated product (Christie, 1989).

4.2 Uranium

Uranium is of great interest in the SBF Basin, which is characterised as a uranium occurrence in South Africa. The SBF coal is well known for its uranium content, which is calculated to be between 650 and 1000 ppm as well as some molybdenum (Viljoen *et al.,* 2010). In total, there is approximately 77 072 tonnes of uranium, which makes this basin a potential source for uranium (Kruger, 1981; Christie, 1989; Snyman, 1998; Loubser, 2007).

The uranium mineralised zone is found in the upper part of the Irrigasie Formation (equivalent of the Beaufort Group) and in the roof of the coal seams. The average thickness is 1m with an average grade of 0.16 – 1.0 kg/ton of U_3O_8 (Cole, 2009) and the inferred resource of U_3O_8 is estimated at 0.09 Mt at 2.2 kg/ton (Creamer, 2010). The only significantly mineralised zones are found in the central (1000 km^2) and north-eastern (600 km^2) parts of the basin, where the palaeovalleys were flanked by Bushveld Complex granites. The coal zone is uraniferous in sites where it is unconformably overlain by the fluvially-deposited Molteno Formation. This formation contains abundant detritus, including pebbles derived locally from the Bushveld Complex granite (Kruger, 1981).

The uranium is disseminated throughout the carbonaceous shale roof to the upper coal seam and in the coal zone. It has been identified to be in uranium-bearing minerals such as coffinite, aurelite and oyamalite (Kruger, 1981); however, the uranium is predominantly held in organo-metallic compounds (Cole, 2009).

4.3 Underground Coal Gasification

UCG is an *in situ* combustion method that converts coal underground, into a combustible gas, therefore providing a clean and convenient source of energy from coal seams where conventional extraction methods are not economically, environmentally or technically suitable. The gas is utilised for industrial heating, power generation or hydrogen and natural gas production (Walker, 1999; Coal-UCG, 2002; Green and Armitage, 2001). It is applicable to coal seams that are at a great depth and are more than 3m thick such as those found in the SBF Basin. Although there are currently no exploitation licences for UCG in the SBF Basin, it is believed that the basin holds a potential for it.

There has been a great improvement in evaluating resources that can be feasibly extracted using UCG and in the methods used with each stage of development. Various methods are applied for UCG operations. A Soviet method is normally employed and encompasses regularly spaced sets of vertically drilled holes, with 10 to 15m spacing dependent on the permeability of the coal. The holes are connected by hydro-fracturing and burning between the holes (Figure 4-2). Burning starts from one set of holes towards another

parallel set forming a gasification front. As the burning migrates, additional rows of holes are brought into operation as required (Beath et al., 2001).

Underground gasification removes the need for strip mining and transportation of coal. However, UCG produces large amounts of CO_2, and the coal combustion wastes that are left behind can contaminate local groundwater, and have caused major contamination in UCG pilot projects (Coil et al., 2012).

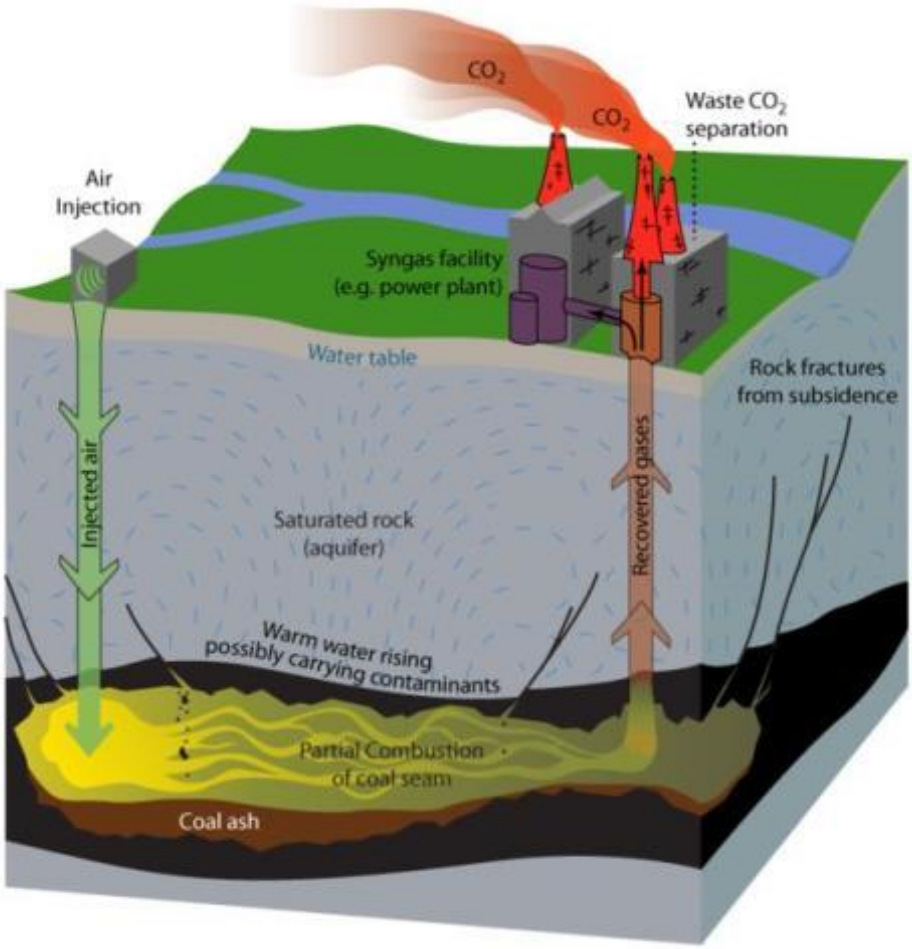

Figure 4-2: Illustration of the UCG process (Coil et al., 2012).

The Eskom pilot plant in South Africa (near Majuba power station) involves the assessment of local sites, environmental impact, technology, geology and costs, and was commissioned in January 2007 and has run continuously ever since (Eskom Website):

- The gas cleaning plant and condensate separation plant for a 15,000Nm3/hr co-firing demonstration have been commissioned.
- Mine production can be ramped up to provide the necessary gas flow for a co-firing demonstration in Unit 4 at Majuba Power Station.
- Initial co-firing at Majuba power station was achieved in October 2010.
- The design phase for a 100-140 MWE open cycle gas turbine demonstration plant using UCG gas is currently underway.

4.4 Coal Bed Methane

Coal Bed Methane (CBM) is a natural gas formed during coalification and a portion of this remains trapped under pressure in the coal seam and surrounding rock, in cleats, fractures and other spaces within the coal. The amount of trapped methane gas depends on coal rank and coal seam depth. As the coal rank increases, the ability for it to retain methane increases. Pressure increases with depth and the absorption capacity of coal increases with pressure. Therefore, the deeper coal seams generally contain more methane than shallow seams of the same rank (Jeffrey, 2002). Shallower coals are degassed as the methane migrates due to low pressure.

CBM is recovered from untouched coal by releasing the gas located both within the coal and adsorbed onto the surface of the coal and surrounding rock. Coal seams are injected with a high pressure water, foam and sand mix (Figure 4-3). The high pressure fractures the coal for some distance around the borehole (Jeffrey, 2002). The sand holds the fractures open, enabling the water and gas to flow to the well bore and to the surface. CBM offers a method of extracting methane from unworked coal without adversely affecting the physical properties of the coal (USEPA, 1998).

A pre-feasibility study in the SBF Coalfield was completed in January 1996 and involved the Department of Minerals and Energy, Southern African Development Community, U.S. Trade and Development Agency, U.S. Department of Energy, Natural Buttes Gas Corporation and Advanced Resources International (World Bank and USEPA, 1998). The analysis conducted in the study indicated that there was a potential methane production of 0.7million m^3, which could be utilised by consumers in the immediate vicinity. A recommendation was made to proceed with a budgeted risk managed exploration program to confirm the production potential (Jeffrey, 2002). This was to have been done through exploratory drilling in order to understand the risk potential through *in situ* gas recovery parameter evaluation (World Bank and USEPA, 1998). CBM offers an alternative to meet South Africa's energy shortages, creating strong potential for growth in this industry.

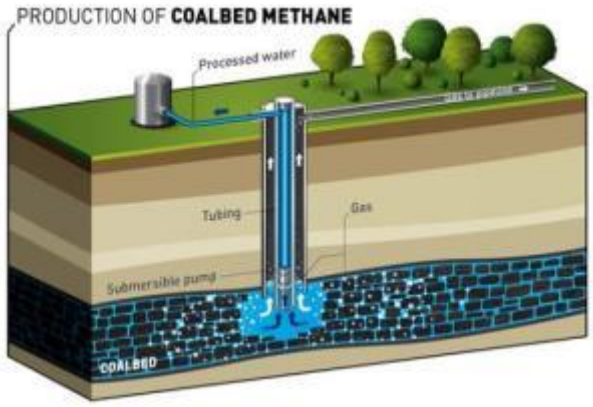

Figure 4-3: Illustration of the production of coal bed methane (www.total.com).

4.5 Current Exploration and Mining

The Springbok Flat area is considered favourable for the occurrence of CBM due to the presence of extensive coal deposits at depths suitable for CBM development and preservation. The following are a few of the known companies looking into the economic potential in the SBF Basin, most of which are concentrating on CBM potential.

Table 4-1 and Figure 4-4 indicate companies and their approximate locations of petroleum exploration and production rights in the SBF area, as well as areas that are currently (as of July 2013) under application.

Table 4-1: Companies with petroleum rights in the SBF Basin indicated in Figure 4-4.

Petroleum Exploration in the SBF Basin	
Number	Company
A	Silver Wave Energy
B	Umbono CBM
C	Umbono
D	Umbono CBM
E	Msix

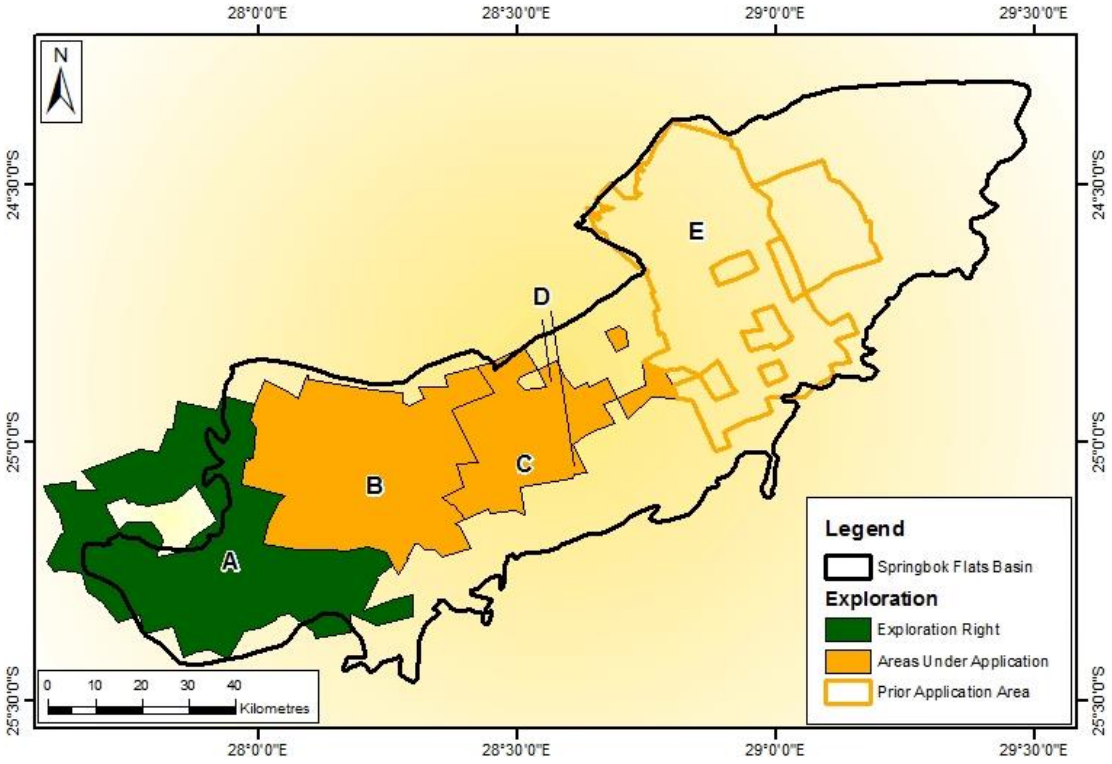

Figure 4-4: Location of Petroleum Exploration in the SBF Basin (adapted from the Petroleum Exploration and Production Activities in South Africa Map July 2013, www.petroleumagencysa.com)

5 Methods of Investigation

The SBF Basin is located in a very flat terrain, and has very few outcrops available for mapping that are open to the public (Figure 1-2). For this reason, this thesis became predominantly a desktop study. The Council for Geoscience (CGS) in Pretoria supplied the information they had on the SBF Basin, borehole data and chemical analyses performed on the coal from various boreholes.

The data provided by the CGS was compiled by many different geologists and therefore, was not consistent. The borehole data covered a large area, and the ideal way of sorting through the data was to break it down into separate areas (Figure 5-1). The areas were chosen by geographically separating the basin to almost equal size portions, and based on borehole density. The areas that had a higher borehole density (such as Areas 1 to 4) were segregated into smaller sections, where areas 6 and 7 had a much lower borehole density and therefore segregated into larger sections. Once this was done it was simpler to filter the data into data sets of appropriate information required for the various investigation methods.

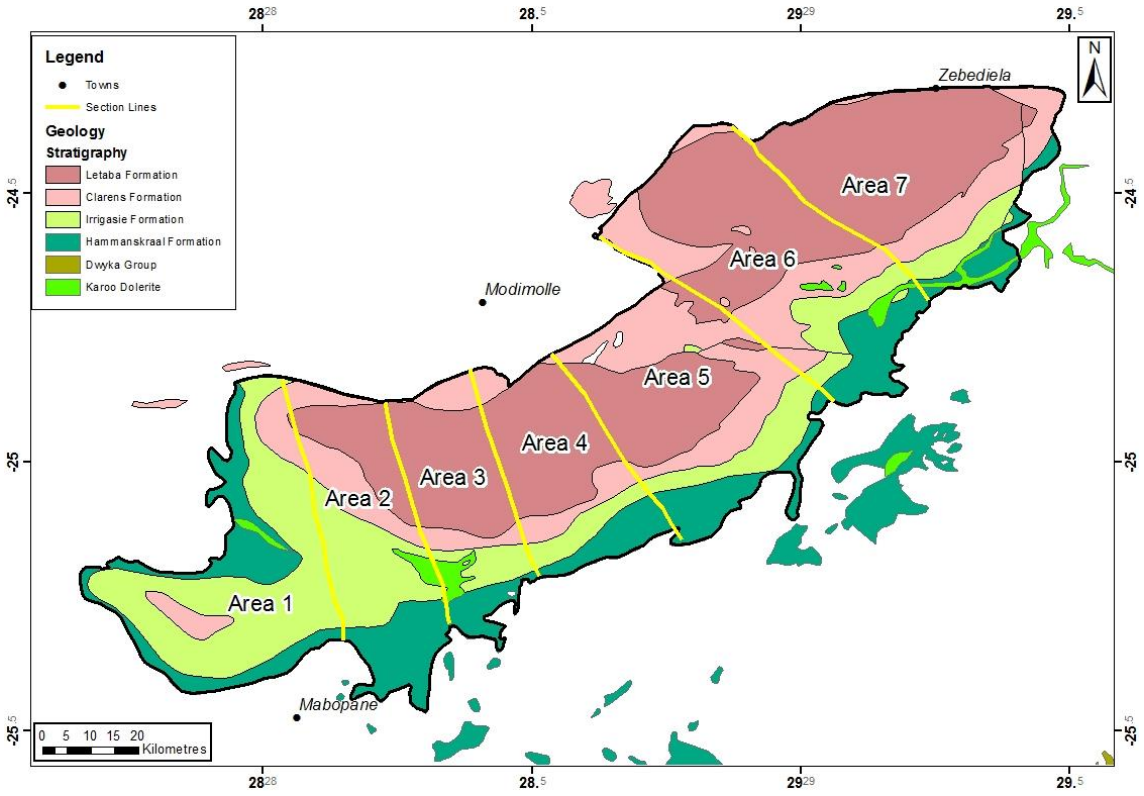

Figure 5-1: The SBF Basin divided into separate study areas.

Once the data were filtered and sorted, different methods of investigation were chosen that would assist in the study of the evolution of the basin. These are:

Table 5-1: Methods of investigation and the programs used to execute them.

Methods of Investigation	Programs used
Georeferencing and digitizing	ArcGIS 9.3
Borehole Logs	Golden Software Strata 3
Fence Diagrams	Golden Software Strata 3
Isopach contouring	Golden Software Surfer 10
Structural contouring	Golden Software Surfer 10
Multicomponent Maps	Golden Software Surfer 10
Geophysics	Outside Source

5.1 Access Database

The data were compiled into an Access Database for ease of data sorting and control. Access enables the management of all the borehole information in one file. Within an Access database file, you can use:

- Tables to store your data.
- Queries to find and retrieve just the data that you want.
- Forms to view, add, and update data in tables.
- Reports to analyse or print data in a specific layout.

The tables created were those containing data for the Collar information, Lithological Logs, and Analysis Logs of the boreholes received from the CGS (Appendix 1: Database Description). These tables were then all linked using the borehole ID's. Various queries were created to assist in the analyses utilised in this study, for example, a query that retrieves lithological logs for a specific area, or one that retrieves the first intersection of a specific formation in all the borehole logs.

5.2 ArcGIS

Many have characterized ArcGIS as one of the most powerful of all information technologies because it focuses on integrating data from multiple sources and creates a cross-cutting environment for collaboration. Like a map, a GIS is layer-based and like the layers in a map, GIS datasets represent collections of individual features with their geographic locations and shapes, with descriptive information stored as attributes. With ArcGIS it is possible to design and build geographic databases, create and manage GIS workspaces and datasets, perform editing and data compilation, make maps and 3D visualizations and perform geo-processing.

The data collected from the CGS and from literature were integrated into GIS, thereby making it easier to sort and correlate data efficiently. This provided a work bench from whence data analysis can begin and results be drawn for discussions.

5.3 Borehole Logs and Cross-sections

To create cross-sections, it is essential to have boreholes with correct coordinates, depth and thickness values, lithology type and detailed descriptions. To create fence diagrams, boreholes were chosen that formed a cross-section over the different selected areas of the basin (Figure 5-2). The boreholes needed to have the full stratigraphy of the basin-fill, reaching down to the basement. Unfortunately, the majority of the boreholes were drilled to a depth where the coal seams were found, and then further drilling ceased.

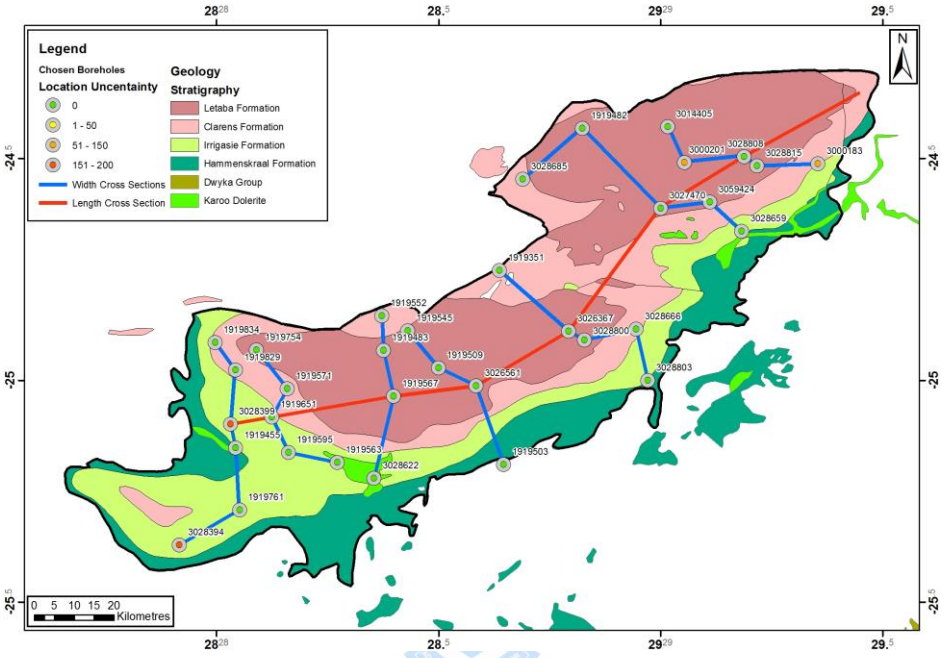

Figure 5-2: Geological map of the SBF Basin indicating the locations of the boreholes chosen and cross-section lines.

The boreholes that were chosen (Figure 5-2) needed to be checked to verify whether the lithology and their descriptions correlated, and then put into a format that is compatible with the program Strater. Strater is a well log and borehole plotting software package. There are 12 log types available in Strater, line/symbol, crossplot, depth, zone bar, bar, percentage, post, classed post, complex text, graphic, lithology and well construction logs. For this study only depth, zone bar and complex text log were used.

Initially, a scheme was created for use in all the borehole logs (see appendix). Schemes contain detailed information of how the data relate to drawing properties. For example, a lithology log uses lithology schemes, which contain keywords, such as granite, clay, etc. Each of these keywords is assigned a fill pattern, contact line properties, line properties, and text properties. Schemes can be reused, meaning you do not have to go through the process of assigning properties each time you create a log.

Once the scheme was approved, the data were imported into the Strater format, and logs were created for each borehole. These logs indicated the different strata at different depths with the geological descriptions alongside them. Since the same scheme was used

for all the borehole logs created, it became easier to correlate them and construct fence diagrams.

The logs from each area were arranged together in order, with estimated distances between them. The different rock types and rock descriptions were then used to link the stratigraphic units together and form cross-sections (blue lines in Figure 5-2) orientated approximately across the elongation direction of the preserved basin. The central borehole logs from each of these cross-sections were linked together to form a cross-section through the length of the basin (red line in Figure 5-2).

5.4 Structure and Isopach Contouring

Structure and isopach contour maps are required in order to illustrate basin-fill geometry, basin shape and basin orientation. These plots are also drawn to illustrate attitude of the selected stratigraphic horizons within the basin. The stratigraphic horizons chosen for this basin are the Dwyka, Ecca, Drakensberg/Letaba Groups, and the Elliot, Molteno, Clarens Formations. On a broad scale, structure contours, particularly at deeper levels within the basin, reveal the location of sub-basins, depocentres and axes of uplift. They may outline subtle syn-depositional topography that had important effects on the local palaeogeography and facies patterns.

The definition of the term isopach is a line of equal thickness for a particular rock unit. To illustrate basin-fill geometry, isopach maps should be drawn for the entire basin-fill and for selected stratigraphic intervals, such as those stated above. In areas of structural complexity, it may be impossible to draw significant information from just structure contour maps, as post-depositional tectonic events may have occurred and altered the strata. Isopach maps reveal the basin-fill in its original, undeformed form and reveal something about syn-depositional structure.

The program utilized in the construction of the structure and isopach maps was Golden Software Surfer 9 and 10, a contouring, gridding, and surface mapping package for scientists. Surfer is a grid-based mapping program that interpolates irregularly spaced XYZ data into a regularly spaced grid. The grid is used to produce different types of maps including contour, vector, image, shaded relief, 3D surface, and 3D wireframe maps. This study utilized the contour, image, shaded relief and 3D surface maps.

5.5 Multicomponent Maps

This type of map displays data plotted as a ratio of lithofacies components, and depicts the variations between two or three lithofacies end-members which are selected to emphasize variations across the basin. For this study the ratio of argillaceous versus arenaceous rocks was used: sandstone and conglomerates against mudstones, siltstones and shales. In general, grain size of clastic sediment indicates the relative amount of energy required to transport the different grains which are then deposited when that energy no longer pertains. The variation of lithologies in clastic environments, such as in the SBF Basin, are caused by the hydrodynamic sorting of coarse to fine grains. How coarse and

how fine these deposits are depends on the current strength and the grain size range of available detritus during the time of deposition. The areas of coarser material would suggest areas where there was higher energy, for example, a river system. Where areas of finer material are located, it suggests that the energy is lower, for example in a lacustrine environment (Miall, 1990). Creating these maps will assist in determining the possible location of depocentres and sub-basins, subtle variations in clastic grain size, and between areas of high and low hydrodynamic energy.

In this investigation, the following aspects are going to be applied to siliclastic sediments (cf., Miall A.D, 1990):

- The climate has no constraint, as sediments occur worldwide and at all water depths;
- Being both terrestrial and marine;
- The grain size of sediments reflects the hydraulic energy in the environment during deposition;
- When comparing compositions of rocks, the presence of mud indicates the settling out from suspension;
- Finally laminated sediments are mostly formed in quiet-water environments:
    - Laminated pelagic mudrocks;
    - Prodelta deposits;
    - Delta plain lagoonal and fluvial overbank muds;
- Thicker beds form in a variety of high-energy wave or current dominated environments;
- An interbedding of contrasting lithofacies may be environmentally indicative in that they, for example, record an alteration of quiet-water mud sedimentation and higher energy flow conditions which result in the deposition of rippled sand;
- Shallow-water sand bodies result from the interaction of currents and waves;
- Bioturbation is preserved in sediment that was deposited during fair weather conditions;
- Widespread changes in hydraulic regimes that are evident in sediments usually indicate changes in sedimentary environments;
- In general, the bed thickness is proportional to the depositional energy level.

5.6 Geophysics

Working at Shango Solutions during part of my master's preparation proved to be extremely beneficial to my thesis. I was lucky enough to acquire geophysical data (Figure

5-3) from Mr. B. Green in 2011, in the form of gravity and magnetic images of the study area. Gravity and magnetic data are used to delineate broad basin configuration. Mr. B. Green supplied images indicating major anomalies, faults and dyke delineations, not all relating directly to the SBF, but to the region. All interpretations made from these diagrams are my own analyses.

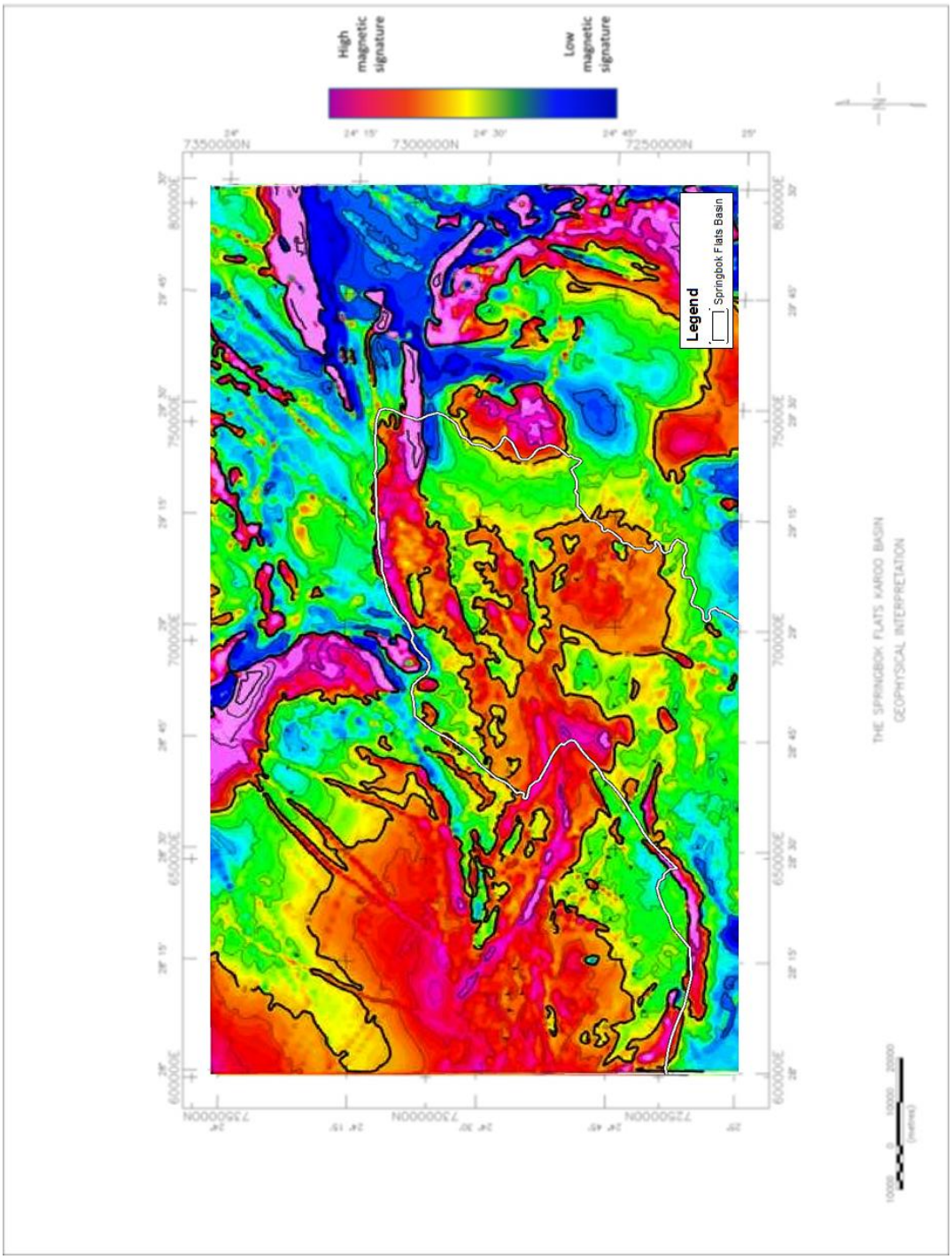

Figure 5-3: Example of regional aeromagnetic data courtesy of Mr. B. Green (2011).

6 Data

6.1 Data Description

Data were acquired from the Council for Geoscience in the form of a borehole Excel database (see Appendix 1: Database Description). The first file considered was a header file indicating the captured and un-captured boreholes, which contained the collar information for each borehole such as the coordinates and the location uncertainty of those coordinates, farm names and numbers, borehole ID numbers, etc. This information assists in acquiring a spatial understanding of the distribution of the boreholes (Figure 6-1).

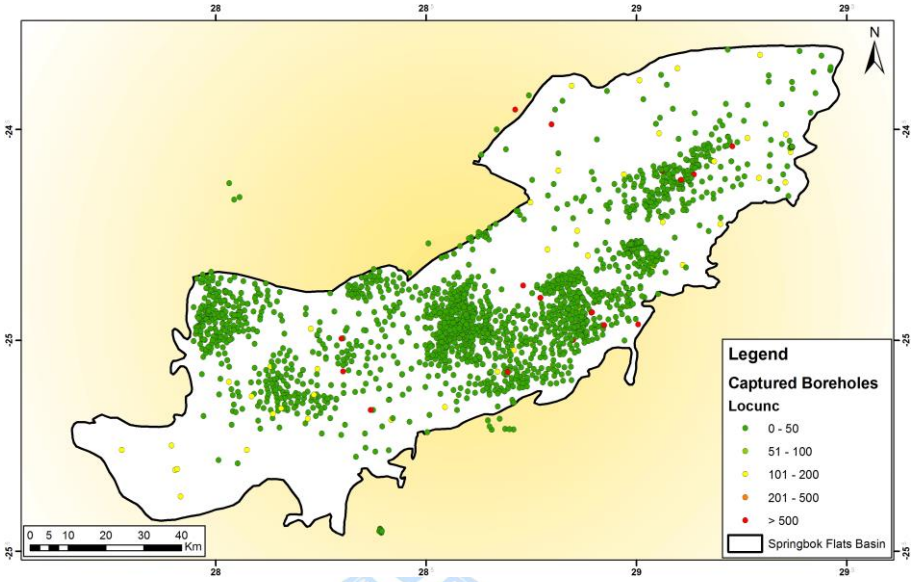

Figure 6-1: Spatial distribution of the borehole database, illustrating the locality uncertainty and capture status.

The second file to be investigated was the lithology file. This file has the captured borehole's lithology log information in the form of "To" and "From" depths, Stratigraphy and the Lithological description. These lithology descriptions were given a Stratigraphic Code (see Appendix 2: Lithological Code) which assisted in classifying the lithology. A status of each entry is given in the form of "M" and "P". "M" represents the lithology of the main hole, and "P" is a detailed description of the coal seam in that log.

The final file to be considered is that of the Analyses file, which has all the analyses for the boreholes captured. The variables captured are the Calorific Value (CV), the percentage of Fixed Carbon, Ash, H_2O, Volatiles, Phosphorous and Sulphur in the coal sample. Also documented are the information pertaining to which float or sink analyses were done, and the overall raw analyses.

These files were all combined into an Access database, enabling the ability to easily compare tables, run queries, and to combine and create new tables with only the information that is needed for a specific task.

6.2 Data Statistics

To get a better understanding of the data, simple statistics were performed. The first calculation performed was how many of the boreholes were able to be utilised in the different methods of investigation. Only boreholes with information that was captured could be used in the majority of the analyses, and the results are indicated in Table 6-1. This can be displayed in ArcGIS to assist in choosing which boreholes to use in the cross-section analyses. Figure 6-2 indicates the versatility of the database, using the status and the locality uncertainty.

Table 6-1: Status of the borehole database.

Status	Number of Boreholes
Un-Captured	1091
Captured	906
Total	1997

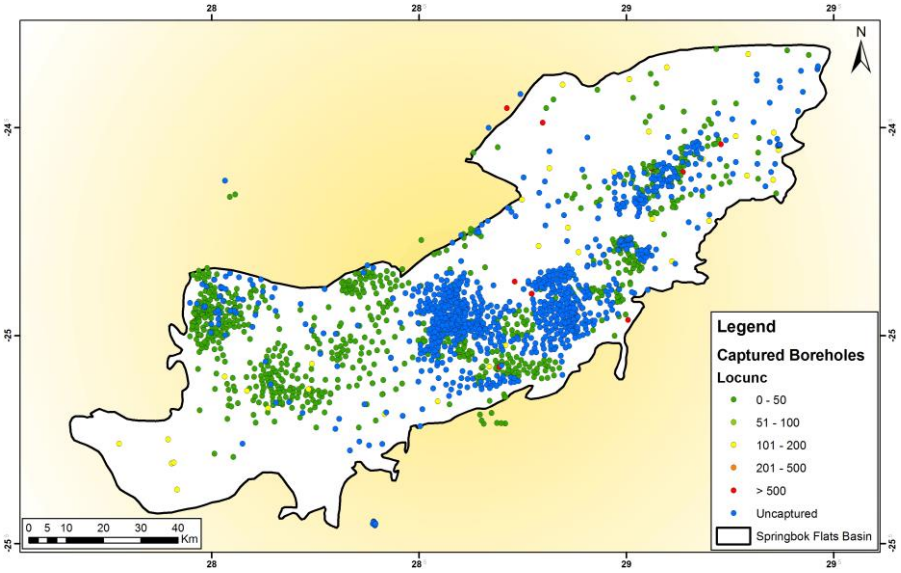

Figure 6-2: Spatial distribution of the borehole database indicating captured/uncaptured boreholes and the locality uncertainty of the captured boreholes.

The data utilised needed to have sufficient information to carry out the analyses, for example, the boreholes which have analysis data would be more useful to utilise (Figure 6-3). Using these methods, a selection of quality borehole data was made.

With using data captured by various people, there is always a risk of errors inherent in the data. Many of the cores which were logged for this area have been lost or discarded over the years, and therefore the data could not be checked for accuracy. For the purpose of this study, the data used are assumed to be 100% accurate.

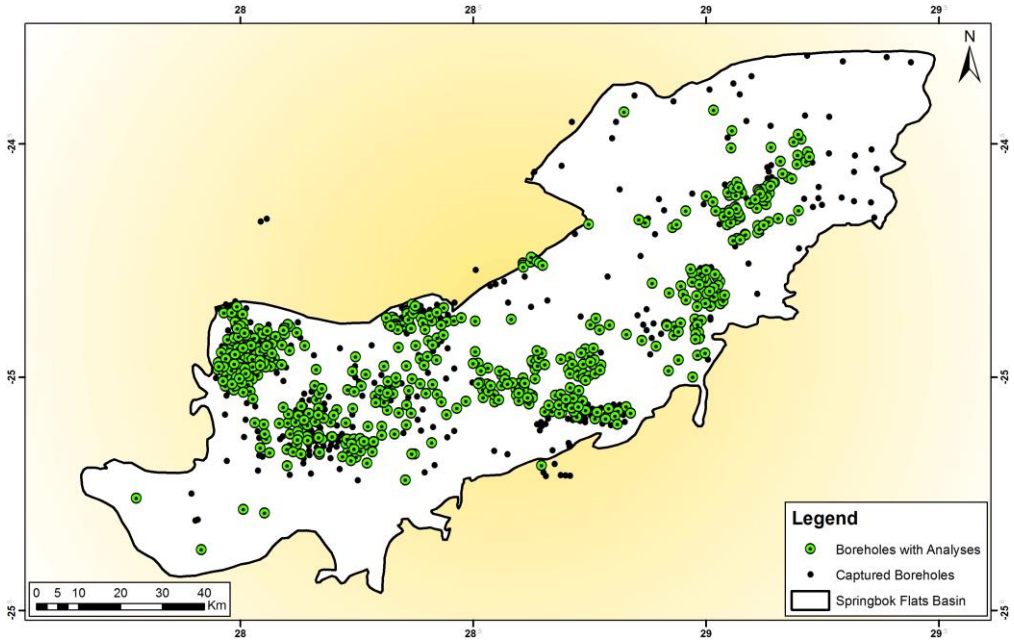

Figure 6-3: Spatial distribution of the "boreholes with analyses" data.

6.3 Errors inherent in the data

The dataset obtained from the Council for Geoscience was a product of collecting various data from the different companies who drilled in the SBF area. The age of the logs captured range from 1947 to 2006, and they were captured by many individuals, and therefore human errors are inherent in the datasets. Throughout the sorting of the data for the purpose of this study, many errors were corrected, and where the information was noticeably incorrect, these data were omitted from the dataset and not used in the analyses. In addition to human errors, many of the boreholes drilled were for the purpose of identifying economic layers, so little care was taken when logging the rest of the stratigraphic column.

The following assumptions were made:

- Data used was assumed to be 100% accurate
- Data capturing methods are assumed to be the same for all boreholes captured
- Interpretation of stratigraphy was assumed correct
  - Except where obvious misinterpretations were made, these data were either corrected or omitted from the dataset.
- Conversions made from feet to metres was assumed to have undergone quality control and quality assurance, and assumed to be correctly converted

In the analyses, it was evident that these errors crept through. For example, in the contour plots where there are outliers in the data, a small ring of tight contours appears. This indicates that the data used from that borehole were incorrectly captured. In these cases, these anomalies were taken into account as ghost anomalies, and not interpreted with the rest of the data. Boreholes logs utilised for the cross-sections appeared to be of high quality.

7 Regional Results

Using the Access Database created for the SBF Basin, it was simple to run queries to extract information for each of the formations. Datasets were compiled for each of the predominant stratigraphic units in the SBF Basin using the borehole lithology data: i.e. Ecca, Beaufort, Molteno, Clarens, Elliot and Letaba.

The boreholes in the Ecca Formation dataset for example, had only the log lithologies that fall within the Ecca Group, and Vryheid and Volkrust Formations. These datasets were used in the following map compilations.

7.1 Structural Contour Maps

The depth to the top contacts of each layer were identified and assigned to that borehole's location, to create a x,y,z plot in Surfer. A grid was then created using this information in order to create the contour plots seen in Figure 7-1 and Appendix 3: Structural Contour Maps. Prior to structural interpretation, the errors in the data were first identified so that they were not taken into consideration. There are two anomalies identified that represent outliers in these Ecca data and these are not to be considered structural. They appear as two tightly contoured high elevation (>1000 a mamsl) points in the 600 mamsl region. In the Clarens Formation in area 2, there is another error in data identified and omitted from the structural interpretation. These two boreholes were identified to be borehole id's 3028406 and 3026637, and were intentionally left in the data so as to act as examples of inherent errors. It is also noted that these two anomalies are only found in the Ecca Group plot, which suggests that the lower contact of the Beaufort Group was misinterpreted to be deeper than it actually is.

Another anomaly identified was along the southern boundary of the basin in the south eastern corner of area 3 (Figure 5-1), where it is indicated that there is an extension of the structural basin. In this area there are only 2 boreholes with information. This anomaly is present throughout the strata as having a lower elevation than the surrounding lithology. Due to the limited data in this region, it is unclear as to whether this is a structural depocentre or an error in the data, therefore a further investigation into this area is required.

One of the principal structures identified was a major fault striking along the central northern boundary of the basin that has faulted the strata down by about 1000m, causing the strata to dip at approximately 1-5 degrees. The direction at which the strata dip is radial away from the fault, ranging from a north-easterly direction in the west of the basin, to north-westerly to the centre of the basin. A similar structure which appears to be an extension of this fault can be identified in the north eastern section of the basin (Areas 6 and 7 in Figure 5-1) which has faulted the strata down by approximately 850m. Again, the strata in the vicinity of this fault dip in a radial direction outwards. These major lineaments are evident throughout all the formations, except for the Letaba Basalts. This is an indication that these faults are of the same family of structures and that they occurred prior to or were syndepositional with the basalts.

In the western area of the basin (area 2 in Figure 5-1) there appears to be a deep trough following a south-easterly trend. This valley appears to be very narrow and has a steep gradient in the Ecca Group, becoming gentler in the Beaufort Group. However, as we move through the younger strata, this valley once again becomes steeper in gradient. This could suggest a fault in the region striking in a south-easterly direction, which was active during the Ecca deposition, then dormant during the Beaufort deposition, and then reactivated during the deposition of the remaining strata. This valley does not appear in the Letaba Formation and was therefore no longer active.

The shape of the basin represents a half-graben structure in a bowl shape (radial), with the central region (areas 4 and 5 in Figure 5-1) having a higher elevation. This elevated section is evident throughout the strata and represents the deposition elevation prior to the down-faulting of the strata by 1000m. This feature gives the basin the characteristic of having two depocentres.

7.2 Isopach Maps

The top and the bottom contact depths of each formation were extracted out of the datasets in order to calculate the thicknesses of the strata. The top contact depth was subtracted from the bottom contact depth to calculate the thickness, and this value was assigned to the individual borehole locations. Following the procedure used in the compilation of the structural contour maps, a grid for each formation was created, and the Isopach maps can be seen in Figure 7-2 and Appendix 4: Isopach Contour Maps.

Similar to the structural maps, in the Ecca Group one can identify outliers which represent boreholes that were incorrectly interpreted. These two anomalies are not indicated in the other stratigraphic formations, which suggests further that the bottom contact of the Beaufort was incorrectly interpreted and at a greater depth than it should have been.

The Ecca Group does not appear to have a large variability in thickness throughout the basin. If one ignores the two anomalies, it is evident that the average thickness of Ecca in the basin is in the order of 20 metres. There are however a few locations where this thickness extends to approximately 60 metres in the northern regions. In the eastern-most part in the basin, there appears to be an area of thicknesses around 60-80 metres. This could suggest that area is a palaeo-low where Ecca sediments accumulated to a greater thickness.

The Beaufort Group is approximately 10-20 metres thick on average in the northern regions and in the southern portion of the Beaufort Formation there appears to be a palaeo-low where the strata is of a greater thickness than the surrounding areas, of about 50-100 metres thickness.

The Molteno Formation appears to range from 25-50 metres in thickness throughout the basin. To the south and in the central regions of the basin, the strata appear to be 30-45 metres in thickness, and thin towards the north. This corresponds with the Beaufort Group and could suggest a similar environmental regime and a depocentre in this region.

Above the Molteno Formation is the Elliot Formation. It appears that during Elliot times, the depocentre that was evident in the previous formations has shifted to a more central region in the SBF Basin. The formation ranges in thickness from 20-150 metres, the thickest succession being in the centre of the basin, with the thinner regions to the north and south.

The Clarens Formation shows another shift in the depocentre back to where it was during the deposition of the Beaufort and Molteno formations. Also indicated in this succession is an area of greater thickness (approximately 150-160 metres) in the region where the major lineament was identified. This suggests that this lineament was possibly active as a syn-depositional fault during accumulation of the Clarens Formation.

The last formation to be investigated is the Letaba Formation. This plot indicates the most prominent feature that was identified in the structural contour plots, the major north-westerly lineament. This is noted as a confirmation that there is a major fault along the northern boundary of the basin, where the Letaba basalts in that region are approximately 1000m thick. This lineation is not as dominant in the other strata other than the Clarens Formation; this suggests that the faulting began to occur during the deposition of Clarens sediment, but was not a major structural feature until the eruption of the Letaba Basalts which re-activated the fault and propagated it further along the boundary of the SBF basin.

7.3 Multicomponent Maps

For this process, the lithology code column was used. All lithologies that fall within the arenaceous type were grouped together and given as a ratio to the argillaceous lithologies within each borehole. For example, the Ecca Group that was intersected by borehole A had 40% arenaceous rocks, and 60% argillaceous rocks. A grid was created using the percentage argillaceous rocks (60% for borehole A) that were allocated to each borehole, and the plots can be seen in Figure 7-3 and in Appendix 5: Multicomponent Maps. The darker the colour of the plot indicates the finer-grained sediments of the formation and the lighter for coarser-grained. The grain size rating used is based on the grain size average of that rock, with 0 being 100% argillaceous (fine grained, clayey lithologies), and 5 being 100% arenaceous (coarse grained, sandy lithologies).

The Ecca Group in the multicomponent map indicates related characteristics with those found in the isopach maps of the same formation. For instance, in the far east of the basin, an area of finer-grained lithologies is identified and corresponds to the same area in the isopach map that indicates a thicker succession. This suggests that there was locally a palaeo-low that subsequently filled up with Ecca sediment. A similar anomaly occurs in the centre of the basin (area 3), where argillaceous material corresponds with an area of thicker accumulation.

Similar patterns occur throughout the formations where the isopach maps and multicomponent maps can be correlated. The Beaufort Group shows a strong correlation in area 3, where the isopach map indicates an area of thicker succession, and the multicomponent map indicates an area of coarser grained material. This correlation differs

from that in the Ecca Group, as the sediment was deposited under different environmental conditions. The Ecca Group is known to be a braided river deposit, and the lithology in the database concurs with this statement which can be seen in the multicomponent map. Therefore the thicker fine-grained deposits are most likely lake sediments. The Beaufort Group, according to literature and the borehole database, is likely to be a meandering fluvial environment, so the areas of thicker coarse-grained occurrence are likely to be river channels, with surrounding flood plains of finer-grained sediment. A similar correlation is found in the Elliot Formation.

In the Molteno and Clarens Formations, the correlation between the isopach and multicomponent map reverses again, where areas of greater thickness are associated with areas of finer-grained, more argillaceous sediments. These differences in correlation suggest that it is environment type dependant. If the presiding environment is wetter in nature, then the areas of thicker succession occurred in areas of higher energy.

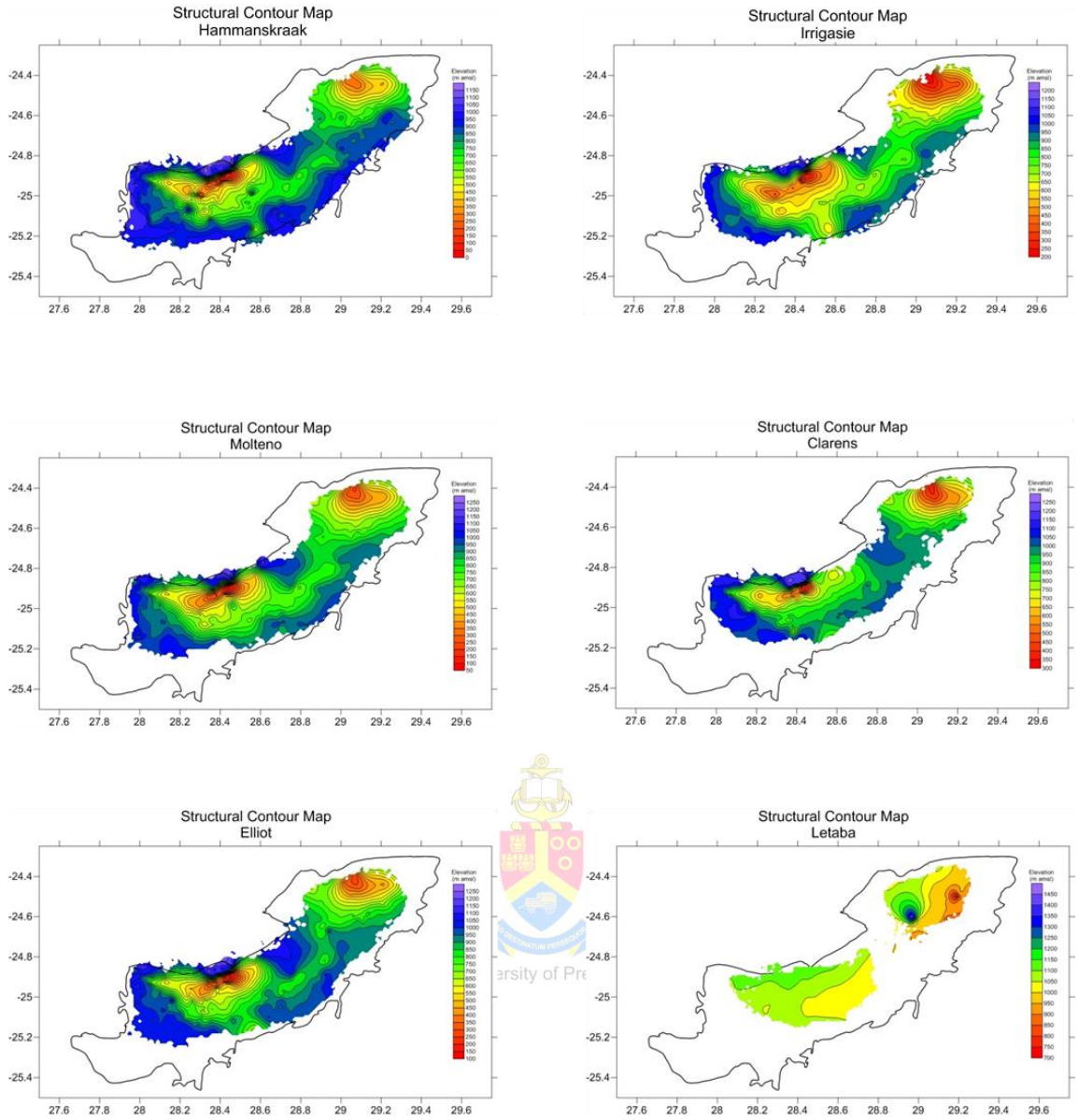

Figure 7-1: Structural Contour plots of the upper contact of the Karoo Supergroup strata found in the SBF Basin.

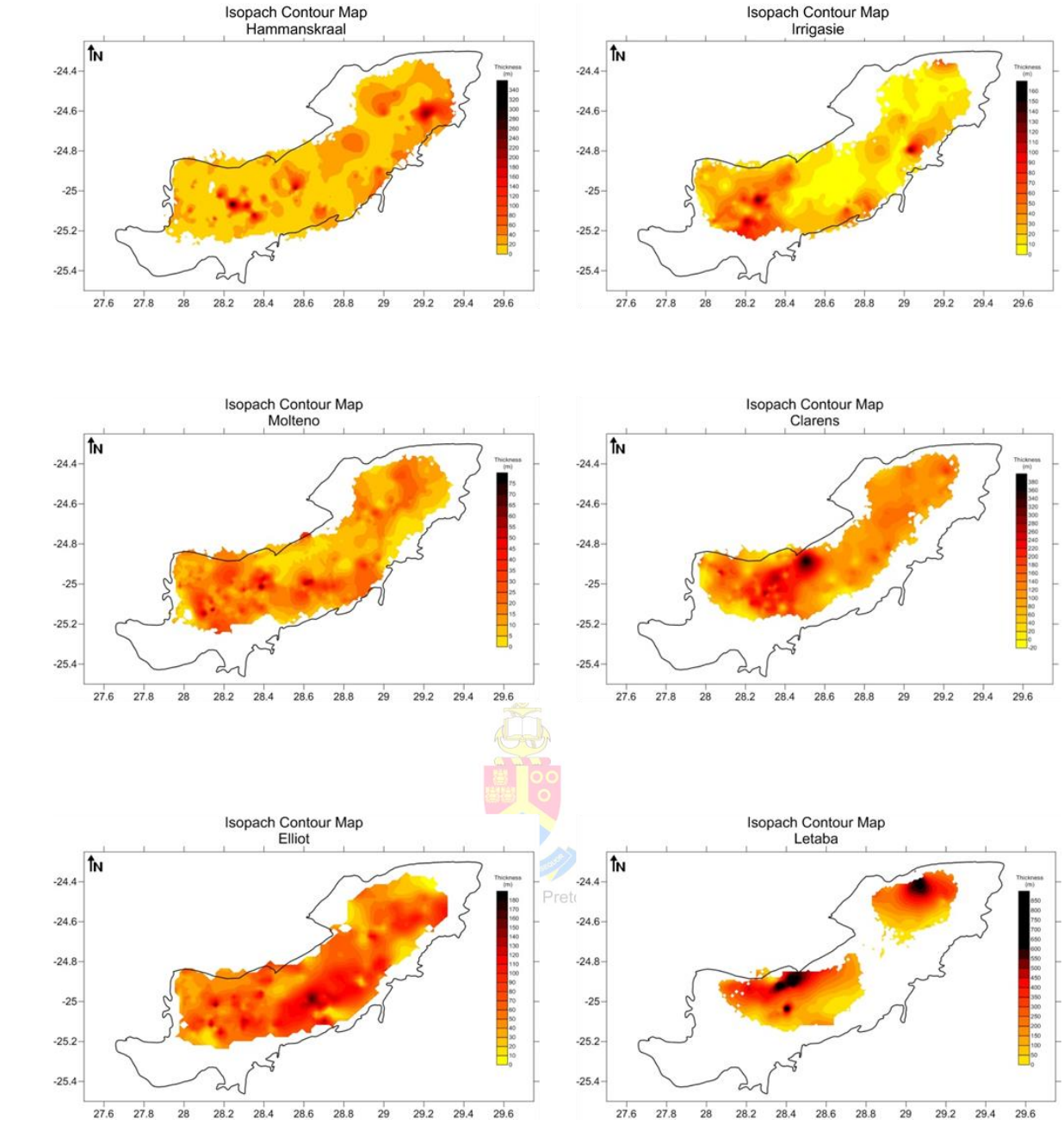

Figure 7-2: Isopach plots of the Karoo Supergroup strata found in the SBF Basin.

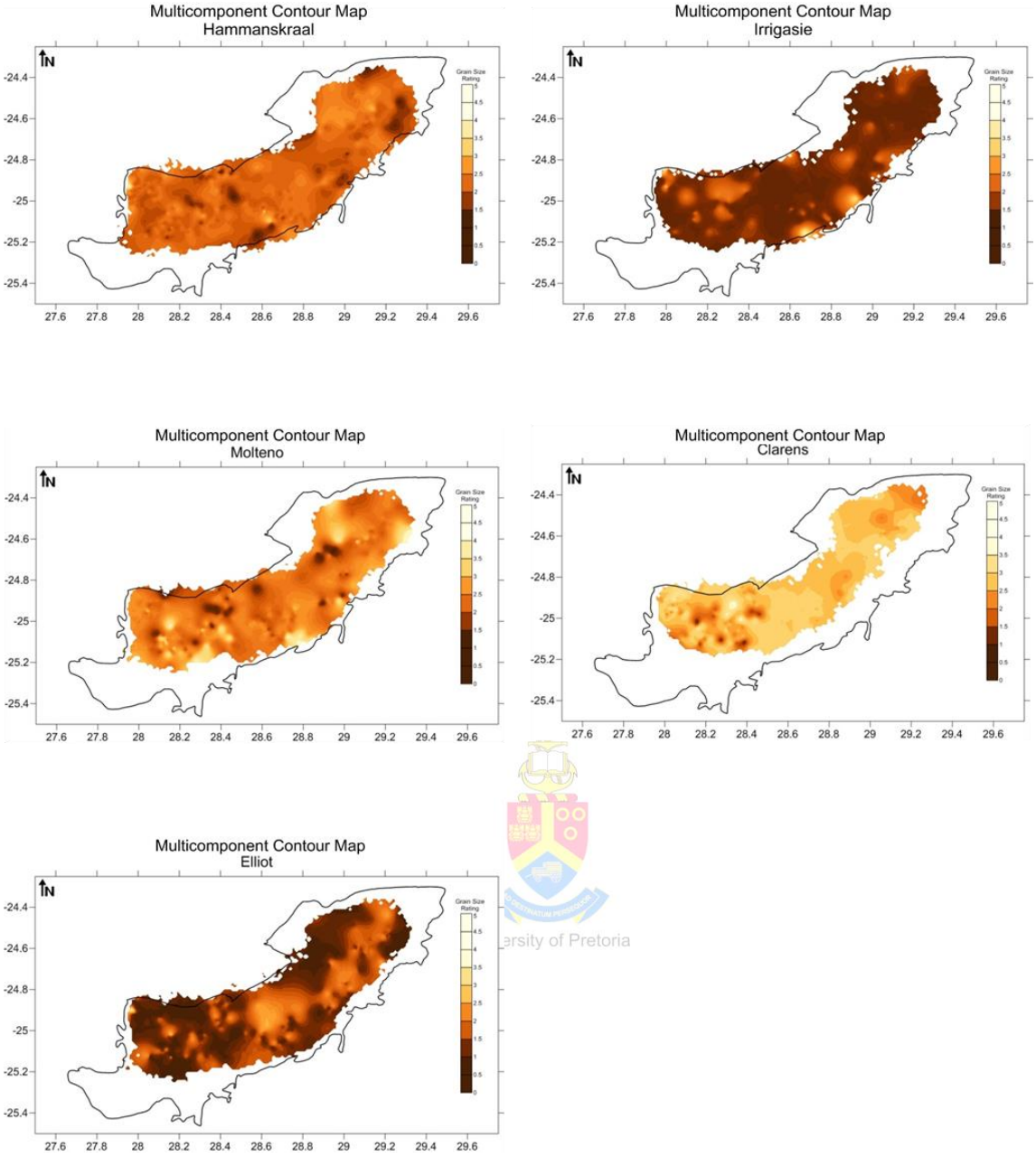

Figure 7-3: Multicomponent plots of the Karoo Supergroup strata found in the SBF Basin.

7.4 Geophysical Evidence

Using the gravity and magnetic data of the area, major faults and dyke systems in the area of the SBF Basin were delineated courtesy of Mr. B. Green (2011). The lineaments identified are not all of the same age as the SBF, but reflect all the dykes and faults for that area. By georeferencing the images supplied by Mr. B. Green (2011), Figure 7-4 was constructed and indicates the proposed locations of the major faults (Black), the major dykes (Green) and the minor dykes (Red).

Figure 7-4 indicates a rose diagram that was constructed with the fault directions; the fault system follows a strong NW-SE trend as well as a NE-SW trend. The faults that are orientated in a NE-SW direction show a large variation in direction, ranging from NNE to ENE, suggesting a variation in the direction of the primary force that created the faults. These faults have a similar direction to that of the Thabazimbi-Murchison Lineament (TML) fault that lies to the north of the basin, which was a pre-depositional weakness in the basin floor (Good and De Wit, 1997). The faults which are striking in a NW-SE orientation have a similar trend to faults found to be associated with the Karoo Supergroup and Cape Fold Belt (CFB).

The dyke clusters in the area are concentrated to the north of the basin and follow an ENE orientation. This trend is reflected in the known dyke clusters of the Save-Limpopo dyke swarm (SLDS) associated with the breakup of the Gondwana Supercontinent (Hastie *et al.,* 2014).

7.5 Geophysical Anomalies

The geophysical anomalies delineated courtesy of Mr. B. Green (2011) indicate two separate sub-basins that fall in the SBF area (Figure 7-4). The major sub-basin has similar characteristics to the Main Karoo Basin, and has a NNE-SSW strike that trends towards a more southerly direction. This basin is seen to extend further south of the known SBF's boundary and could suggest an extension of the basin that has since been eroded. Evidence for this can be seen in the many outliers of the Ecca Group to the south of the preserved basin (Figure 3-1).

The smaller Karoo sub-basin in the south western region of the SBF does not exhibit any directional characteristics, and it is clearly separate from the larger Karoo sub-basin to the east.

The mafic sill anomalies lie to the north of the basin, which indicates that there was a possible extension of the SBF basin to the north, leaving the current basin as the preserved basin.

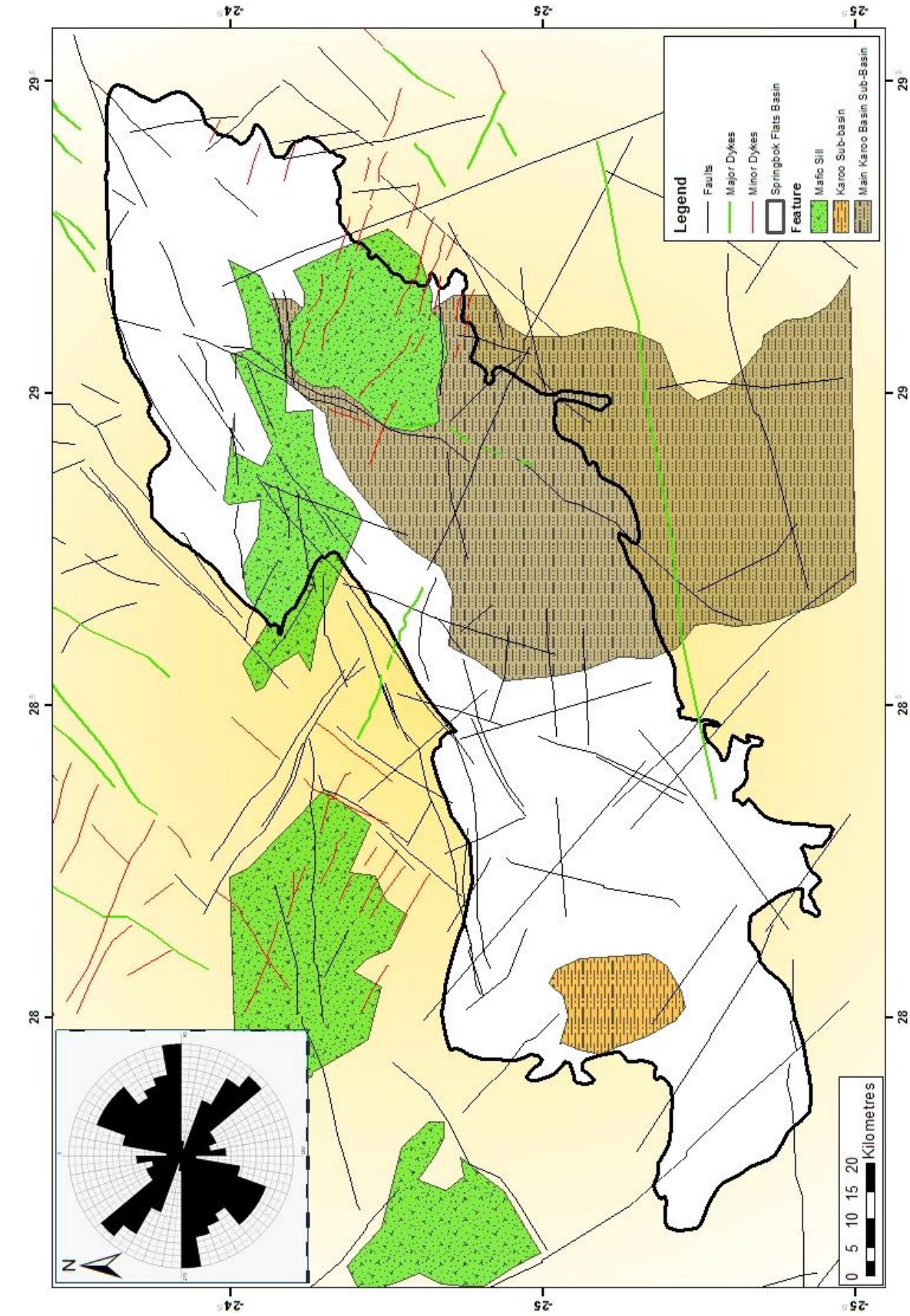

Figure 7-4: Geophysical anomaly delineation courtesy of Mr. B. Green (2011).

7.6 Borehole identification

In order to get a better understanding of the basin and the strata in it, it is important to have a closer look at the boreholes provided. The following data constraints were investigated in order to select the boreholes used for the cross-sections:

- Coordinate confidence
- Depth
- Strata thickness
- Lithology intersected
- Description detail
- Analyses availability

The location of the boreholes selected plays an important role in the accuracy of the cross-sections. The borehole database provided by the Council for Geoscience had data relating to the uncertainty of the location. These data were used to identify boreholes that had the lowest location uncertainties, and boreholes of less than 200 metres uncertainty were used where possible. The possible borehole options were reduced by removing those boreholes that had more than 200 metres uncertainty (Figure 7-5).

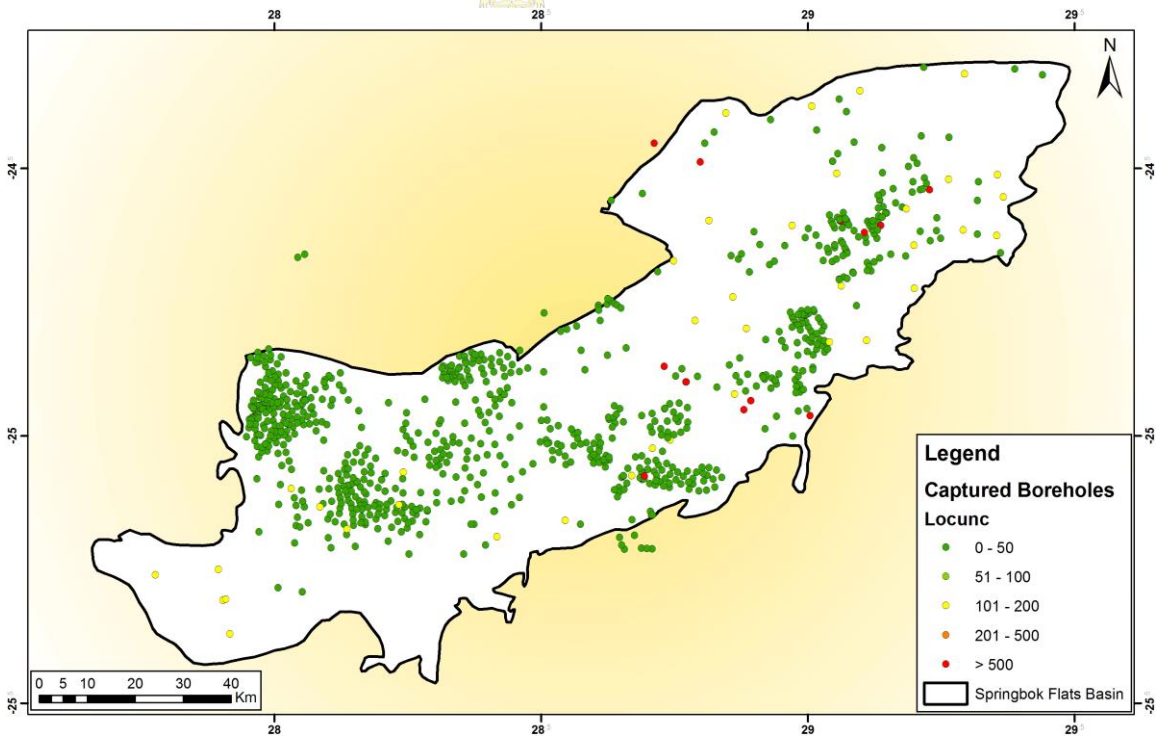

Figure 7-5: Database distribution illustrating the location uncertainty of the boreholes.

Boreholes that did not provide sufficient information in the log were excluded from the selection, as detailed lithology and stratigraphy is required in order to produce a useful log. To create a cross-section indicating the possible geometry of the basin fill, it is required that the boreholes that are selected extend to the basement of the Karoo deposits. However, the

majority of the boreholes were drilled in order to identify coal depth and quality, and due to drilling expenses, the holes were not extended further than the floor of the coal layer. Boreholes that extended to the Dwyka Group were given priority, however due to the lack of these boreholes; the deepest holes in that region were used.

The boreholes that had the best information taking consideration of all the constraints stated above, were chosen for the cross-section analyses and are listed in Table 7-1.

Table 7-1: Selection of boreholes to be used in the cross-section analyses.

Area	Farm Name	Borehole ID	Coal Analyses Available	Depth (m)	Area	Farm Name	Borehole ID	Coal Analyses Available	Depth (m)
1	Reguit	1919834	Yes	190.15	5	Cyferfontein	1919351	Yes	81.05
	Newlands	1919829	Yes	331.70		Gegund	3026367	Yes	382.75
	Haakdoornbult	1919842	Yes	243.84		Roodevlakte	3028800	Yes	283.00
	Leeuwkraal	1919454	Yes	213.39		Vlakplaats	3028666	Yes	142.57
	Kalkbank	1919761	Yes	224.15		Leeuwkuil	3028803	Yes	119.30
	Buffelsdoorn	3028394	Yes	177.00	6	Vlakfontein	3028685	Yes	167.25
2	Droogelaagte	1919754	Yes	534.85		Rietlaagte	1919482	Yes	720.73
	Vlaklaagte	1919571	Yes	312.87		De Hoop	3027470	Yes	317.10
	Welgelegen	1919651	Yes	291.37		Hoogbult	3059424	Yes	296.60
	Wolfhuiskraal	1919591	Yes	112.11		Vrischgewaagd	3028659	Yes	74.70
	Vaalbuschbult	1919563	No	145.03	7	Blinkwater	3014405	Yes	783.33
3	Buiskop	1919332	Yes	211.13		Hulpfontein	3000201	Yes	667.82
	Roodekuil	1919483	Yes	1001.70		Merwede	3028808	Yes	476.23
	Vlaklaagte	1919570	Yes	670.84		Morgenzon	3028815	Yes	327.30
	Ruimte	3028622	Yes	69.00		Frischgewaagd	3027497	No	269.52
4	Tweefontein	1919545	Yes	1072.00					
	Rosedale	1919509	Yes	517.00					
	Afzet	3026538	Yes	353.13					
	Rooikop	1919503	Yes	68.63					

7.7 Delineation of SBF Basin Influencing Faults

Once the boreholes were chosen, logs were created in order to see which strata were intersected and how they correlated (Appendix 6). It was clear from the initial cross-sections created (using Golden Software Strata) that there was significant faulting in the basin. To understand the apparent structure, the faults delineated by Mr. B. Green (2011) were plotted in ArcGIS, superimposed on the structural, isopach and multicomponent contour plots created in Section 7, and comparisons were made. Furthermore, values from the borehole database displaying the depths of the first coal intersected (Figure 7-6) were plotted, with the geology as a base map. It is possible to turn the different layers on and off, and to compare all the components. Using this information together with previous studies on the basin (McDonald and Waldeck, 2008), it was possible to calculate which of the faults

indicated by Mr. B. Green (2011) had an effect of the Karoo strata, and the approximate movement of the faults (Figure 7-7).

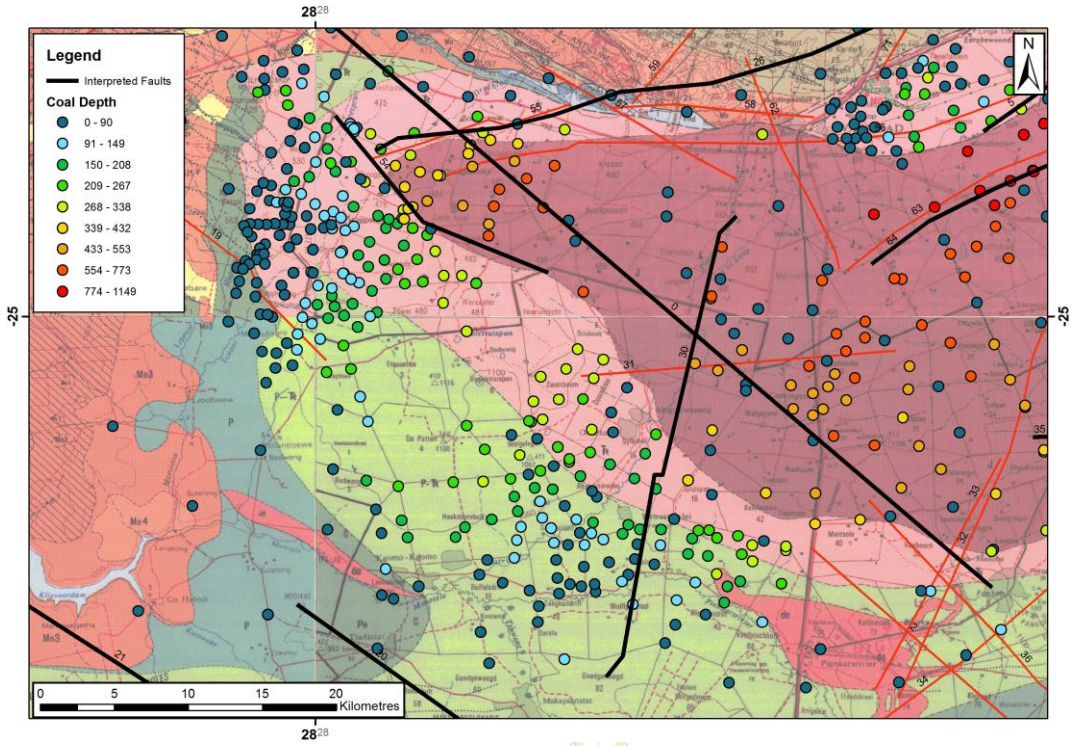

Figure 7-6: Boreholes plotted according to depth of first coal intersection over a geological map (Geological survey, 1:250 000 geological series maps).

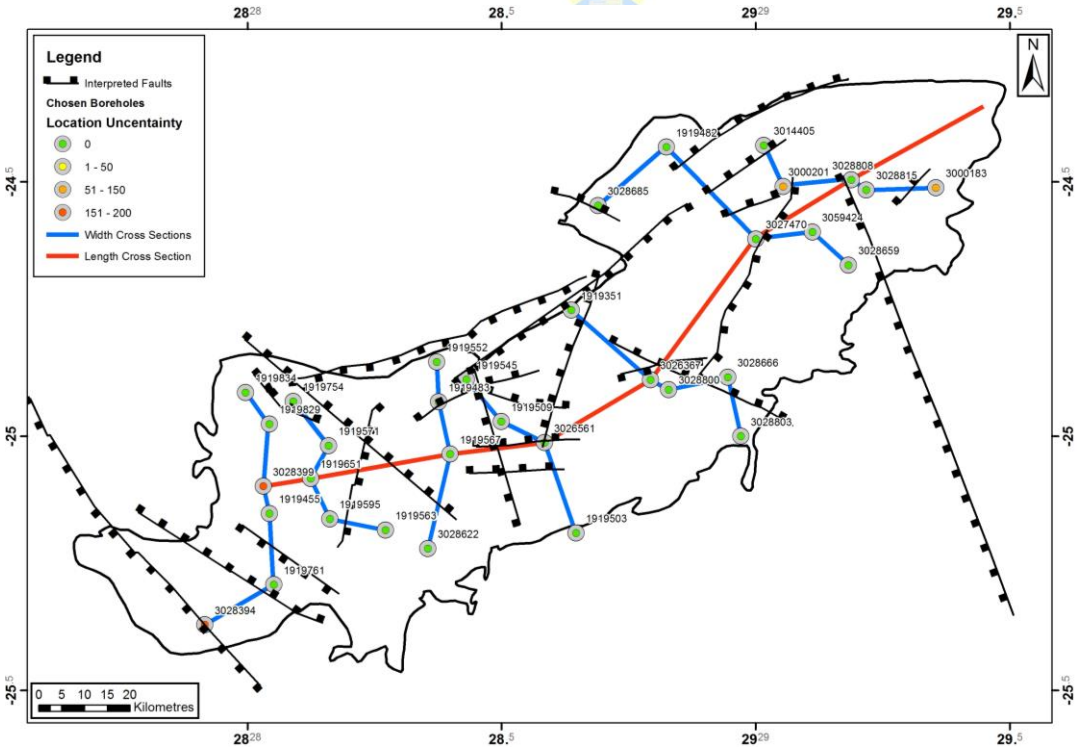

Figure 7-7: Calculated movement of fault blocks.

7.8 Introduction to Cross-sections

The cross-section lines were superimposed on the local geology (Geological survey, 1:250 000 geological series maps) and SRTM data in order to assist in determining the geometry of the cross-sections. Figure 7-8 indicates what the different blocks represent in the cross-section maps to follow.

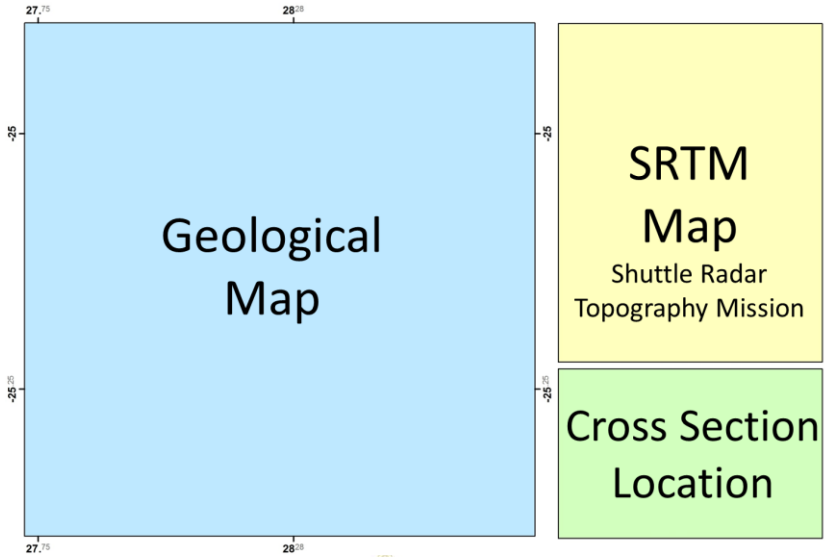

Figure 7-8: Legend for Cross-section maps that follow.

This study is primarily based on the CGS Borehole Database, and therefore several assumptions were made. In this database, many different nomenclatures were used for the different strata. For example, the Irrigasie Formation includes the Beaufort Group and the Elliot and Molteno Formations. Underlying these is the Hammanskraal Formation which correlates with the Vryheid Formation. Table 7-2 illustrates the correlated strata from the database to those in previous studies. The lithologies for the cross-sections were grouped into successions based on Johnson et al. (2006).

The definition in The Oxford English Dictionary, 10th ed. (2002), of a dyke is an intrusion of igneous rock cutting across strata, where a sill is a tabular sheet of igneous rock intruded between and parallel with existing strata. Igneous intrusions were identified in the CGS Borehole Database as either intrusion or dyke, and no reference to sills was made. Due to the coarseness of the distribution of boreholes chosen for the cross sections, it is difficult to clarify whether an igneous intrusion is a dyke or a sill. For the purpose of this study, when an intrusion is specifically referred to as a dyke in the database, it is assumed to be a dyke. If it is referred to as an igneous intrusion, and is not able to be clarified specifically as a dyke or a sill, it will be referred to as an igneous intrusion.

Table 7-2: Nomenclature of the SBF stratigraphy over time compared to stratigraphy identified in the CGS Database.

<table>
<tr><th colspan="2">Du Toit (1954); Haughton (1969)</th><th>S.A.C.S. (1980)</th><th>De Jager, (1983); Mc Rae, (1988)</th><th>Johnson et al. (2006)</th><th colspan="2">The CGS Database</th></tr>
<tr><td rowspan="3">Stormberg Series</td><td>Bushveld Amygdaloid</td><td>Letaba Formation</td><td>Letaba Formation</td><td>Letaba Formation</td><td>Letaba Formation</td><td>Drakensberg Group</td></tr>
<tr><td>Bushveld Sandstone</td><td>Clarens Sandstone Formation</td><td>Clarens Sandstone Formation</td><td>Clarens Formation</td><td colspan="2">Clarens Formation</td></tr>
<tr><td>Bushveld Mudstone</td><td rowspan="2">Irrigasie Formation</td><td>Elliot Formation</td><td rowspan="2">Irrigasie Formation</td><td colspan="2">Elliot Formation</td></tr>
<tr><td rowspan="3">Ecca Series</td><td rowspan="2">Upper Ecca Shale Stage</td><td>Molteno Formation</td><td colspan="2">Molteno Formation</td></tr>
<tr><td rowspan="3">Ecca Group (formations not named)</td><td>Beaufort Group</td><td>Volkrust Formation</td><td>Beaufort Group</td></tr>
<tr><td>Middle Ecca Coal Measures Stage</td><td>Vryheid Formation</td><td rowspan="2">Hammanskraal Formation</td><td rowspan="2">Vryheid Formation</td><td rowspan="2">Ecca Group</td></tr>
<tr><td>Lower Ecca Shale Stage</td><td>Pietermaritzburg Shale Formation</td></tr>
<tr><td colspan="2">Dwyka Series</td><td>Not Named</td><td>Dwyka Group</td><td>Dwyka Group</td><td colspan="2">Dwyka Group</td></tr>
</table>

The created logs that were used for the cross-sections were cross referenced with boreholes in the database to get an understanding of each formation. With the comparison of correlating formations in the lithological database, a trend for each formation developed. Taking into account the literature and results determined from the maps compiled, these trends could then be documented.

Logs of each of the boreholes were created in Golden Software Strata and can be found in Appendix 6. Detailed logs of the different coal zones found in the boreholes were also drawn up indicating the analyses of RAW coal data; these assist in confirming which zone the coal layer belongs to. However, not all the coal layers had undergone analyses and then the logs are left blank. The detailed coal logs can be found in Appendix 7.

7.9 Area 1

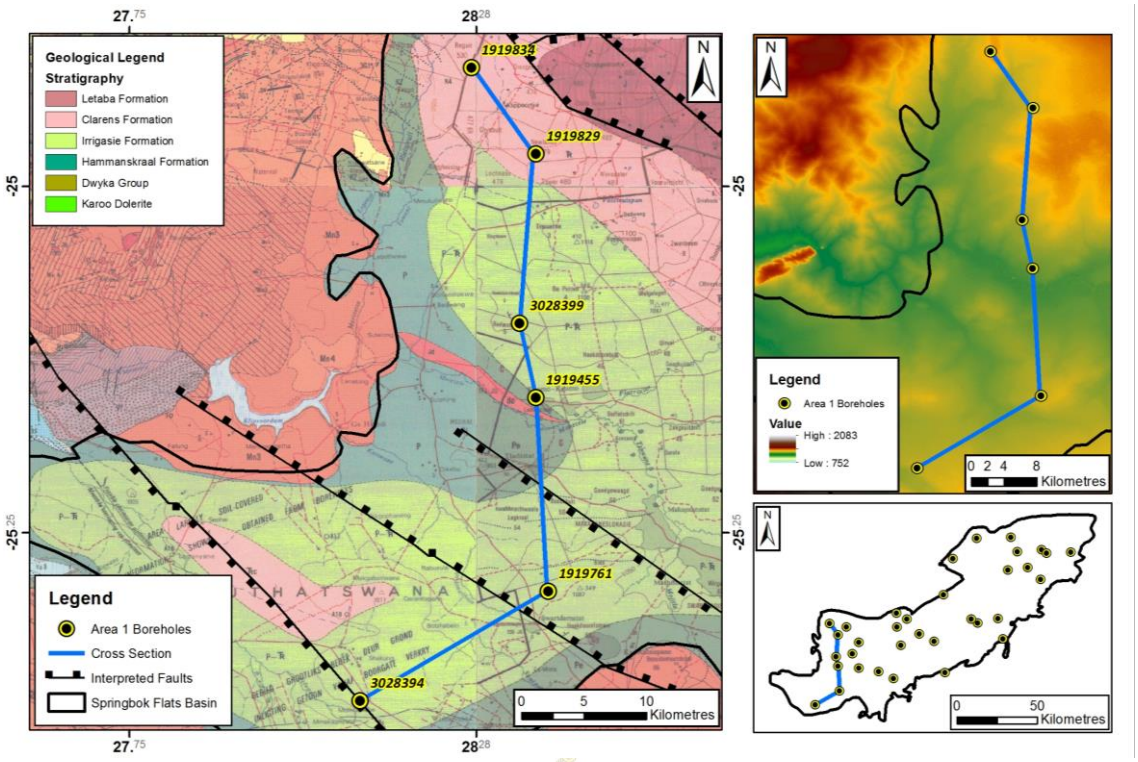

Figure 7-9: The spatial distribution of boreholes and cross-section line in Area 1.

The cross-section for Area 1 (Figure 7-9 and Figure 7-10) was compiled using boreholes in the southern-most section of the basin (Table 7-1). In this area the surface geology ranges from the Letaba Formation in the north east, and down to the Ecca Group along the boundary. The surface topography of the area is generally very gentle, with the highest elevation to the north, near borehole 1919834, and the lowest elevation can be found about 25 km to the west of borehole 1919455.

The section line crosses two major conjugate normal faults which form a graben in the southern region of Area 1. The graben block has faulted the strata down by approximately 100 to 120 metres. The Elliot Formation within the graben structure is considerably thicker than to the north of the faulting, unlike the previous successions of Ecca, Beaufort and Molteno Formations. This suggests that the graben structure formed prior to the deposition of the Elliot Formation, and this succession subsequently filled the graben basin.

Borehole 1919829 indicates that the strata are at a greater depth when correlated to the other selected boreholes. However, these strata do not appear to be structurally influenced, but have that depth as a result of the palaeotopography. This region appears to be the depocentre of the sedimentary sub-basin. The strata in this region appear thicker than in the region of boreholes 3028399 and 191455, this indicates that this depocentre was active during the deposition of the Ecca Group. The Irrigasie Formation is thicker in borehole 3028399 than its correlates in 1919829 where the Ecca Group is relatively thick. This change in thickness indicates that there was a shift in the depocentre of the sub-basin.

The Lower Coal Zone (LCZ) is more prominent in the northern region of Area 1, and is comprised of alternating coal, bright coal and mudstone. In the northern section of Area 1, the coal has a CV around 17 MJ/kg, ash of between 30% and 50% and volatiles in the order of 28 %. In the central region of Area 1, the LCZ seems to all but disappear, with the only occurrence being carbonaceous shale with a few bright stringers. The UCZ makes its appearance in this region, with the coal zone being approximately 6 metres in thickness, consisting of alternating bright coal and carbonaceous shale with a high ash content of around 45-60%. There is a major dyke that occurs deep below the LCZ in the north, in borehole 1919829, and in between the LCZ and UCZ as one moves to a more central location of Area 1 in boreholes 3028399 and 191455, where the coal has been devolatilised, as well as having very low CVs (±15 MJ/kg) and elevated ash content (± 55% ash). Within the graben structure in Area 1, the LCZ becomes more substantial once more, with CVs around 17 MJ/kg, ash of 40-55% and volatiles of 18-24%. In the most southerly region of Area 1, the LCZ disappears, leaving only the UCZ which appears as carbonaceous shale with a few bands of mixed coal having a very high ash content of around 60-80%.

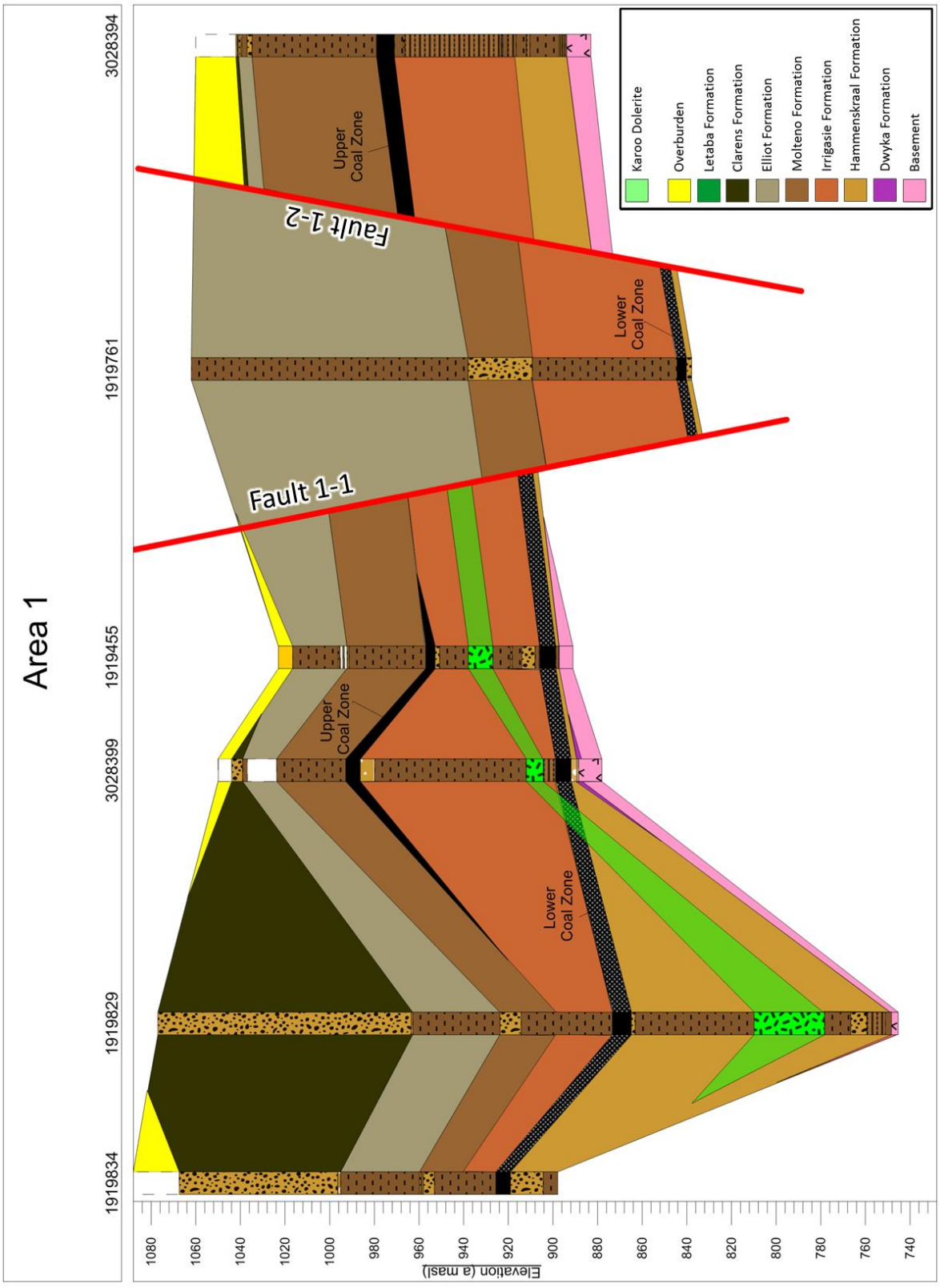

Figure 7-10: Cross-section through Area 1.

7.10 Area 2

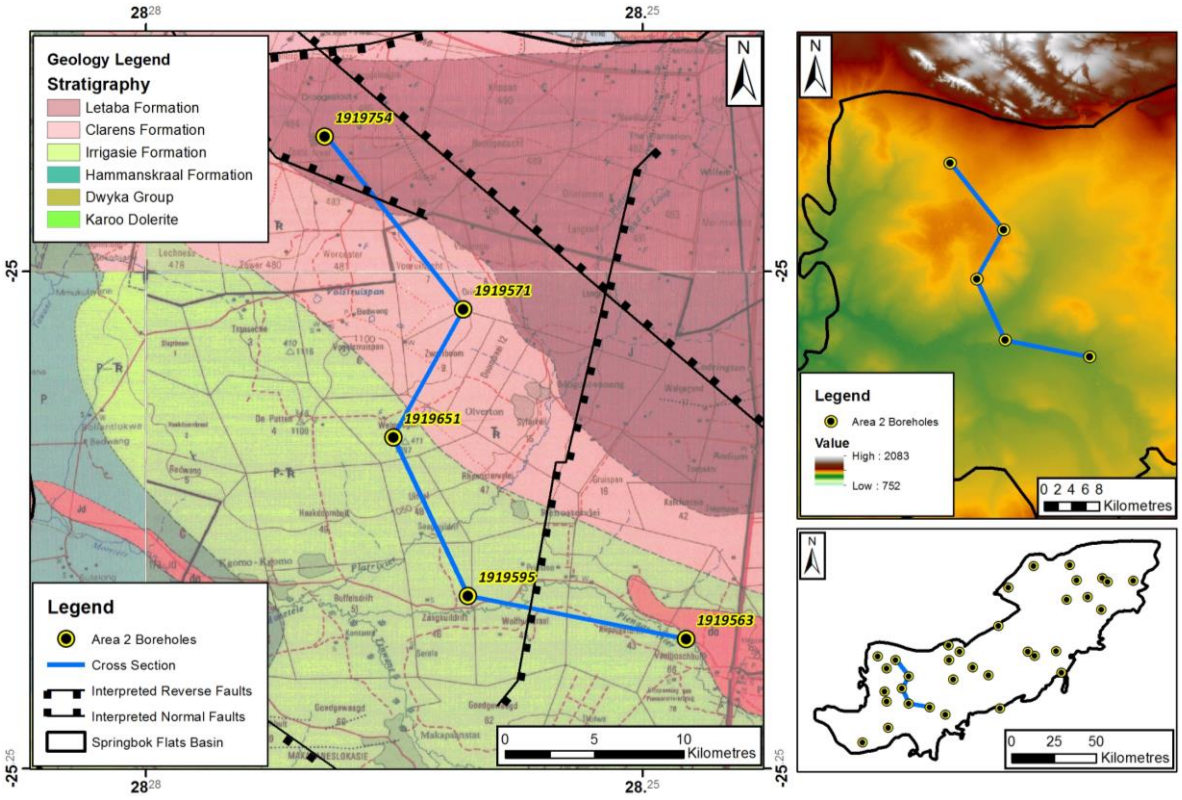

Figure 7-11: The spatial distribution of boreholes and cross-section line in Area 2.

The section line for Area 2 (Figure 7-11 and Figure 7-12), traverses gently undulating topography. The higher elevations are to the north, and the lower elevations in the central regions of the area. The cross section crosses over lithologies from the Letaba, Clarens, and the Irrigasie Formations on surface. It is also intersected by two major normal faults. Fault 2-1 which is intersected in the north strikes in a south-easterly direction, and the fall of ground is around 200 m on the northern side. This fault runs along the contact of the Letaba basalts and the Clarens Formation. Fault 2-2 that is intersected by the cross-section is not evident on surface geology; however it has been delineated from the geophysical interpretations. It has a NNE strike, and has a fall of ground to the east of approximately 100m.The maximum depth recorded for this section exceeds 520 metres below surface (mbs) to the north, and becomes shallower to the south where it reaches a depth of 145 mbs. A dyke is intersected in boreholes 1919595 and 1919651 at depths of approximately 160 mbs. At borehole 1919561 the dyke is located above the LCZ, and moves beneath the LCZ in borehole 1919595.

In the central region of Area 2, at boreholes 1919571 and 1919651, there is a thicker deposition of Elliot and Molteno Formations; this appears to correlate with the shift of the depocentre mentioned in Area 1, moving from the northern regions in Area 1, to the centre regions of Area 1 and Area 2. These formations thin out towards borehole 1919595 in the southern region, which suggests a palaeohigh in this region.

Fault 2-2 in the southern region of Area 2 was active throughout the deposition of the Molteno and Elliot Formations, as these successions appear to be thicker to the south of the fault, in the hanging wall. It is unclear as to whether this fault was active throughout the deposition of the Karoo deposits, as the boreholes do not reach a sufficient depth, and the younger formations have not been preserved.

The LCZ is the only coal zone to be intersected by the chosen cross-section. The deeper coal can be found in the north at 518.40 mbs and has a thickness of 7.2 m. The LCZ in this region consists of alternating layers of mudstone and bright coal. It has a high ash content of 60%, with some layers having a much lower ash content of 20%. The CV ranges from 10 to 25 MJ/kg and the volatiles are found to be in the order of 18 to 32 %. The coal further south becomes less bright, and more shale-like with pyritic bands. In this region the coal has lower ash content around 40-50%, with the CVs around 15MJ/Kg. The coal thickness increases to 8-10 metres in thickness.

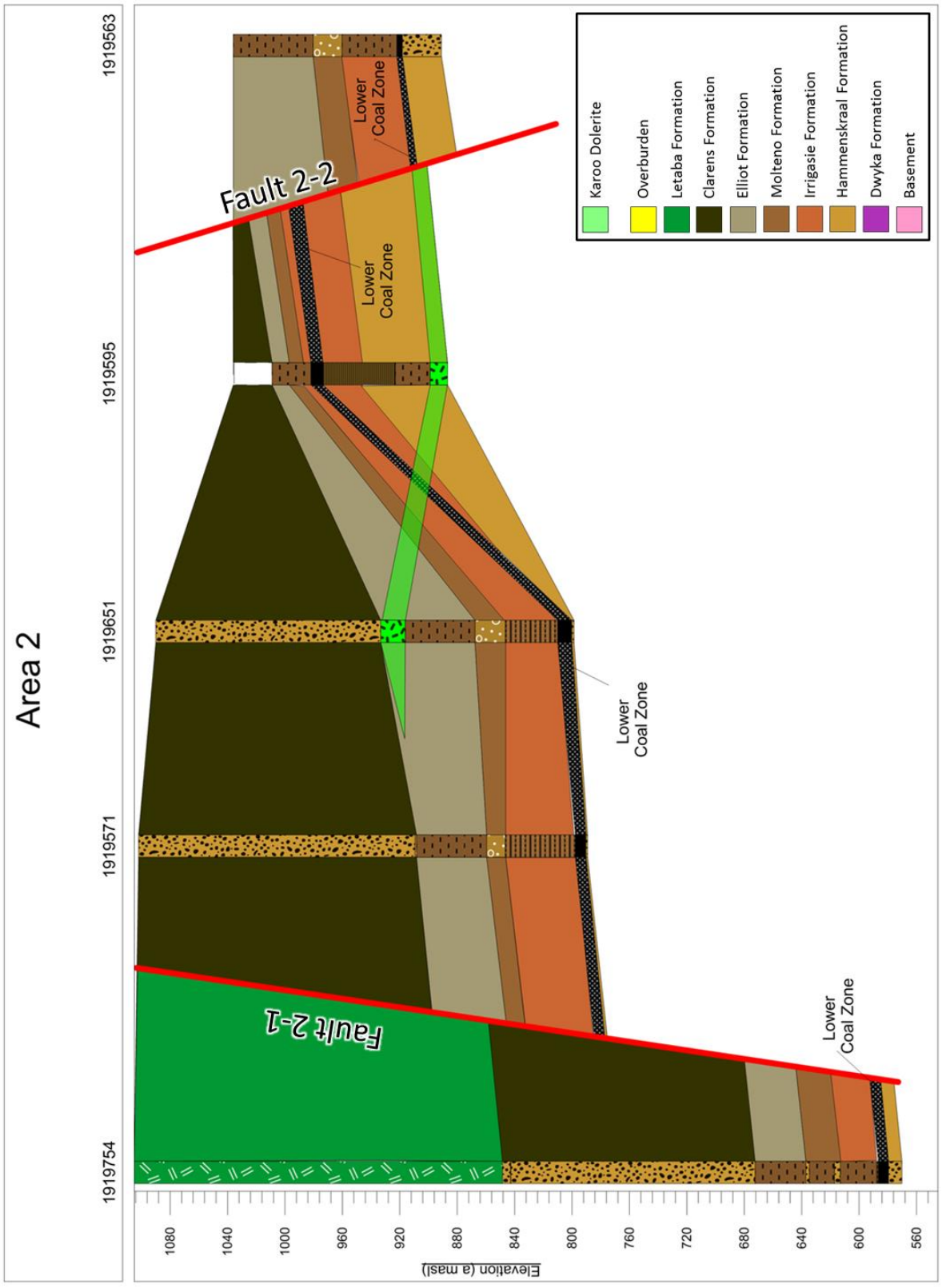

Figure 7-12: Cross-section through Area 2.

7.11 Area 3

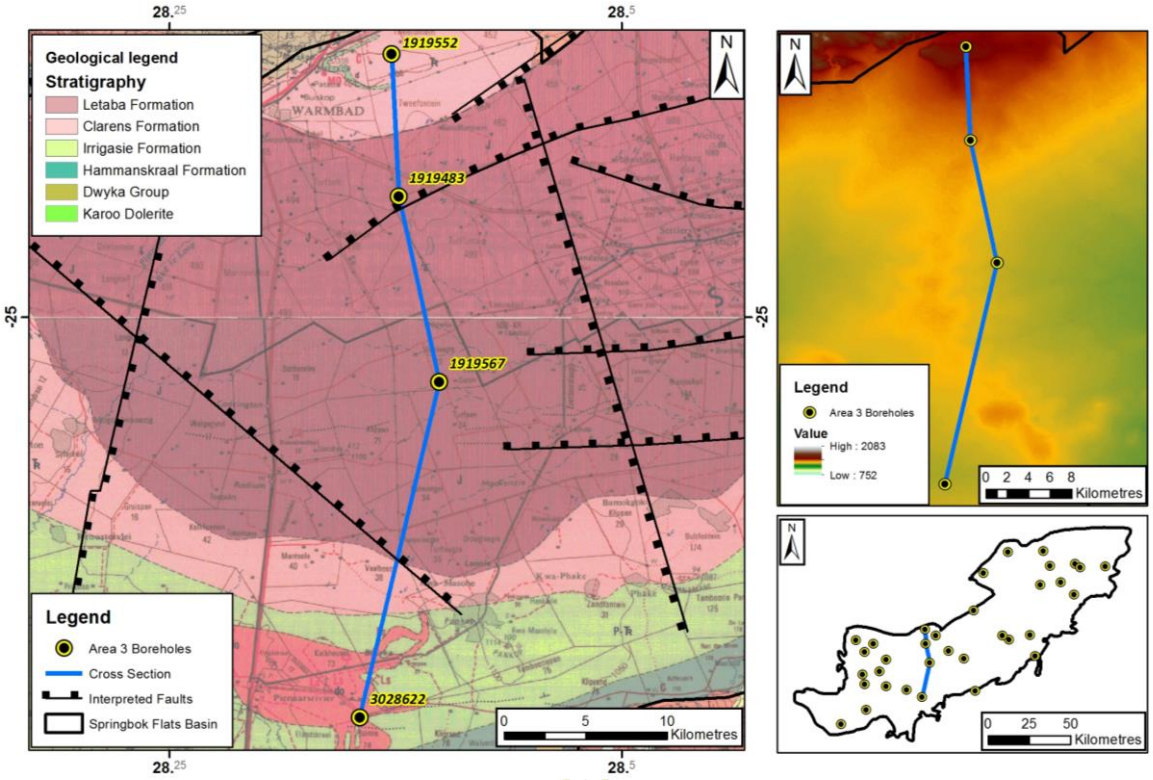

Figure 7-13: The spatial distribution of boreholes and cross-section line in Area 3

The cross-section for Area 3 (Figure 7-13 and Figure 7-14) begins in the north with borehole 1919522 at an elevation of 1203 mamsl and follows a gentle down-gradient to the south to the last borehole 3028622 at 1060 mamsl. The cross-section runs along a local topographic high and watershed in the area. The surface geology intercepted ranges from the Letaba to the Irrigasie Formation (Beaufort Group).

This cross-section traverses over three major faults. The first two faults (Fault 3-1 and Fault 3-2) intersected from the north are a conjugate graben pair that has a down-throw of approximately 850 m and a south-westerly strike. Fault 3-1 runs along the contact of the Letaba basalts and the Clarens Formation, whereas Fault 3-2 was identified using geophysical data. These faults appear to be of a similar strike to those identified in Section 7.1 that runs along the northern boundary of the SBF basin. Fault 3-3 is a south-easterly striking normal fault with a down-throw of roughly 400 m to the north.

In the area of borehole 1919552, north of the Fault 3-1, the strata are relatively shallow, with the UCZ being intersected at 192 mbs and the LCZ being at a depth of approximately 270 mbs. A dyke is intersected at a depth of 64 mbs and has a thickness of around 22 m. The UCZ in this area displays alternating layers of shale and bright coal, and has a thickness of around 5 m. The Ash content varies from less than 25% in the middle of the zone, to over 75% near the top and bottom contacts. The CV is in the order of 25 MJ/kg, H_2O of between 2.5 and 5% and the volatiles around 30%.

The strata within the graben pair faults and to the south of these faults do not appear to have had a significant change in stratigraphic thickness for the Clarens, Elliot and Molteno formations. This lack of change signifies that this graben structure occurred after deposition of these formations and there is limited influence of palaeotopography evident in the cross-sections. The effect of the fault on the Irrigasie Formation could not be determined due to the lack of boreholes that extend deeper than this horizon.

Only the LCZ was intersected by the chosen borehole (1919483) and is approximately 996 mbs. The LCZ in this region exhibits the typical alternating shale and coal layers, although the coal is mostly dull, with a few layers of bright coal towards the top of the seam. The thickness of this zone is around 9 m. The bright coal layers, and shales about 2 metres below them, have a CV of just under 25 MJ/kg, Ash content of 27 %, H_2O of 2 and a Volatile content averaging around 30%.

The central region of the cross-section has the lower coal zone (LCZ) sitting at about 653 metres below the surface, having been down-faulted by the Fault 3-3 in the south. Borehole 191567 intersects an igneous intrusion at a depth of 548 mbs, which is about 1 m below the UCZ. The igneous intrusion occurred after deposition of the coal zone as it has slightly devolatilised and burnt the coal in that region. The intrusion magma does not appear to have been too hot, as the coal still has a Volatile content of around 15%, although the Ash content averages around 50%.

The Molteno Formation shows no significant variation in thickness which suggests that there was no lateral variation in this area during its deposition. To the south, the Clarens Formation has been completely eroded, whereas the Elliot Formation has been partially eroded in this area. Fault 3-3 has resulted in the down throw of the strata to the north, and has left the strata to the south relatively intact. The depth of the UCZ to the south of Fault 3-3 is approximately 60 mbs, and the LCZ was not intersected by boreholes in this area. The UCZ in this region has an exceptionally high Ash content averaging around 75% and volatiles of around 10%, which suggests that it has been burnt.

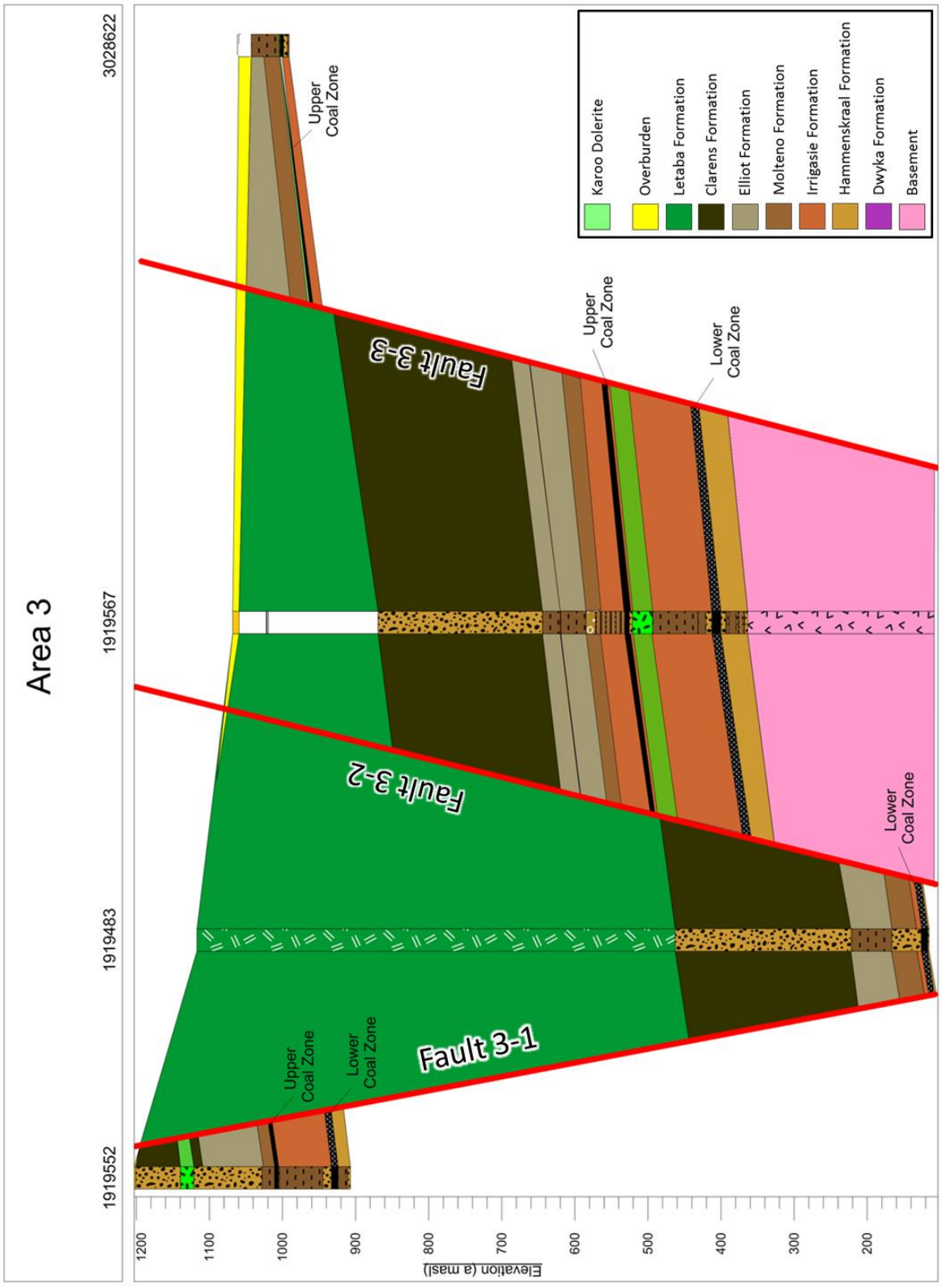

Figure 7-14: Cross-section through Area 3.

7.12 Area 4

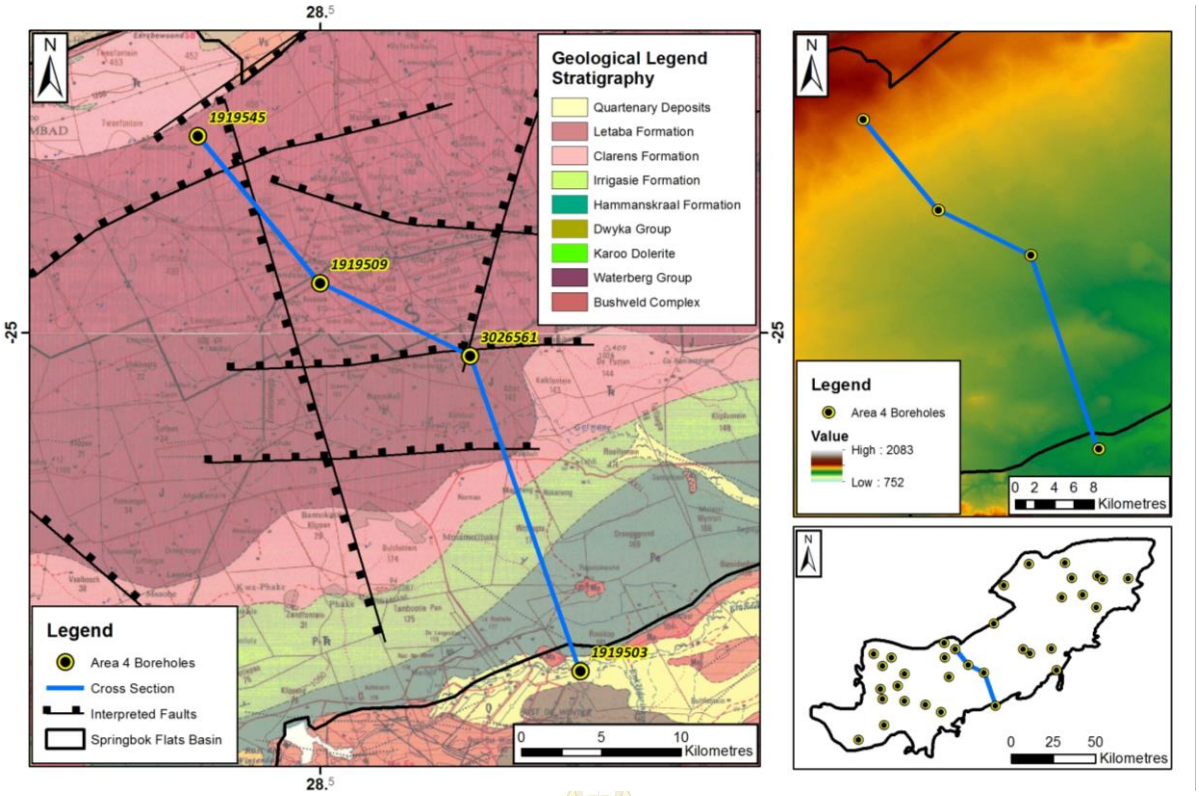

Figure 7-15: The spatial distribution of boreholes and cross-section line in Area 4.

The elevation for the northern-most borehole (1919545) selected for the Area 4 cross-section is 1135 mamsl (Figure 7-15 and Figure 7-16). The topography follows a gentle slope to the south along the cross-section line and has a minimum elevation of 975 mamsl at borehole 1919503. The surface lithologies that are traversed from north to south are the Letaba, Clarens, Irrigasie Formations, and lastly the Ecca Group along the southern margin of the SBF Basin. The southern-most borehole 1919503 appears to be outside the basin and drilled into the Bushveld Complex. However, on closer examination of the lithologies recorded, it was concluded that this borehole records the lithologies of the SBF Basin. The location uncertainty of this borehole has been recorded as 0 m, and therefore suggests that the southern boundary of the SBF Basin may need to be adjusted on the map shown above.

Borehole 1919545 has a drill depth of 1072 mbs, and is located between a normal fault that characterises the contact between the Clarens Formation and the Letaba Basalts to the north, and Fault 4-1 to the south (Figure 7-16). This northern fault, not indicated on the cross- section, appears to have faulted the strata down by approximately 700-800m. Further south the cross-section intersects 3 other normal faults which have caused fall of ground to the north of each fault. These faults appear to have similar strike directions to that of the major fault along the northern boundary of the SBF Basin identified in Section 7.1.

The Clarens Formation strata do not show significant variation in thickness throughout the cross-section, indicating a lack of lateral variation during deposition. The Elliot and Molteno Formations, however show an increase in thickness towards the northern

and central regions respectively of Area 4. The Elliot Formation then thins out towards the southern boundary of the SBF Basin. The Molteno Formation's strata thickness is thin in the southern and northern regions (around 10 m thickness), but thicker in the central region in borehole 3026561 (about 20 m thickness). Another point to be noted is that the underlying Irrigasie Formation has a thickness of around 10 m in the northern region and thickens towards the south-central region to almost 100 m. This variation in the location of the thickest section of each formation could suggest a shifting of the basin's depocentre over time, as has been suggested for the previous areas discussed.

The Elliot Formation in boreholes 1919545 and 3026561 is present in a strata thickness of approximately 100 m, unlike its correlative thickness in borehole 1919509 which is about 40 m. This suggests that the faulting occurred syn-deposition towards the end of the Elliot Formation, with the central fault occurring last. These faults were then re-activated during the breakup of Gondwana.

The LCZ has been intersected by all the selected boreholes and the UCZ only by borehole 3026561. In the northern regions of Area 4, the LCZ has a high Ash content around 60% and a low CV of less than 15%. It is characterised by alternating bands of carbonaceous siltstone and dull to dull lustrous coal. The coal zone is found to be at a thickness of around 4 metres. The LCZ in the central region of Area 4 is characterised by carbonaceous shale with bright coal laminae, with a diminished thickness of about 1.5 m. The UCZ is present in the central regions and is in the form of alternating bands of carbonaceous to weakly carbonaceous shale and bright coal that is pyritic in places. The Ash content is in the order of 30-60% with a volatile percentage of 20-25%. The thickness of the UCZ is around 7m. Only the LCZ is intersected in the southern region and is typically an alternating coal and carbonaceous shale package. The coal is bright and exhibits calcite veins and pyrite lenses locally. The quality of the coal in this zone has marginally increased with an Ash content of between 40-55%, Volatiles of 25-30% and a CV between 20-25%.

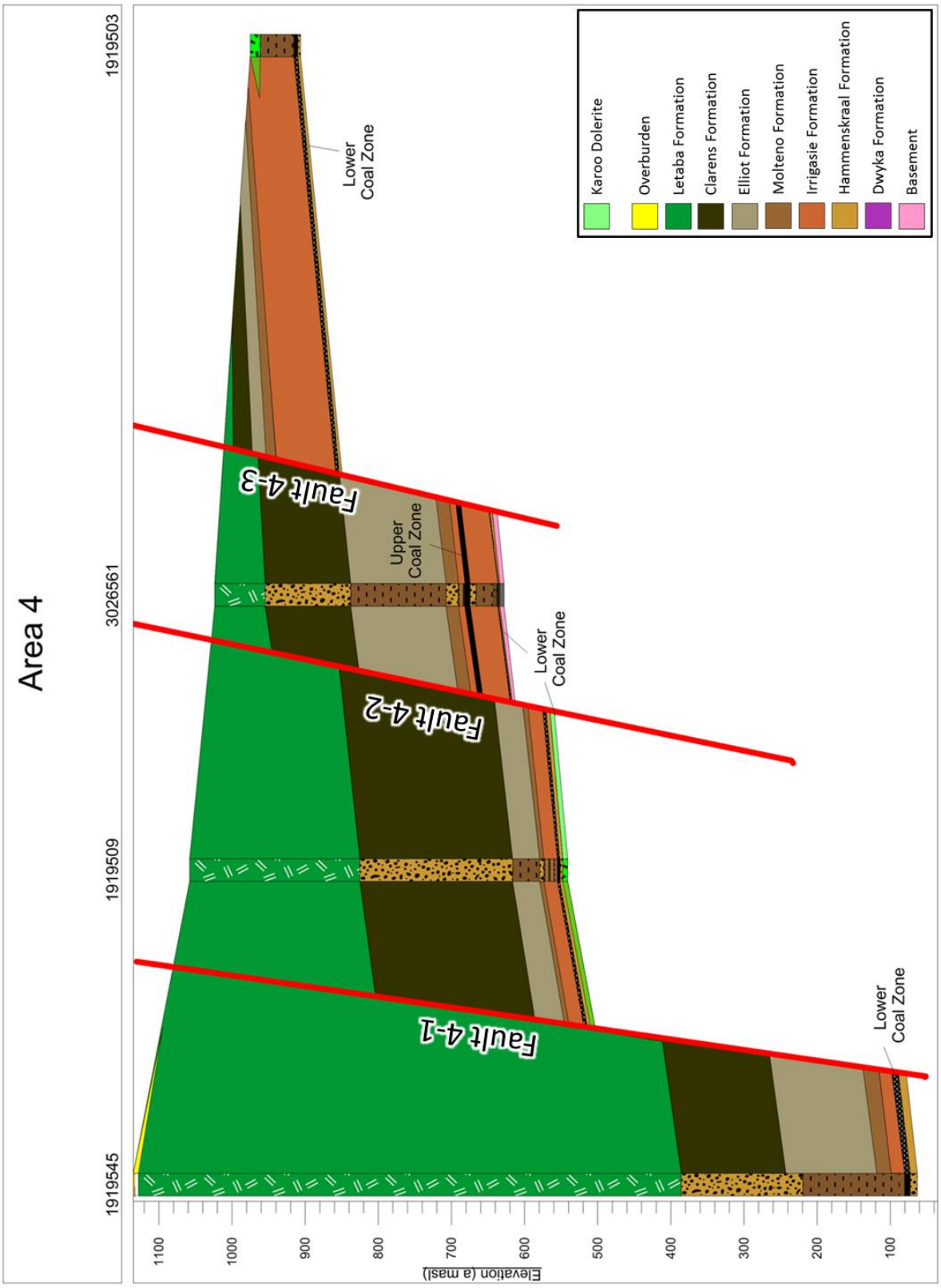

Figure 7-16: Cross-section through Area 4.

7.13 Area 5

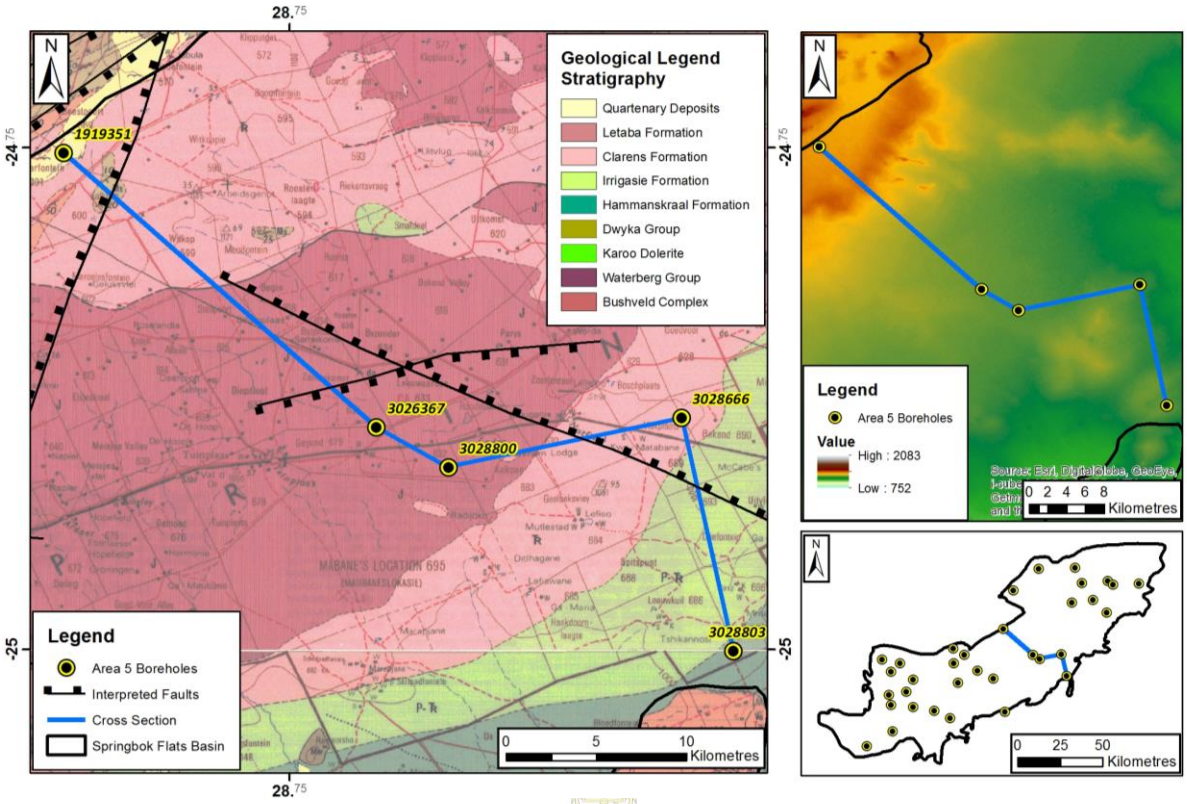

Figure 7-17: The spatial distribution of boreholes and cross-section line in Area 5.

The topography of Area 5 is characterised by an elevated northern region with gentle undulating hills towards the south. Borehole 1919351 in the north has an elevation of 1106 mamsl with the southern-most borehole 3028803 having a slightly lower elevation of 1020 mamsl (Figure 7-17 and Figure 7-18). The cross-section begins in the north with surface geology of the Clarens Formation, and then in the central region the surface lithology is dominated by the Letaba Formation. To the east of borehole 3028800 the Clarens Formation is once again outcropping, and moving further south the Irrigasie Formation is intersected followed by the Hammanskraal Formation.

Three faults are intersected by the cross-section which affects the strata in the central region of Area 5. Faults 5-1 and 5-2 appear to be a conjugate pair, which resulted in the strata being downthrown to the south of it by approximately 800 metres. Fault 5-2 cutting off borehole 3028666 is intersected twice, and appears to be an oblique normal fault, with the greater fall of ground being to the north of this borehole.

The Beaufort Group in this section is characterised by a limited thickness in the north, thickening in the central region and once again thinning to the south. The Molteno Formation shows a similar trend, although in borehole 3028800 it is extremely thin at about 2 metres and thickens towards the south to approximately 20 metres in borehole 3028803. The Clarens Formation appears to have a uniform thickness laterally of about 100 metres.

The LCZ is intersected in the northern-most boreholes, e.g., 1919351, and is not found in the other boreholes. It occurs here as alternating bands of carbonaceous siltstone

and shale, with dull and bright coal. The coal layers in this zone are poorly developed and occur as dull lustrous coal or bright coal interbanded with shale. There are pyritic lenses and nodules towards the base with a calcite vein in the centre of the zone. The entire zone has a high Ash content ranging from 50 to 80%, with highly variable Water and Volatile values. The CVs are between 0 and 25 MJ/kg.

The coal intersected by the remaining boreholes belongs to the UCZ and this is better developed than the LCZ to the north. The thickness of the coal zone in Area 5 is approximately 7 metres and there is very little lateral variation in this thickness from north to south. It is developed as alternating carbonaceous shale and bright calcitic coal which is slightly pyritic towards the roof of this seam. The centre of the coal zone exhibits the best qualities, with an Ash content around 25%, Volatile content around 30%, Water around 2% and a CV averaging around 20-25%.

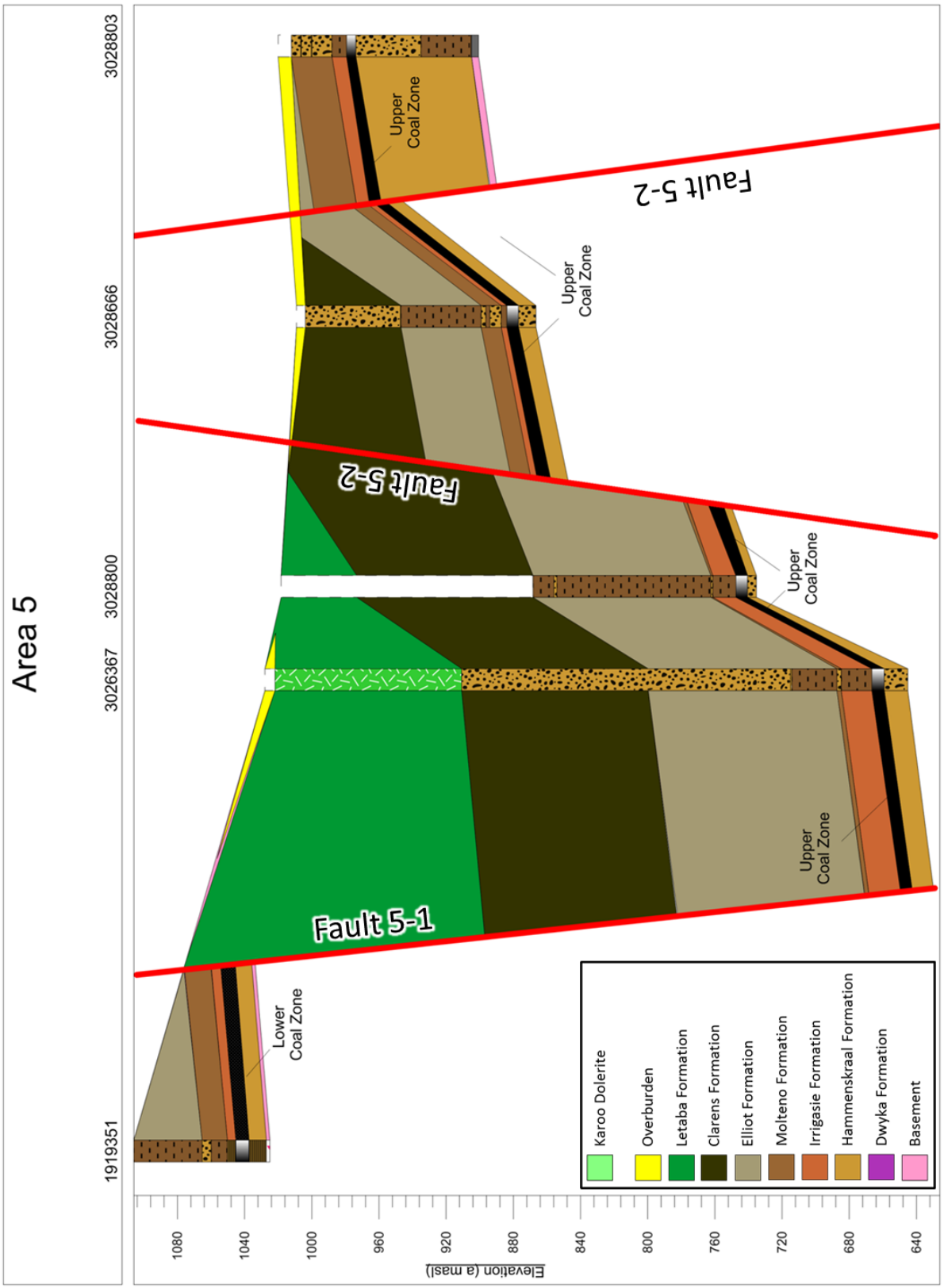

Figure 7-18: Cross-section through Area 5.

7.14 Area 6

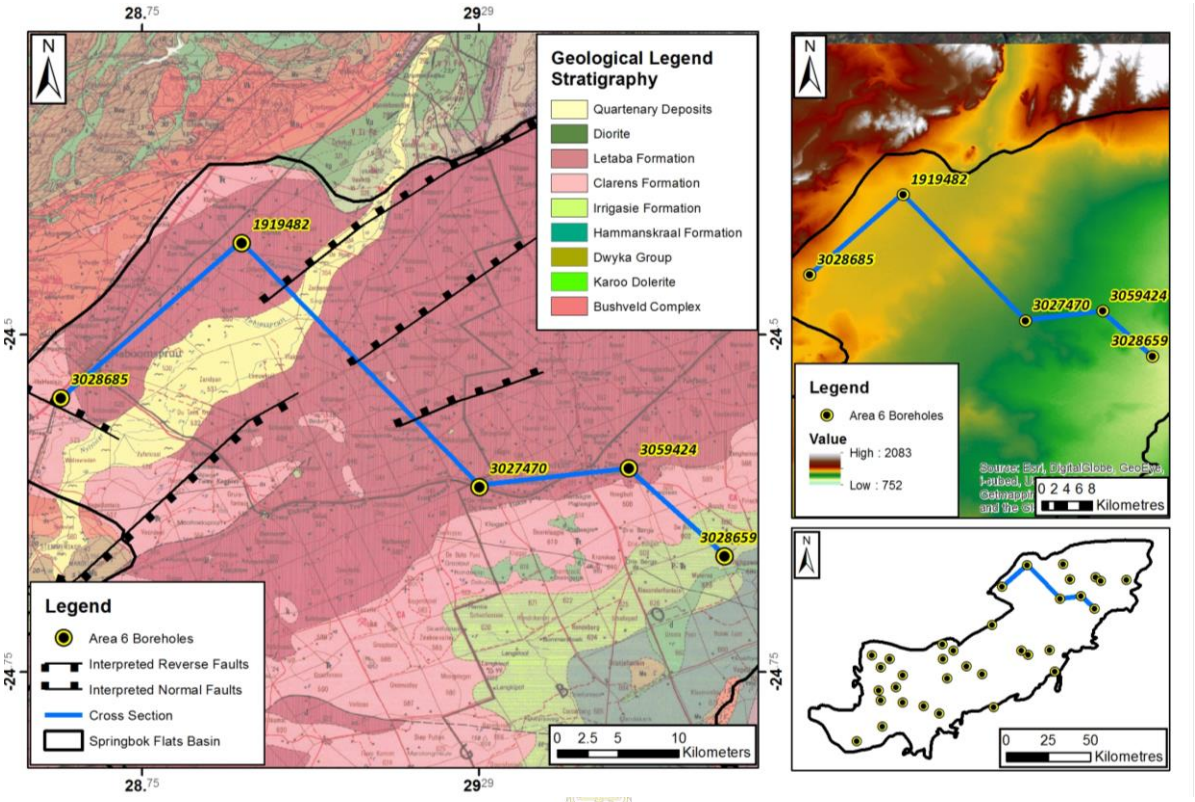

Figure 7-19: The spatial distribution of boreholes and cross-section line in Area 6.

Figure 7-19 shows the location of the cross-section compiled for Area 6 which can be found in Figure 7-20. The density of boreholes found in the area is very sparse, which made it difficult to get a good understanding of the geology. The results discussed below are made with what information was available.

The higher ground is found to the north of Area 6, and has a gentle slope down to the south east near borehole 3028659. The surface lithologies traversed by the cross-section start with the Clarens Formation near borehole 3028685, and as one moves in a north easterly direction the lithology changes abruptly to the Letaba Formation. The Letaba Formation is the surface geology for much of this section until past borehole 3059424. To the south of borehole 3059424 and until borehole 3028659, the surface lithologies change from Letaba to Clarens Formation and then finally into the Irrigasie Formation.

The cross-section through Area 6 intersects 4 normal faults, where Fault 6-1 is striking approximately NW-SE, and the remaining three (Faults 6-2 to 6-4) strike in a north-easterly direction, with the fall of ground to the north west of the faults. These three faults have different degrees of fault displacement, the northern-most fault (Fault 6-2) having the most at approximately 440 m fall of ground. Fault 6-3 has less at around 200 m fall of ground and Fault 6-4 has the least at about 150 m fall of ground.

The boreholes in this region do not extend to the basement or the Dwyka Group of the SBF succession, and therefore it is not possible to determine the succession thickness of the Ecca Group or the evolution of these sediments. The Beaufort Group has been identified

as having an average thickness of 10 metres in the northern region of Area 6, thinning out to about 5 metres in the central regions, and thickening to about 25 metres along the southern boundary of the SBF.

The Elliot and Molteno Formations indicate very little lateral variation in thickness from north to south, other than in the central regions where the Beaufort Group similarly thins. This could suggest that there was a palaeohigh in this region around borehole 3027470. The Elliot and Molteno Formations become thicker in the region of borehole 3059424, where the Beaufort Group is markedly thinner. The Clarens Formation shows a marked increase in thickness from the north to the south of Area 6. This indicates that the depocentre location during the deposition of the Clarens Formation was further to the south.

The Lower and Upper coal zones are intersected by the selected cross-section, with the LCZ only found in the northern region, and the UCZ in the southern region. The LCZ in borehole 1919482 is poorly developed with 2 metre thick layers of mudstone in between the dull pyritic coal. Calcite veins are present with coaly shale layers. The Ash content exceeds 60%, and the CV is low at around 10 MJ/Kg. The UCZ is intersected by the last three boreholes in the south of the cross-section, and is relatively thin at around 4 metres. In borehole 3027470 the coal is present in alternating carbonaceous shale and highly pyritic bright coal strata. Near the roof of the coal zone there is a very high Ash content (above 80%), though just below this in the bright coal, the ash content is around 25%, and with a CV of 27%. Volatiles are high in this 1 metre thick bright coal at about 33%. The UCZ intersected by borehole 3059424 and 3028659 is poorly developed and highly pyritic with thin bands of bright coal within carbonaceous shale. The analyses taken at the bright coal bands indicate an Ash content of around 20-25%, high Volatiles around 30% and CVs of 25 MJ/kg.

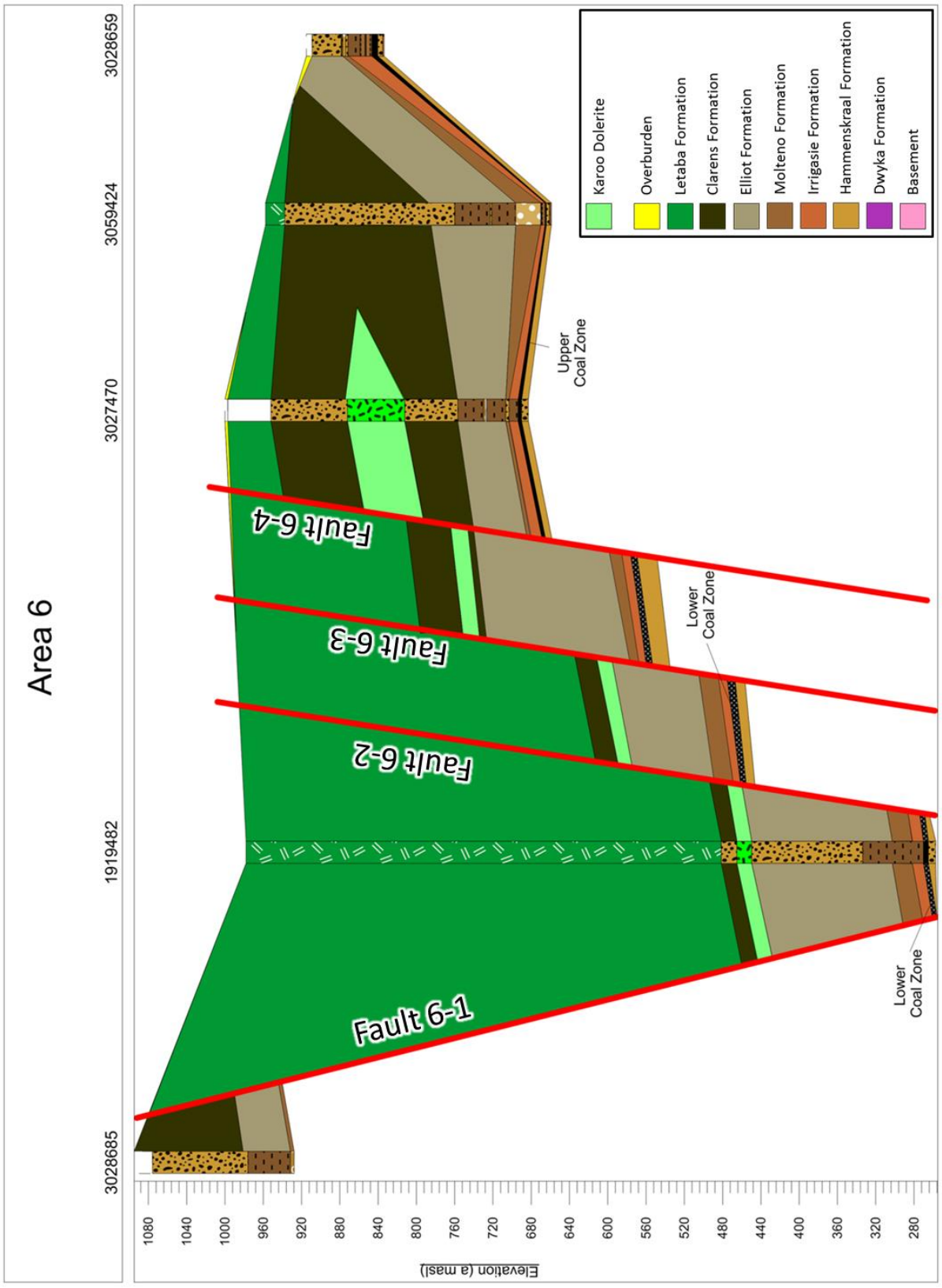

Figure 7-20: Cross-section through Area 6.

7.15 Area 7

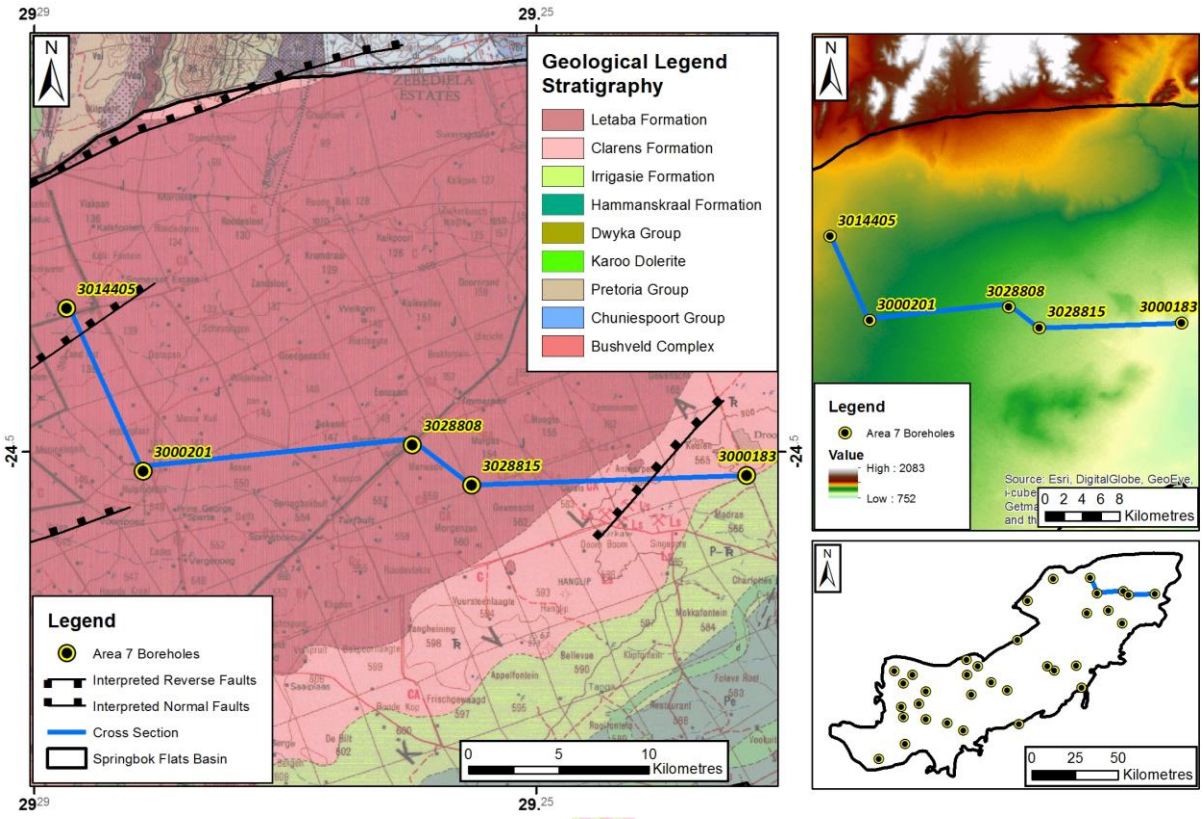

Figure 7-21: The spatial distribution of boreholes and cross-section line in Area 7.

Figure 7-21 shows the location of the cross-section compiled for Area 7 which can be found in Figure 7-22. Similar to Area 6, there is a very low borehole density for this area. Many assumptions needed to be made based on limited information, and are discussed below.

The SRTM data for this area indicates that the elevation in the northern region is higher than in the south, where there is a gentle slope from borehole 3014405 which has a starting elevation of 1060 mamsl, to borehole 3000183 which has an elevation of 933 mamsl. The Letaba Formation dominates this cross-section, with the Clarens and Irrigasie Formations only having a surface presence in the southern part of this area.

Three normal faults are intercepted by the chosen cross-section, all three showing similar strike directions and similar fall of ground of about 100-150m, although deeper in the northern part of the area, and shallower to the south. The strata dip in a northerly direction with the shallow strata being in the south.

The strata thickness in the area of borehole 3028815 appears to be thinner than further north and south, and is evident in the Beaufort Group, and the Molteno and Elliot Formations. Similar to Area 6, this indicates that this area was possibly elevated during deposition as a palaeohigh. The Clarens Formation however becomes thicker to the south, as evident in borehole 3028815, although it is not present in borehole 3000183 as it has since been eroded.

The LCZ is intersected by borehole 3014405 in the northern region and by borehole 3000183 to the south. The LCZ in the northern region is characterised by alternating bands of carbonaceous shale and bright coal with many carbonaceous shale laminae. The Ash content is high at over 50%, and the Volatiles average around 20% for the top 1.5 metres of the 4 metre thick coal zone. The LCZ intersected in the south is poorly developed and occurs as a 3 metre carbonaceous shale layer with bright coal stringers. No analyses were undertaken of this coal zone.

The coal seams intersected by the other boreholes all belong to the UCZ and are found in the central region of Area 7. This seam becomes progressively thicker from north to south until borehole 3028815. However, this seam becomes practically non-existent in borehole 3000183 and is only present in the form of coaly shale. In borehole 3000201, the coal seam is approximately 4 metres in thickness with Ash content of around 25%, Water around 1.5% and Volatiles around 30%. It is characterised by alternating carbonaceous shale and bright coal which is calcitic and pyritic in places. However, the carbonaceous shale is of higher proportion than the coal. Further south in borehole 3028815, the bright coal ratio to carbonaceous shale increases, and the coal is extremely pyritic in the centre of the seam. The Ash and Volatile contents vary throughout the seam, with the best qualities averaging around 25% Ash and 35% Volatiles, with the worst averaging around 80% Ash and 7% Volatiles. The Water content in this region averages around 2% throughout the seam.

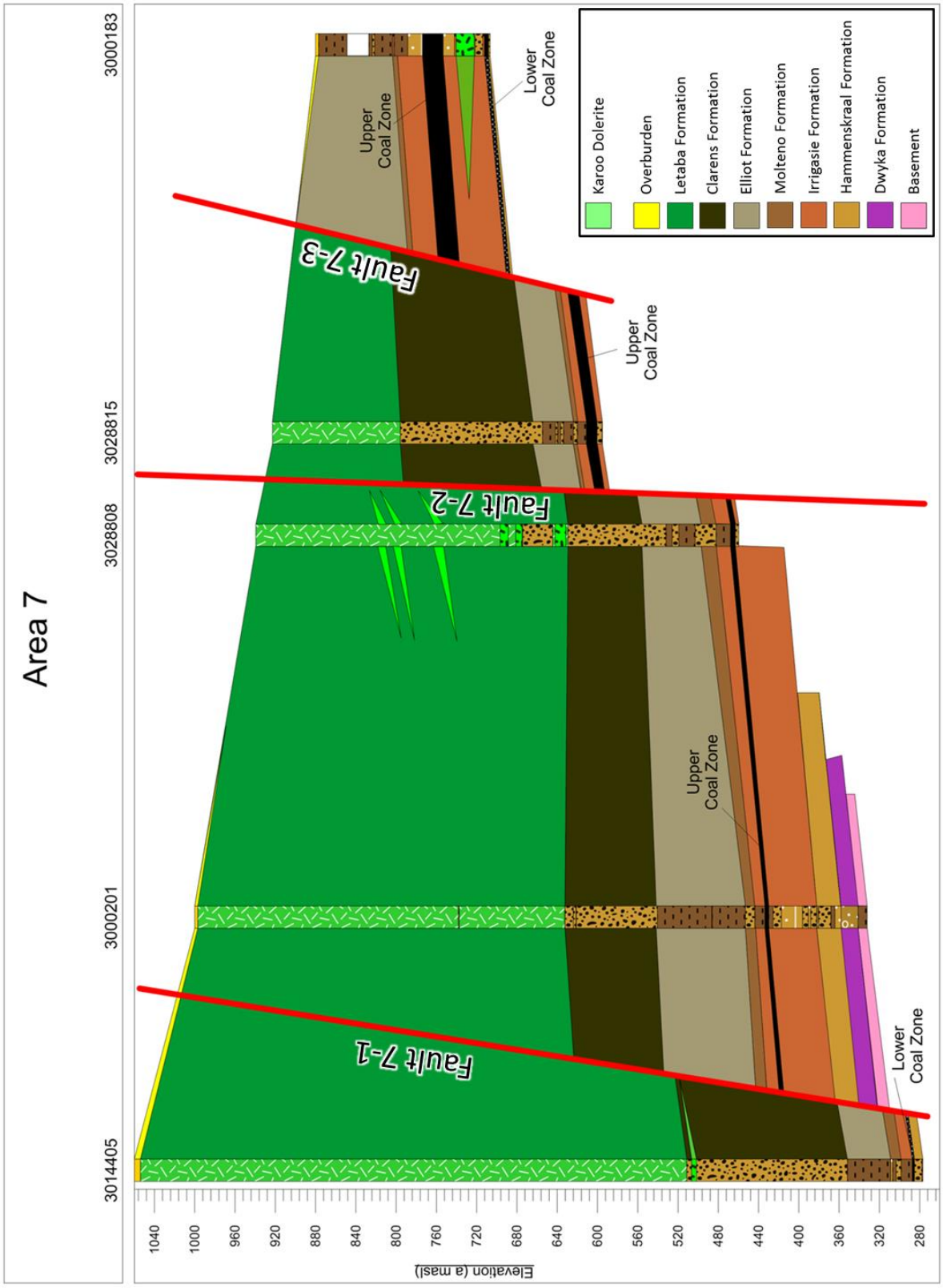

Figure 7-22: Cross-section through Area 7.

7.16 Total Area

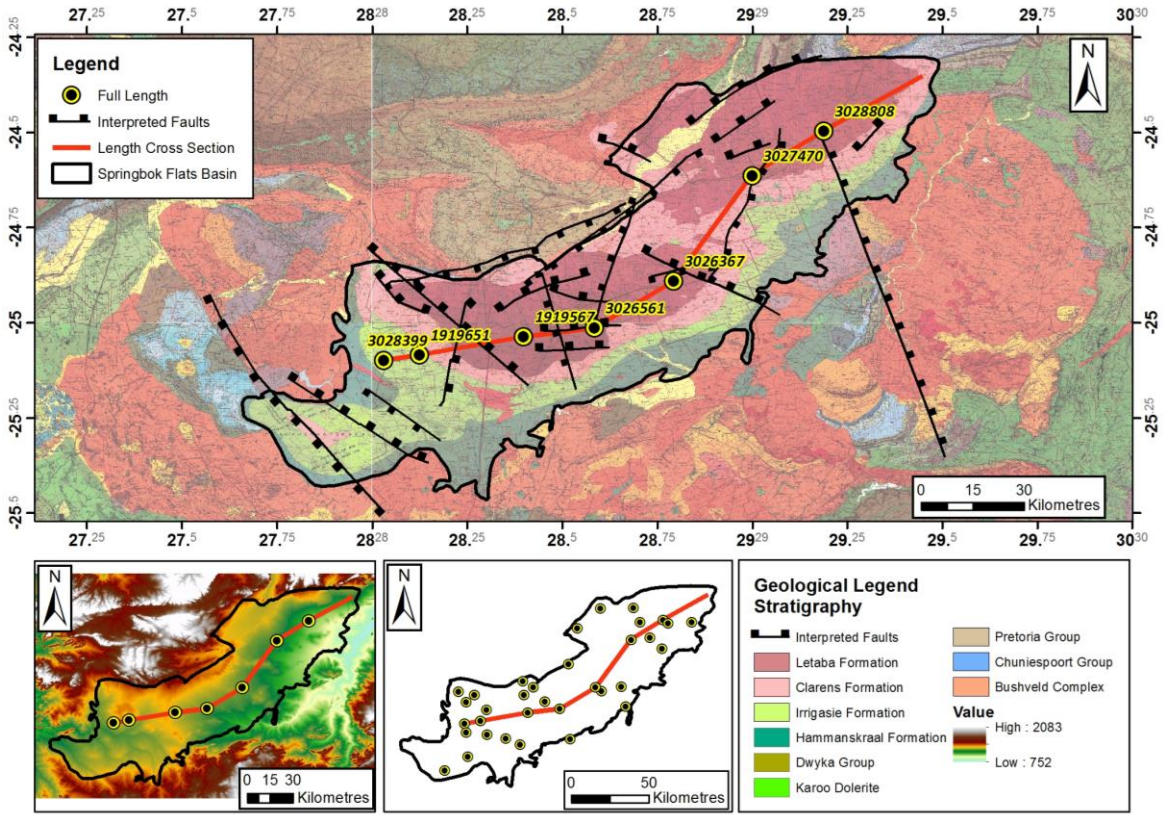

Figure 7-23: The spatial distribution of boreholes and cross-section line for the length of the basin.

This cross-section links all the areas together with a line through the length of the preserved SBF basin, and can be found in Figure 7-23 and Figure 7-24. The topography follows a similar elevation through the basin, although it is slightly elevated in the west when compared to the north-eastern section of the basin. The surface geology that this cross-section traverses covers the Karoo Supergroup in the SBF. Moving from west to east, the Irrigasie Formation is the first lithology identified on surface, going up in succession to the Letaba Formation. In the centre of the basin, there is a break in the Letaba Formation, exposing the Clarens Formation on surface. Moving further in an easterly direction, the Letaba Formation once again is exposed.

Many normal faults are intersected by the cross-section and have broken the strata in many places. The basement is intersected by four of the boreholes utilised, and shows varying depths. The basement in the southern-most area (Area 1) is rather shallow when compared to Area 3, and then becomes shallower towards the centre of the basin. To the north of borehole 3026561, the basement once again drops in depth, although not intersected by the boreholes; this is evident in the drop of strata. This cross-section clearly indicates the two sub-basins in the south west and the north east, with the boundary in the centre of the basin in Area 5.

The Beaufort Group in this section appears to have a large thickness in the western regions of the basin, and thins out towards the north east. A similar phenomenon occurs with the Molteno Formation which also indicates a marked reduction in thickness to the east. The Elliot Formation shows a different trend to its predecessors as it is thinner in the west, thickens in the centre of the basin, and then once again thins out in the eastern region of the basin. The Clarens Formation is the strata with the greatest cumulative thickness; unfortunately at the edges of the basin it has been exposed and eroded away, rendering the task of identifying its geometry difficult. However, a trend is noted that the thickness of the Clarens Formation increases in the south western sub-basin and more so in the north-eastern sub-basin. These trends are noted and will be discussed further in Section 7.17.

Another major item to be noted is the occurrence of the coal zones throughout the basin. In the south-western region of the basin, the LCZ is dominant and thins out towards the east. In the north eastern region the UCZ becomes important with a less variable thickness when compared to the LCZ.

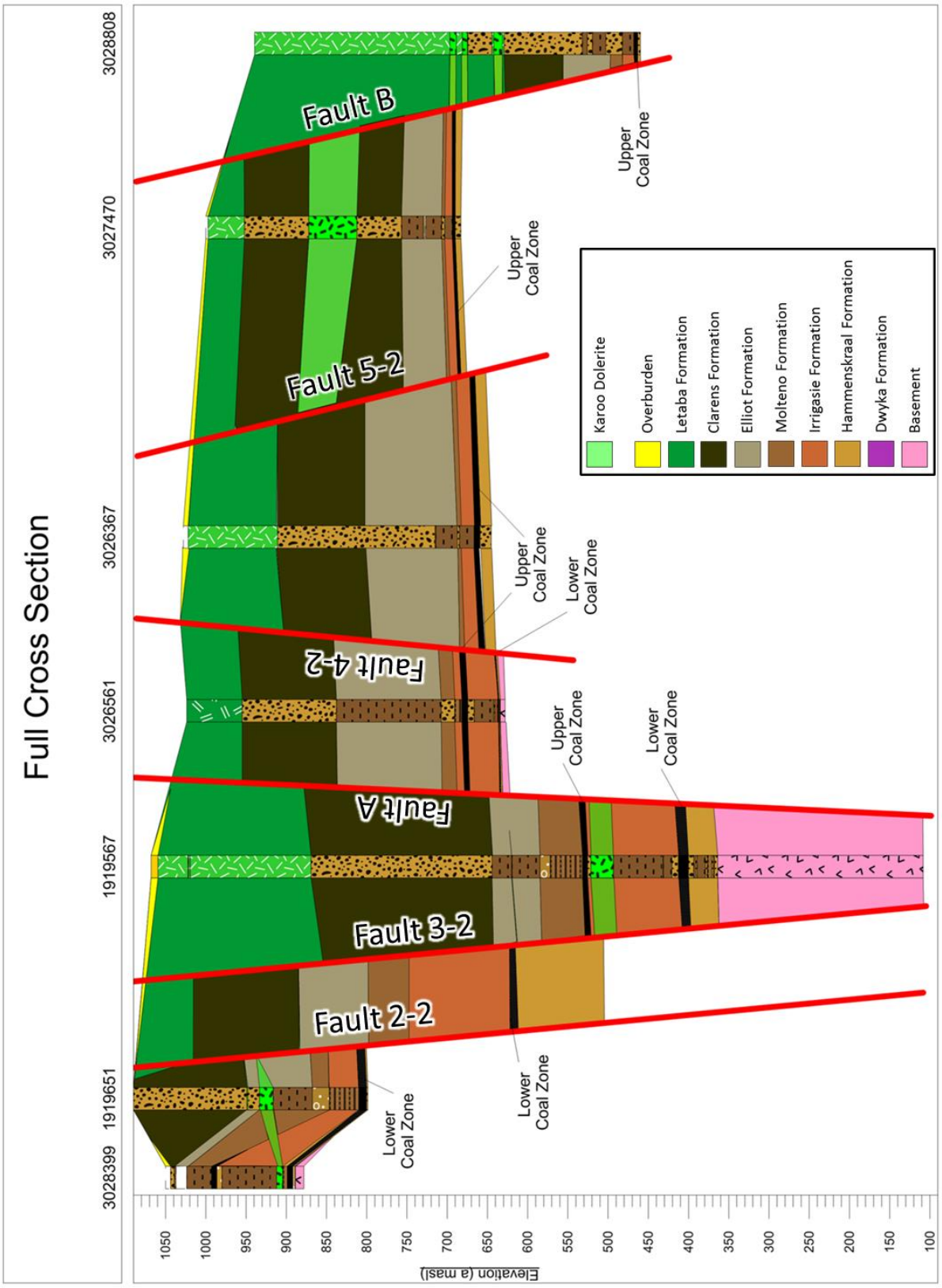

Figure 7-24: Cross-section through the length of the basin.

7.17 Stratigraphy

A summary was compiled based on the information provided in the database, and heavily relies on the accuracy and competency of the data capturers, and the individuals who logged the core. This summary can be found in Figure 7-25. There were slight differences in the lithologies of specific successions with the correlated strata in the Main Karoo Basin, and these will be discussed further in Section 8.

Thicknesses of the various successions were difficult to determine considering the geometry of the basin. The strata thin towards the edges and thicken towards the depocentre (Section 7.2). An average thickness was calculated for each formation/group, and the values calculated did not reflect the true thicknesses. A percentile (or a centile) is a measure used in statistics to indicate the value below which a given percentage of observations in a group of observations fall. The 95th percentile says that 95% of the time, the value is below this amount. Similarly, the remaining 5% of the time, the value is above that amount. The 95% percentile was calculated for the thickness of each strata, and can be seen alongside the average values in Figure 7-25.

It should be noted that further investigations and analyses are required in order to confidently confirm the correlations, with the use of palaeontological investigations and dating techniques.

Simplified Stratigraphy of the Springbok Flats Basin

Depth (mbs)	Log	Formation	Lithology Description	Thickness Statistics (m) Average South	95th %ile South	Average North	95th %ile North
0 – 620		Drakensberg	Grey to green-grey speckled **hornblende basalt** flows with reddish-grey amygdaloidal flow tops, of up to 50m thickness. The flows are generally massive with occasional flow structures. The occasional sedimentary xenolith has been identified along with tuff layers	207	629	150	504
640 – 740		Clarens	Medium grained white **sandstone** occurs at the top of the succession, grading into fine grained **muddy red sandstone**. The basal metre of the Clarens succession exhibits bedding and slump structures. The quartzitic sandstone is cross-bedded towards the base, becoming mottled and fine-grained, well sorted and massive towards the top. Also present within these sandstones are thin mudrock or siltstone intercalations which occur sporadically.	127	234	106	166
760 – 800		Elliot	Alternating **mudstones, siltstones and sandstones** that are purple-grey towards the base, becoming brick red and iron rich at the top. Planar and ripple cross-bedding is present with distinct bedding and slump structures in places, as well as bands of conglomerate, calcite nodules throughout. Bioturbation has also been identified in some of the boreholes towards the base of the succession.	66	133	68	119
820		Molteno	Grey **mudstone** and **fine-grained sandstone** at the base of the succession, grading to **coarse grained sandstones and conglomerates** towards the top of the succession. Towards the central and northern regions of the SBF there is a basal grit with upward fining cycles of sandstone grading into purple **shale**.	18	42	15	29
840		UCZ	Interbedded **carbonaceous shale** and **bright coal** layers. Calcitic and pyritic in places. Found in the central and north-central regions of the SBF Basin	6	8	5	8
		Irrigasie	Gradational base, and becomes dominated by **mudstones** and **siltstones**, with channels of **fine-grained sandstones**, The sedimentary rocks exhibit carbonaceous red-purple colouration at the base of this succession, becoming khaki towards the top.	27	70	20	70
860		LCZ	The southern basin exhibits higher coal qualities than in the northern region for the LCZ, exhibiting thicker sequences of **bright and dull coal** interbedded with thin layers of **carbonaceous mudstone**. The LCZ in the northern region of the basin exhibits thicker layers of interbedded **carbonaceous shales and mudstone**, with thinner layers of **bright coal**	6	9	5	8
		Hammanskraal	Basal **mudstones** that are calcareous in places, grading into **medium to coarse grained immature sandstones** with interbedded **coaly shales**. The top of the Ecca succession displays **carbonaceous siltstones** and **mudstones** with thin sandy laminae. Also present in the Ecca succession is evidence of bioturbation and leaf fragments.	17	51	18	70
880 – 900		Dwyka	**Tillite** with basement granite and Waterberg Group red sandstone pebbles. Pebbles are angular and rounded and set in a dark grey argillaceous matrix.	3	5	13	25

Figure 7-25: Summary of SBF Stratigraphy and Lithology, indicating thickness statistics for the northern and southern regions of the basin.

8 Discussion

8.1 Sedimentary Evolution of the SBF Basin

The borehole database that has been utilised for this study indicates that there are only 76 boreholes that intersect the full Ecca Group, the Dwyka Group and the underlying basement lithologies. For these units the interpretations made are based on what little data were available.

8.1.1 Pre-Karoo Rocks

76 boreholes from the borehole database were identified that intersect Karoo basement rocks. Utilising this information together with the 1:250 000 geological series map (Geological Survey) as well as Roberts (1992) interpretation of the basement lithologies, it was possible to construct an estimated basement map of the SBF Basin with inferred basement lithology boundaries (Figure 8-1).These boundaries and extents could not be precisely determined due to the absence (in some areas) or otherwise paucity of boreholes that extend into the basement lithologies.

The Chuniespoort Group (lower Transvaal Supergroup) is present in the northern–most floor region of the basin. A major anticline extends into the basin, below the Karoo and Waterberg sediments. The older Chuniespoort sedimentary rocks are shale and quartzite in thin alternating layers, which are dipping at approximately 40°. Moving in a westerly direction the recrystallized dolomites of the Malmani Subgroup of the Chuniespoort Group occur. This recrystallization is a result of contact metamorphism due to the intrusion of the Bushveld Complex.

The Pretoria Group (upper Transvaal Supergroup) is present just south of the Chuniespoort Group and is characterised by greenish-grey quartzite, well bedded and cross bedded in several horizons. This succession has an average dip of 30°.

Bushveld granite is the dominant basement lithology for the SBF basin. It occurs as the basement rock for the majority of the southern region of the basin. To the north boreholes intersected indicated coarse grained granite, pink to pale red in colour.

The Rooiberg Group lies predominantly in the centre of the basin and comprises white coloured rocks with reddish parts of decomposed, fractured felsite and is porphyritic in places. These rocks are indicated in borehole logs as being decomposed and bleached to a white colour.

The central-to-northern regions of the basin are dominated by the lower Waterberg Group sedimentary rocks. A few boreholes indicated these sedimentary rocks as belonging to the Loskop Formation; however the proximity to the Main Waterberg basin and the distance from the Middelburg Basin suggested that these interpretations could have been mistaken. However, Barker et al. (2006) suggest that the Loskop and correlated formations can be viewed as “proto-Waterberg” deposits, making any distinction essentially academic. The lithology is also characteristic of that of the Waterberg succession, with red shale,

alternating with reddish-grey medium grained quartzites and sandstones. The average dip is approximately 15°, and the quartzites are well bedded. These deposits represent the possible extension of the Nylstroom Sub-basin (Waterberg Group) prior to the Karoo deposition and the subsequent reactivation of the Zebedelia Fault in the Thabazimbi-Murchison Lineament relay system as a normal fault around 0.182 Ga (Good and De Wit, 1997). Palaeo-valleys are evident along the northern boundary of the Waterberg deposit which exposes the underlying granite and felsite lithologies. The Waterberg and Rooiberg Group basement rocks lie beneath the shallowest part of the SBF Basin, on the palaeo-highland between the two sub-basins.

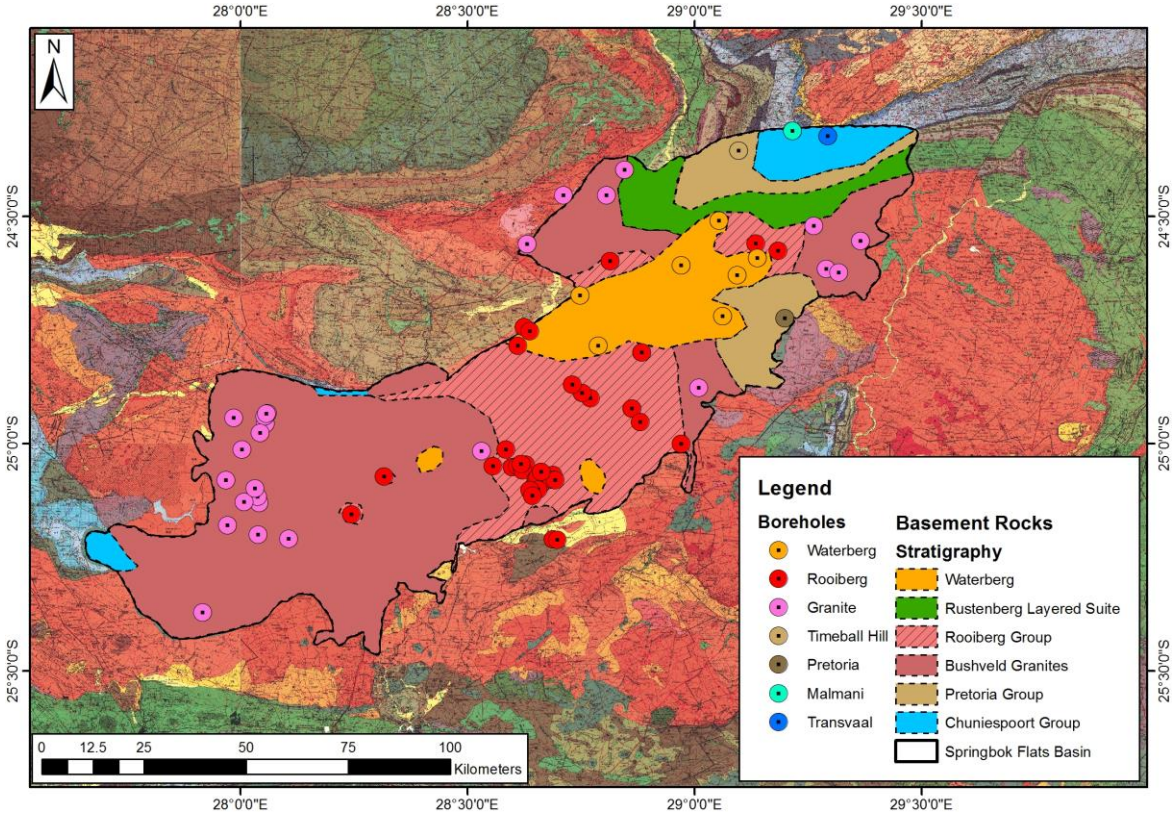

Figure 8-1: Basement lithologies of the SBF Basin (Base map: Geological Survey, 1:250 000 Geological Series).

8.1.2 Late Carboniferous

The late Carboniferous Dwyka Group in the SBF is poorly understood, and there is still little information available for this unit. The Dwyka Group lies unconformably on the undulating Precambrian floor rocks in the SFB. In the relevant boreholes the sedimentary rocks are characterised by tillite which comprises of basement granite pebbles and Waterberg Group red sandstone pebbles, which are angular to rounded and set in a dark grey argillaceous matrix. Some boreholes indicate that there is no Dwyka Group accumulated or preserved and go directly into basement rock. This evidence suggests that the late Carboniferous sediments of the Dwyka Group were only deposited in certain locations, indicating either an erosional event that removed sediment that had accumulated, or, more likely, an undulating palaeo-topography similar to that found in the Free State coal

basins (Esterhuizen and van Heerden, 2011). Where sediment was deposited and preserved, it was most commonly in the form of tillite rock, and the lack of identification of dropstones suggests continental ice sheet environment with interglacial lakes with debris flows. These occurrences confirm that which Catuneanu et al. (2005) suggested, that the preserved Dwyka sediments in the SBF basin are associated with continental ice sheets which were located on the fore-bulge of the Karoo retro-arc foreland basin.

Local development of grounded ice lobes separated by ponds and outwash fans occurred during the later Dwyka (Smith, 1990). It is understood that the general direction of ice movement within the forebulge area was from north to south (Catuneanu et al., 2005), indicating a palaeo-topographic profile dipping to the south. This however, cannot be confirmed at this stage due to lack of data.

Some Dwyka sedimentary rocks are present in a number of the boreholes where the Dwyka was preserved as shale and mudstone beds which overlie the tillites and, in some places, interbedded with tillite. This provides evidence for the theory that the area now known as the SBF drifted out of the polar latitudes, and that extensive melting occurred resulting in a broad epeiric sea to the south in the Main Karoo Basin, and broad lakes in the SBF basin (Smith, 1990). It is during this time that there is a gradational change to the Ecca deposits.

8.1.3 Early to Middle Permian

The Permian Vryheid Formation equivalent in the SBF, namely the Hammanskraal Formation was deposited during the relaxing of the Cape Fold Belt (CFB), and subsequent subsidence of the fore-bulge (Section 2). This resulted in the deposition of basal mudstones that are calcareous in places, grading into medium to coarse grained immature sandstones with interbedded coaly shales. This sequence suggests that the palaeoenvironment was that of a low energy environment, moving into a higher energy setting. The calcareous mudstones suggest that there was palaeosol development (cf. Miall, 1990). This would allow for the establishment of vegetation, which is evident in the upper zone of the sequence as coaly shale. The immature sandstone interbedded with coaly shales suggests that there were periods where coarser grained material was carried by water and deposited on top of the palaeosols and a period where the vegetation was allowed to grow. When correlating these to the stratigraphy in the Main Karoo Basin, it is supported that the method of sediment transport was by water. This then suggests that there were periodic flooding events (cf. Smith, 1990; Cadle *et al.,* 1993)).

The top of the Ecca succession displays carbonaceous siltstones and mudstones with thin sandy laminae. These rock types suggest that there was an alteration of quiet-water mud and silt sedimentation and higher energy flow conditions which resulted in the deposition of thin sand layers (cf. Roberts, 1992). Also present in the Ecca succession is evidence of bioturbation and leaf fragments, indicating that the sediment was deposited under cool to fair climatic conditions that supported a variety of life (cf. Miall, 1990; Cadle *et al.,* 1993).

It is known in previous studies that the environmental settings during the period from the end of the Dwyka deposition to the late Ecca changed from glaciation to perma-frost and eventually to cool, wet climatic conditions (cf. Smith, 1990; Cadle *et al.,* 1993). The climate change to more fair conditions resulted in the rapid melting of the continental glaciers which led to a transgressive shoreline, fluvial and deltaic environments to develop with meandering river systems being dominant. A closer investigation of the Multicomponent map (Figure 7-3) for this period indicates that the rivers in the southern regions of the basin appear to be draining to the SSW, where the rivers in the northern region are draining to the south. This is determined by the fan like features indicated by the finer grained sediment, where the tip of the fan is proximal, and the broader areas of the fan are the more distal area of the river. The flexural subsidence resulted in the formation of wide deltas and meandering rivers which is evident in the Multicomponent map in Figure 7-3 and would result in the rock formations stated above in the uppermost Hammanskraal Formation. This setting supported the growth of vegetation and subsequently the deposition of the organic, carbon-rich muds under anoxic conditions (cf., Smith, 1990), which are evident in the SBF Vryheid Formation equivalent.

It is in this Ecca succession that it becomes evident that there are two sub-basins forming in the SBF Basin, specifically with the deposition of the LCZ (Figure 8-2). The LCZ was deposited during the Mid-Permian era in two sub-basins, one in the southern region and one in the northern region of the SBF. The southern basin exhibits higher coal qualities than in the northern region for the LCZ, showing thicker sequences of bright and dull coal interbedded with thin layers of carbonaceous mudstone (cf. Roberts, 1992). The LCZ in the northern region of the basin exhibits thicker layers of interbedded carbonaceous shales and mudstones, with thinner layers of bright coal. This could suggest that the southern region of the SBF Basin during this period of its evolution experienced lower energy levels with the development of a more established swamp like environment, than the northern region, where energy levels appear to have been higher with more frequent flooding events and the vegetation more sporadic. The divide between these two basins is marked by the thinning out of the coal seam, to become layers of carbonaceous shale with the occasional dull lustrous coal stringer, in the centre of the basin.

The termination of the inferred marsh environment was in part due to a second uplift event of the Cape Fold Belt, which resulted in the marsh environment changing to flood plains and meandering rivers, and covered by the Late Permian deposits of the Volkrust Formation equivalent in the SBF.

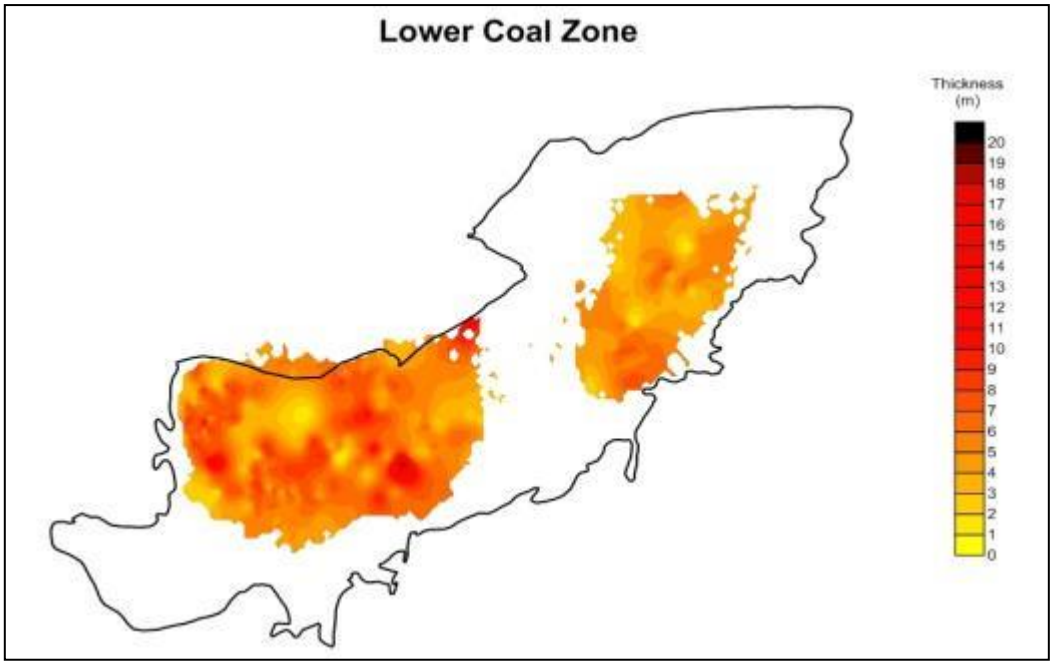

Figure 8-2: Isopach map of the Lower Coal Zone in the SBF Basin.

8.1.4 Late Permian to Middle Triassic

During this era in the evolution of the SBF Basin, the Volkrust Formation equivalent (Irrigasie Formation) (Beaufort Group) was deposited. The lithologies for this sequence in the borehole database indicate that this succession does not have a gradational base as in the Main Karoo Basin, which suggests a period of no deposition and of erosion. This succession appears to be overlying the Vryheid Formation equivalent coals, where it becomes dominated by mudstones and siltstones, with channels of fine-grained sandstones. This suggests a low energy environment where sediment is being deposited from suspension. The fine-grained channels of sandstone suggest poorly developed high sinuosity river channels, with the mud and siltstone deposited from shallow water bodies (cf., Miall, 1990). The sedimentary rocks exhibit red-purple colouration with carbonaceous zones at the base of this succession, suggesting the presence of an anoxic environment and a reduction in vegetation. These carbonaceous zones coincide with the noted black shales around the world that link to the P-Tr Mass Extinction Event, providing evidence towards the long term development of anoxic shallow waters (Knoll *et al.*, 2007).

The colour of the lithology then becomes khaki coloured towards the top, which could result from the lack of carbon material. This coincides with the suggested global warming associated with the P-Tr Mass Extinction event (cf. Knoll *et al.*, 2007; cf. Pace *et al.*, 2009). Pebble conglomerates have also been identified with up to 10cm long clasts of Waterberg fragments, which may have resulted from flooding events. The dominant inferred environmental setting is braided river systems turning into a more fluvial-deltaic type environment with the development of deltas pro-grading into lakes (cf., Smith, 1990).

There is a clear climate change indicated in these sediments during the transition from end-Permian to Early Triassic, as the environmental settings changed from an environment

which was becoming settled and allowing the establishment of vegetation, to one where there was a sudden change where vegetation become more sporadic and allowed for braided river systems to develop. The transition from the Ecca to Beaufort lithologies is also not gradational, suggesting a sudden change in events. These points provide further evidence to the global warming theories put forth by Knoll et al. (2007), and the suggestion that this mass extinction event occurred rapidly.

The Isopach map for this period (Figure 7-2) indicates that the two depocentres identified in the previous succession appear to have shifted further apart, with an elevated area in the centre of the basin. This is evident in the isopach and multicomponent maps for the Beaufort Group, which indicates thicker deposits of coarser grained material in the far southern and far northern regions of the basin. This suggests a possible channel deposit that flooded into a shallow lake during wet seasons (cf. Roberts, 1992). Similarly in the northern region of the basin, there are thicker deposits than in the centre, although smaller in area than in the south. The centre of these maps is dominated by fine grained materials and thin deposits, which suggest low energy environments with slow rates of deposition. Plotting the isopach map for the UCZ (Figure 8-3) indicates that this central region of the basin hosted thicker vegetation conducive to coal development, which resulted in the deposition of the UCZ.

The UCZ is dominated by interbedded carbonaceous shale and bright coal layers, with a high frequency of interbedding occurring along the southern boundary of the basin where the coal layers are thickest. The higher frequency of interbedding in the UCZ coals indicates variations in the water level and flooding events. The coal seam which is deposited closer to the depocentres and along the northern boundary of the basin becomes increasingly poor in quality, with less shale-coal interbedding frequency. This interbedding suggests that the extensive vegetated areas were drowned by fine sediment during wet periods. The change in the coal-shale interbedding frequency between the centres of the coal deposit and the outer boundaries of the coal occurrences suggests that the areas closer to the two sub-basin depocentres were flooded more often and for longer periods of time than in the centre of the basin. The increased thickness of the coal in the southern regions and the difference in coal-shale interbedding frequencies of the south versus the north coincide with the previously suggested northern sub-basin being smaller and less substantial than the southern sub-basin (cf. Roberts, 1992).

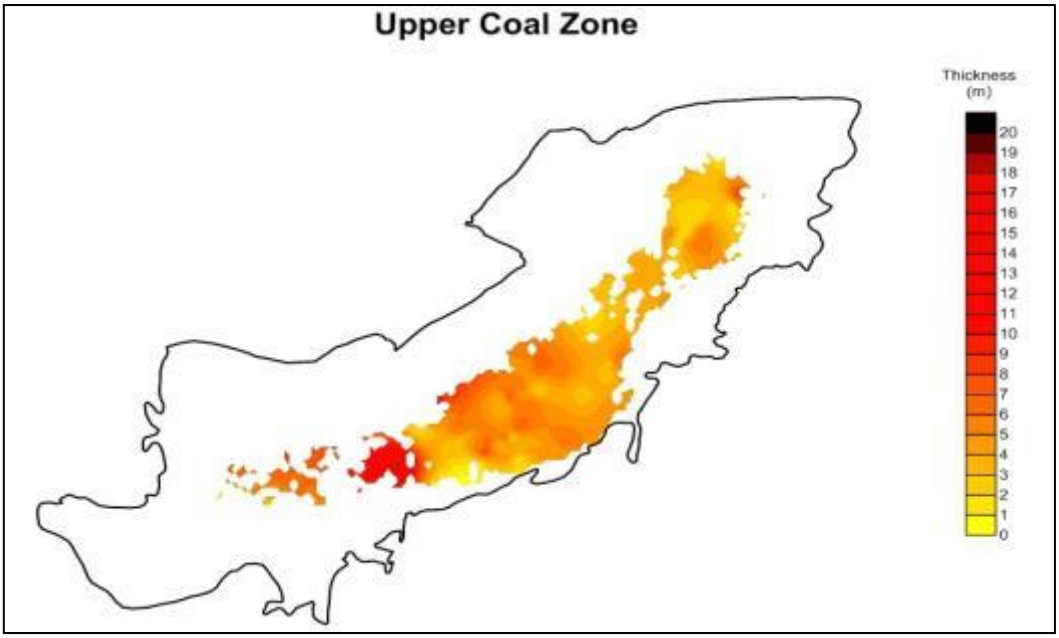

Figure 8-3: Isopach map of the Upper Coal Zone in the SBF Basin.

8.1.5 Middle Triassic

The Middle Triassic saw the deposition of the Molteno Formation. This succession in the southern region of the SBF Basin is dominated by mudstone and fine-grained sandstone at the base of the succession, grading to coarse grained sandstones and conglomerates towards the top of the succession. Towards the central and northern regions of the SBF there is a basal grit with upward fining cycles of sandstone grading into purple shale. The Molteno Formation in the SBF suggests that this period is characteristic of braided rivers which later developed into localised floodplain deposits as sinuosity possibly increased (cf., Miall, 1990).

The colour variations start with light grey sandstones and mudstones at the base of the formation, the upward succeeding yellow orange and final red purple colours all indicate ferruginous staining. This change in colour suggests that there is an increase in oxidation conditions as the climate becomes progressively warmer and drier (cf. Johnson *et al*. ed., 2006), which indicates a slight recovery after the P-Tr Extinction Event.

Previous successions suggested, through thickness patterns, that there were two sub-basins, north and south, within the SFB. The Molteno thickness patterns indicate that the locus of deposition of the southern sub-basin becomes elongated towards the centre of the SFB. The northern sub-basin is also trending towards a more central deposition location. The Molteno succession is thickest in the south, and thins out towards the centre of the preserved basin closer to the northern boundary. In the northern region of the basin the Molteno Formation thickens again, but not to the same extent as in the south, which suggests that the capacity of this sub-basin to accommodate sediment is being reduced.

8.1.6 Late Triassic

The Late Triassic marked the beginning of the thick deposits of the Elliot Formation. The depocentre of the basin appears to have shifted towards the central parts as this is where the thickest deposits are found as can be seen in the isopach maps. Additionally, the multicomponent map for the Elliot Formation indicates that the sediments are coarser grained along the centre of the basin than in the southern region and along the boundary of the basin. The typical rock types found in the SBF in this Formation comprise of alternating mudstones, siltstones and sandstones as well as bands of conglomerate and calcite nodules throughout. The colouring of this succession is purple-grey towards the base, becoming brick red, iron rich at the top (cf. Bordy *et al.,* 2004). The alternating mudstones, siltstones and sandstones are indicative of a lacustrine environment (cf. Roberts, 1992). The finer grained deposits suggest a loessic type environment with sufficient energy levels to deposit the finer grains, as was as playa-lake development. The coarser grained sediments are indicative of either a flooding event (conglomerates) or a period of a higher energy environment, possibly an increase in collective precipitation volumes over time. There is evidence of planar and ripple cross-bedding present with distinct bedding and slump structures in places. The cross bedding suggests channelized bar and dune bedforms (cf. Roberts, 1992).

Bioturbation has also been identified in some of the boreholes towards the base of the succession indicating fair weather conditions (cf. Roberts, 1992; cf. Bordy *et al.,* 2004). In order for bioturbation to be well preserved, the sediment through which these animals were burrowing was required to be soft and moist, yet stiff enough not to collapse as they moved through it. These structures indicate that the environment was not periglacial, and was however moving towards a more tropical environment. Due to the lack of evidence of bioturbation further up in the sequence, along with the increasing coarser grained sediments with predominantly reddish colouring occurring implies an aridification and oxidising environment with possible flash-flooding of the environment towards the end of the deposition of the Elliot Formation (cf. Roberts, 1992).

Both the isopach and multicomponent map of this age indicate channelization, with a distinct trend following the coarser grained sediment, which corresponds to the thickest areas. This indicates the likelihood of large relatively unconfined braided systems with occasional floods, allowing for the thicker deposits of the Elliot Formation (cf., Miall, 1990).

8.1.7 Late Triassic to Early Jurassic

During this transition from fluvial-lacustrine deposits of the Elliot Formation to more aeolian environments, the Clarens Formation of the Late Triassic to Early Jurassic was deposited. The base of the Clarens succession exhibits bedding and slump structures in a fine grained muddy red sandstone, suggesting a playa lakes environment similar to that found in the later deposits of the Elliot Formation (cf., Smith, 1990). This implies a gradational contact between these two formations. These sediments grade into a quartzitic sandstone with cross bedding towards the base, becoming mottled and fine-grained. Present

within these sandstones are thin mudrock or siltstone intercalations which occur sporadically. Further up the succession this quartzitic sandstone is well sorted becoming massive towards the top, which could suggest windblown movement of sediment in a dry environment (cf., Smith, 1990). The intercalations identified in these strata are indicative of ephemeral river systems and small inland lakes, and the fact that they are sporadic and become increasingly sporadic towards the top of the succession is indicative of a change of enhanced aridification (cf. Roberts, 1992). The massive sandstone deposits are typical of large parts of the preserved aeolian deposits of the Clarens Formation in the Main Karoo Basin (cf. Johnson *et al*. ed., 2006; cf. Roberts, 1992).

The lithology of the Clarens Formation in the SBF Basin represents a changing environment from fluvial-lacustrine to an arid aeolian environment (cf. Roberts, 1992). The isopach map of the Clarens indicates one depocentre just west of the centre of the basin. The maximum thickness is in a similar location as the prominent structure along the northern boundary of the basin (Section 7.7), and could indicate growth faulting during sedimentation, occurring prior to the breakup of Gondwana. This thickening is also evident in the cross section in Area 3 (Section 7.11) which corresponds to the faults identified.

The movement of the Gondwana supercontinent to more equatorial latitudes combined with the flexural uplift of the fore-bulge caused by another compressional event of the Cape Fold Belt resulted in the aridification of the SBF Basin during the Late Triassic to Early Jurassic.

8.1.8 End of Early Jurassic

Similar to the Main Karoo Basin, the end of the Karoo Supergroup in the SBF is marked by the Jurassic outflow of flood basalts. The boreholes indicate a spatial cessation of the deposition of the Clarens Formation, suggesting a rapid outpouring of widespread basaltic lavas. The lavas indicate amygdaloidal flow tops, flow structures and are generally massive which is characteristic of low-viscous flows. The occurrence of tuff layers found in the Letaba Formation indicates that there were periods of pyroclastic eruptions during breaks in outpouring of flood basalts (cf. Roberts, 1992).

The preserved deposits of the basalts indicate two sub-basins, which suggest that this central section was not affected by the faulting event. The dolerite dykes identified by Mr. B. Green (2011) indicate that there is a high likelihood that the Letaba basalts extended further north of the SBF Basin (Figure 8-4) and that fault control played a role along the northern boundary (cf. Roberts, 1992).

The structural contour and isopach maps for all the Karoo successions indicate that there was a major faulting event that resulted in the down-throw of the Karoo strata that occurred during the outpouring of the Letaba Basalts. It was this major normal fault slip along the northern boundaries of the SBF Basin that resulted in the tilting of the strata and subsidence of the Karoo strata in the north by a kilometre of throw. This will be further discussed in Section 8.2 to follow.

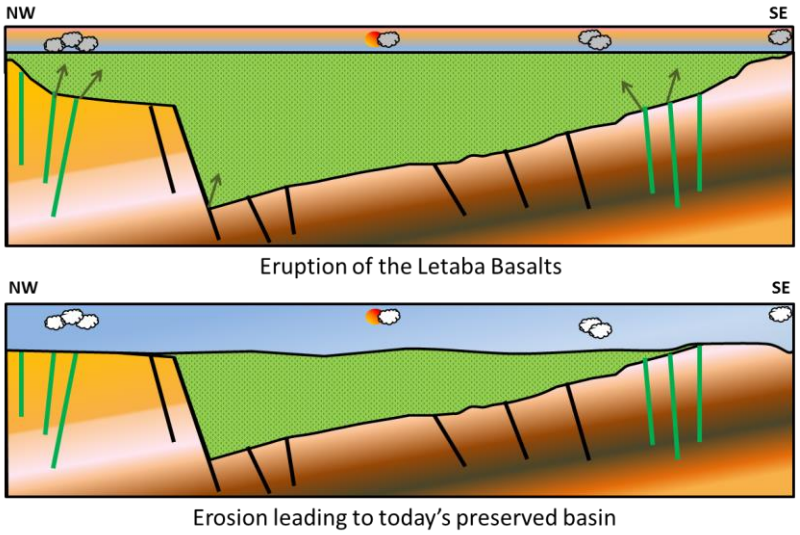

Figure 8-4: Illustration of the eruption of the Letaba basalts and subsequent erosion.

8.2 Tectonic Development of the SBF Basin

A widely accepted theory for the origins of the Karoo Supergroup in the various basins in southern Africa is the flexural retro-arc foreland basin system, as for example discussed by Catuneanu et al. (1998; also 2005). In this work it is recognised that there is a direct relationship between episodic uplift in the Cape Fold Belt (CFB) and the progradation of sediments into the various sub-basins in the flexural system. Figure 8-5 indicates the flexural and surface profiles which illustrate the evolution of the foreland system during stages of orogenic loading and unloading (Catuneanu et al., 1998). The SBF basin would be located on the forebulge in these diagrams.

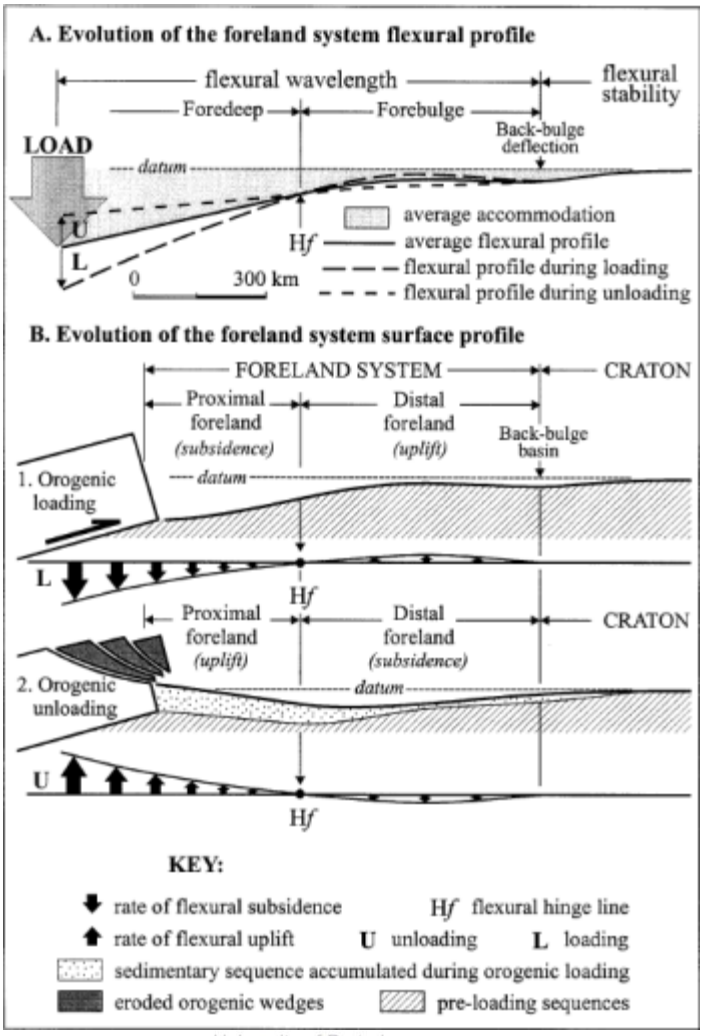

Figure 8-5: Flexural and surface profiles illustrating the evolution of the foreland system during stages of orogenic loading and unloading (Catuneanu et al., 1998).

8.2.1 Basin Extent

In Catuneanu et al. (1998), the changes in the flexural wavelength of the basin is discussed which effects the positioning of the hinge line of the foreland basin. Sedimentation within the Karoo basins that are related to this retro-arc foreland basin system was closely related to the orogenic cycles of loading and unloading in the CFB. During orogenic loading, the foredeep subsides allowing for the accommodation of sediments, and the forebulge in fact undergoes flexural uplift (Figure 8-5). The flexural foredeep and forebulge undergo out-of-phase subsidence and uplift in response to orogenic loading and unloading, and this is evident in the sedimentation discussed above. The Volksrust Formation correlated strata in the SBF (Irrigasie Formation) for example is correlated to the Ecca Group in the south of Main Karoo Basin. However, towards the northern boundary of the Main Karoo Basin, this unit actually interfingers with the overlying strata (cf. Johnson *et al*. ed., 2006), and in the case of the SBF Basin, it falls within the Beaufort Group. This suggests a lag in the deposition of sediment in the SBF Basin compared to the Main Basin succession deposited in the foredeep.

Catuneanu et al. (1998) also discuss the migration of the hinge line in this foreland system. The pattern of the hinge line migration is shown in Figure 8-6, which indicates the flexural peripheral bulge advancing towards the Kaapvaal craton during the Late Carboniferous-Permian periods in response to the unloading of the orogenic front. The hinge line then migrates back towards the CFB during the Triassic-Middle Jurassic as there is orogenic loading. During the Late Triassic-Middle Jurassic there was orogenic unloading again.

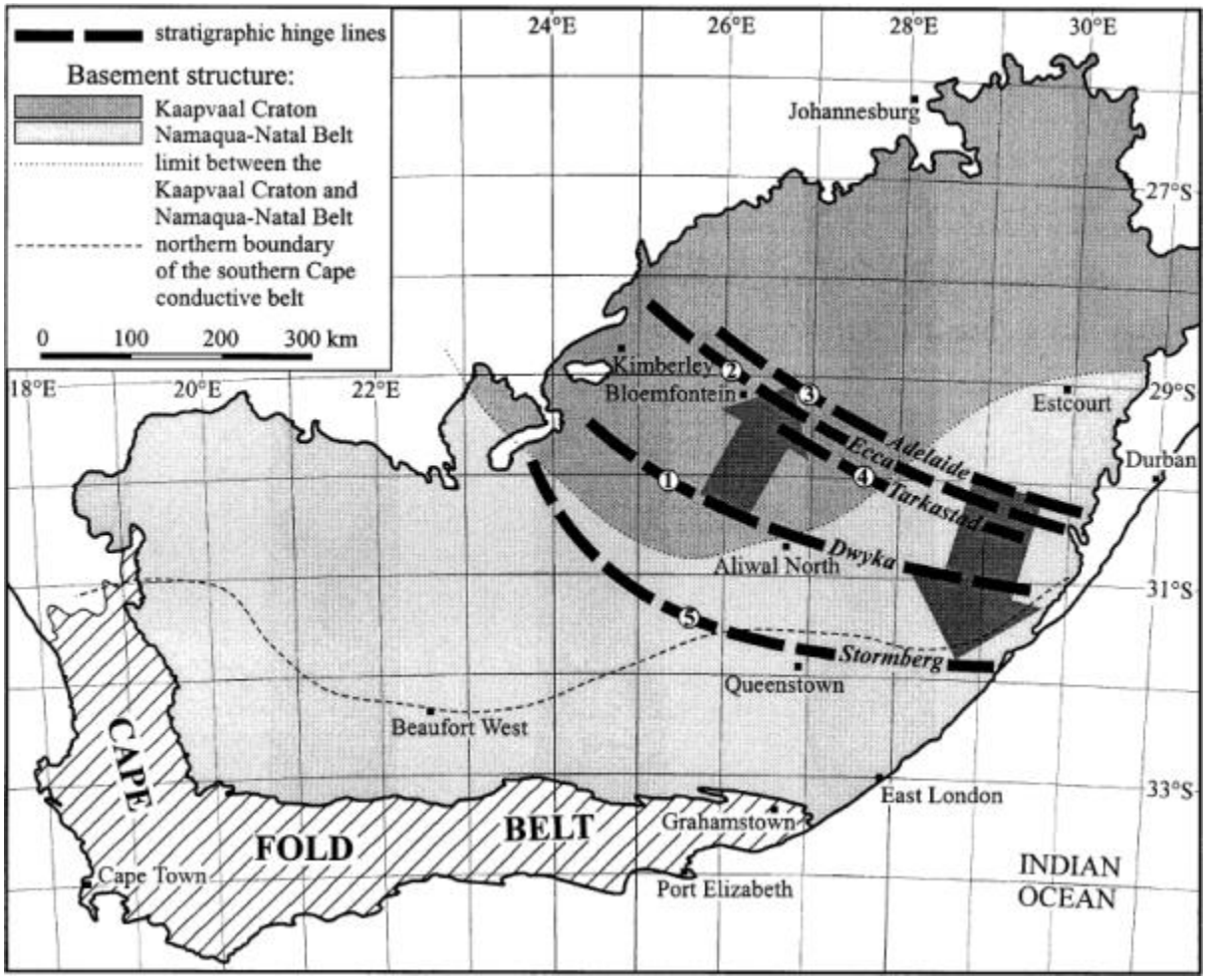

Figure 8-6: Position of the stratigraphic hinge line migration at consecutive time-slices (1 – 5, in chronological order). Arrows indicate migration of hinge line (Catuneanu et al., 1998).

Studies, as well as the evidence stated in Section 8.1, indicate that the Karoo stratigraphy can be split up into two distinct successions, the Lower and Upper Karoo. The Lower and Upper Karoo is separated by the Permian-Triassic Boundary (Catuneanu et al., 1998), as well as being denoted by this shift in the hinge line migration.

It is therefore inferred, that the early positions of the hinge line during the Lower Karoo sedimentation of the Dwyka and Ecca Groups would have resulted in the deposition of these formations on the forebulge in the SBF Basin to be further south than the sediments of the Middle Karoo (Beaufort to Molteno). As the hinge line moved further north, so would

the depocentres of the successions being deposited. With investigation of the Geological Maps of South Africa and the geology south of the current SBF Basin, outliers of both the Dwyka and Hammanskraal Formation (Ecca Group) are identified, thus supporting the hypothesis that the these successions were deposited further south (Figure 8-9). Given the proximity of the Main Karoo Ecca deposits to those outliers identified, it could be argued that the two basins, the SBF and Main Karoo Basin, might have been one basin during deposition of the Dwyka and Hammanskraal formations.

There are no outliers of the Middle to Upper Karoo sediments to the south of the SBF, which does not necessarily indicate that there were no sediments deposited here, as it is could indicate that these sediments have since been eroded. However, the original basin was not much larger than it is today, as the upper strata in the preserved basin tend to thin and coarsen towards the current SBF non-faulted boundaries.

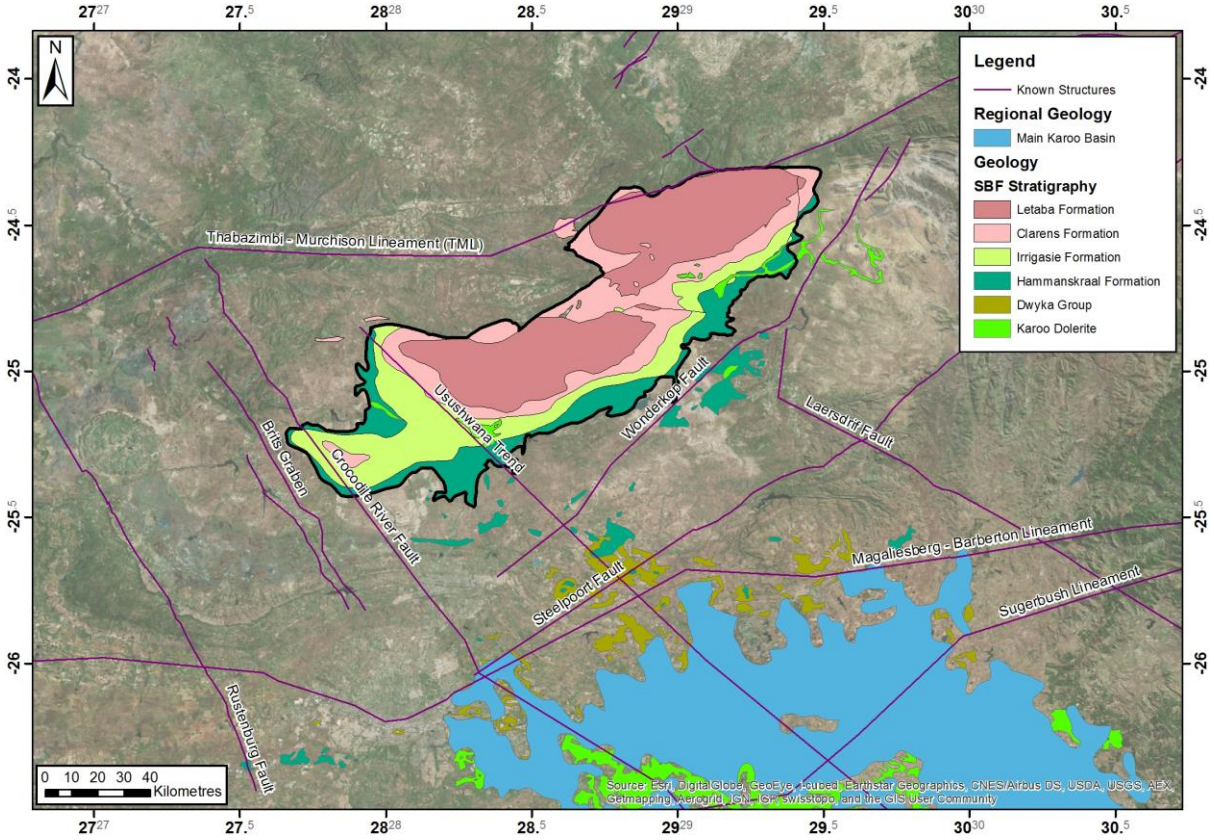

Figure 8-7: Outliers of the Dwyka and Hammanskraal Formations south of the SBF Basin.

8.2.2 Depocentre Migration

After collision of the palaeo-Pacific ocean plate with the African plate that created the initial stages of the Cape Fold Belt (CFB), the weaker Pan-African basement was easily deformed and thus subsided further in comparison to the more rigid crust of the Precambrian Kaapvaal craton (Bumby and Guiraud, 2005).The SBF Basin lies on this more rigid crust, and therefore underwent a more brittle deformation style. Throughout the sedimentation of the Karoo sediments in the SBF Basin, this flexing of the fore-bulge is evident. There is one major uplift event of the Cape Fold Belt that is evident in the SBF Basin.

The Cape Fold Belt underwent its first paroxysm event that initiated the deposition of the Karoo sediments during the Late Carboniferous era. As the fore-deep sub-basin was pushed down, the fore-bulge underwent uplift with formation of the SBF sub-basin therein, distally from the southern orogenic belt (Figure 8-5).

The fault systems in the SBF Basin follow a strong ENE-WSW trend, particularly along the northern boundary of the preserved basin. These faults have a similar direction to that of the Thabazimbi-Murchison Lineament (TML) that lies to the north of the basin which suggests a reactivation of the TML relay system during the final deposition of the Karoo Supergroup (cf. Good and De Wit, 1997). The minor faults in the basin have been active throughout the duration of the deposition of the Karoo sediments due to the repeated pressures put on them by the episodic uplift in the Cape Fold Belt. These faults later underwent major slip during the breakup of Gondwana. Due to the proximity of the SBF Basin to the TML, a major weakness in the craton, it is likely that there was some influence of this major lineament with the location of the SBF deposits.

The continued loading and unloading of the Cape Fold Belt orogeny led to the weakening of the continental crust in the vicinity of the TML, which caused the strata to dip towards the TML. This dip of the crust in this region becomes evident in the later SBF deposits where, in the Clarens Formation, the thickest succession is found closer to the strike of the Zebedelia Fault. This evidence demonstrates that there may have been growth faulting and the onset of early rifting occurring during the later Karoo deposition in the SBF Basin.

The movement of the depocentre as shown in the Isopach Maps of the different successions over time is also indicative of altering tectonic framework and specifically of changing subsidence patterns (Figure 8-8). The major depocentre of the southern sub-basin of the SBF Basin moves from the southern region of the preserved depository towards the centre thereof, essentially moving north towards the TML. The northern sub-basin also shows the depocentre moving slightly north towards the centre of the preserved basin, once again towards the TML. This adds to the evidence that the lower Karoo successions were deposited further south, and the middle to upper successions further north, relating to the migration of the hinge line. Figure 8-8 indicates the Vryheid-equivalent LCZ and Volkrust-equivalent UCZ deposits and the change in depocentre locations. It was during the transition between the two successions that the hinge line migration direction changed.

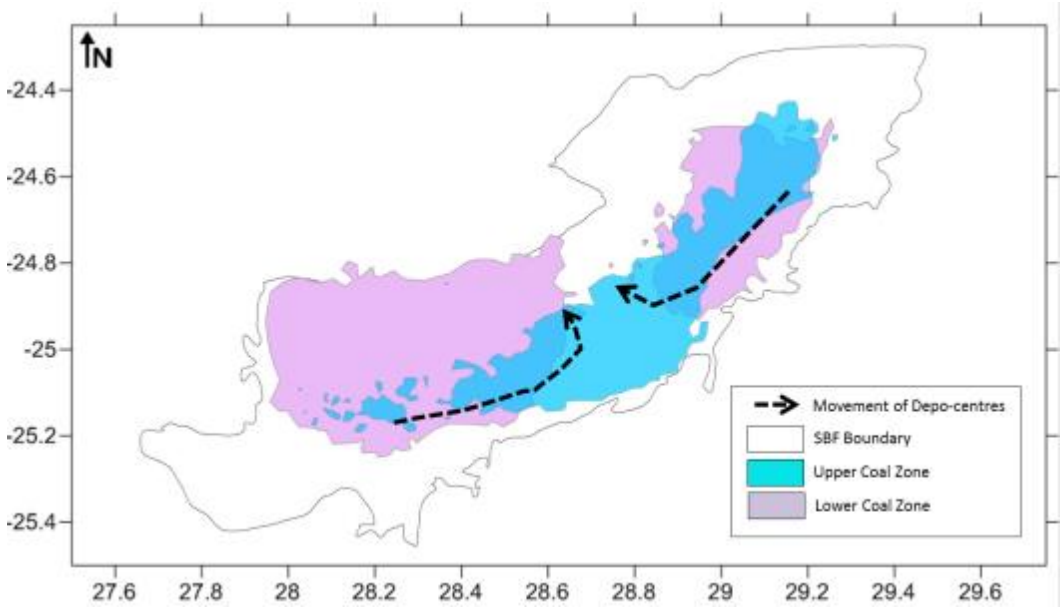

Figure 8-8: Illustration indicating the apparent movement of the two sub-basins' depocenters utilising the comparison of the LCZ and UCZ occurrences.

8.2.3 Tectonic Evolution

The cross sections developed in Section 7.9 to 7.16 were investigated in order to identify the possible ages of the faulting delineated by Mr. B. Green. By comparing correlating thicknesses of each stratigraphic unit either side of the fault, it is possible to see which strata were affected, and which were not. If the correlating stratigraphy indicated a change in thickness either side of the fault, it is highly likely that that fault was active during deposition. Alternatively, if the thickness of the strata were not affected, it could be inferred that the fault was not active during deposition.

Due to the inconsistent data for all the Karoo strata in the SBF, there is very little evidence of any major tectonic events for the Lower Karoo sequences. The main tectonic event that is evident in the Upper Karoo is a marked structural inversion of the CFB during the Beaufort Group and Early Molteno Formation. Literature shows that there was a ± 3km uplift, known as the Namaqua Uplift, which resulted in erosion north of the CFB (Rowsell and de Swardt, 1976). Figure 8-9 indicates the interpreted ages of fault delineations in the SBF Basin with Figure 8-10 indicating the Rose Diagram constructed from data in Figure 7-4 which relates fault trends to major tectonic events affecting the SBF Basin.

The two sub-basins identified in the SBF are both bounded in the north by two physically unconnected faults that share a similar orientation to that of the TML relay system. These major faults are not indicated in the strata below the Letaba Basalts (See Section 7.1). Displacement of these faults appears to have occurred post-depositionally of the underlying strata.

It became evident that the minor dyke orientations were controlled by structures that had similar orientations to lineations that occurred prior to the Gondwana breakup. This suggests that the emplacement of the dykes were via weak points in the crust, and intruded

along the faults. The major dyke orientations are similar to the TML orientation, and those lineations related to the Gondwana breakup (cf. Hastie *et al.,* 2014).

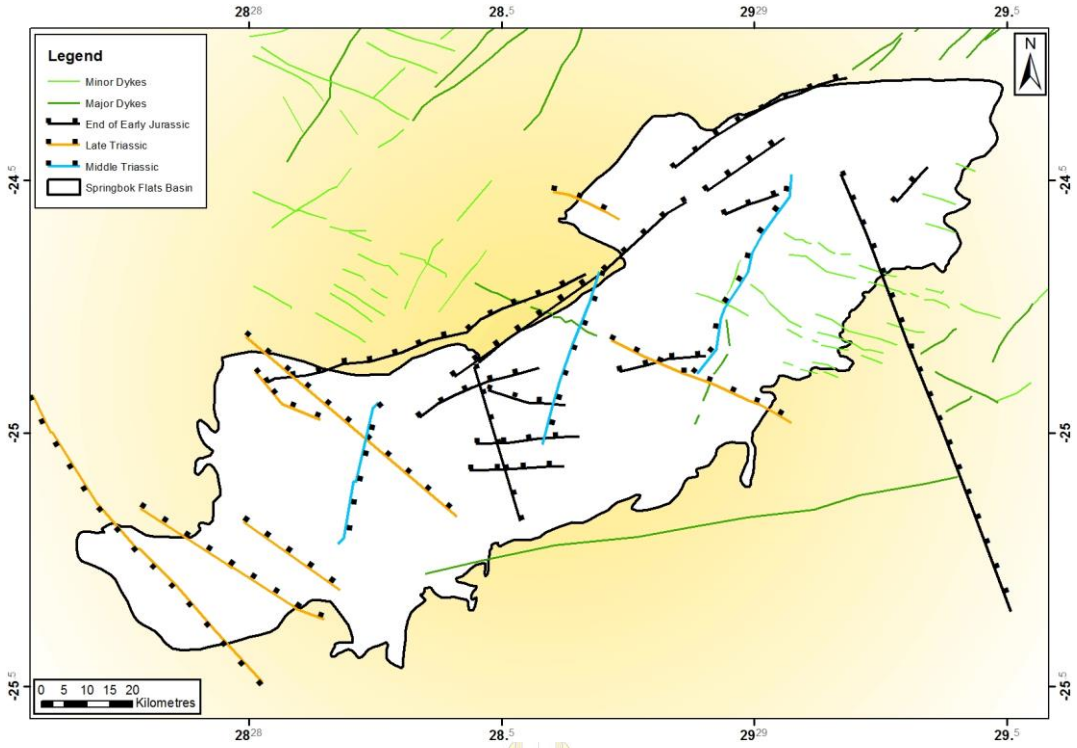

Figure 8-9: Map indicating the interpreted ages of fault delineations in the SBF Basin.

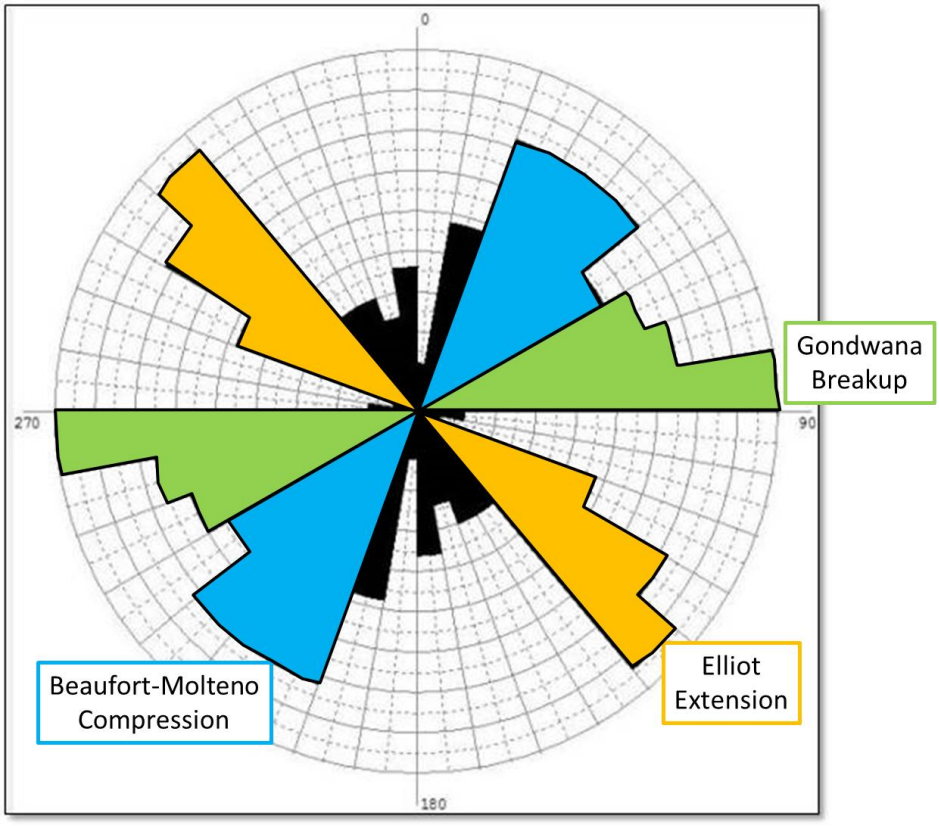

Figure 8-10: Rose diagram indicating grouping of structural lineation strikes in the SBF.

9 Summary and Conclusions

This study was aimed at elucidating an evolutionary history of the SBF Basin by utilising methods of basin analysis and literature search, and to establish how the basin relates to other Karoo Supergroup basins in southern Africa with emphasis on the Main Karoo Basin. The genetic model of the retro-arc flexural foreland rift basin was compared to the inferred depositional environments and was found to be a logical interpretation of the basin's evolution.

The onset of the Karoo Stratigraphy in the SBF was due to uplift resulting from the mid-carboniferous assembly of Pangea. During the Lower Karoo deposition, lithospheric subsidence was facilitated by crustal-scale faults, resulting in the deposition of the glacial Dwyka and Lower Ecca sediments. Flexural subsidence was occurring in the forebulge due to the relaxing of the initial compression of the CFB. The forebulge did not subside as rapidly as the foredeep, as it is situated on the competent Kaapvaal Craton, and this can be seen in the thin successions of the Dwyka and early Ecca Group deposited. The later Ecca succession was characterized by greater subsidence with little accompanying brittle deformation. The lower Beaufort Group was a deltaic basin and was terminated towards the end of the Permian period, identified by a significant fauna and flora change as suggested in Section 8.1.3.

The termination of the Beaufort Group was also marked by a ± 3km uplift, known as the Namaqua Uplift, and erosion north of the Cape Fold Belt. This resulted in structural inversion during the Beaufort Group and Early Molteno Formation. Evidence of this in the SBF is shown by a change in deposition dynamics of the Molteno Formation, as well as the faulting that occurred during this succession. These uplift events resulted in uplift in the foredeep which resulted in the compression of the forebulge. Once these events subsided, the forebulge relaxed and underwent extension. The Elliot Formation formed during this unloading of structural relief and relaxation of basin-forming stresses. The upper Elliot and Clarens formations and Letaba Basalts exhibit the transition from sinistral strain of the late Karoo Basin to the dextral tectonics of the Gondwana breakup that terminated the basin deposition.

The Karoo sediments in the SBF Basin clearly represent the broad spectrum of the same set of palaeoenvironments that are recognised in the Main Karoo Basin rocks. These reflect the progressive infilling of the Karoo Basins, the changing tectonic framework as well as the migration of Gondwana from polar to tropical latitudes. However, due to the development of the SBF basin on the forebulge, the compression of the CFB had the opposite effect, where it resulted in uplift of the fore-bulge and subsidence of the foredeep. This subsequently resulted in the SBF correlated Karoo sedimentary successions to be markedly thinner than those of the Main Karoo Basin, and in some cases, certain strata are completely absent.

During the breakup if the Gondwana supercontinent, an extensional basin formed by reactivation of older structures such as the TML as a result of displacement on the principle shear zones. This resulted in the preservation of the SBF strata in the basin today.

10 Recommendation for Further Studies

Various questions have been identified that require further understanding. This study is a baseline and preliminary investigation into the SBF Basin, and may act as a canvas to which more in-depth investigations may be added. Possible fields of investigation include:

- Quality assurance and quality control of the borehole database with core samples;
    - This will allow for more accurate analyses of the data and a higher confidence in the outcomes.
- An addition of more boreholes into the cross sections in the different fault blocks to get more defined cross sections
- Southern extension of the SBF basin;
- Source and distribution of the Uranium occurrences in the coal zones and mudstones, and how they relate;
- CBM potential of the SBF Coals;
- CGS potential of the SBF Coals;
- Palaeontological investigation to determine the correlative ages of the SBF strata and the Main Karoo Basin strata;
- A study into the basement lithology of the SBF Basin;
    - Possible extension of the Nylstroom Sub-basin, Waterberg Group, beneath the SBF;
- P-Tr extinction event evidence in the SBF.

11 Acknowledgements

Starting with the institute that made this study possible, the University of Pretoria and the Geology department, this dissertation could not have been written completed Professor Pat Eriksson, who not only served as my supervisor but also gave me guidance and support throughout my academic career. Dr Adam Bumby likewise played an important role in my project, although not formally my co-supervisor, he assisted me with any questions I put forward.

Outside of the University, I'd like to thank Coal Tech for supporting this study financially, as well as supplying the many connections required to obtain the research necessary. The time that I have been working at Shango Solutions has taught me vital skills

that assisted in pushing this project to new levels and exciting discoveries. Interacting with the high quality staff has given me the knowledge to better understand the methodology and interpretations used.

Mr. B. Green has been a great help to the regional understanding of the SBF basin with his extensive knowledge of geophysics, and his contributing of geophysical information of the area.

12 References

Bordy, E. M., Hancox, P. J. and Rubidge, B. S. (2004).Basin development during the deposition of the Elliot Formation (Late Triassic – Early Jurassic), Karoo Supergroup, South Africa.*South African Journal of Geology,* 107, pp. 397 – 412.

Bredell, J.H., 1987. South African coal resources explained and analysed. *Report, Geological Survey of South Africa*, pp. 154 (unpubl.).

Bumby A.J and Guiraud R, 2005.The geodynamic setting of the Phanerozoic basin of Africa. Journal of African Earth Sciences 43, pg 1-12.

Cadle, A. B., Cairncross, B., Christie A., and Roberts, D. L. (1993). The Karoo basin of South Africa: Type basin for coal-bearing deposits of southern Africa. *International Journal of Coal Geology,***23**, 117-57.

Catuneanu, O., Beaumont, C., Waschbusch, P., (1997a). Interplay of static loads and subduction dynamics in foreland basins: reciprocal stratigraphies and the ‘‘missing’’ peripheral bulge. Geology 25(12), 1087–1090.

Catuneanu, O., Hancox, P.J., Rubidge, B.S., (1998). Reciprocal flexural behaviour and contrasting stratigraphies: a new basin development model for the Karoo retroarc foreland system, South Africa. *Basin Research,* **10**, 417–439.

Catuneau, O. (2004). Retroarc foreland systems – evolution through time. J. Afr. Earth. Sci. 38, 225-242.

Catuneanu O., Wopfner H, Eriksson P.G, Cairncross B, Rubidge B.S, Smith R.M.H, Hancox P.J (2005). The Karoo basins of South-Central Africa. *Journal of African Earth Sciences*, **43**, pp. 211-253.

Chevallier, L. and Woodford, A.C. (1999). Morpho-tectonics and mechanisms of emplacement if the dolerite rings and sills of the western Karoo, South Africa. *S. Afr. J. Geol.,* **102**, 43-54.

Christie, A.D.M., 1989. Demonstrated coal resources in the SBF coalfield. Report, Geological Survey of South Africa, pp. 69 (unpubl.).

Cole, D., (2009). A review on Uranium deposit in the Karoo supergroup of Southern Africa, Council for geoscience, pp. 1-9.

DeCelles, P.G. & Burden, E. T. (1992) Non-marine sedimentation in the overfilled part of the Jurassic-Cretaceous Cordilleran foreland basin: Morrison and Cloverly Formations, central Wyoming, USA. Basin Res., 4, 291–314.

Esterhuizen, G. and van Heerden, G. (2011). Free State Coalfields: Geological characteristics of the depositional environments, structural-geological features and the distribution of coal seams. Free State Coal Indaba. Presented by Karin van der Merwe. 16 pp.

Geological Survey, 1974. 1:250 000 Geological Series 2426 Thabazimbi, Geological Survey, Pretoria

Geological Survey, 1978. 1:250 000 Geological Series 2428 Nylstroom. Geological Survey, Pretoria

Geological Survey, 1978. 1:250 000 Geological Series 2528 Pretoria. Geological Survey, Pretoria

Geological Survey, 1981. 1:250 000 Geological Series 2526 Rustenburg. Geological Survey, Pretoria

Giles, K. A. & Dickinson, W. R. (1995). The interplay of eustasy and lithospheric flexure in forming stratigraphic sequences in foreland settings: an example from the Antler foreland, Nevada and Utah. In: Stratigraphic Evolution of Foreland Basins (Ed. by S. L. Corobek & G. M. Ross), Spec. Publ. SEPM, 52, 187–211.

Good, N. and De Wit, M. J., (1997). The Thabazimbi-Murchison Lineament of the Kaapvaal Craton, South Africa: 2700 Ma of episodic deformation. *Journal of the Geological Society*, 154, pp 93–97.

Green, B. (2011). Aeromagnetic and Gravity geophysical images for the SBF region, not published.

Haughton S.H, (1969). Geological history of Southern Africa. The Geological Society of South Africa, Cape and Transvaal printers Ltd., Cape Town.

Hemming, M., (2009). Environmental impact assessment for a coal bed methane exploration right application SBF project. Pp 1-32.

Jeffrey, L.S., (2005). Characterization of the coal resources of South Africa. *The Journal of the South African Institute of Mining and Metallurgy.*95-102.

Johnson, M.R., (1976). Stratigraphy and Sedimentology of the Cape and Karoo sequences in Eastern Cape Province. Unpublished PhD. thesis, Rhodes University, Grahamstown, 366pp.

Johnson, M.R., Anhaeusser, C.R. and Thomas, R.J. (editors), (2006).The geology of South Africa. Geological Society of South Africa, Johannesburg, and Council for Geoscience, Pretoria, pp. 691.

Johnson, M. R., Van Vuuren, C. J., Hegenberger, W. F., Key, R. and Shoko, U. (1996). Stratigraphy of the Karoo Supergroup in southern Africa: An overview. *Journal of African Earth Sciences*, 23, No. 1, pp. 3 – 15.

Kruger, S.J., 1981. ‘n Mineralogiese ondersoek van die asfraksie van steenkool van die Springbokvlakte-Steenkoolveld. M.Sc. thesis, Rand Afrikaans University, Johannesburg,166 pp. (unpubl.).

Loubser, T., 2007. Uranium 2007: Resources, Production and Demand (The Red Book). A Joint Report by the OECD Nuclear Energy Agency, South Africa and the International Atomic Energy Agency (IAEA). OECD Publishing, 422 pp.

Miall, A. 2010, Principles of Sedimentary Basin Analysis, *Springer Berlin Heidelberg*. 3rd edition, 616 pages.

McDonald, A.J., and Waldeck, H. G., (2008).An Independent Competent Person's Report on HolGoun's Coal and Uranium Assets in the SBF Coalfield, HolGoun Energy (Pty) Ltd, Report Number 381289/HolGoun 2008 IER-05, SRK Consulting, 1-114.

Oxford English Dictionary. (2002) 10th ed. Oxford: Oxford University Press.

Pace, D. W., Gastaldo, R. A. and Neveling, J. (2009).Early Triassic aggradational and degradational landscapes of the Karoo Basin and evidence for the climate oscillation following the P-TR Event. *Journal of Sedimentary Research,* 79, pp. 316 – 331.

Roberts, D.L., (1992), The SBF basin – a preliminary report, *Geological Survey of South Africa Report.*1992-0197, 23 p.

Rust, I.C., (1975).Tectonic and sedimentary framework of Gondwana basins in southern Africa. *In: Campbell, K.S.W. (Ed.), Gondwana Geology* (3rd Gondwana Symposium). Australian National University Press, Canberra, pp. 537–564.

Smith, R. M. H. (1990). A review of stratigraphy and sedimentary environments of the karoo Basin of South Africa. *Journal of African Sciences*, 10, No. ½, pp. 117 – 137.

Smith, R. M. H., Eriksson, P. G. and Botha, W. J. (1993).A review of the stratigraphy environments of the Karoo-aged basins of Southern Africa. *Journal of African Earth Sciences*, 16, No. 1/2 , pp 143 – 169.

Smith, R.M.H. and Ward, P.D.,(2001).Pattern of vertebrate extinctions across an event bed at the Permian-Triassic boundary in the Karoo Basin of South Africa. Geology 29 (12), 1147–1150.

South African Committee for Stratigraphy (SACS) (1980). Stratigraphy of South Africa: part 1, Lithostratigraphy of the Republic of South Africa, South West Africa/Namibia and the Republic of Bophuthatswana, Transkei and Venda, Department of Mineral and Energy Affairs, Geological Survey, Pretoria

Snyman, C.P., (1998). Coal. In: Wilson, M.G.C., Anhaeusser, C.R. (Eds.), The Mineral Resources of South Africa. Handbook 16, Council for Geoscience, Pretoria, pp. 136–205.

Tankard, A., Welsink, H., Aukes, P., Newton, R. and Stettler, E. (2009).Tectonic evolution of the Cape and Karoo Basins of South Africa. *Marine and Petroleum Geology*, 26, pp 1379 – 1412.

Turner, B. R. (1975). The stratigaphy and sedimentology history of the Molteno Formation in the Main Karoo Basin of South Africa and Lesotho. Ph. D. Thesis (unpubl.), Univ. Witwatersrand, Johannesburg, pp 314.

Turner, B. R. (1978). Sedimentary patterns of Uranium mineralization in the Beaufort Group of the southern Karoo Basin of South Africa. In: Fluvial Sedimentology. (Edited by Mia U, A. D.) Merru Canad. Ass. Petrol. Geol. 5 859 pp., Toronto.

Turner, B. R. (1983). Braidplain deposition of the Upper Traissic Molteno Formation in the Main Karoo (Gondwana) Basin, South Africa. Sedimentology 30, pp 77 – 89.

Turner, B. R. and Thomson, K. (2005).Discussion on 'Basin development during deposition of the Elliot Formation (Late Triassic), Karoo Supergroup, South Africa' (South African Journal of Geology, 107, 397 – 412).*South African Journal of Geology*, 108, pp. 448 – 453.

Visser, H. N., and Van Der Merwe, S. W., (1959), The Northeastern SBF Coal Field: Records of bore-holes 1 to 27 drilled for the Department of Mines. Geological Survey, Bulletin 31, pp 1-97.

Walker, F. and Poldervaart, A. (1949).Karoo dolerites of the Union of South Africa. *Bull. Geol. Soc. Amer.,* **60,** 591-706.

Appendices

Appendix 1: Database Description

Collar File	
Column	**Description**
Status	Whether the borehole has been captured or un-captured
Seqno	The sequence number (CGS usage)
Farmname	Farm name
Farmno	Farm number
Regdist	Registered district
Boreholeid	Borehole ID number (CGS Given)
Company no	Original borehole number
Depth from	Depth of first rock intersection
End depth	End depth of the borehole
Drill date	Date that drilling was completed
Comments	General comments
Map	Map on which borehole is located (CGS usage)
Latitude	Latitude coordinate
Longitude	Longitude coordinate
Elevation	Elevation of Borehole
Lox	X Coordinate in LO Projection
Loy	Y Coordinate in LO Projection
Locunc	Location uncertainty
Declat	Declination Latitude WGS84
Declon	Declination Longitude WGS84

ithology File	
Column	**Description**
No	Entry number
Status	Whether the borehole has been captured or un-captured
Seqno	The sequence number (CGS usage)
Farmname	Farm name
Farmno	Farm number
Regdist	Registered district
Boreholeid	Borehole ID number (CGS Given)
Company no	Original borehole number
Depth from	Depth of beginning of interval
Depth to	Depth of end of interval
Lithology status	Lithology status where M: main P: coal particulars
Lithology	Lithology code (see appendix*)
Lithology description	Description of the lithology
Stratigraphy	Interpreted stratigraphy
Rank	Stratigraphy rank (Formation/Group/etc.)
Seam name	Coal seam name
Seam rank	Whether the interval is a coal zone or not

Analyses File	
Column	**Description**
Status	Whether the borehole has been captured or un-captured
Seqno	The sequence number (CGS usage)
Farmname	Farm name
Farmno	Farm number
Regdist	Registered district
Boreholeid	Borehole ID number (CGS Given)
Company no	Original borehole number
Seam name	Coal seam name
Seam rank	Whether the interval is a coal zone or not
Sample no	Sample number
Sample from	Depth at which sample was analysed from
Sample to	Depth at which sample was analysed to
Rd from	Analyses type, (Float/Sink/Raw)
Rd to	Analyses type, (Float/Sink/Raw)
Yield	Yield
CV	CV (%)
H2O	Moisture content (%)
Ash	Ash content (%)
Volatiles	Volatile content (%)
Fixed carbon	Fixed carbon content (%)
Sulphur	Sulphur content (%)
Swell	Free-Swelling Index
Roga	Roga Index (0 – 100) Good > 60
Phos	Phosphorous content (%)

Appendix 2: Lithological Code

The database that was provided by the CGS used the codes from table * for a brief description of the logs. These codes were used in the construction of the borehole logs used in the analyses.

Lithology Code	Lithology Name	Parent Code	Parent Name
ALFGR	Alkali-Feldspar Granite	GRNTD	Granitoid
ALFQS	Alkali-Feldspar Quartz Syenite	SYNTD	Syenitoid
ALFSY	Alkali-Feldspar Syenite	SYNTD	Syenitoid
ALRHY	Alkali Feldspar Rhyolite	RHYLT	Rhyolitoid
ALTRC	Alkali Feldspar Trachyte	TRACH	Trachytoid
ALVKT	Alvikite	CACAR	Calcite-Carbonatite
AMPBL	Amphibolite	MET	Metamorphic Rocks
ANDES	Andesite	BSLTD	Basaltoid
ANDST	Andesitoid	VLC	Volcanic Rocks
ANRTS	Anorthosite	PLU	Plutonic Rocks
APLIT	Aplite	PLU	Plutonic Rocks
ARLUT	Arenaceous Lutite	SIL	Siliciclastic Sediments
ARNIT	Arenite	SIL	Siliciclastic Sediments
ARNRD	Arenaceous Rudite	SIL	Siliciclastic Sediments
BASLT	Basalt	BSLTD	Basaltoid
BASNT	Basanite	TEPHR	Tephritoid
BAUX	Bauxite	RESDP	Residual Deposits
BEFOR	Beforsite	DCCAR	Dolomite-Calcite Carbonatite
BIOL	Biolithite	CBNAT	Carbonate Rock
BIRBR	Birbirite	RESDP	Residual Deposits
BLDRS	Boulders	NROCK	Non-Rock Lithologies
BLUSC	Blueschist	MET	Metamorphic Rocks
BMDST	Breccia Mudstone	SIL	Siliciclastic Sediments
BREC	Breccia	SIL	Siliciclastic Sediments
BSLTD	Basaltoid	VLC	Volcanic Rocks
BSST	Breccia Sandstone	SIL	Siliciclastic Sediments
CACAR	Calcite-Carbonatite	CRBNT	Carbonatite
CALAR	Calciarenite	LIMST	Limestone
CALCR	Calcrete	RESDP	Residual Deposits
CALLU	Calcilutite	LIMST	Limestone
CALRD	Calcirudite	LIMST	Limestone
CANEL	Cannel Coal	COALS	Coaly Sediment
CARN	Coarse Arenite	SIL	Siliciclastic Sediments
CARSH	Carbonaceous Shale	CHE	Chemical And Biochemical Sediments
CATCL	Cataclastite	MET	Metamorphic Rocks
CAVIT	Cavity	NROCK	Non-Rock Lithologies
CBNAT	Carbonate Rock	CHE	Chemical And Biochemical Sediment
CDCAR	Calcite-Dolomite Carbonatite	CRBNT	Carbonatite
CGL	Conglomerate	SIL	Siliciclastic Sediments
CHARN	Charnockite	MET	Metamorphic Rocks
CHE	Chemical And Biochemical Sediments	SED	Sedimentary
CHERT	Chert	NONCB	Non-Carbonate Chemical And Biochemical Sediments
CHROM	Chromitite	PLU	Plutonic Rocks
CLAY	Clay	UNCD	Unconsolidated Detrital Sediments
CLCSL	Calc-Silicate Rock	MET	Metamorphic Rocks

Lithology Code	Lithology Name	Parent Code	Parent Name
CLINP	Clinopyroxenite	PYRXN	Pyroxenite
CLSTS	Claststone	CHE	Chemical And Biochemical Sediments
CLYST	Claystone	SIL	Siliciclastic Sediments
CMDST	Conglomeratic Mudstone	SIL	Siliciclastic Sediments
COAL	Coal	COALS	Coaly Sediment
COALS	Coaly Sediment	CHE	Chemical And Biochemical Sediments
COLSH	Coaly Shale/Mudstone/Siltstone	CHE	Chemical And Biochemical Sediments
CONCR	Concrete	MAN	Man-Made
CRBNT	Carbonatite	PLU	Plutonic Rocks
CRUSH	Crushed Rock	MAN	Man-Made
CSST	Conglomeratic Sandstone	SIL	Siliciclastic Sediments
CTUFF	Coarse Tuff	PCL	Pyroclastic
DACT	Dacite	DACTD	Dacitoid
DACTD	Dacitoid	VLC	Volcanic Rocks
DCCAR	Dolomite-Calcite Carbonatite	CRBNT	Carbonatite
DIAMT	Diamictite	SIL	Siliciclastic Sediments
DIATE	Diatomite	NONCB	Non-Carbonate Chemical And Biochemical Sediments
DIORT	Dioritoid	PLU	Plutonic Rocks
DIRIT	Diorite	DIORT	Dioritoid
DOCAR	Dolomite Carbonatite	CRBNT	Carbonatite
DOLAR	Dolarenite	CBNAT	Carbonate Rock
DOLCR	Dolocrete	RESDP	Residual Deposits
DOLMT	Dolomite	CBNAT	Carbonate Rocks
DOLRD	Dolorudite	DOLMT	Dolomite
DOLRT	Dolerite	PLU	Plutonic Rocks
DOLUT	Dololutite	DOLMT	Dolomite
DORB	Dorbank	PED	Pedological Sediments
DSTNT	Disthenite	MET	Metamorphic Rocks
DSULF	Disseminated Sulphide	VOR	Vein / Ore Rock
DUNIT	Dunite	PERDT	Peridotite
ECLGT	Eclogite	MET	Metamorphic Rocks
EHOR	E Horizon	PED	Pedological Sediments
EMERY	Emery Rock	MET	Metamorphic Rocks
EPDRT	Epidiorite	MET	Metamorphic Rocks
EPDST	Epidosite	MET	Metamorphic Rocks
EVPRT	Evaporite	CHE	Chemical And Biochemical Sediments
FALBD	Fahlband		
FARN	Fine Arenite	SIL	Siliciclastic Rocks
FBAFS	Foid-Bearing Alkali-Feldspar Syenite	FOIDS	Foid Syenitoid
FBATR	Foid-Bearing Alkali Feldspar Trachyte	TRACH	Trachytoid
FBDRT	Foid-Bearing Diorite	FOIDD	Foid Dioritoid
FBGAB	Foid-Bearing Gabbro	FOIDG	Foid Gabbroid
FBLAT	Foid-Bearing Latite	TRACH	Trachytoid
FBMDT	Foid-Bearing Monzodiorite	FOIDD	Foid Dioritoid
FBMGB	Foid-Bearing Monzogabbro	FOIDG	Foid Gabbroid
FBMNT	Foid-Bearing Monzonite	FOIDS	Foid Syenitoid
FBSYN	Foid-Bearing Syenite	FOIDS	Foid Syenitoid
FBTRC	Foid-Bearing Trachyte	TRACH	Trachytoid
FECAR	Ferrocarbonatite	CRBNT	Carbonatite
FELST	Felsite	VLC	Volcanic Rocks

Lithology Code	Lithology Name	Parent Code	Parent Name
FELUT	Felutite	NONCB	Non-Carbonate Chemical And Biochemical Sediments
FERCT	Ferruginous Chert	CHE	Chemical And Biochemical Rocks
FERHM	Ferhythmite	NONCB	Non-Carbonate Chemical And Biochemical Sediments
FIBRC	Fibric Peat	PEAT	Peat
FILL	Fill	MAN	Man-Made
FLOST	Flowstone	CBNAT	Carbonate Rocks
FMDRT	Foid Monzodiorite	FOIDD	Foid Dioritoid
FMGAB	Foid Monzogabbro	FOIDG	Foid Gabbroid
FMSYN	Foid Monzosyenite	FOIDS	Foid Syenitoid
FOID	Foidite	FOIDT	Foiditoid
FOIDD	Foid Dioritoid	PLU	Plutonic Rocks
FOIDG	Foid Gabbroid	PLU	Plutonic Rocks
FOIDL	Foidolite	PLU	Plutonic Rocks
FOIDS	Foid Syenitoid	PLU	Plutonic Rocks
FOIDT	Foiditoid	VLC	Volcanic Rocks
FRRCR	Ferricrete	RESDP	Residual Deposits
FSYN	Foid Syenite	FOIDS	Foid Syenitoid
FTUFF	Fine Tuff	PLC	Pyroclastic
GABNR	Gabbronorite	GBBRD	Gabbroid
GABRO	Gabbro	GBBRD	Gabbroid
GARNT	Garnetite	MET	Metamorphic Rocks
GBBRD	Gabbroid	PLU	Plutonic Rocks
GHOR	G Horizon	PED	Pedological Sediments
GNEIS	Gneiss	MET	Metamorphic Rocks
GONDT	Gondite	MET	Metamorphic Rocks
GOSSN	Gossan	RESDP	Residual Deposits
GRANT	Granite	GRNTD	Granitoid
GRAVL	Gravel	UNCD	Unconsolidated Detrital Sediments
GREIS	Greisen	VOR	Vein / Ore Rock
GRNDT	Granodiorite	GRNTD	Granitoid
GRNFS	Granofels	MET	Metamorphic Rocks
GRNLT	Granulite	MET	Metamorphic Rocks
GRNSC	Greenschist	MET	Metamorphic Rocks
GRNTD	Granitoid	PLU	Plutonic Rocks
GSTON	Greenstone	MET	Metamorphic Rocks
GYPCR	Gypcrete	RESDP	Residual Deposits
H1	H1	FIBRC	Fibric Peat
H10	H10	SAPRC	Sapric Peat
H2	H2	FIBRC	Fibric Peat
H3	H3	FIBRC	Fibric Peat
H4	H4	FIBRC	Fibric Peat
H5	H5	HEMIC	Hemic Peat
H6	H6	HEMIC	Hemic Peat
H7	H7	HEMIC	Hemic Peat
H8	H8	SAPRC	Sapric Peat
H9	H9	SAPRC	Sapric Peat
HARDP	Hardpan Carbonate Horizon	PED	Pedological Sediments
HARZB	Harzburgite	PERDT	Peridotite
HBGAB	Hornblende Gabbro	GBBRD	Gabbroid

Lithology Code	Lithology Name	Parent Code	Parent Name
HBPER	Hornblende Peridotite	PERDT	Peridotite
HBPYX	Hornblende Pyroxenite	PYRXN	Pyroxenite
HEMIC	Hemic Peat	PEAT	Peat
HRNBL	Hornblendite	PLU	Plutonic Rocks
HRNFS	Hornfels	MET	Metamoephic Sediments
HUMA	Humic A Horizon	PED	Pedological Sediments
ICE	Ice	WATER	Water
IGN	Igneous Rocks		
IGNIM	Ignimbrite	PCL	Pyroclastic
IRNFM	Iron Formation	NONCB	Non-Carbonate Chemical And Biochemical Sediments
IRNST	Ironstone	CHE	Chemical And Biochemical Sediment
ITBRT	Itabirite	MET	Metamorphic Rocks
JADTT	Jadeitite	MET	Metamorphic Rocks
KIMBR	Kimberlite	PLU	Plutonic Rocks
KOMTT	Komatiite	VLC	Volcanic Rocks
KRTPR	Keratophyre	VLC	Volcanic Rocks
KZGT	Kinzigite	MET	Metamorphic Rocks
LAMPR	Lamprophyre	PLU	Plutonic Rocks
LATIT	Latite	TRACH	Trachytoid
LAVA	Lava	VLC	Volcanic Rocks
LCB	Lithocutanic B Horizon	PED	Pedological Sediments
LDFLL	Landfill	MAN	Man-Made
LEACH	Leachate	RESDP	Residual Deposits
LEPTT	Leptite	MET	Metamorphic Rocks
LHERZ	Lherzolite	PERDT	Peridotite
LIGNT	Lignite	COALS	Coaly Sediment
LIMGT	Limburgite	VLC	Volcanic Rocks
LIMST	Limestone	CBNAT	Carbonate Rocks
LPLTF	Lappilli Tuff	PLC	Pyroclastic
LUARD	Lutaceous Arenaceous Rudite	SIL	Siliciclastic Sediments
LUTAR	Lutaceous Arenite	SIL	Siliciclastic Sediments
LUTIT	Lutite	SIL	Siliciclastic Sediments
LUTRD	Lutaceous Rudite	SIL	Siliciclastic Sediments
MAN	Man-Made	NROCK	Non-Rock Lithologies
MANGN	Manganese Nodules	VOR	Vein / Ore Rock
MANRT	Meta-Anorthosite	MET	Metamorphic Rocks
MARBL	Marble	MET	Metamorphic Rocks
MARN	Medium Arenite	SIL	Siliciclastic Rocks
MARNT	Meta-Arenite	MET	Metamorphic Rocks
MBAST	Meta-Basite	MET	Metamorphic Rocks
MBREC	Muddy Breccia	SIL	Siliciclastic Rocks
MCARB	Meta-Carbonate	MET	Metamorphic Rocks
MCGL	Muddy Conglomerate	SIL	Siliciclastic Sediments
MDIOR	Monzodiorite	DIORT	Dioritoid
MDST	Mudstone	SIL	Siliciclastic Sediments
MELA	Melanic A Horizon	PED	Pedological Sediments
MET	Metamorphic Rocks		
METAN	Meta-Anorthosite	MET	Metamorphic Rocks
MGAB	Monzogabbro	GBBRD	Gabbroid
MGCRT	Magnesicrete	RESDP	Residual Deposits

Lithology Code	Lithology Name	Parent Code	Parent Name
MGNET	Magnetitite	PLU	Plutonic Rocks
MHNBD	Meta Hornblendite	MET	Metamorphic Rocks
MIGMT	Migmatite	MET	Metamorphic Rocks
MLLTT	Melilitite	VLC	Volcanic Rocks
MLTOL	Melilitolite	PLU	Plutonic Rocks
MLUTT	Meta-Lutite	MET	Metamorphic Rocks
MNCRT	Manganocrete	RESDP	Residual Deposits
MONZ	Monzonite	SYNTD	Syenitoid
MSULF	Massive Sulphide	VOR	Vein / Ore Rock
MTASM	Metasomatite	MET	Metamorphic Rocks
MTBST	Metabasite	MET	Metamorphic Rocks
MTSED	Metasedimentary Rocks	MET	Metamorphic Rocks
MTVOL	Metavolcanic Rocks	MET	Metamorphic Rocks
MUD	Mud	UNCD	Unconsolidated Detrital Sediments
MYLON	Mylonite	MET	Metamorphic Rocks
NACAR	Natrocarbonatite	CRBNT	Carbonatite
NCARB	Neocarbonate B Horizon	PED	Pedological Sediments
NCUTB	Neocutanic B Horizon	PED	Pedological Sediments
NONCB	Non-Carbonate Chemical And Biochemical Sediments	CHE	Chemical And Biochemical Sediments
NOR	Not Recorded, Overburden		
NORIT	Norite	GBBRD	Gabbroid
OBSDN	Obsidian	VLC	Volcanic Rocks
OILSH	Oil Shale	COALS	Coaly Sediment
OLCLN	Olivine Clinopyroxenite	PYRXN	Pyroxenite
OLGAB	Olivine Gabbro	GBBRD	Gabbroid
OLGBN	Olivine Gabbronorite	GBBRD	Gabbroid
OLHB	Olivine Hornblendite	HRNBL	Hornblendite
OLHPY	Olivine-Hornblende Pyroxenite	PYRXN	Pyroxenite
OLNOR	Olivine Norite	GBBRD	Gabbroid
OLOPY	Olivine Orthopyroxenite	PYRXN	Pyroxenite
OLPHY	Olivine-Pyroxene Hornblendite	HRNBL	Hornblendite
OLWEB	Olivine Websterite	PYRXN	Pyroxenite
OOZE	Ooze	UNCC	Unconsolidated Chemical Sediments
ORGO	Organic O Horizon	PED	Pedological Sediments
ORTHA	Orthic A Horizon	PED	Pedological Sediments
ORTPY	Orthopyroxenite	PYRXN	Pyroxenite
PBDUN	Plagioclase-Bearing Dunite	PERDT	Peridotite
PBHRZ	Plagioclase-Bearing Harzburgite	PERDT	Peridotite
PBLHZ	Plagioclase-Bearing Lherzolite	PERDT	Peridotite
PBOCP	Plagioclase-Bearing Olivine Clinopyroxenite	PYRXN	Pyroxenite
PBOOP	Plagioclase-Bearing Olivine Orthopyroxenite	PYRXN	Pyroxenite
PBOPX	Plagioclase-Bearing Orthopyroxenite	PYRXN	Pyroxenite
PBOWB	Plagioclase-Bearing Olivine Websterite	PYRXN	Pyroxenite
PBPYZ	Plagioclase-Bearing Pyroxenite	PYRXN	Pyroxenite
PBREC	Pyroclastic Breccia	PCL	Pyroclastic
PBWEB	Plagioclase-Bearing Websterite	PYRXN	Pyroxenite
PBWHL	Plagioclase-Bearing Wehrlite	PERDT	Peridotite
PCB	Prismacutanic B Horizon	PED	Pedological Sediments

Lithology Code	Lithology Name	Parent Code	Parent Name
PCL	Pyroclastic		
PEAT	Peat	CHE	Chemical And Biochemical Sediments
PED	Pedological Sediments	SED	Sedimentary
PEDCB	Pedocutanic B Horizon	PED	Pedological Sediments
PEGM	Pegmatite	PLU	Plutonic Rocks
PELTE	Pelite	MET	Metamorphic Rocks
PERDT	Peridotite	PLU	Plutonic Rocks
PHFDT	Phonolitic Foidite	FOIDT	Foiditoid
PHGAB	Pyroxene-Hornblende Gabbro	GBBRD	Gabbroid
PHNLD	Phonolitoid	VLC	Volcanic Rocks
PHNLT	Phonolite	PHNLD	Phonolitoid
PHNOR	Pyroxene-Hornblende Norite	GBBRD	Gabbroid
PHONL	Phonolite	PHNLD	Phonolitoid
PHOSC	Phoscrete	RESDP	Residual Deposits
PHOSP	Phosphorite	NONCB	Non-Carbonate Chemical And Biochemical Sediments
PHPER	Pyroxene-Hornblende Peridotite	PERDT	Peridotite
PHTEP	Phonolitic Tephrite	TEPHR	Tephritoid
PHYLT	Phyllite	MET	Metamorphic Rocks
PLNTT	Plinthite	RESDP	Residual Deposits
PLU	Plutonic Rocks		
PODZB	Podzol B Horizon	PED	Pedological Sediments
PSMMT	Psammite	MET	Metamorphic Rocks
PSPHT	Psephite	MET	Metamorphic Rocks
PYHB	Pyroxene Hornblendite	HRNBL	Hornblendite
PYRXN	Pyroxenite	PLU	Plutonic Rocks
QANTH	Quartz Anorthosite	ANRTS	Anorthosite
QATR	Quartz-Alkali Feldspar Trachyte	TRACH	Trachytoid
QDIOR	Quartz Diorite	DIORT	Dioritoid
QGAB	Quartz Gabbro	GBBRD	Gabbroid
QGRAN	Quartz-Rich Granitoid	PLU	Plutonic Rocks
QLAT	Quartz Latite	TRACH	Trachytoid
QMDR	Quartz Monzo-Diorite	DIORT	Dioritoid
QMGAB	Quartz Monzogabbro	GBBRD	Gabbroid
QMONZ	Quartz Monzonite	SYNTD	Syenitoid
QRTZ	Quartzite	MET	Metamorphic Rocks
QRTZL	Quartzolite	PLU	Plutonic Rocks
QRTZT	Quartzite	MET	Metamorphic Rocks
QSYN	Quartz Syenite	SYNTD	Syenitoid
QTRAC	Quartz Trachyte	TRACH	Trachytoid
RALUT	Rudaceous Arenaceous Lutite	SIL	Siliciclastic Sediments
RAPB	Red Apedal B Horizon	PED	Pedological Sediments
RAPGT	Rapakivi Granite	PLU	Plutonic Rocks
REGIC	Regic Sand	UNCD	Unconsolidated Detrital Sediments
RESDP	Residual Deposits	PED	Pedological Sediments
RHYDT	Rhyodacite	VLC	Volcanic Rocks
RHYLT	Rhyolitoid	VLC	Volcanic Rocks
RHYOL	Rhyolite	RHYLT	Rhyolitoid
RSB	Red Structured B Horizon	PED	Pedological Sediments
RUBLE	Rubble	MAN	Man-Made
RUDAR	Rudaceous Arenite	SIL	Siliciclastic Sediments

Lithology Code	Lithology Name	Parent Code	Parent Name
RUDIT	Rudite	SIL	Siliciclastic Sediments
RUDLA	Rudaceous Lutaceous Arenite	SIL	Siliciclastic Sediments
RUDLT	Rudaceous Lutite	SIL	Siliciclastic Sediments
SAND	Sand	UNCD	Unconsolidated Detrital Sediments
SAPEL	Sapropelite	COALS	Coaly Sediment
SAPRC	Sapric Peat	PEAT	Peat
SAPRL	Saprolite	RESDP	Residual Deposits
SBREC	Sandy Breccia	SIL	Siliciclastic Sediments
SCARH	Soft Carbonate Horizon	PED	Pedological Sediments
SCGL	Sandy Conglomerate	SIL	Siliciclastic Sediments
SCHST	Schist	MET	Metamorphic Rocks
SED	Sedimentary		
SGRAN	Syenogranite	PLU	Plutonic Rocks
SHALE	Shale	SIL	Siliciclastic Sediments
SIL	Siliciclastic Sediment	SED	Sedimentary
SILCR	Silcrete	RESDP	Residual Deposits
SILT	Silt	UNCD	Unconsolidated Detrital Sediments
SINTR	Sinter	NONCB	Non-Carbonate Chemical And Biochemical Sediments
SLATE	Slate	MET	Metamorphic Rocks
SLTST	Siltstone	SIL	Siliciclastic Sediments
SOAPS	Soapstone	MET	Metamorphic Rocks
SOIL	Soil	PED	Pedological Sediments
SOVIT	Sovite	CACAR	Calcite-Carbonatite
SPB	Soft Plinthic B Horizon	PED	Pedological Sediments
SPEL	Speleothem	CHE	Chemical And Biochemical Sediment
SPH	Hard Plinthic B Horizon	PED	Pedological Sediments
SPILT	Spilite	VLC	Volcanic Rocks
SRALU	Slightly Rudaceous Arenaceous Lutite	SIL	Siliciclastic Sediments
SRARN	Slightly Rudaceous Arenite	SIL	Siliciclastic Sediments
SRLAR	Slightly Rudaceous Lutaceous Arenite	SIL	Siliciclastic Sediments
SRLUT	Slightly Rudaceous Lutite	SIL	Siliciclastic Sediments
SRPTN	Serpentinite	MET	Metamorphic Rocks
SSHOR	Subsoil Horizons	PED	Pedological Sediments
STROM	Stromatolite	CBNAT	Carbonate Rocks
SYEN	Syenite	SYNTD	Syenitoid
SYNTD	Syenitoid	PLU	Plutonic Rocks
TBNIT	Torbanite	COALS	Coaly Sediment
TBREC	Tuff Breccia	PCL	Pyroclastic
TEPHR	Tephritoid	VLC	Volcanic Rocks
THROM	Thrombolite	CBNAT	Carbonate Rock
TILLT	Tillite	SIL	Siliciclastic Rocks
TONAL	Tonalite	GRNTD	Granitoid
TPFDT	Tephritic Foidite	FOIDT	Foiditoid
TPHON	Tephritic Phonolite	PHNLD	Phonolitoid
TPHRT	Tephrite	TEPHR	Tephritoid
TRACH	Trachytoid	VLC	Volcanic Rocks
TRACT	Trachyte	TRACH	Trachytoid
TRAVT	Travertine	CHE	Chemical And Biochemical Sediments
TRHJT	Trondhjemite	PLU	Plutonic Rocks
TROCT	Troctolite	GBBRD	Gabbroid

Lithology Code	Lithology Name	Parent Code	Parent Name
TSHOR	Topsoil Horizons	PED	Pedological Sediments
TUFA	Tufa	CBNAT	Carbonate Rock
TUFF	Tuff	PCL	Pyroclastic
ULMFT	Ultramafitite	VLC	Volcanic Rocks
ULTRM	Ultramafic Rocks	PLU	Plutonic Rocks
UNAKT	Unakite	MET	Metamorphic Rocks
UNC	Unconsolidated Sediments		
UNCC	Unconsolidated Chemical Sediment	UNC	Unconsolidated Sediments
UNCD	Unconsolidated Detrital Sediment	UNC	Unconsolidated Sediments
UTMAF	Ultramafitite	VLC	Volcanic Rocks
UTMOL	Ultramafitolite	PLU	Plutonic Rocks
VEIN	Vein	VOR	Vein / Ore Rock
VERTA	Vertic A Horizon	PED	Pedological Sediments
VLC	Volcanic Rocks		
VOR	Vein / Ore Rock		
WAD	Wad	RESDP	Residual Deposits
WATER	Water	NROCK	Non-Rock Lithologies
WEB	Websterite	PYRXN	Pyroxenite
WEHR	Wehrlite	PERDT	Peridotite
XLDOL	Crystalline Dolomite	CBNAT	Carbonate Rocks
YBAPB	Yellow Brown Apedal B Horizon	PED	Pedological Sediments

Appendix 3: Structural Contour Maps

Appendix 4: Isopach Contour Maps

Appendix 5: Multicomponent Maps

Appendix 6: Lithological Logs

Appendix 7: Coal Zone Lithological Logs and Analyses

Structural Contour Map
Hammanskraal

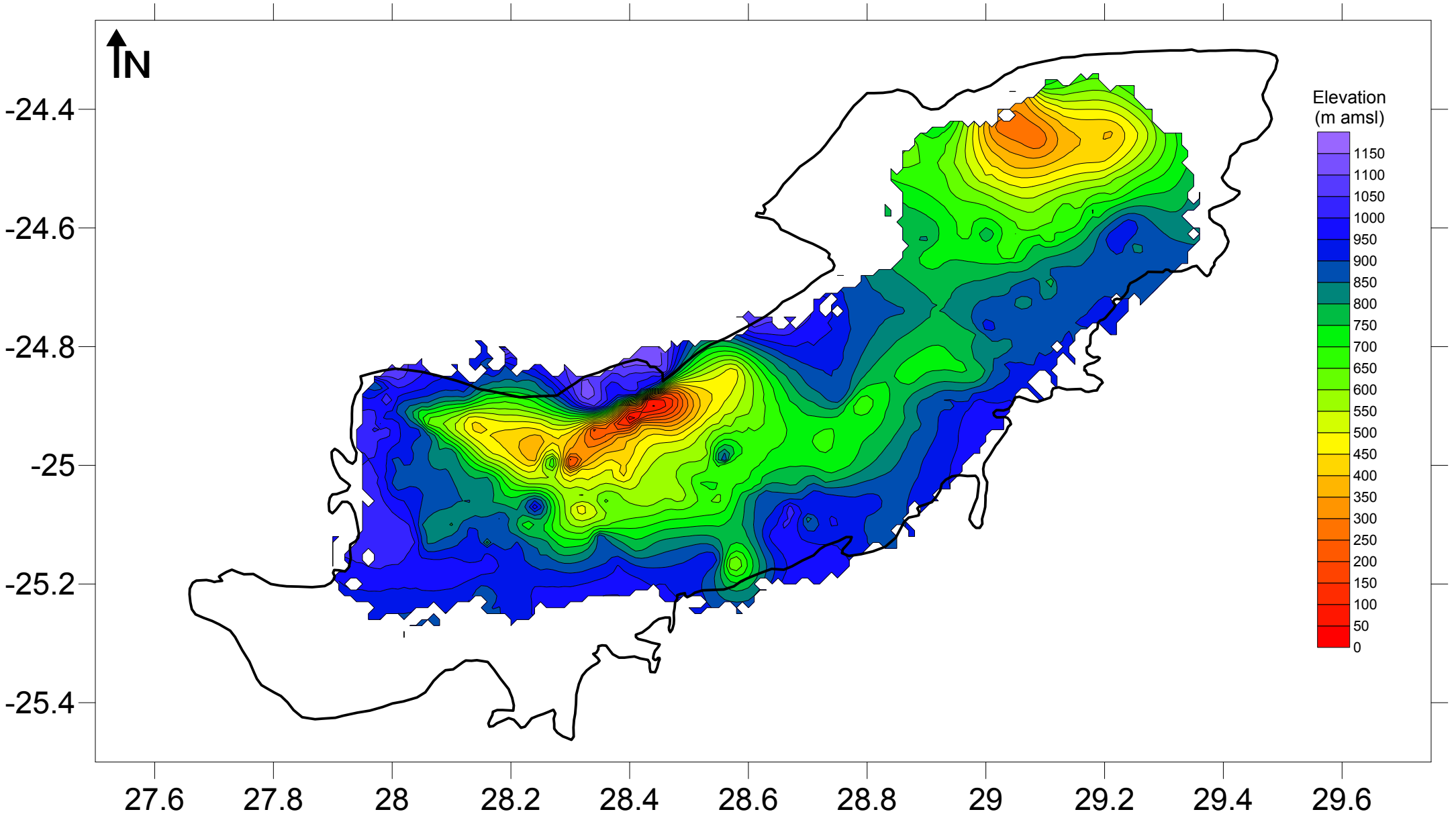

Structural Contour Map
Irrigasie

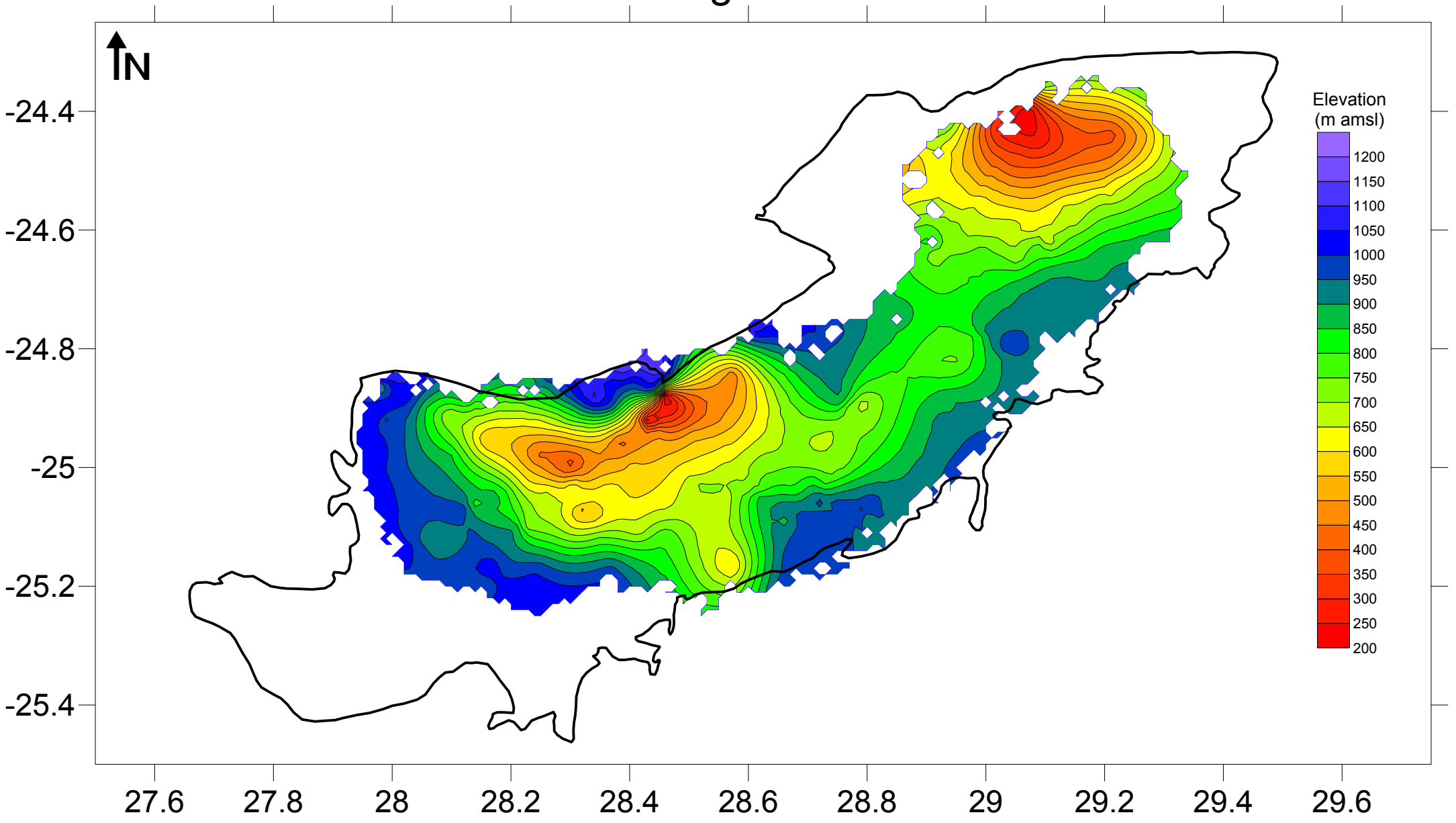

Structural Contour Map
Molteno

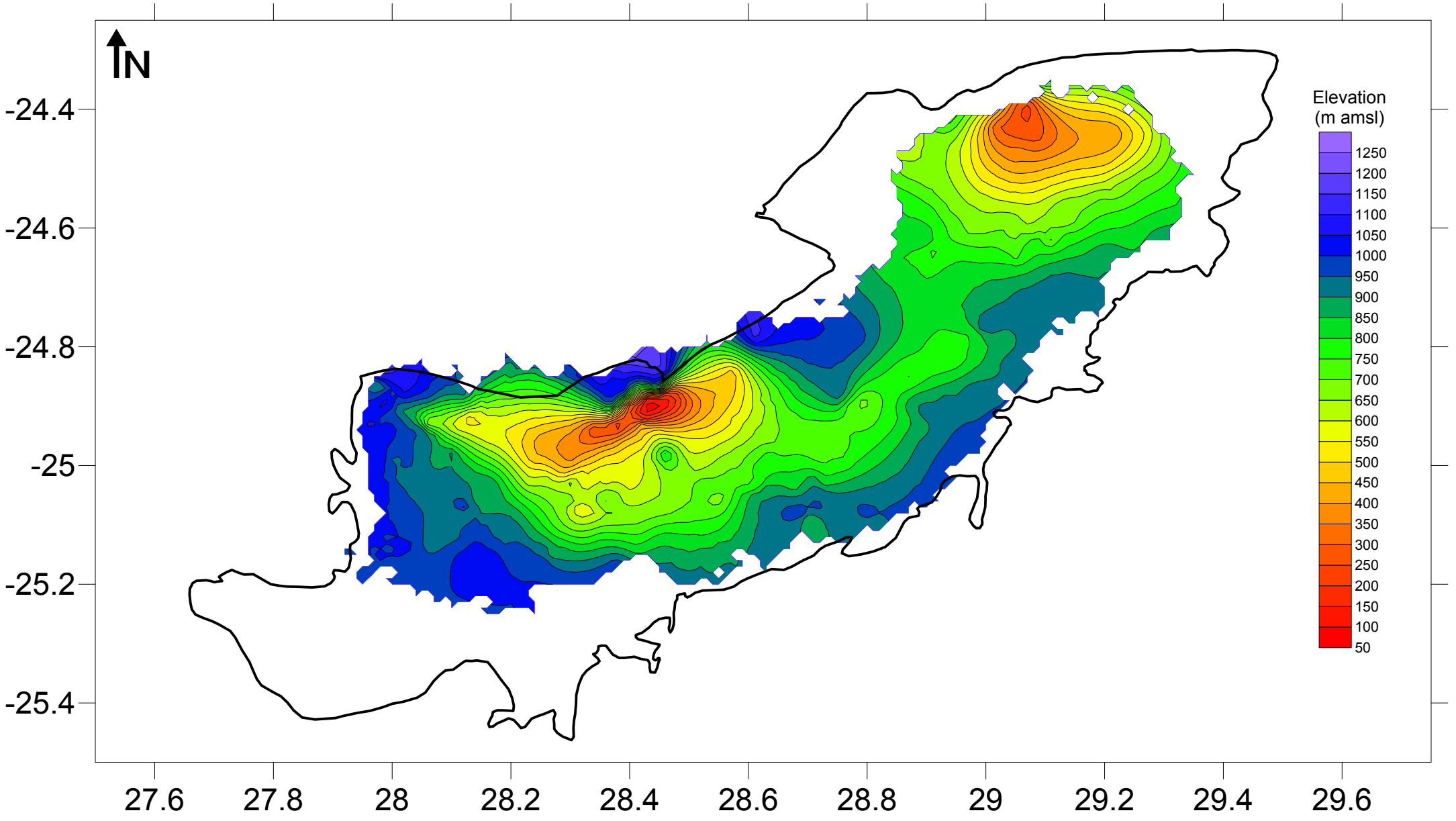

Structural Contour Map
Elliot

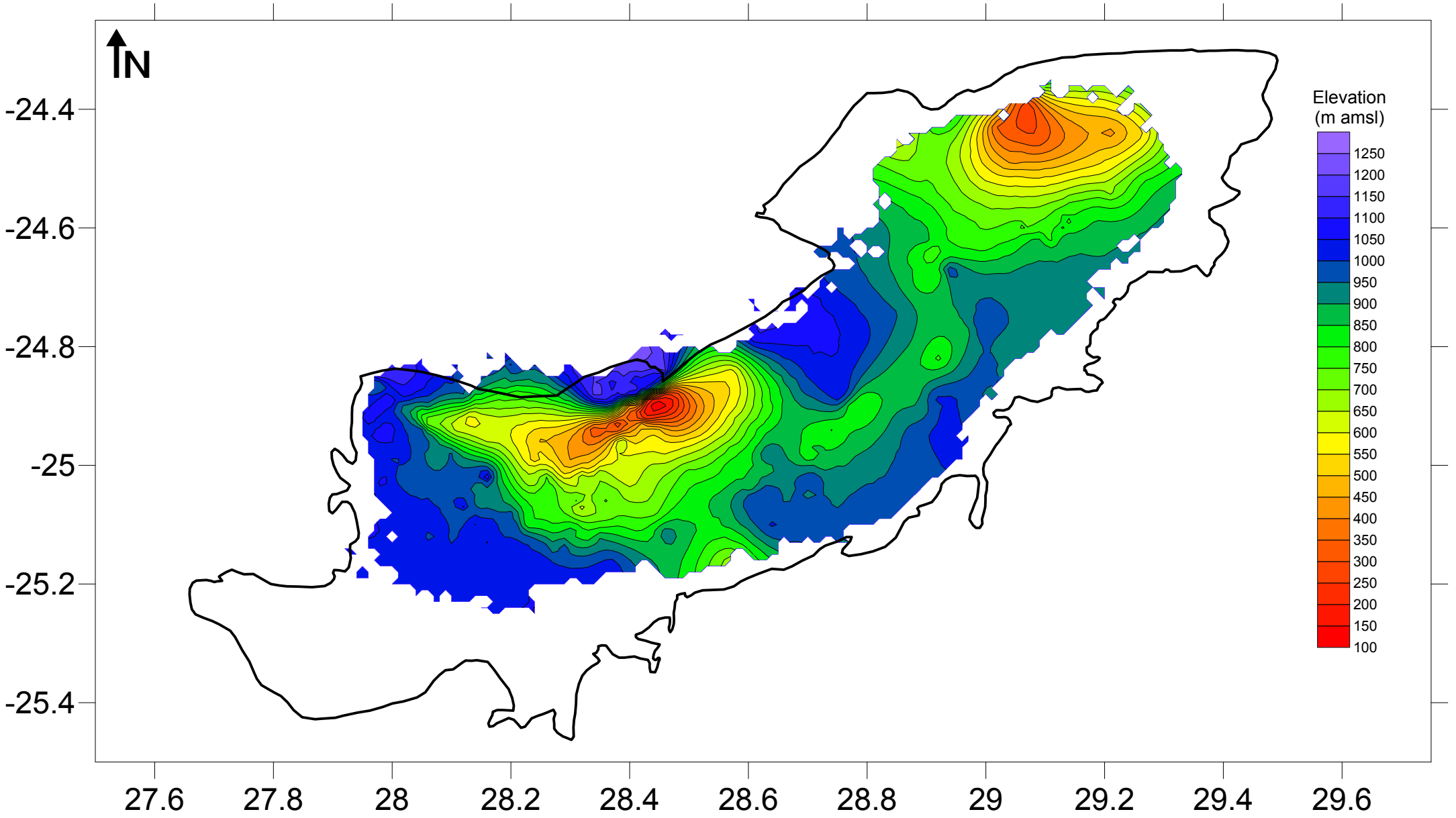

Structural Contour Map
Clarens

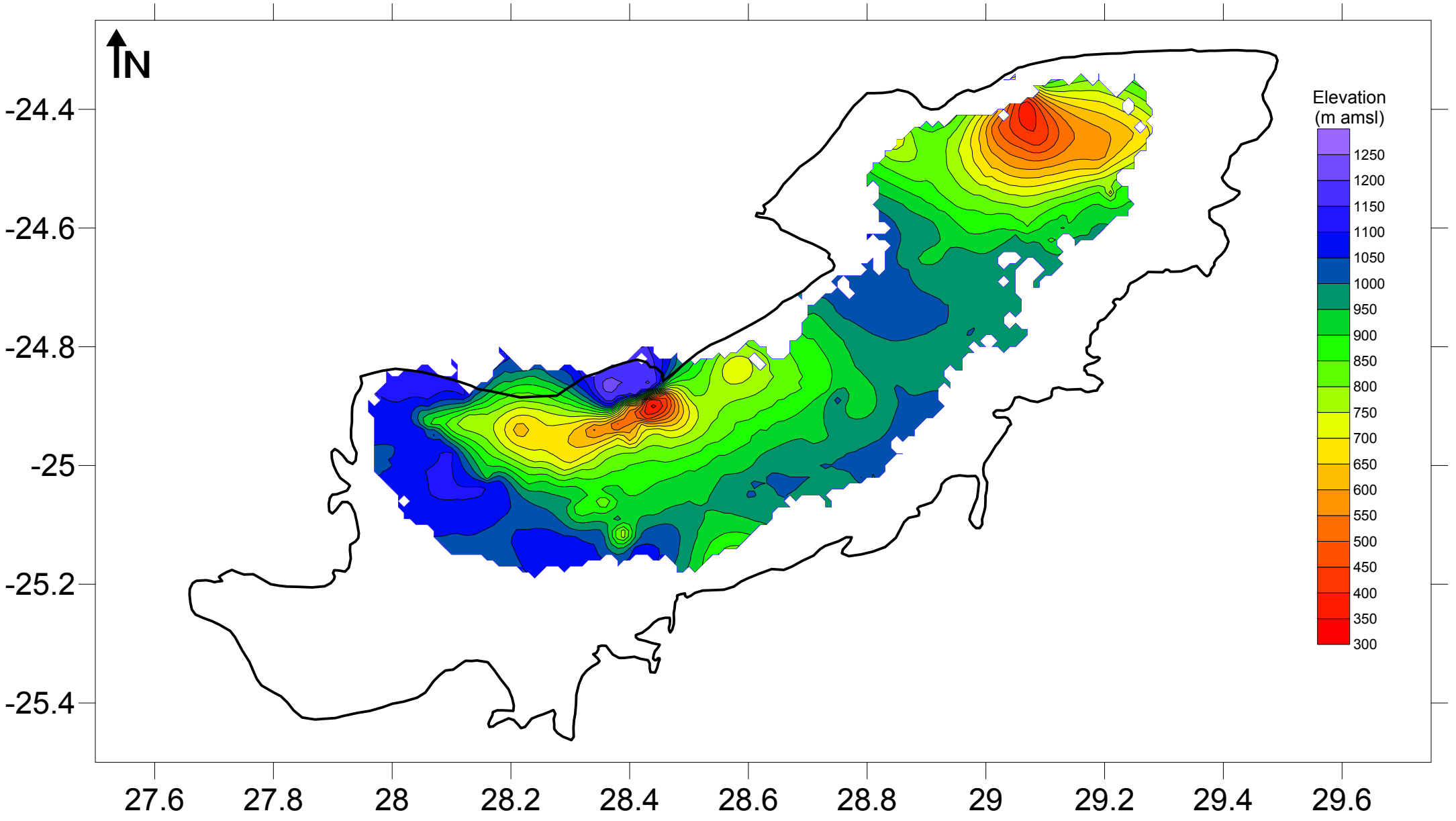

Structural Contour Map
Letaba

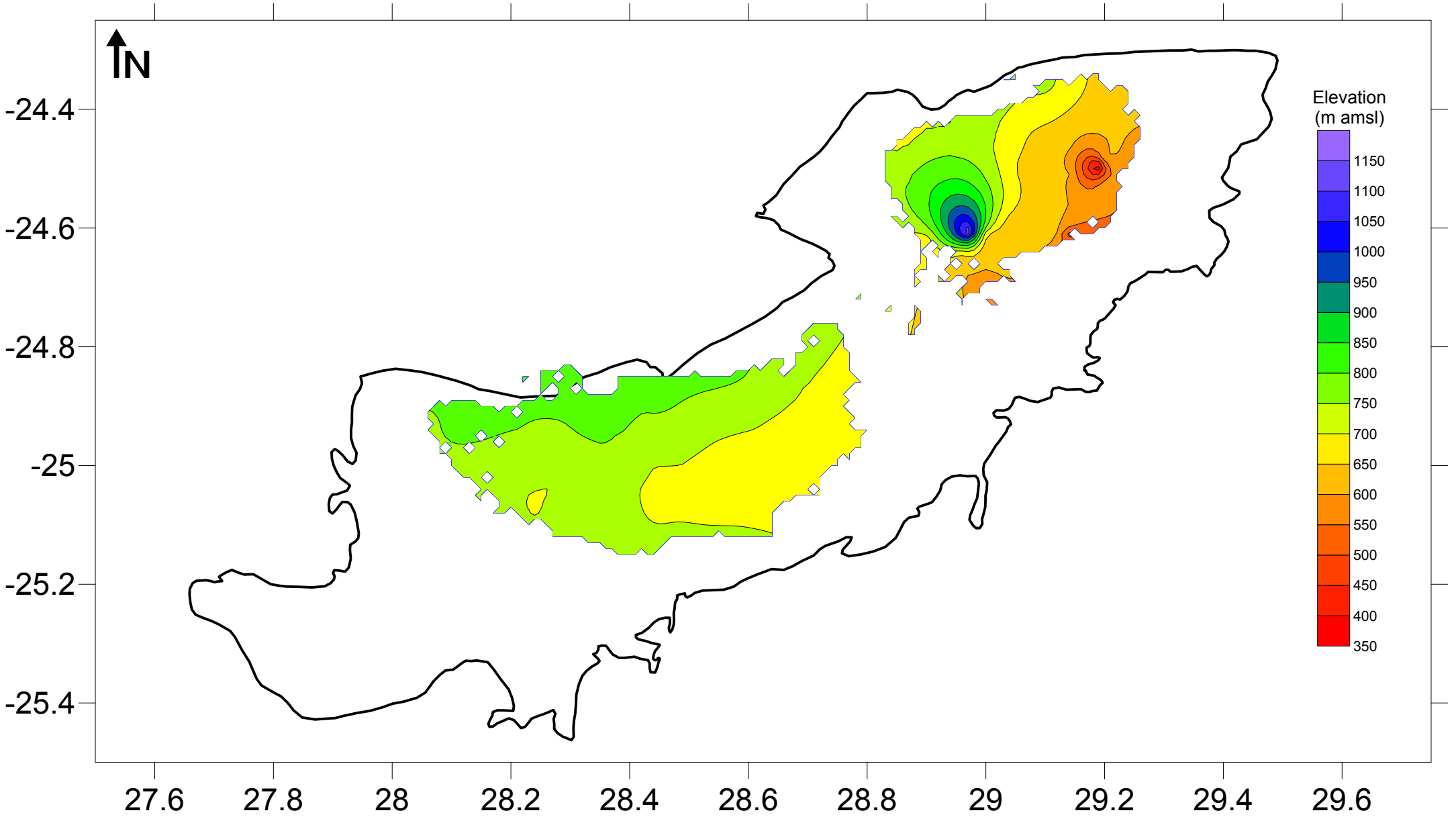

Isopach Contour Map
Hammanskraal

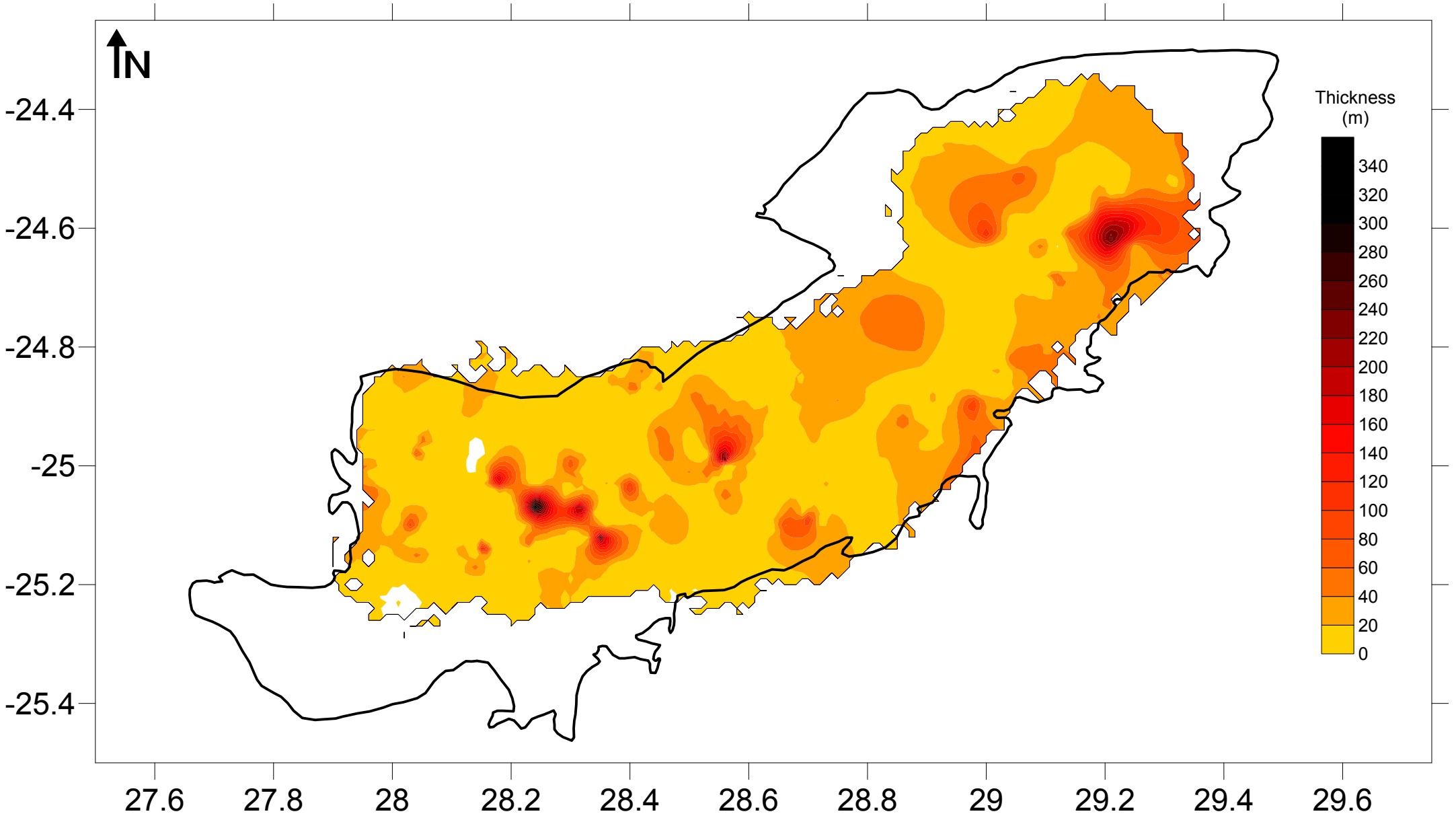

Isopach Contour Map
Irrigasie

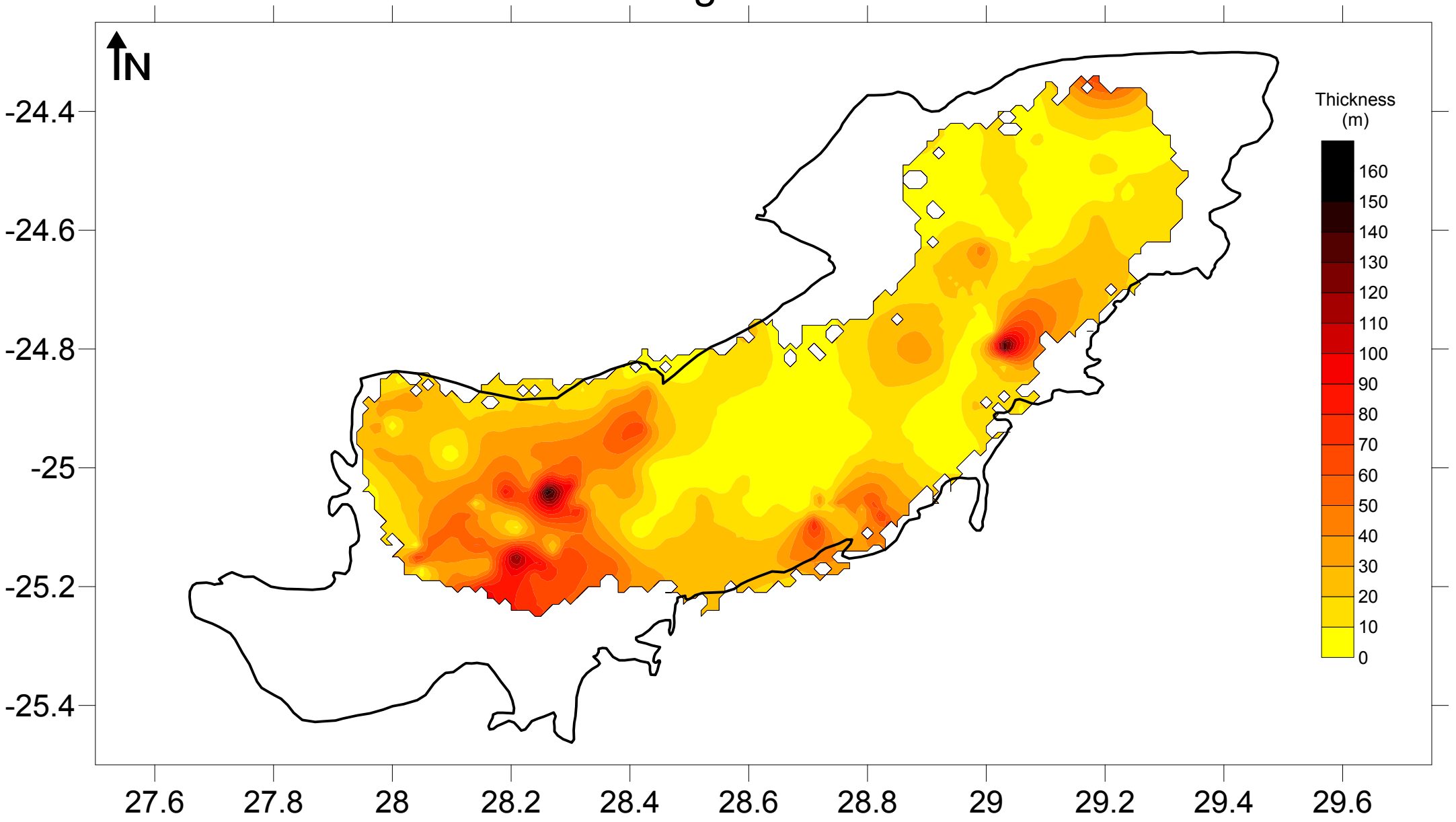

Isopach Contour Map
Molteno

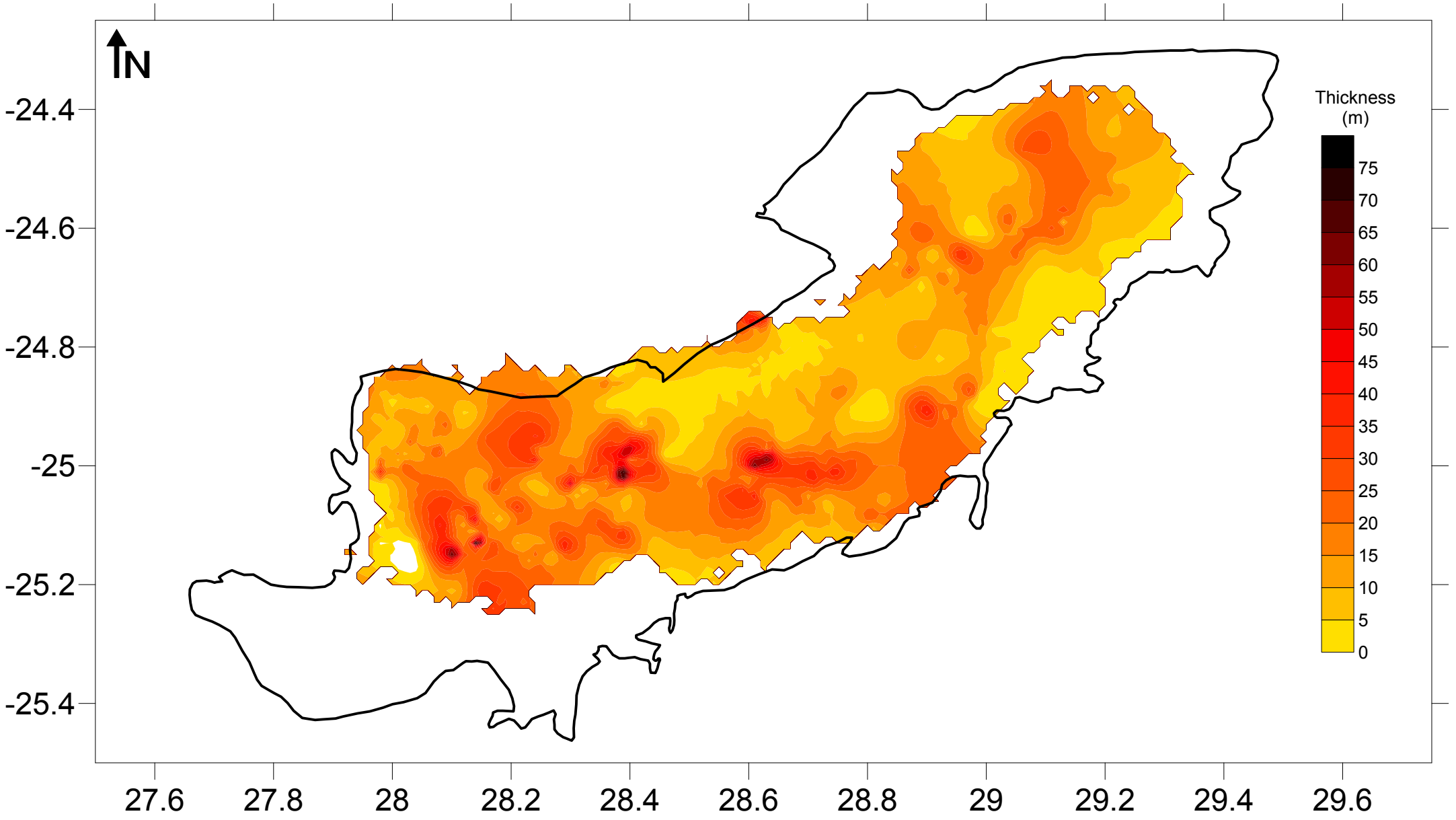

Isopach Contour Map
Elliot

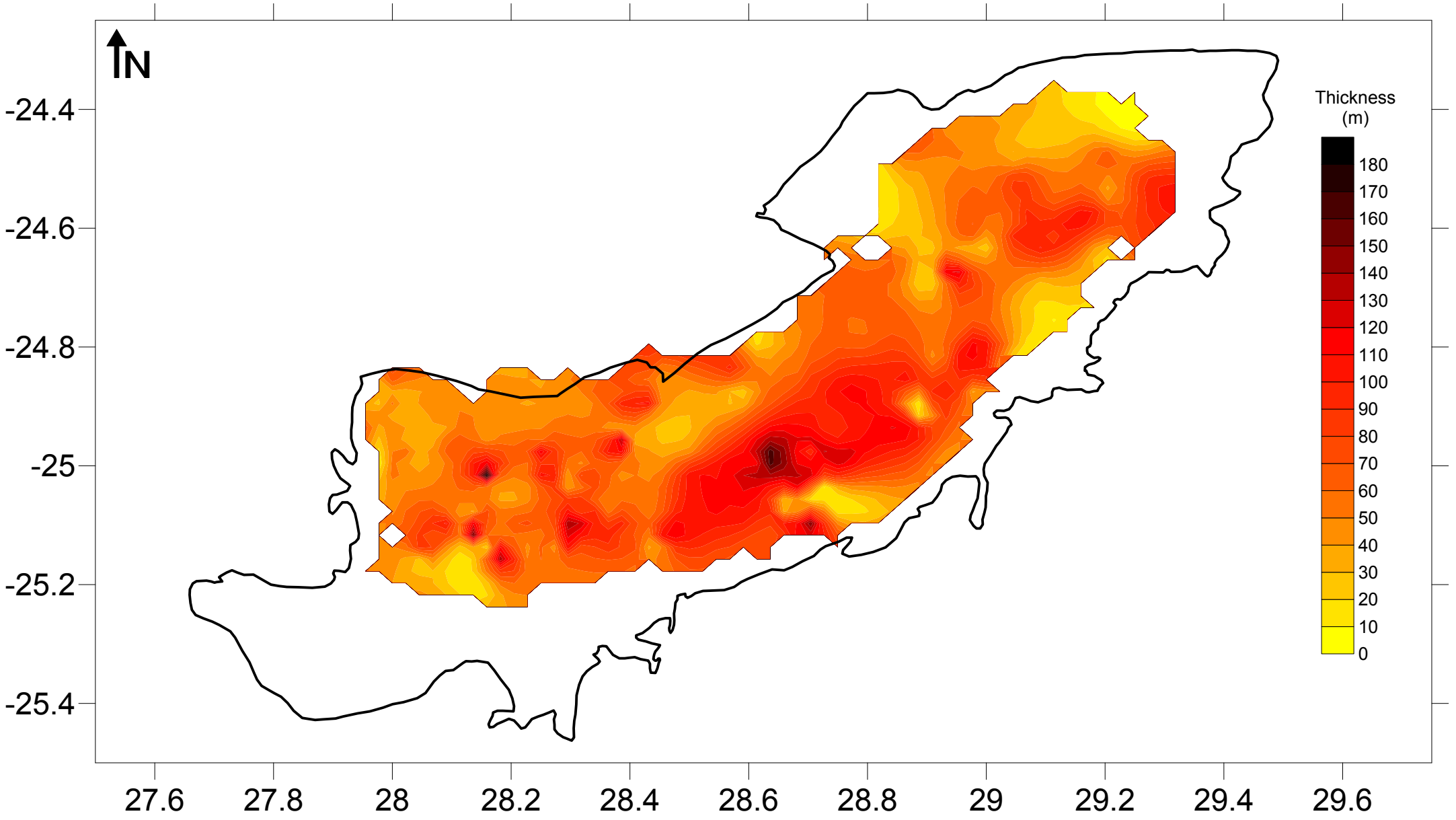

Isopach Contour Map
Clarens

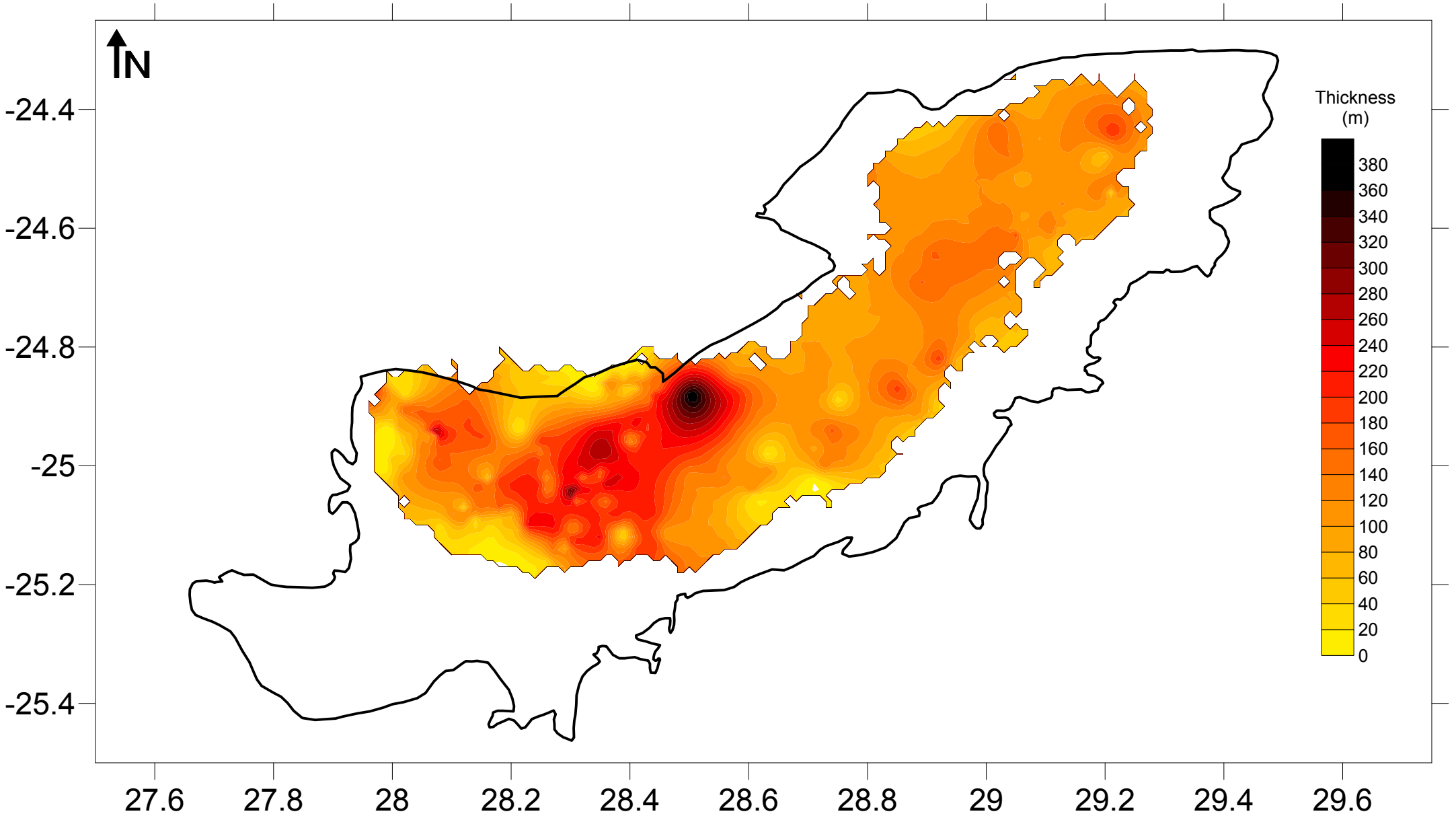

Isopach Contour Map
Letaba

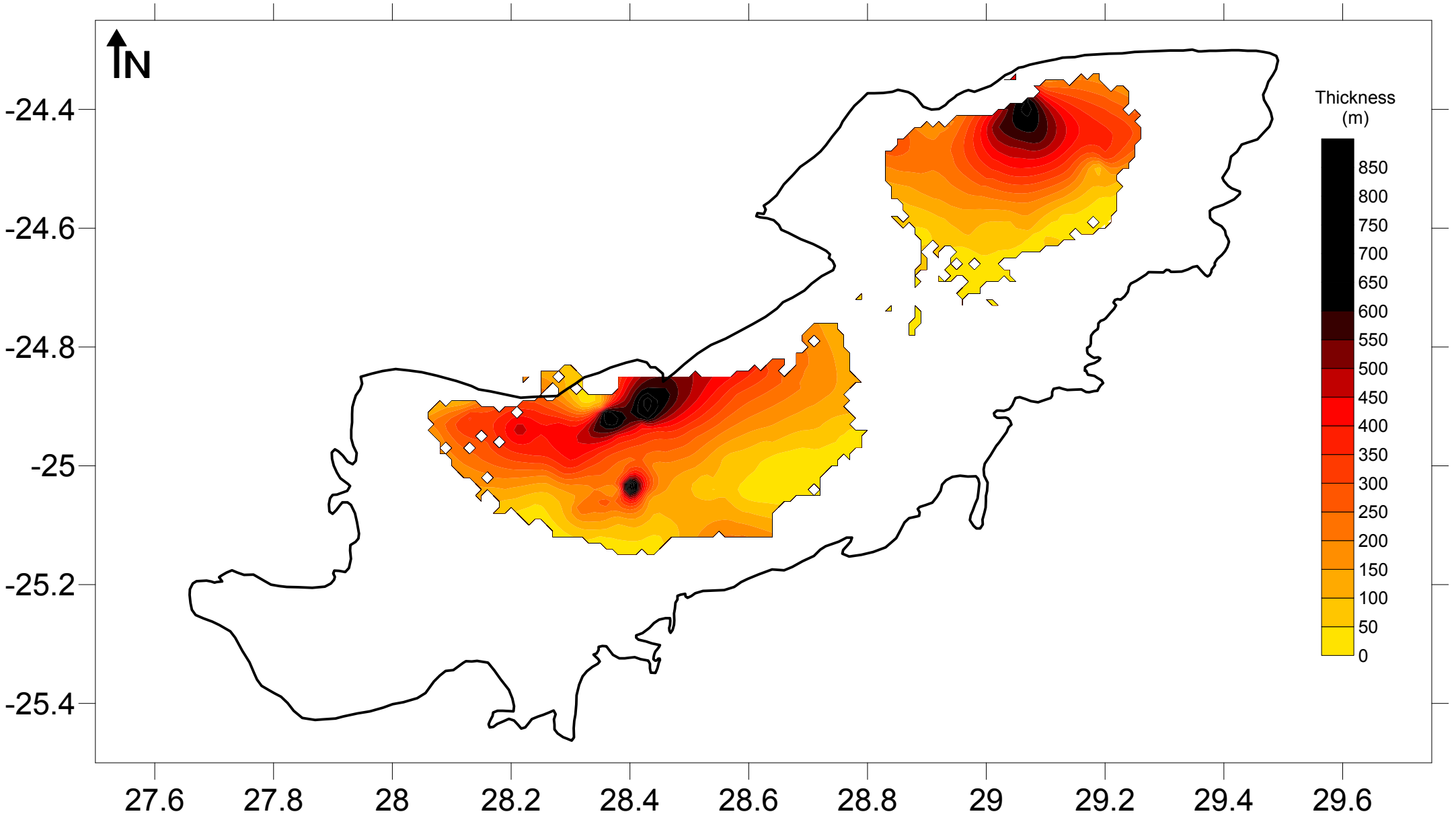

Structural Contour Map
Hammanskraal

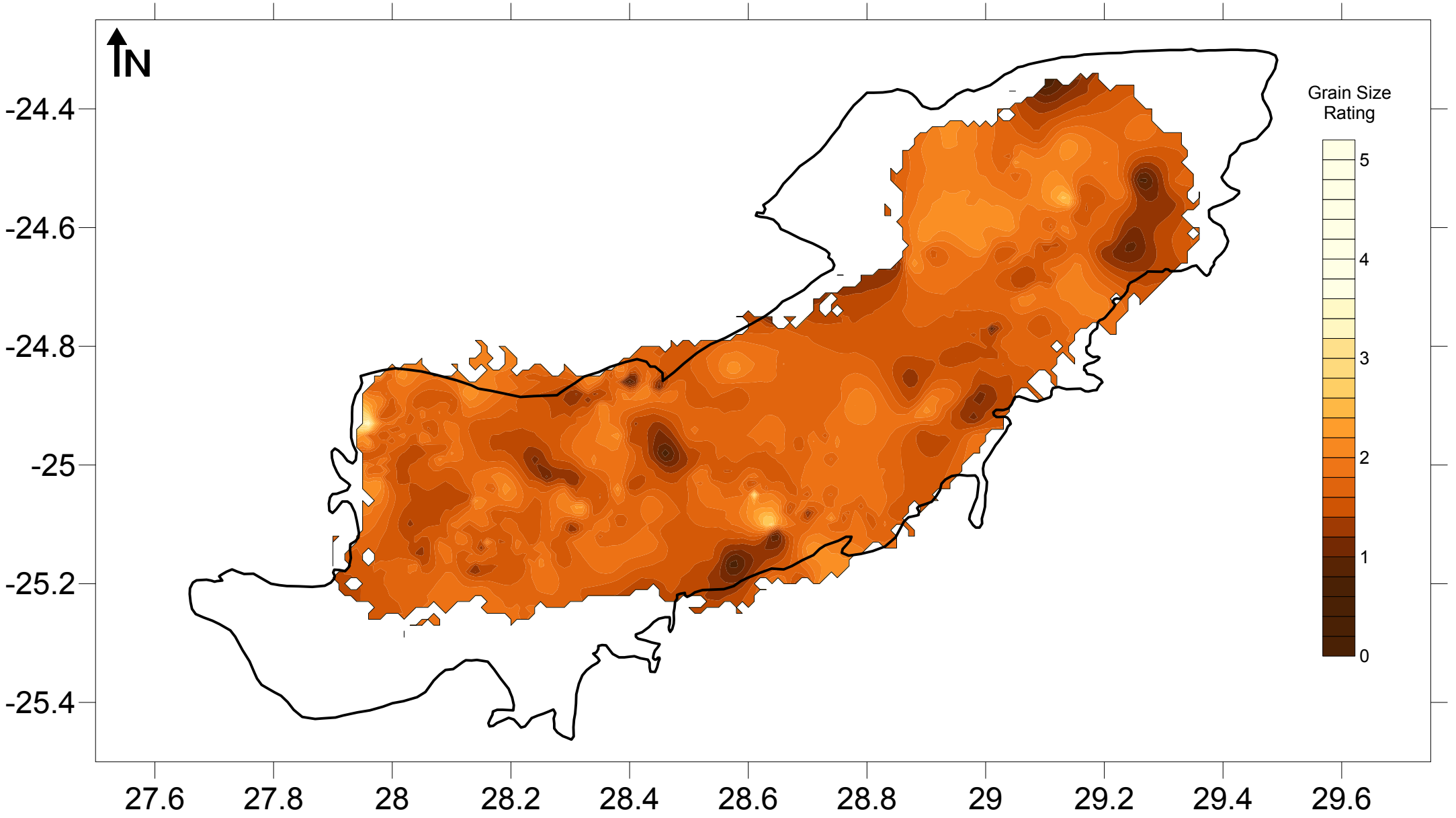

Structural Contour Map
Irrigasie

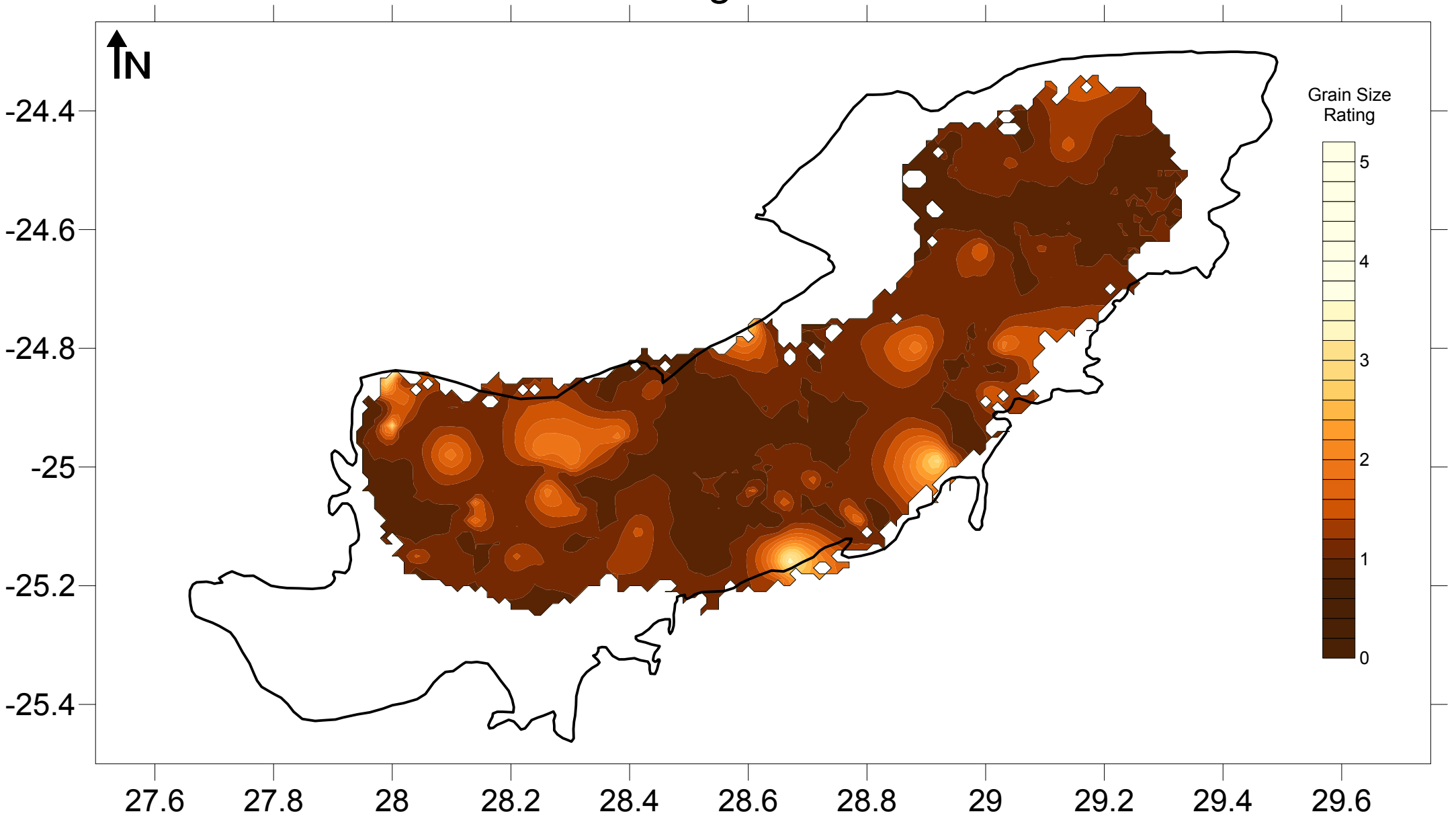

Structural Contour Map
Molteno

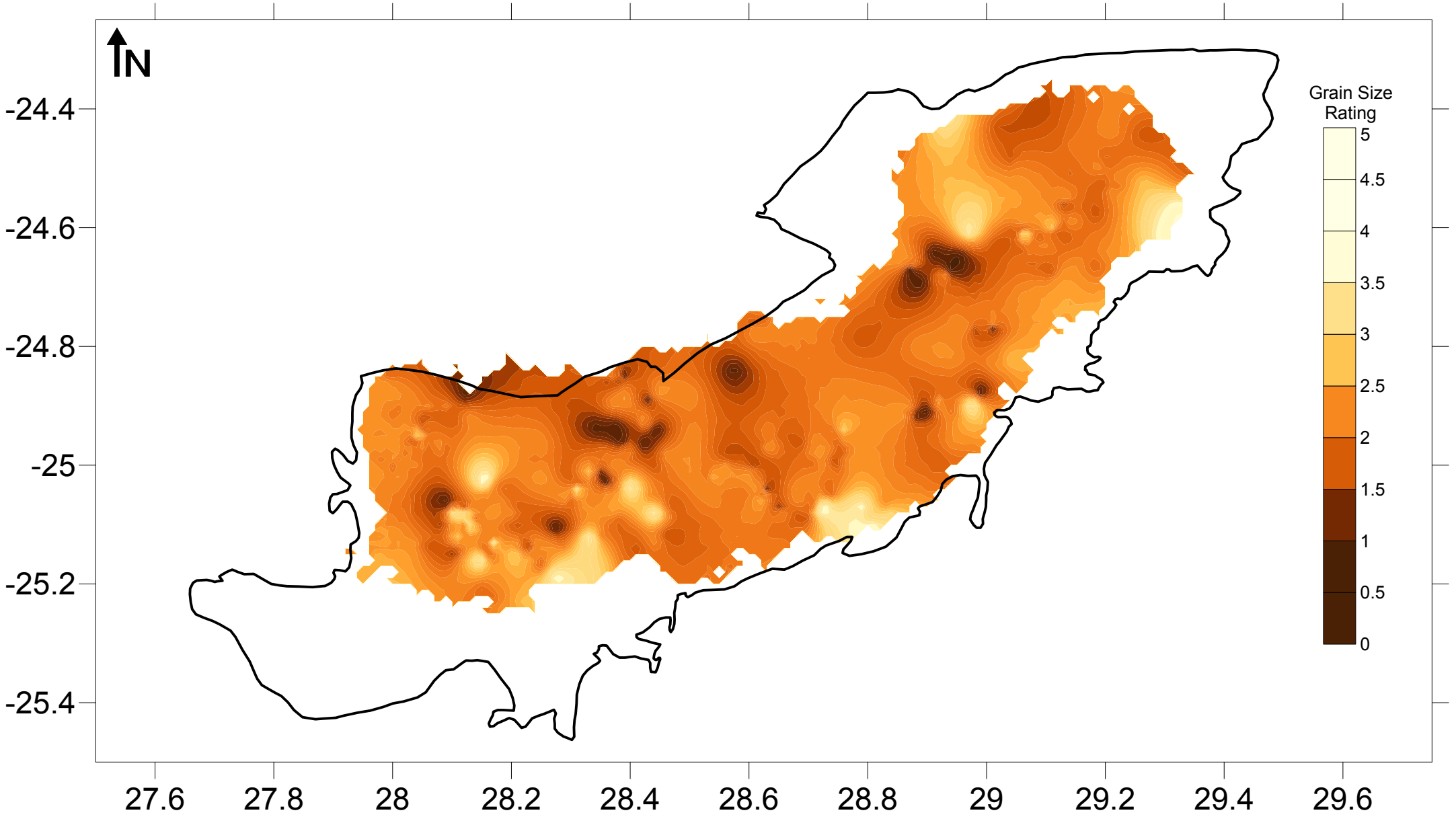

Structural Contour Map
Elliot

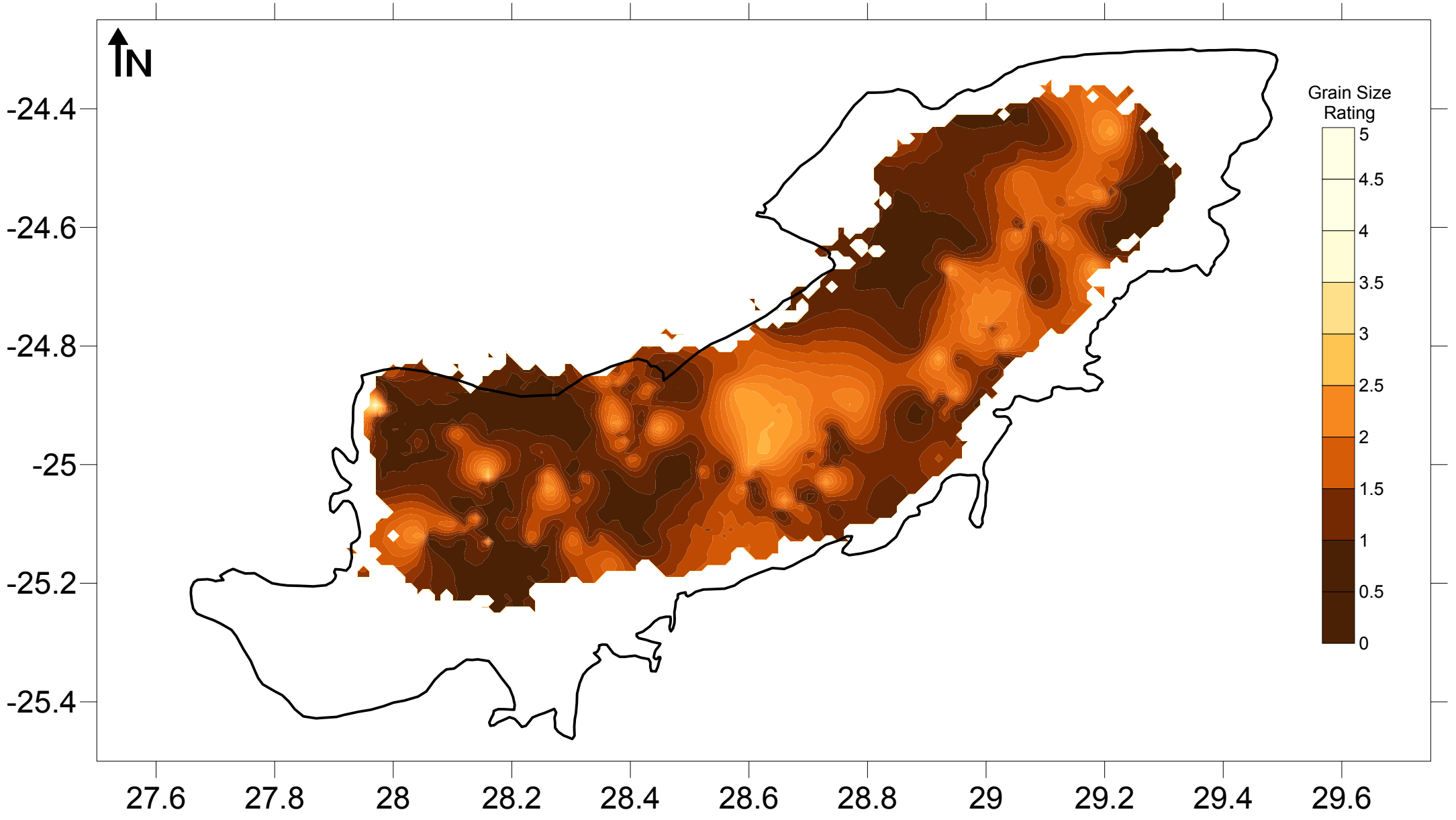

Structural Contour Map
Clarens

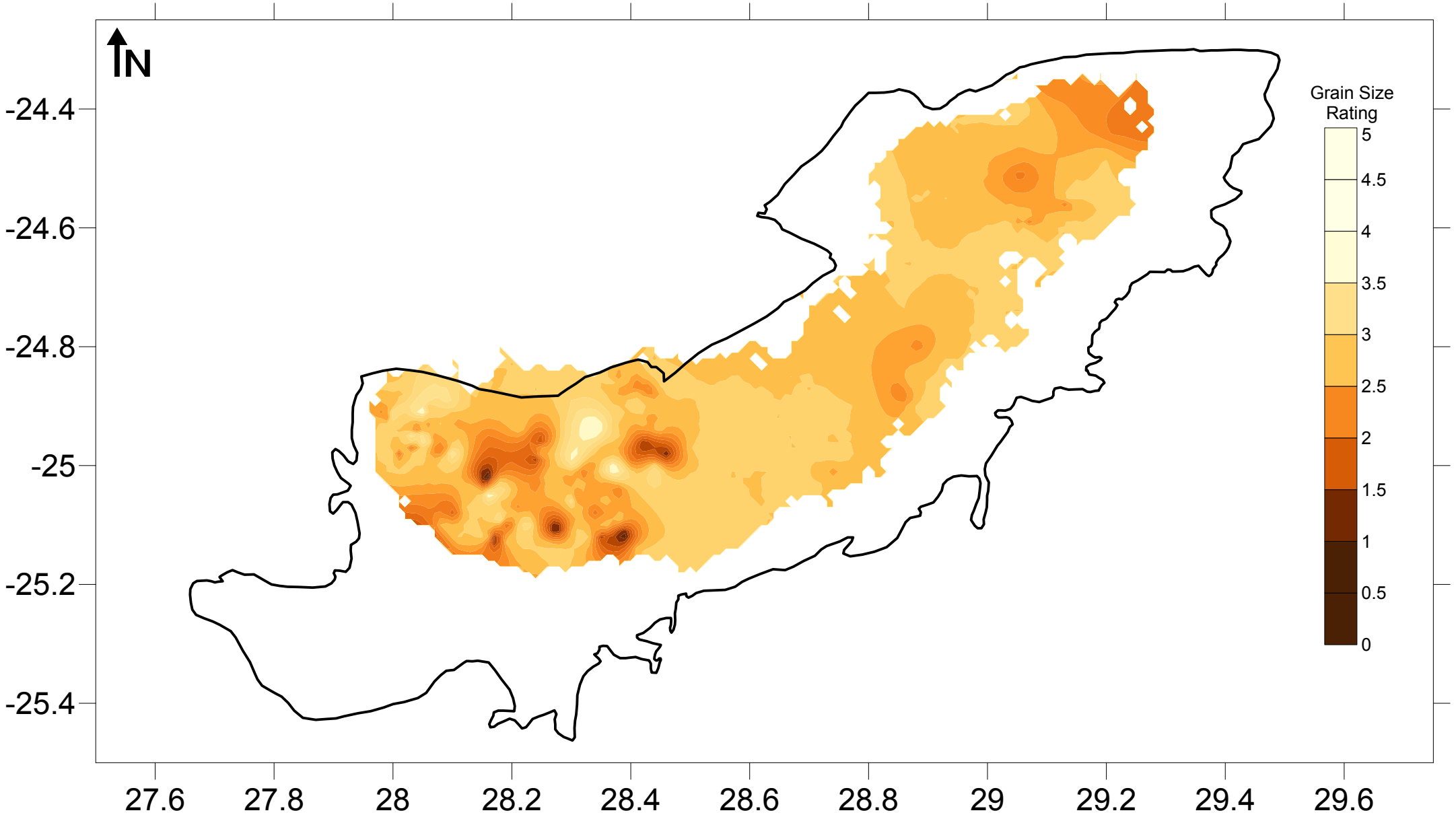

Area 1

Borehole: 1919834

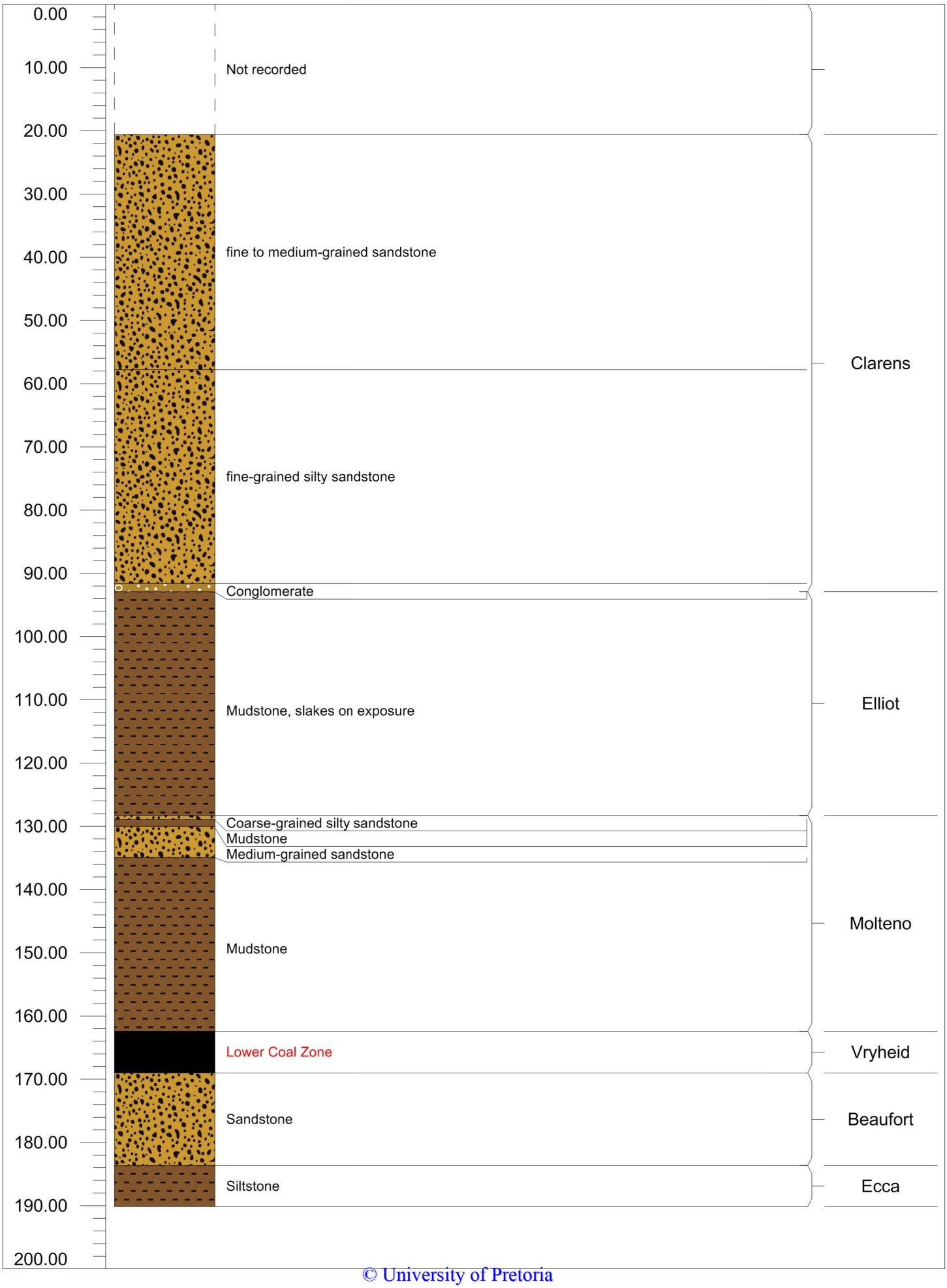

Area 1

Borehole: 1919829

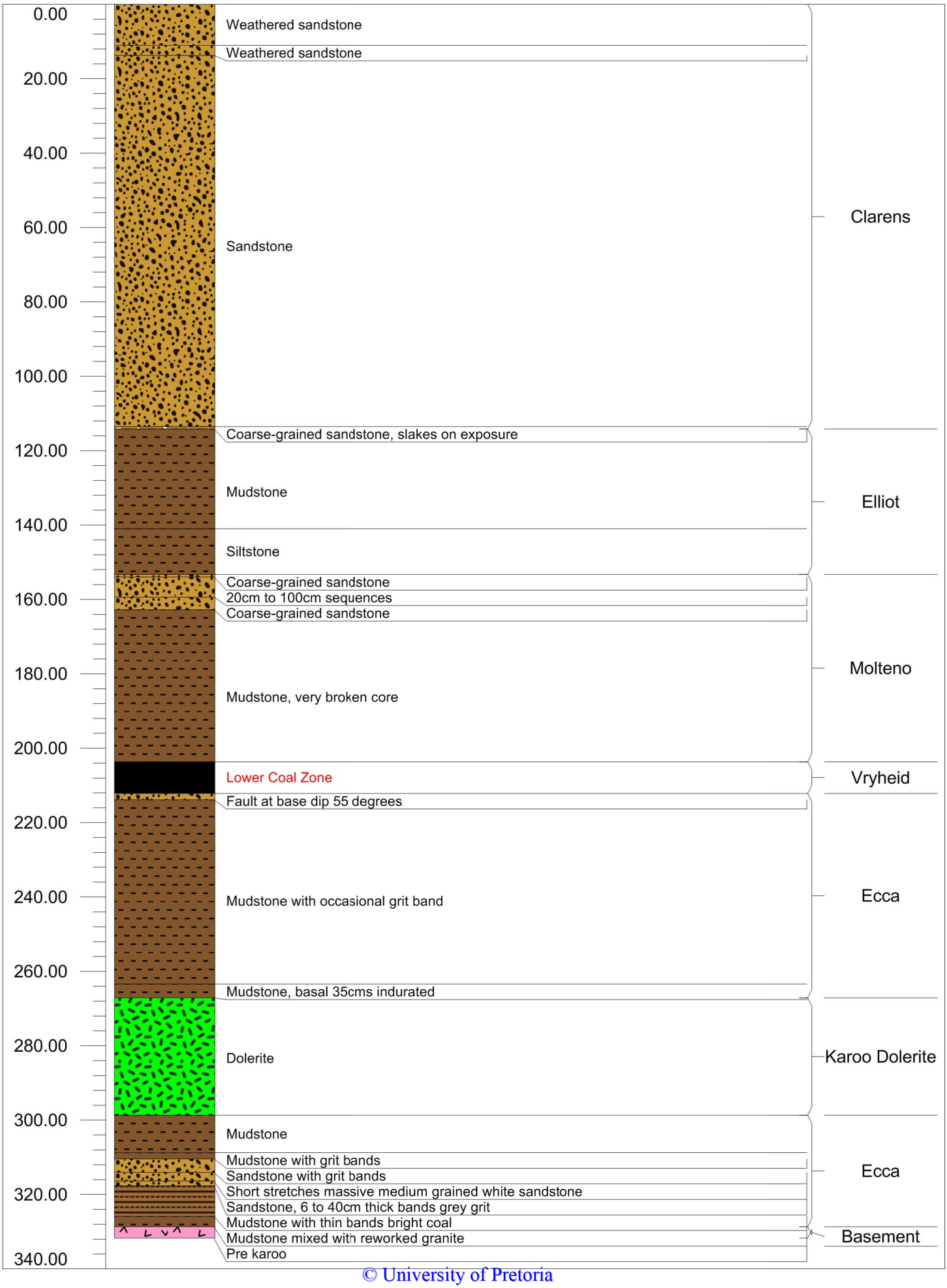

Area 1

Borehole: 3028399

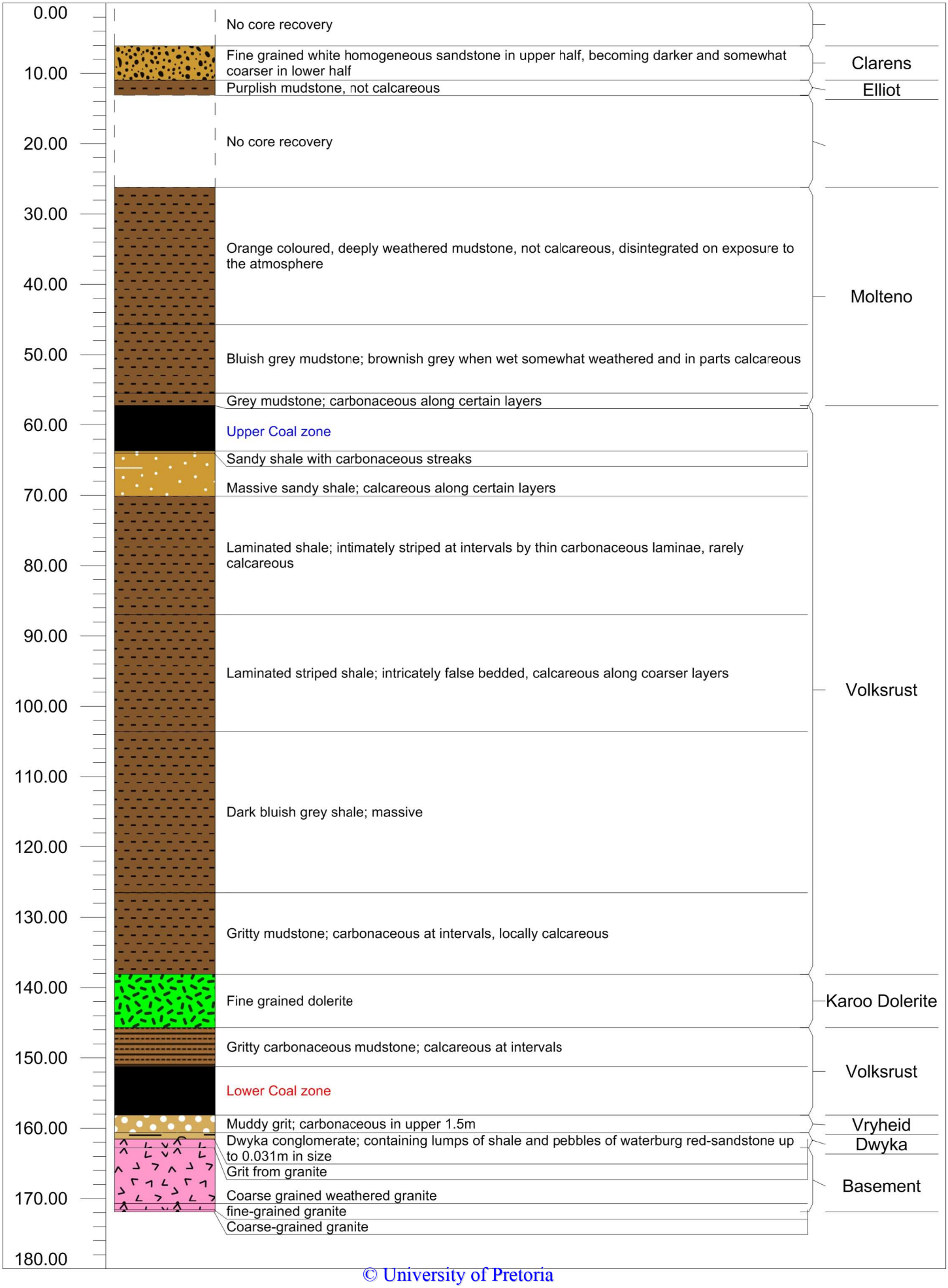

Area 1

Borehole: 1919455

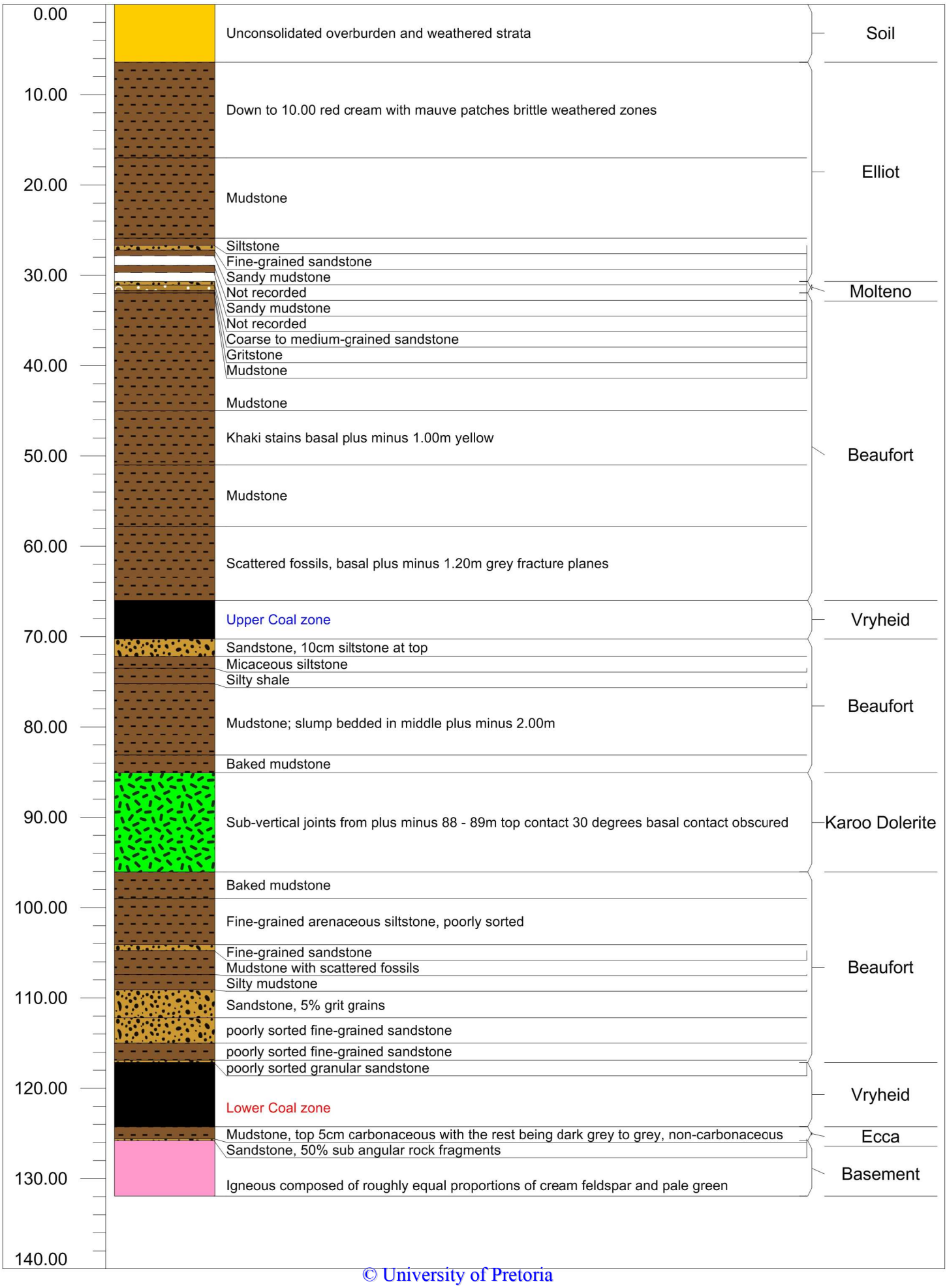

Area 1

Borehole: 1919761

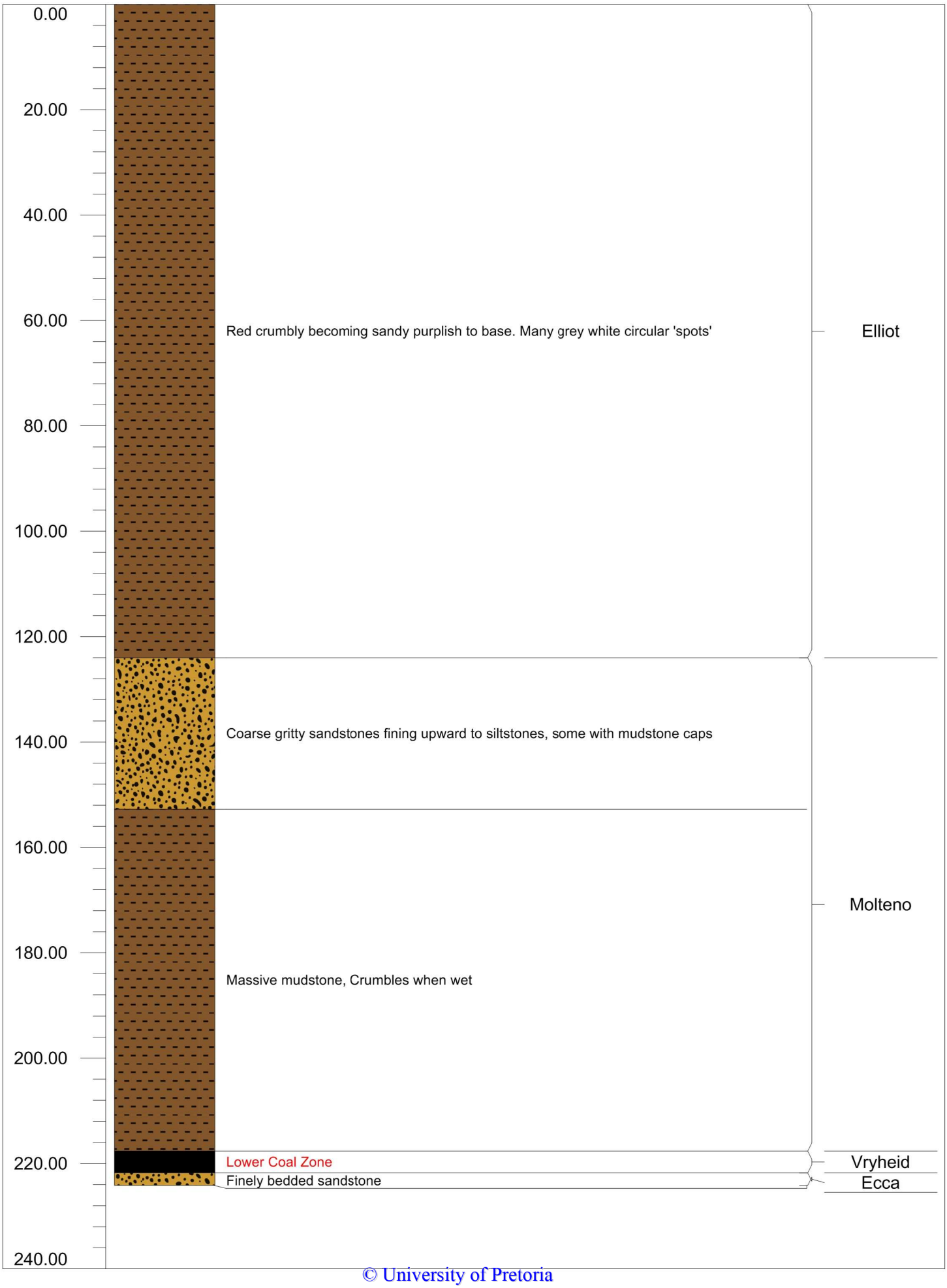

Area 1

Borehole: 3028394

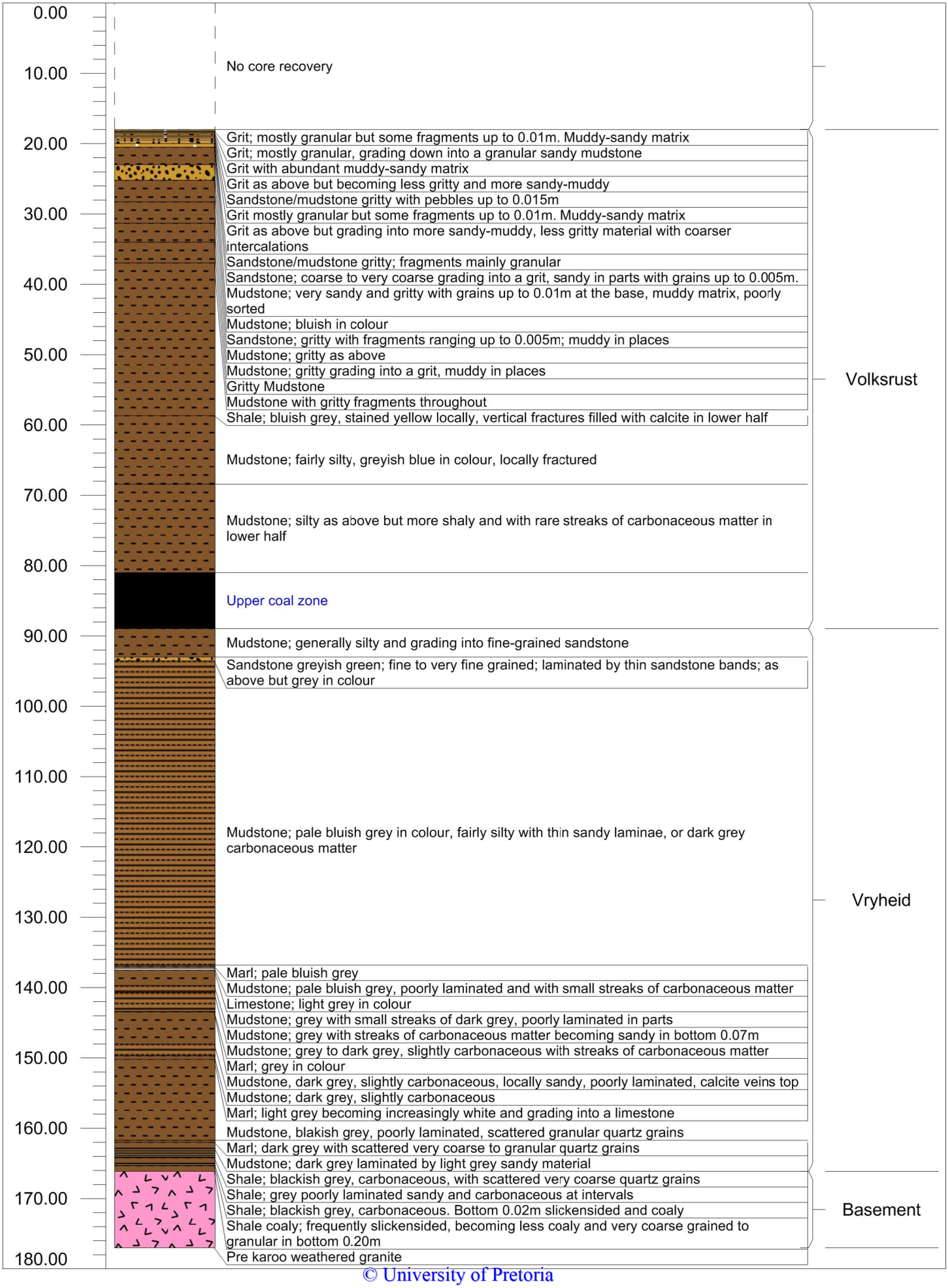

Area 2

Borehole: 1919754

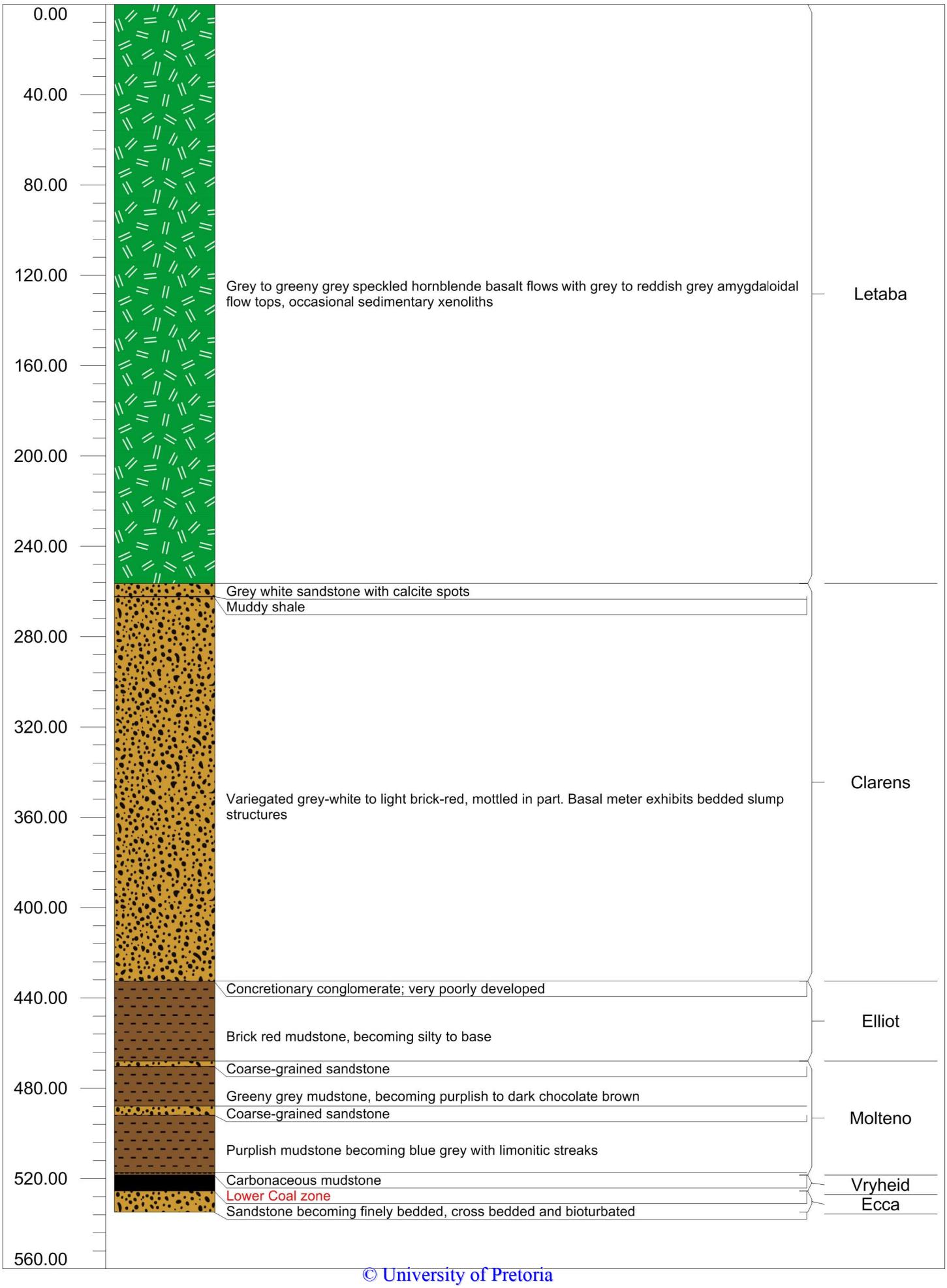

Area 2

Borehole: 1919571

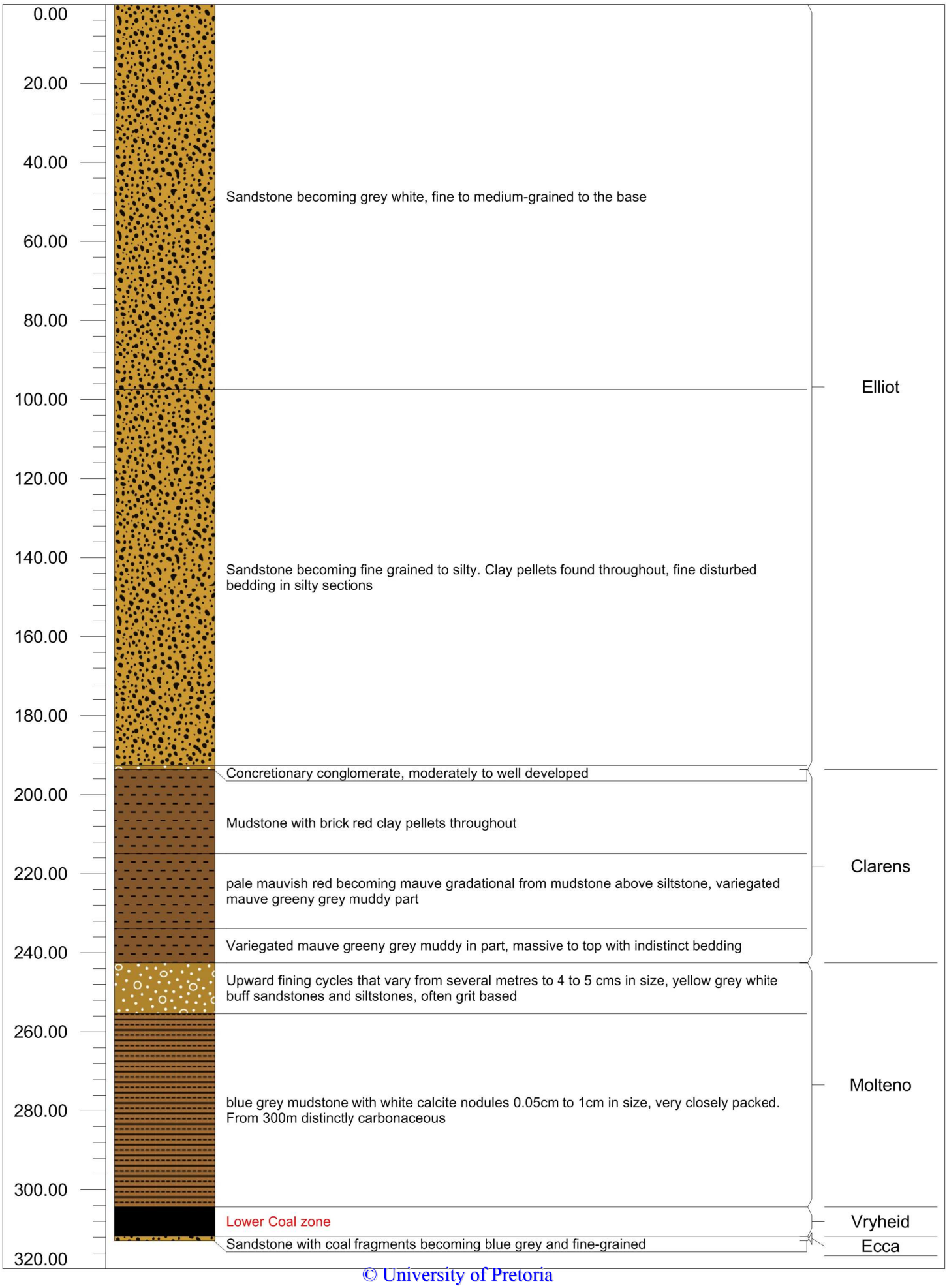

Area 2

Borehole: 1919651

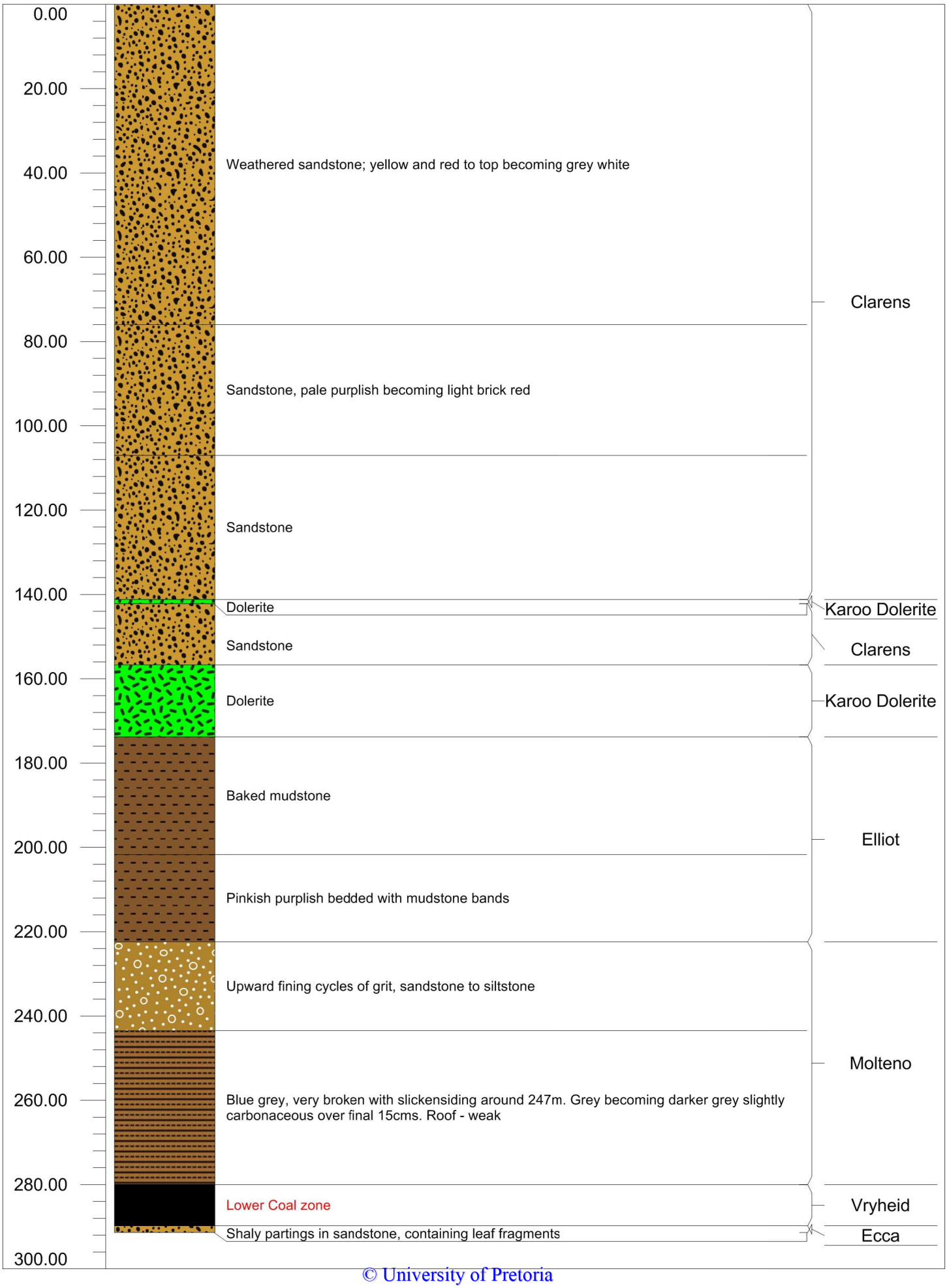

Area 2

Borehole: 1919595

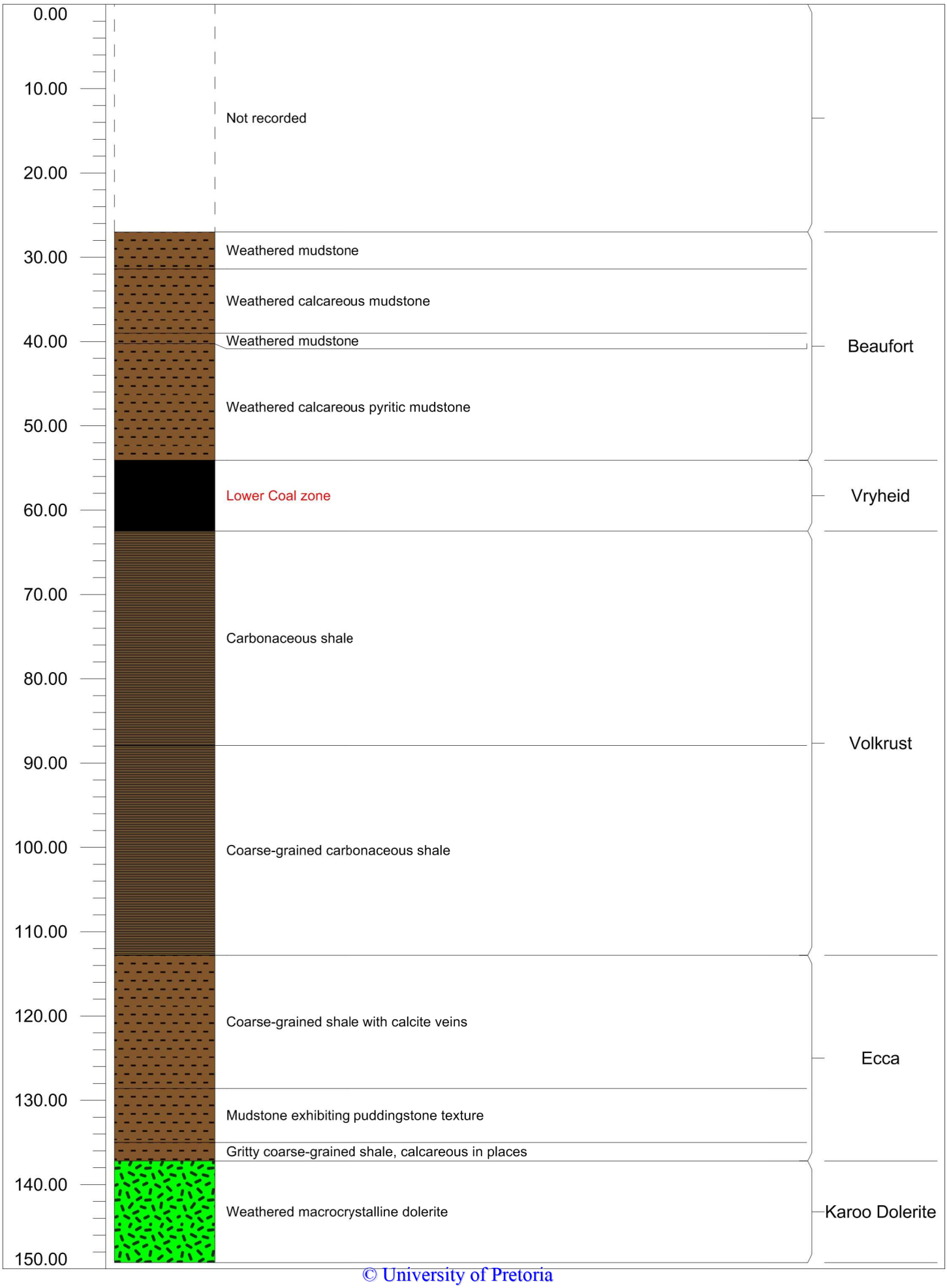

Area 2

Borehole: 1919563

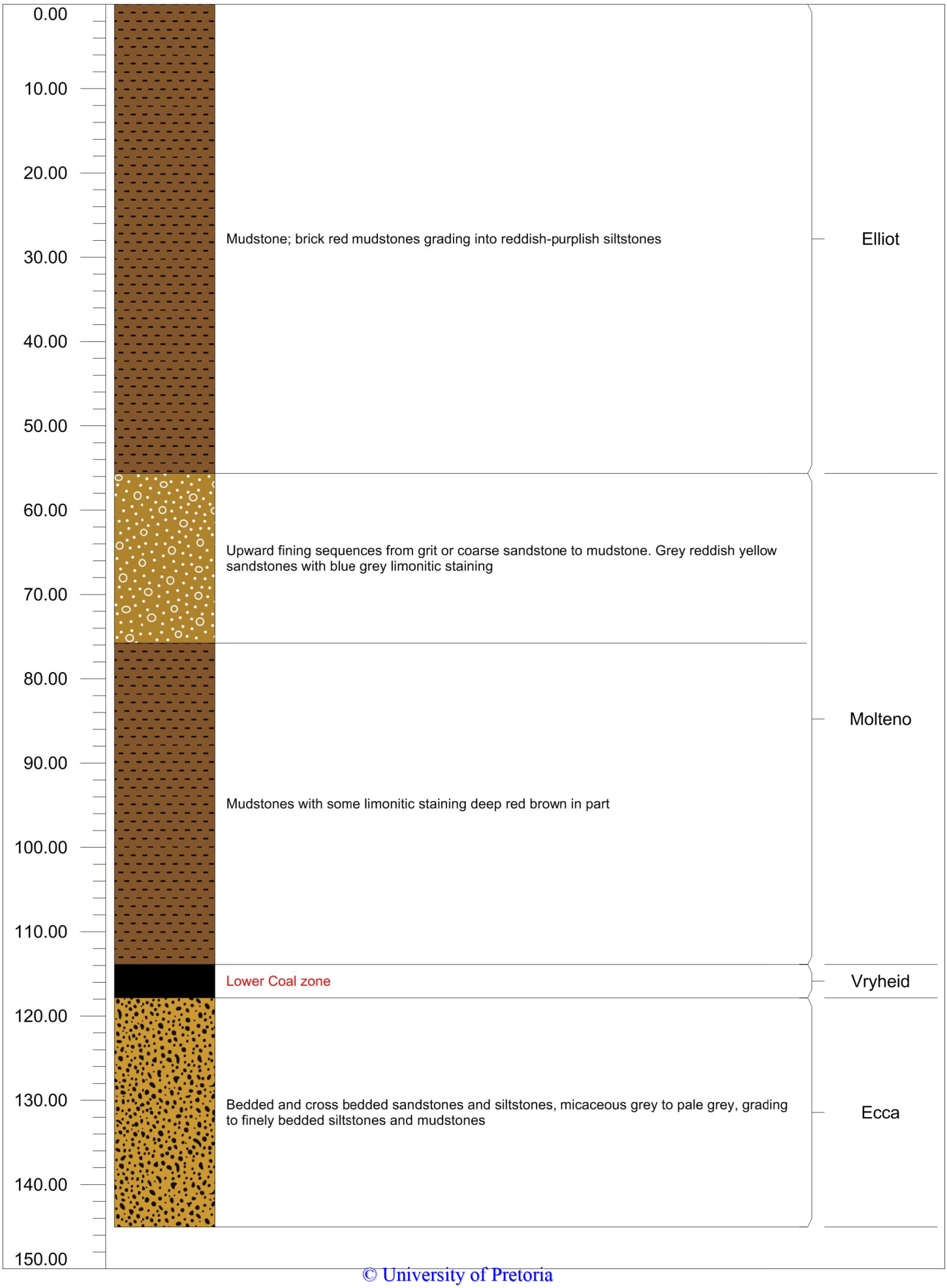

Area 3

Borehole: 1919552

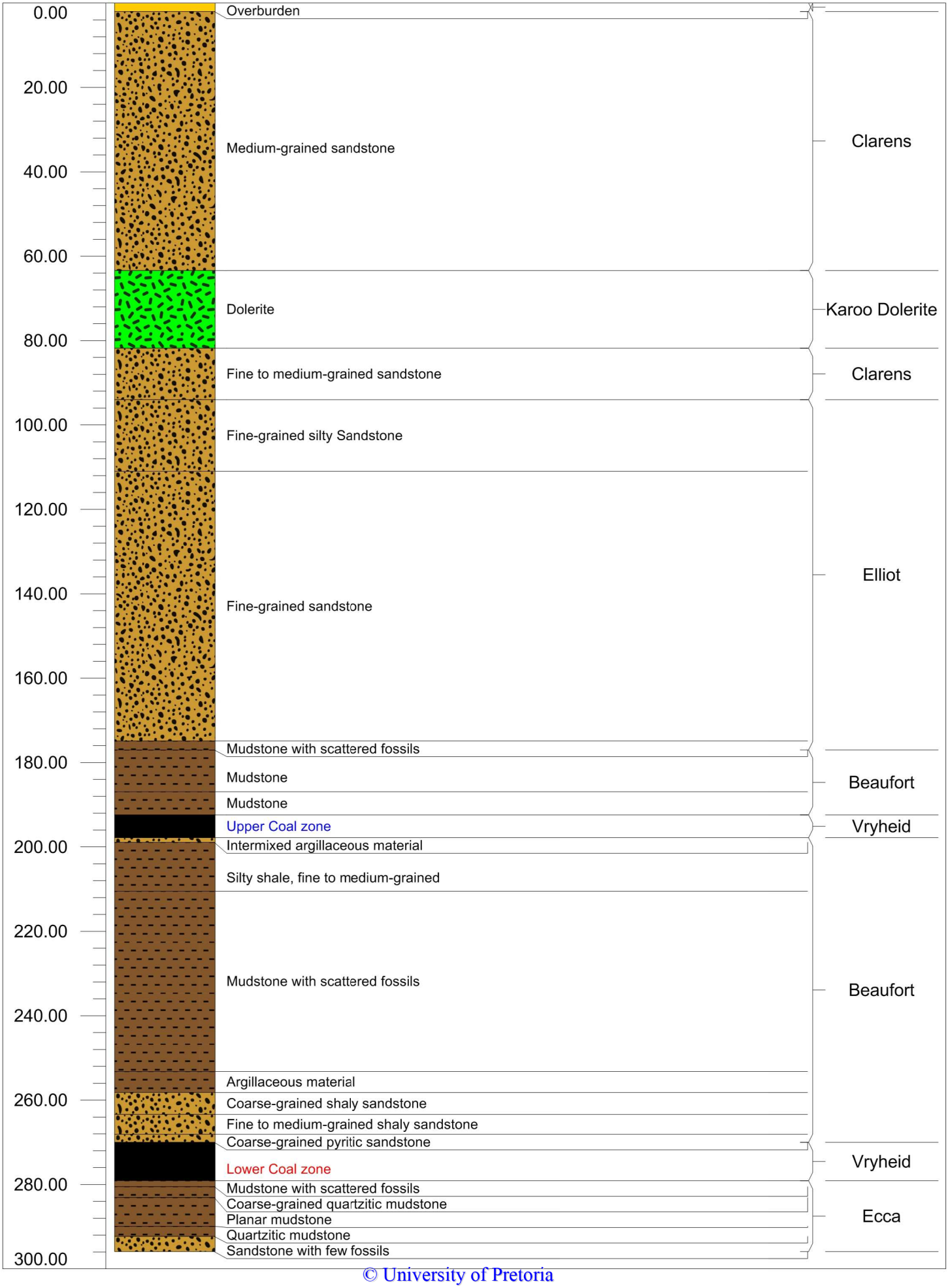

Area 3

Borehole: 1919483

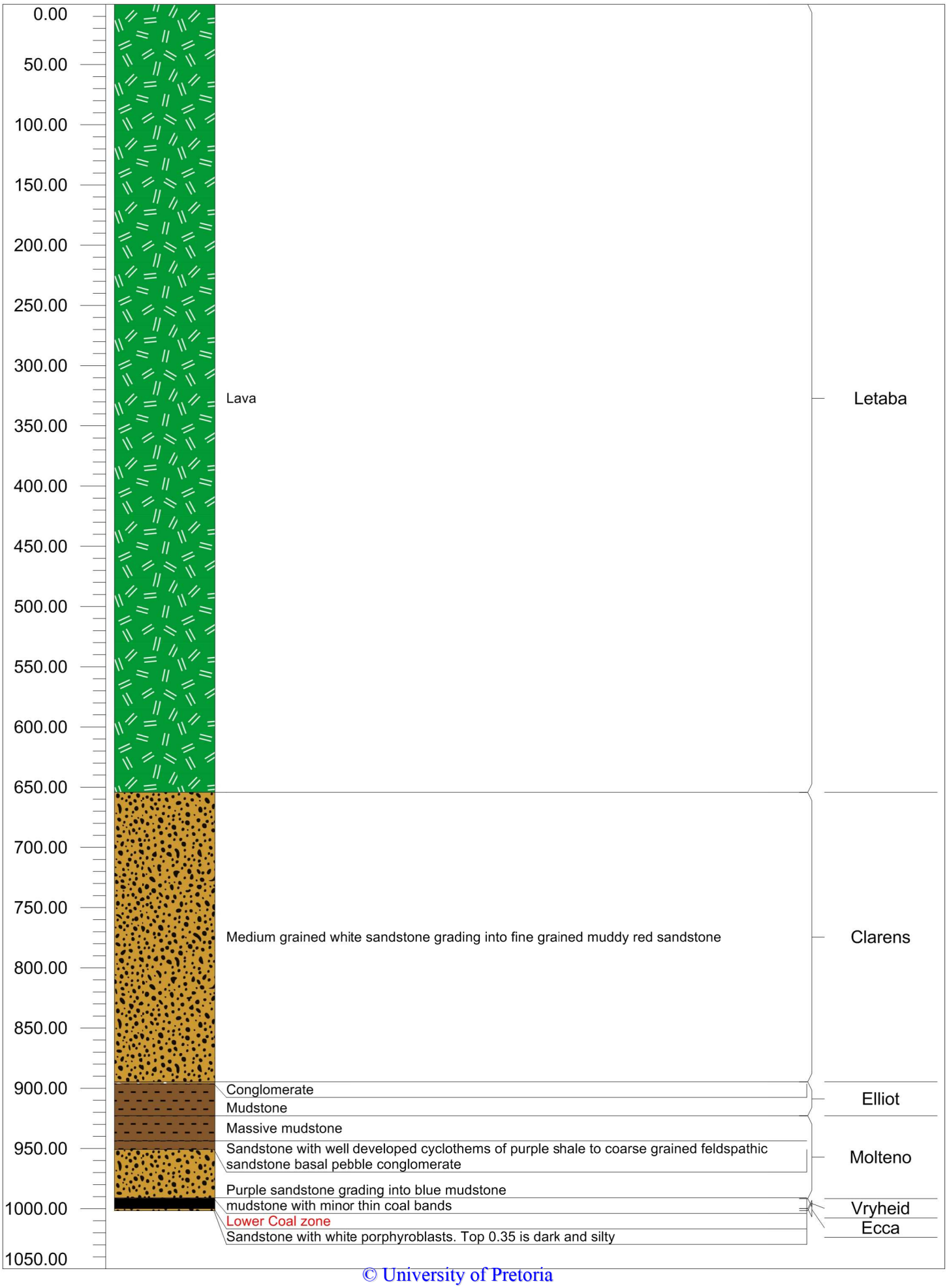

Area 3

Borehole: 1919567

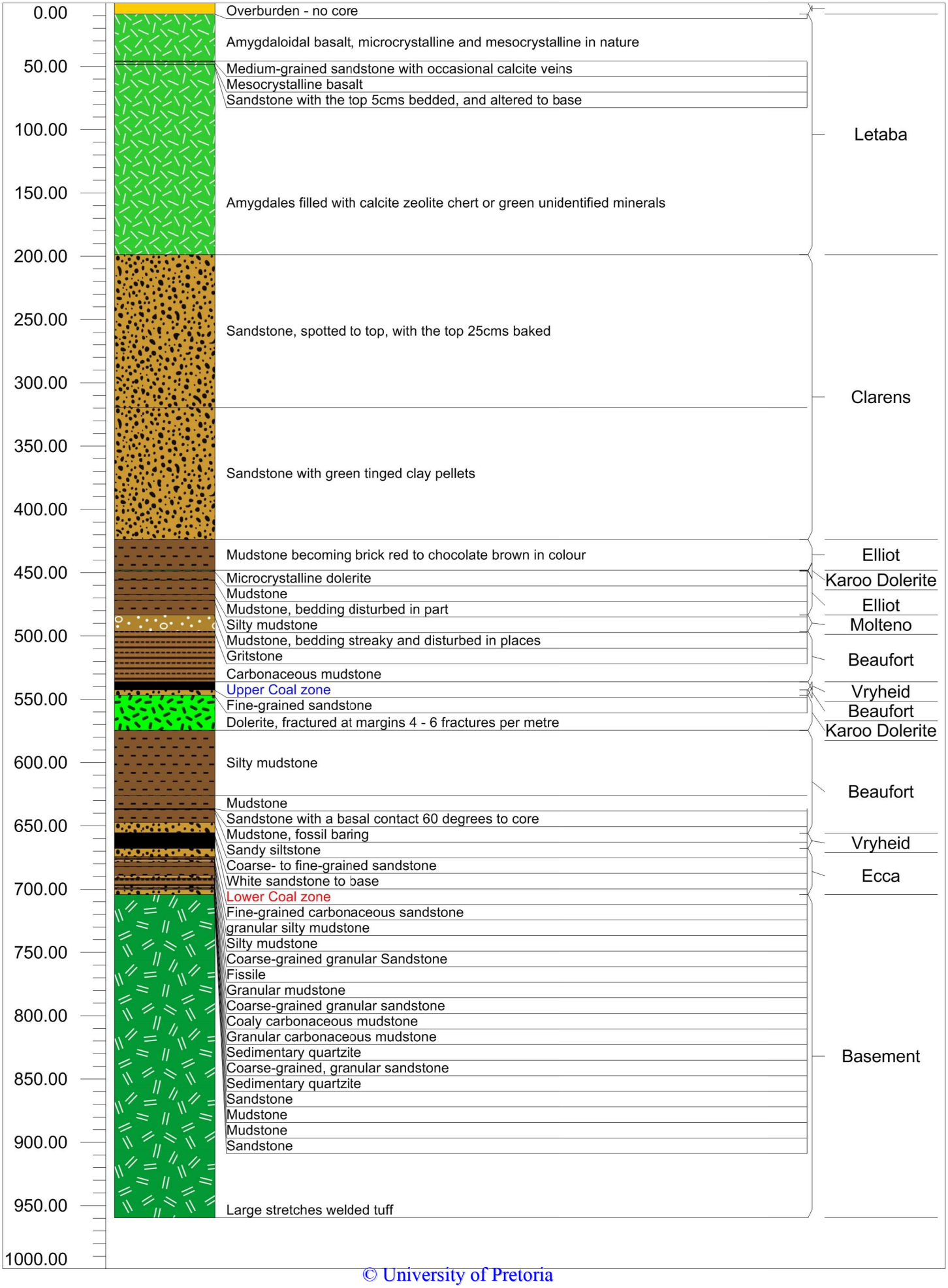

Area 3

Borehole: 3028622

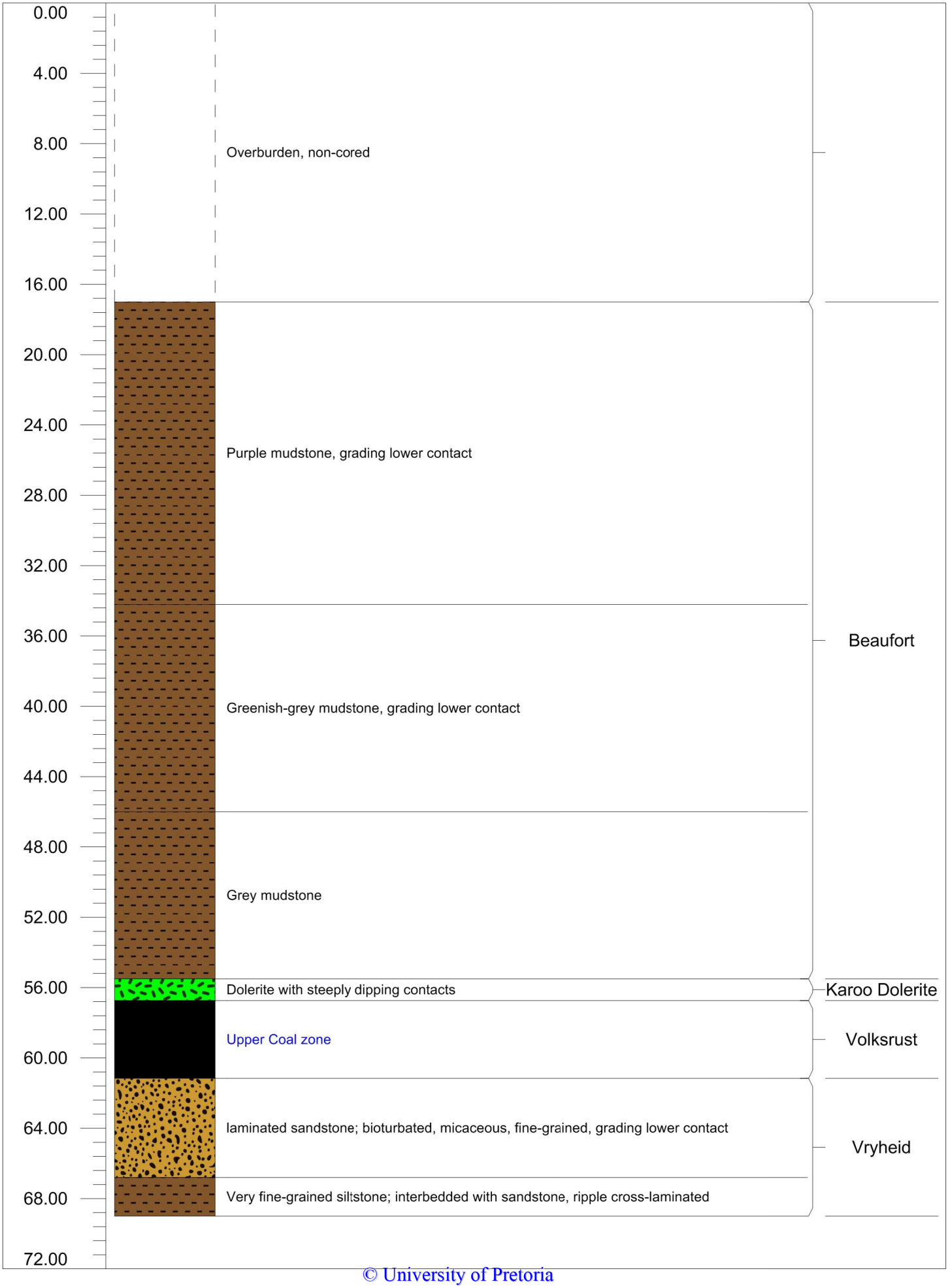

Area 4

Borehole: 1919545

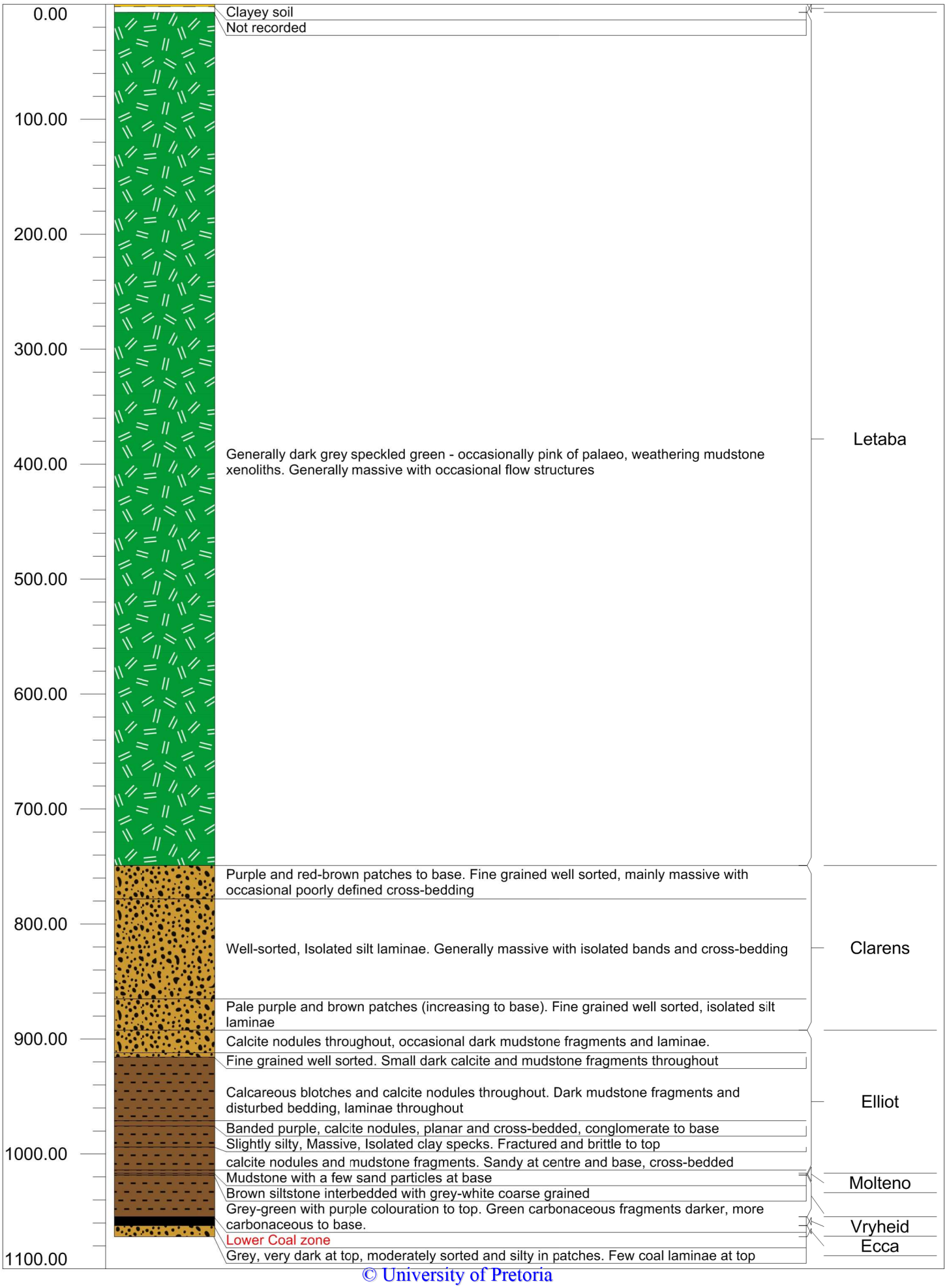

Area 4

Borehole: 1919509

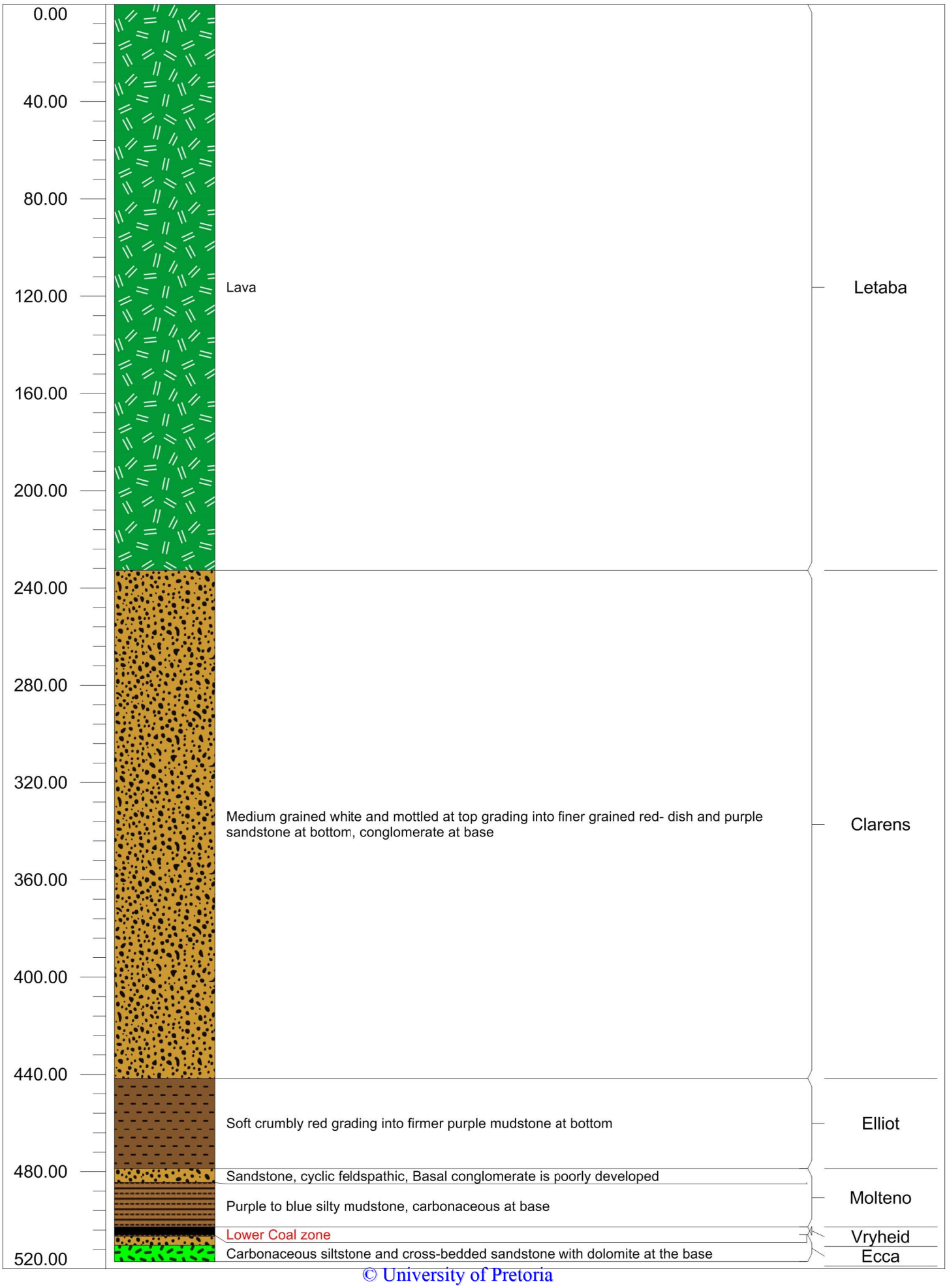

Area 4

Borehole: 3026561

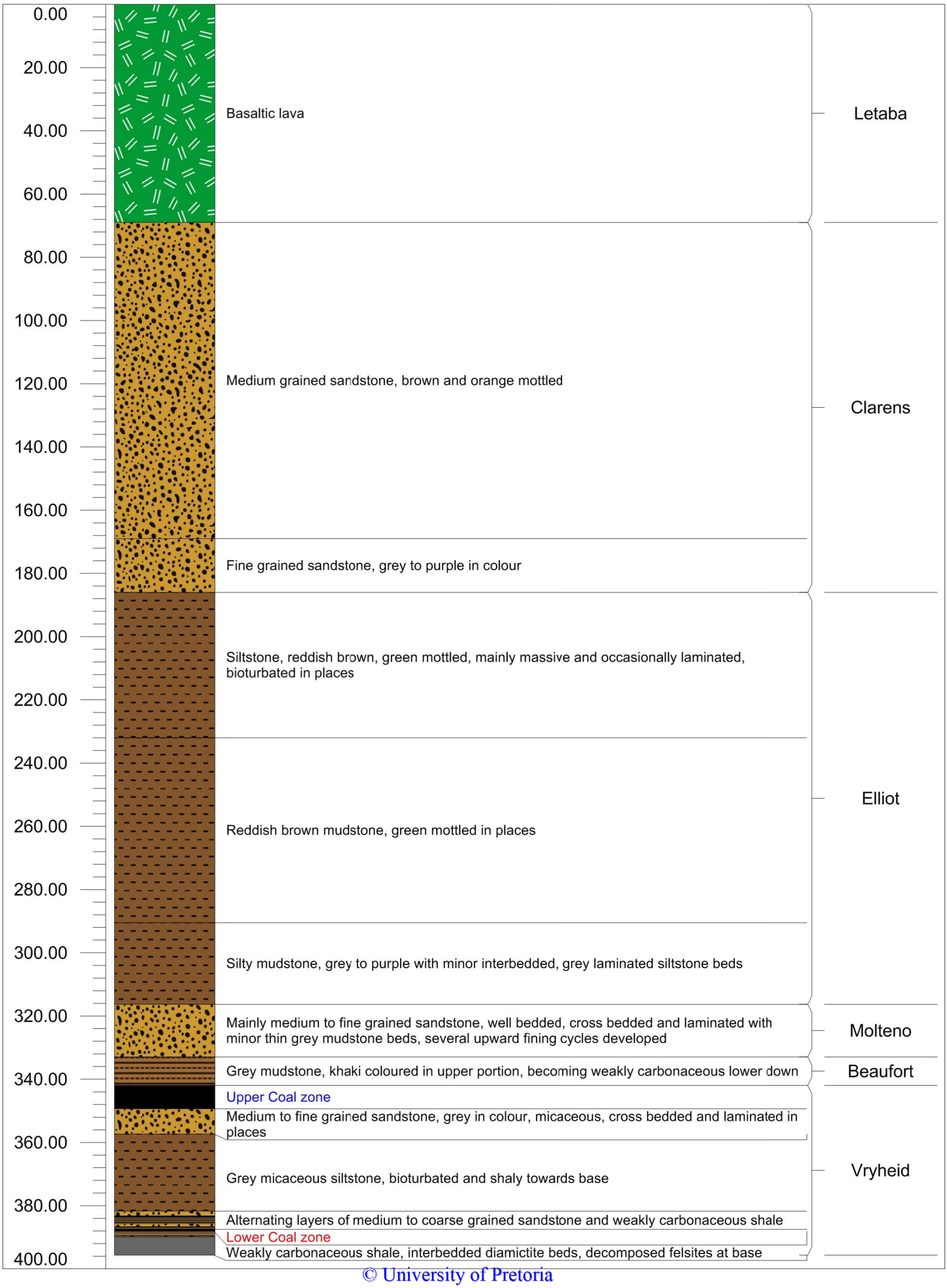

Area 4

Borehole: 1919503

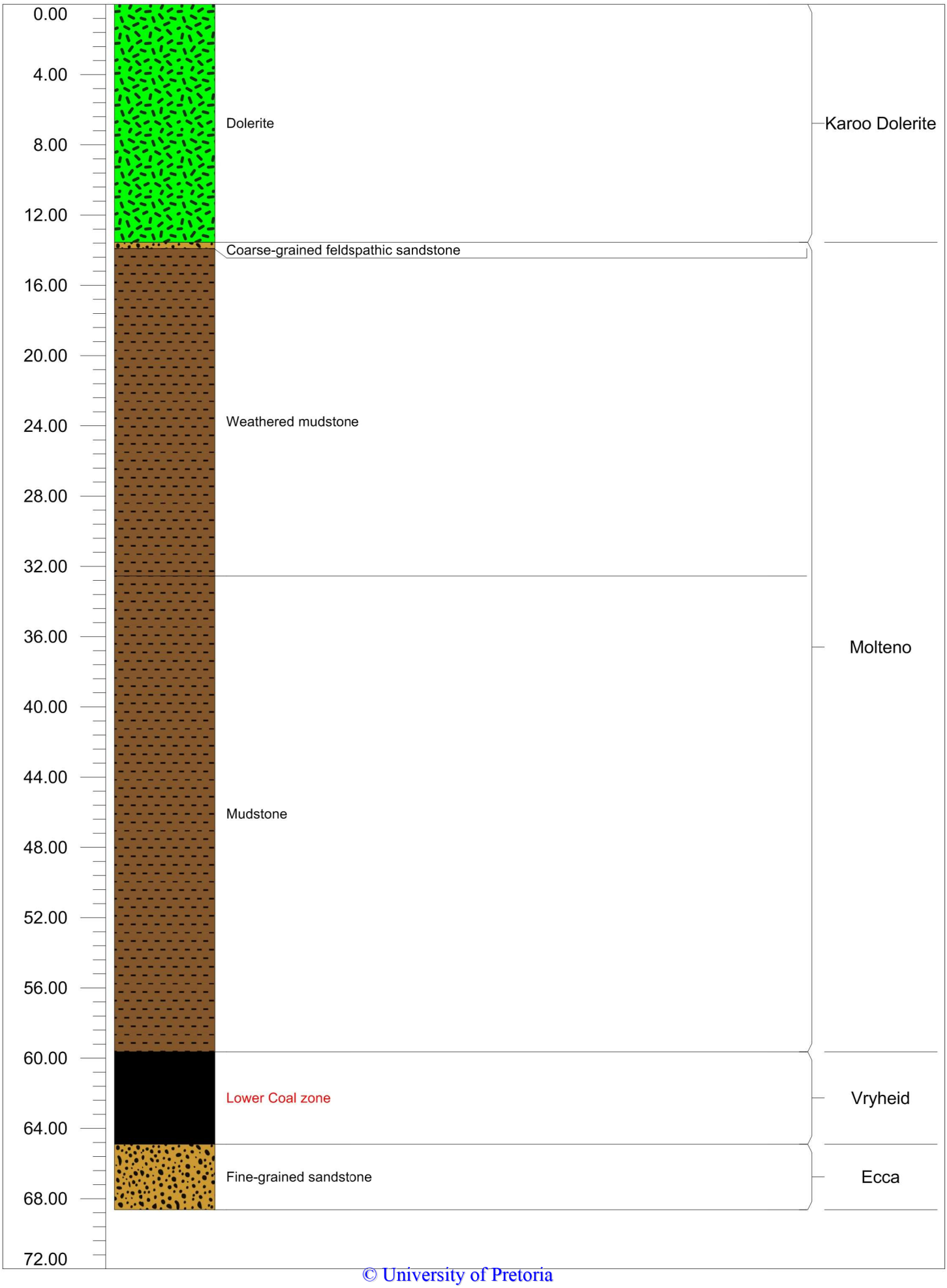

Area 5

Borehole: 1919351

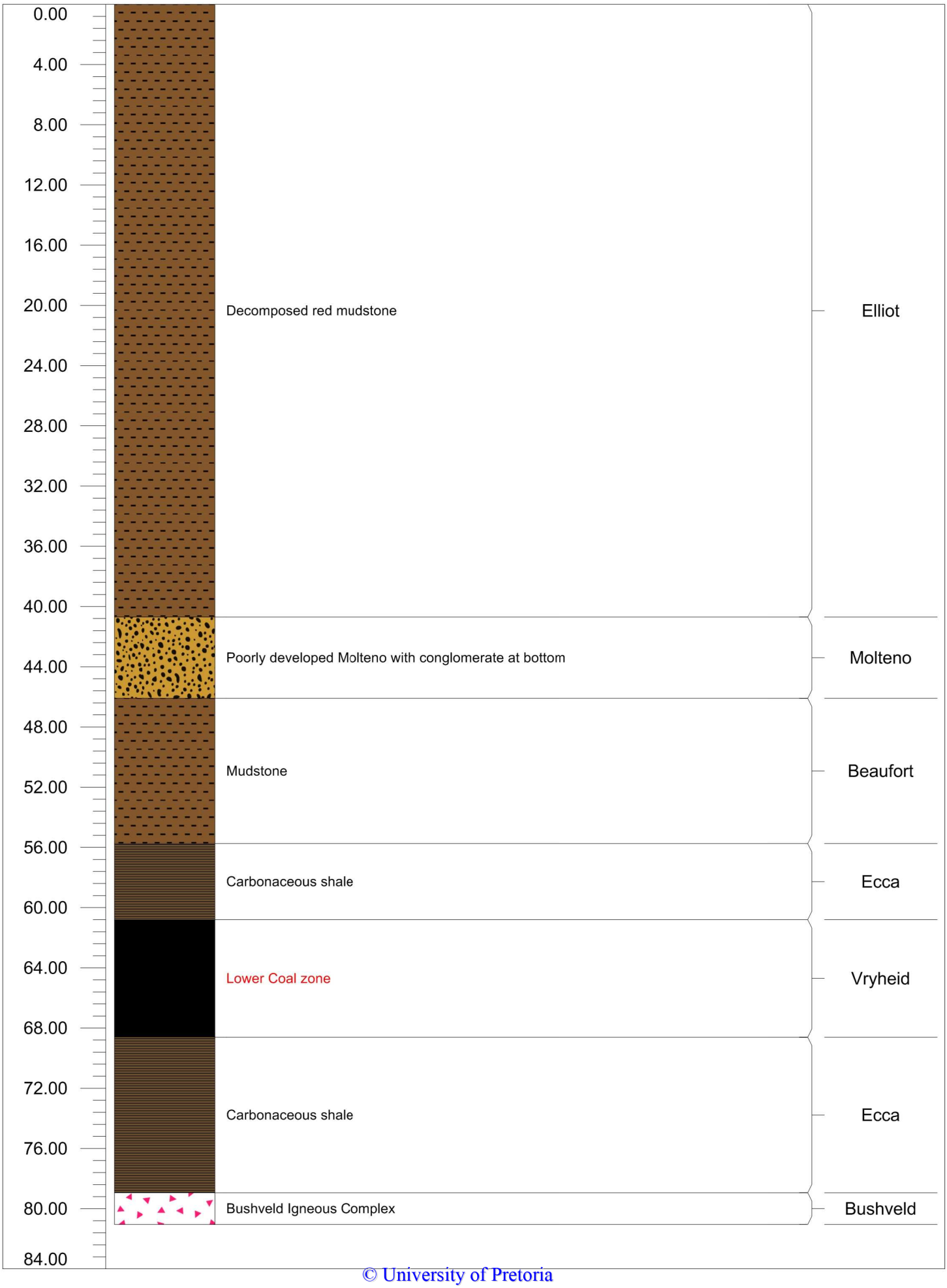

Area 5

Borehole: 3026367

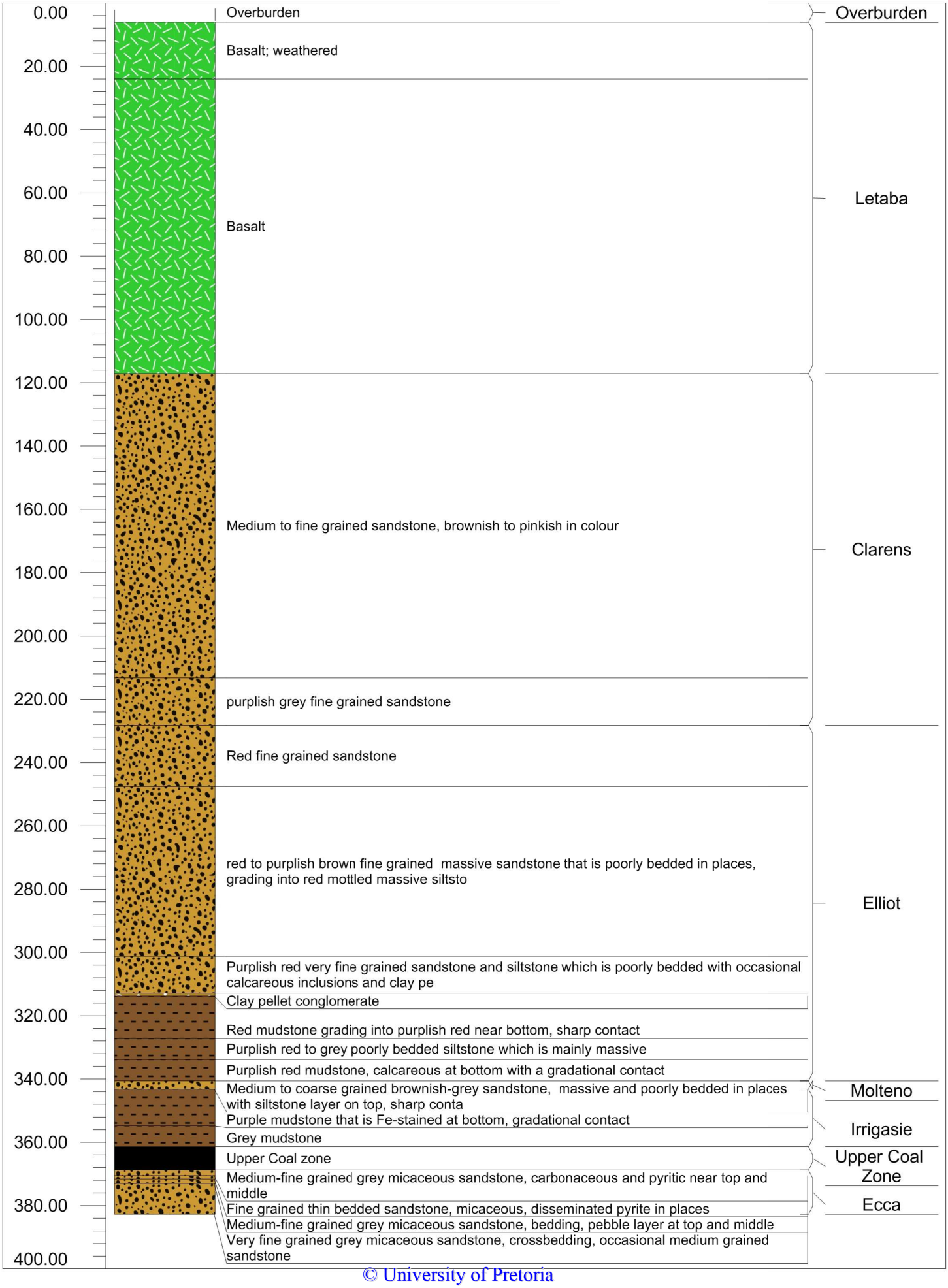

Area 5

Borehole: 3028800

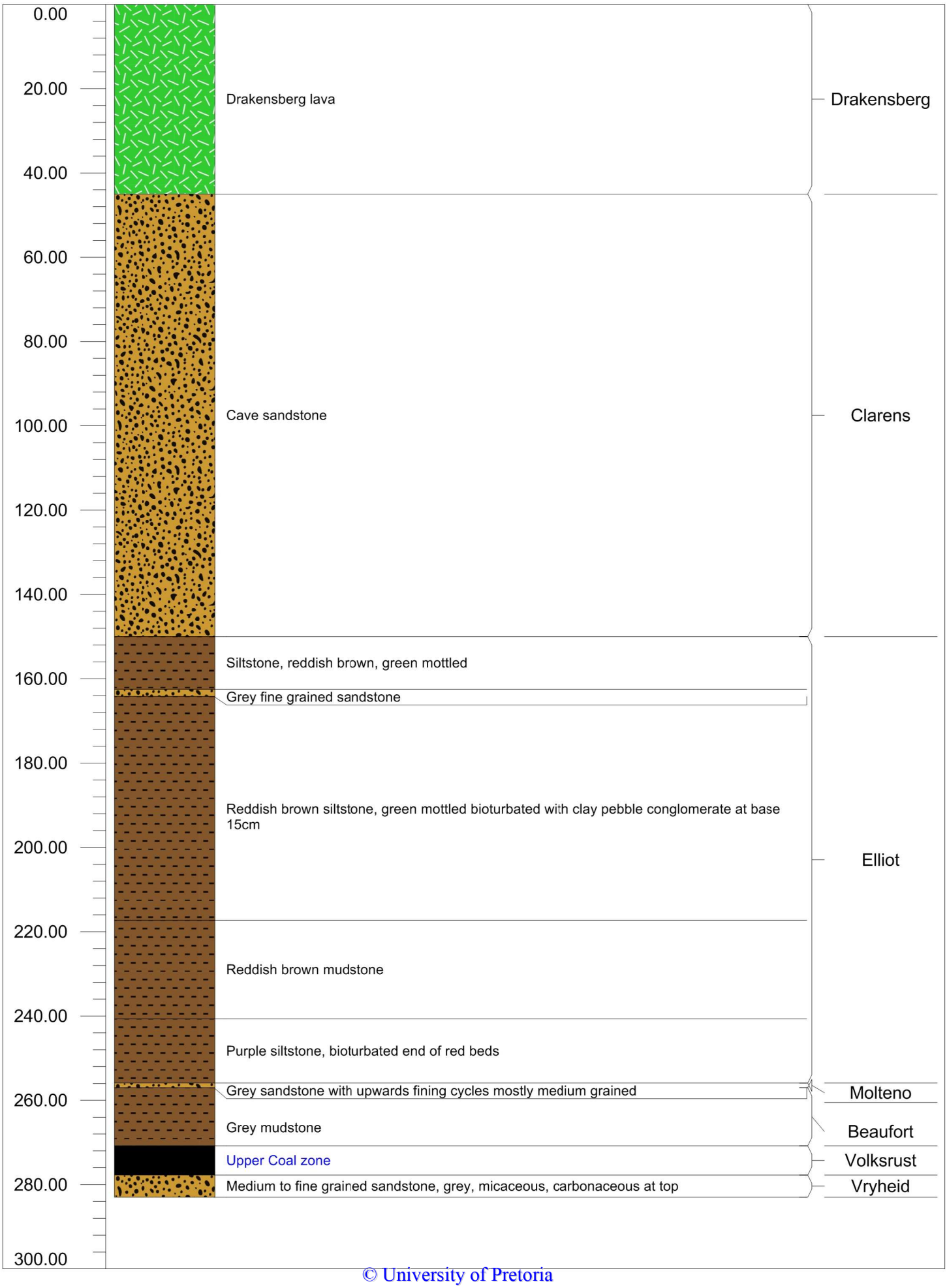

Area 5

Borehole: 3028666

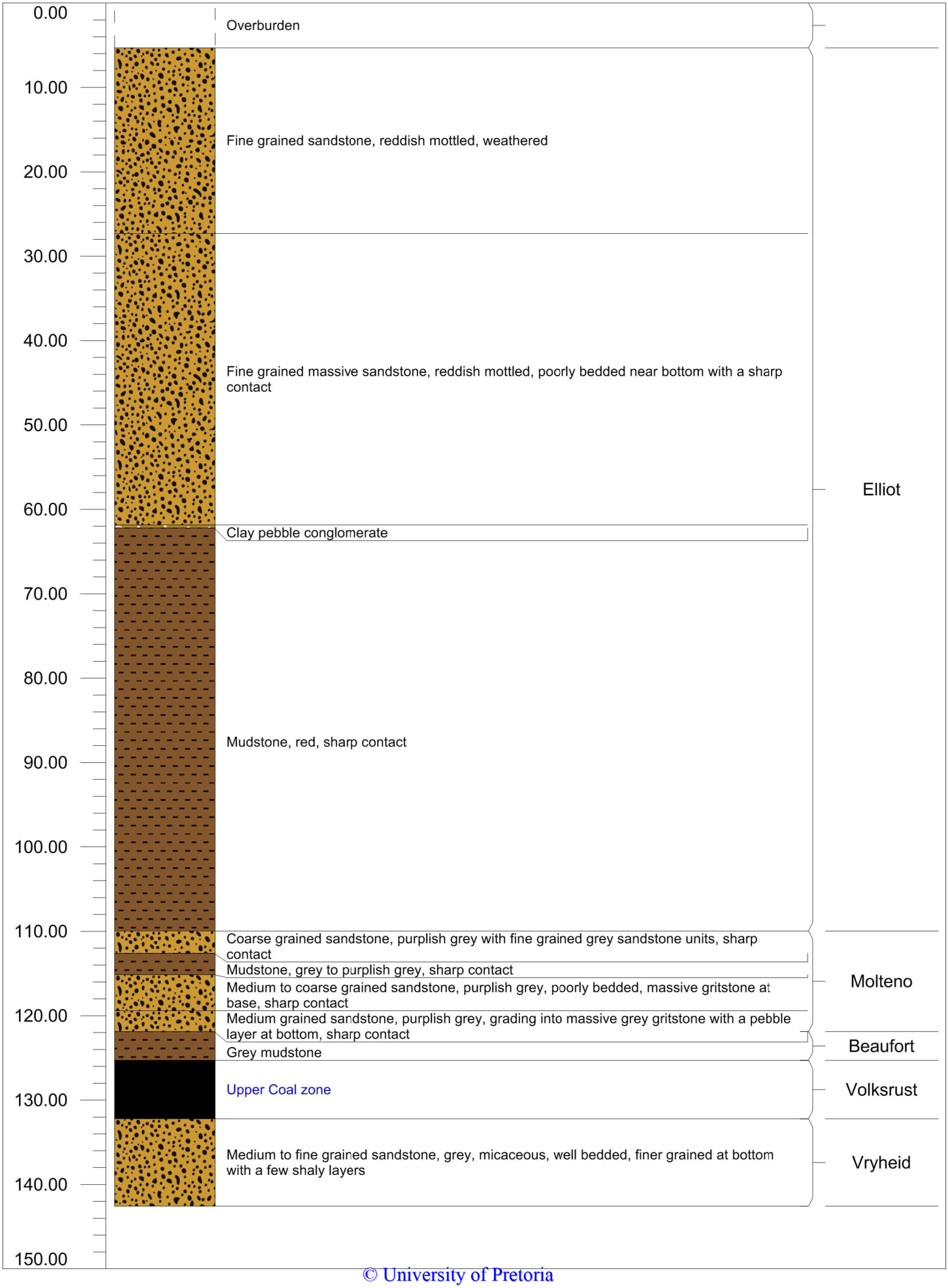

Area 5

Borehole: 3028803

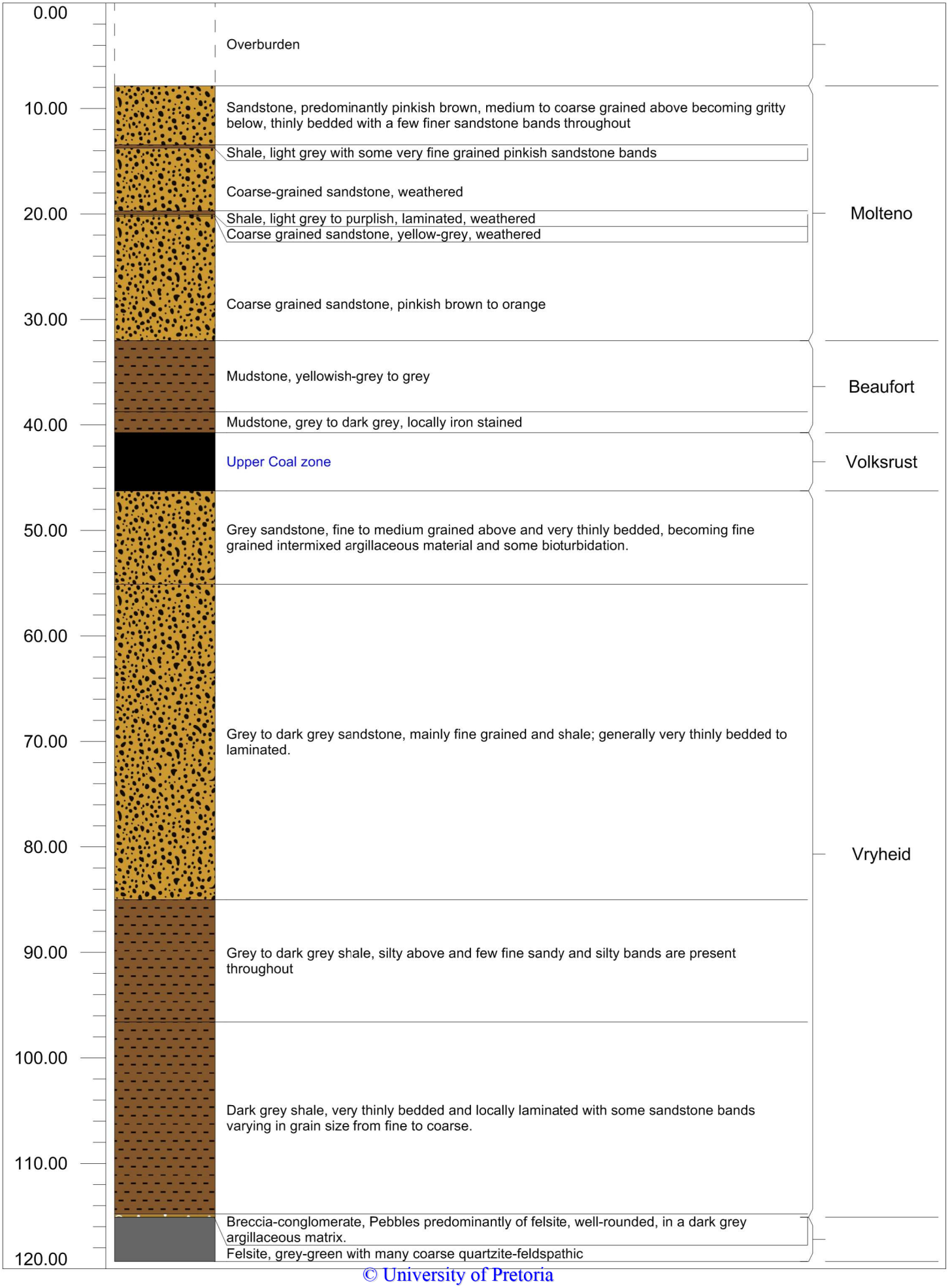

Area 6

Borehole: 3028685

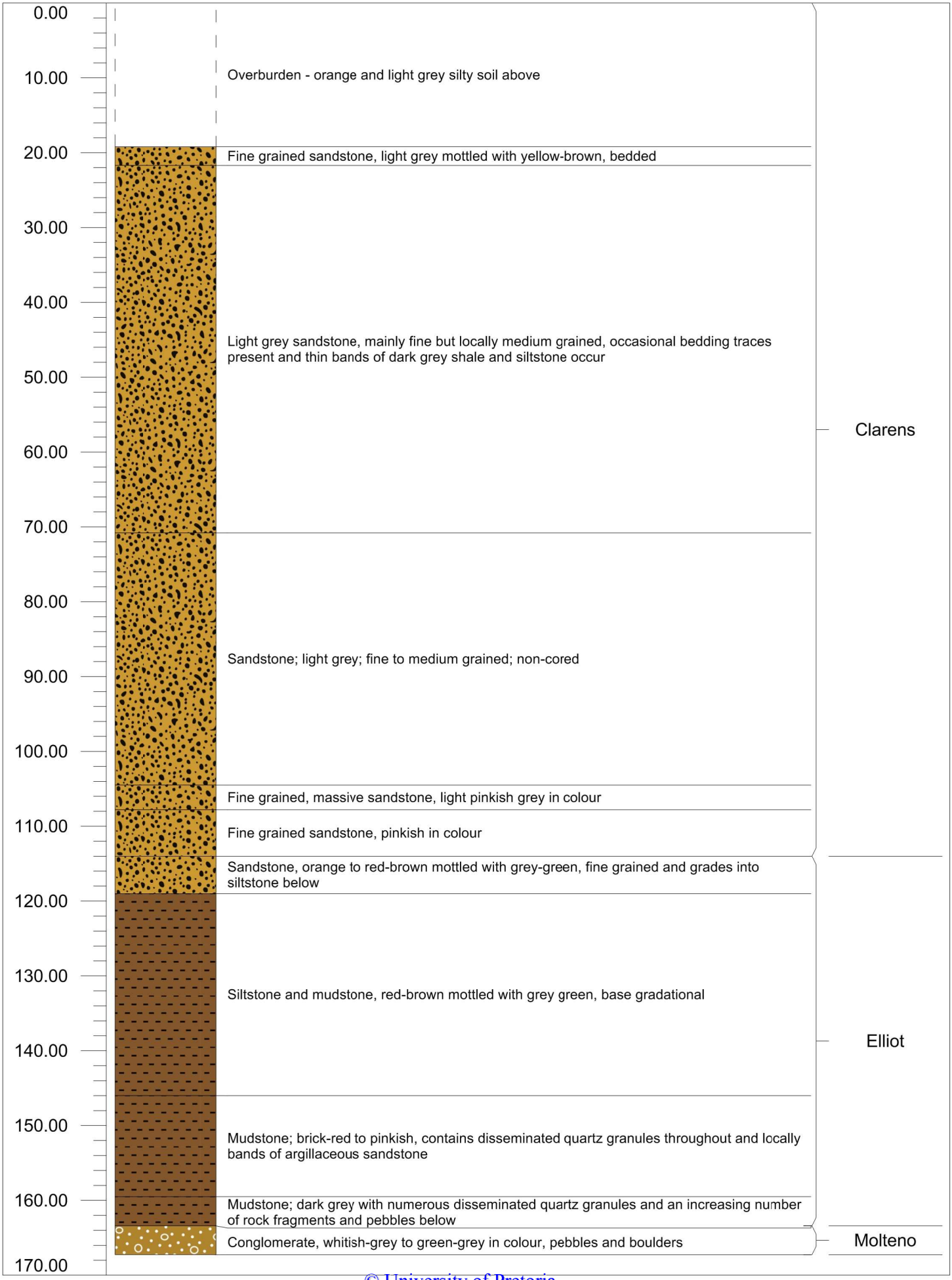

Area 6

Borehole: 1919482

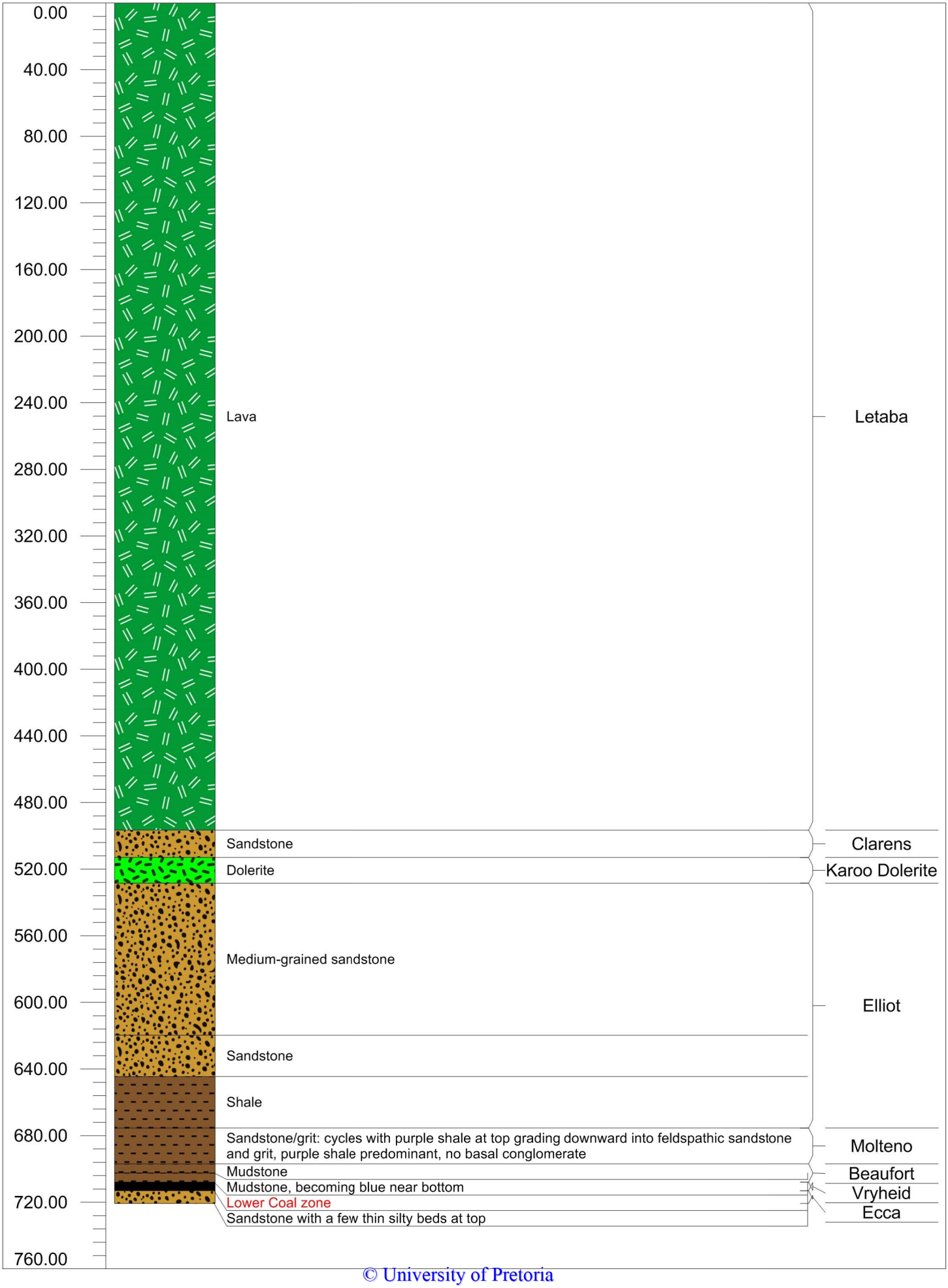

Area 6

Borehole: 3027470

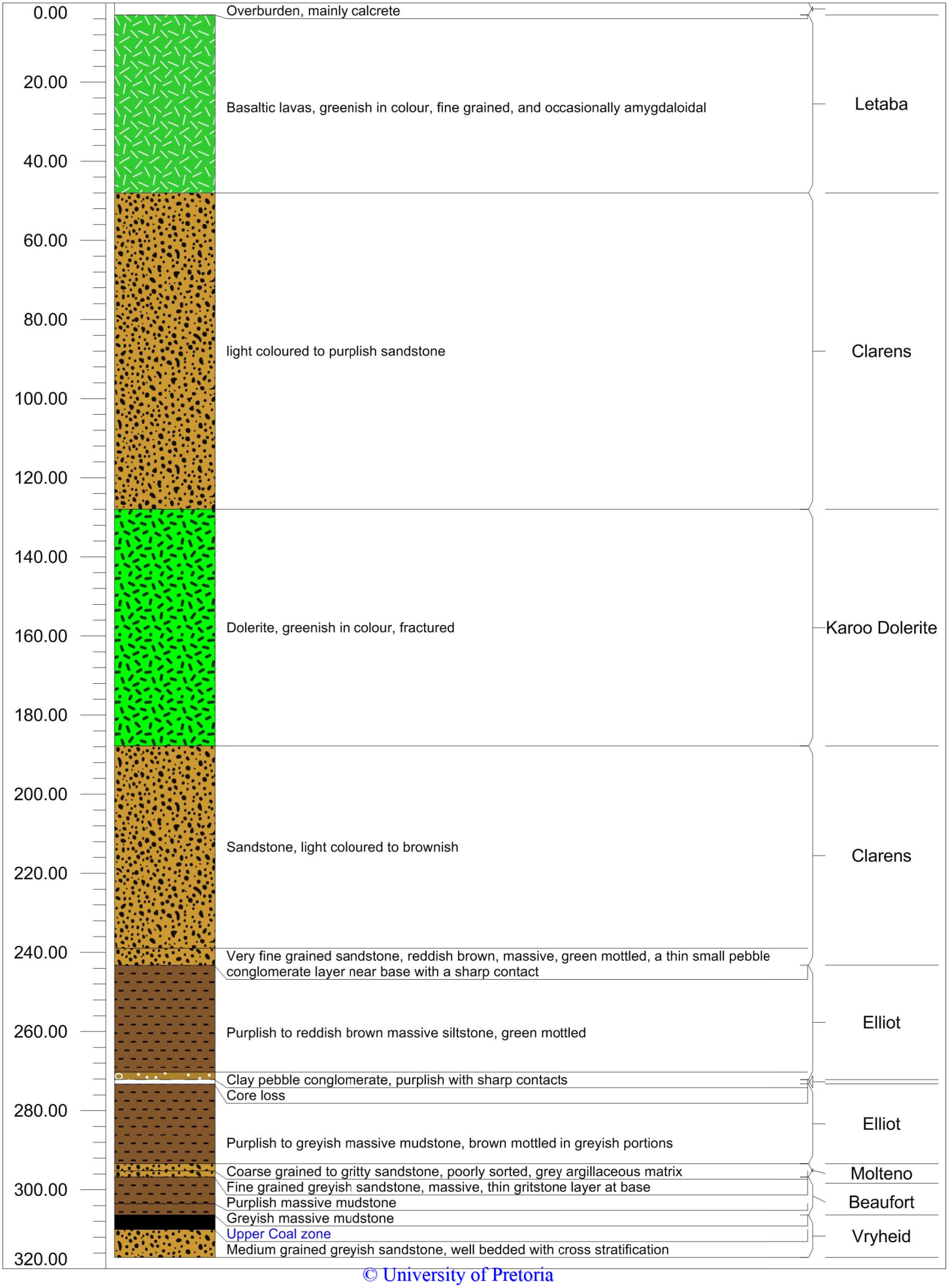

Area 6

Borehole: 3059424

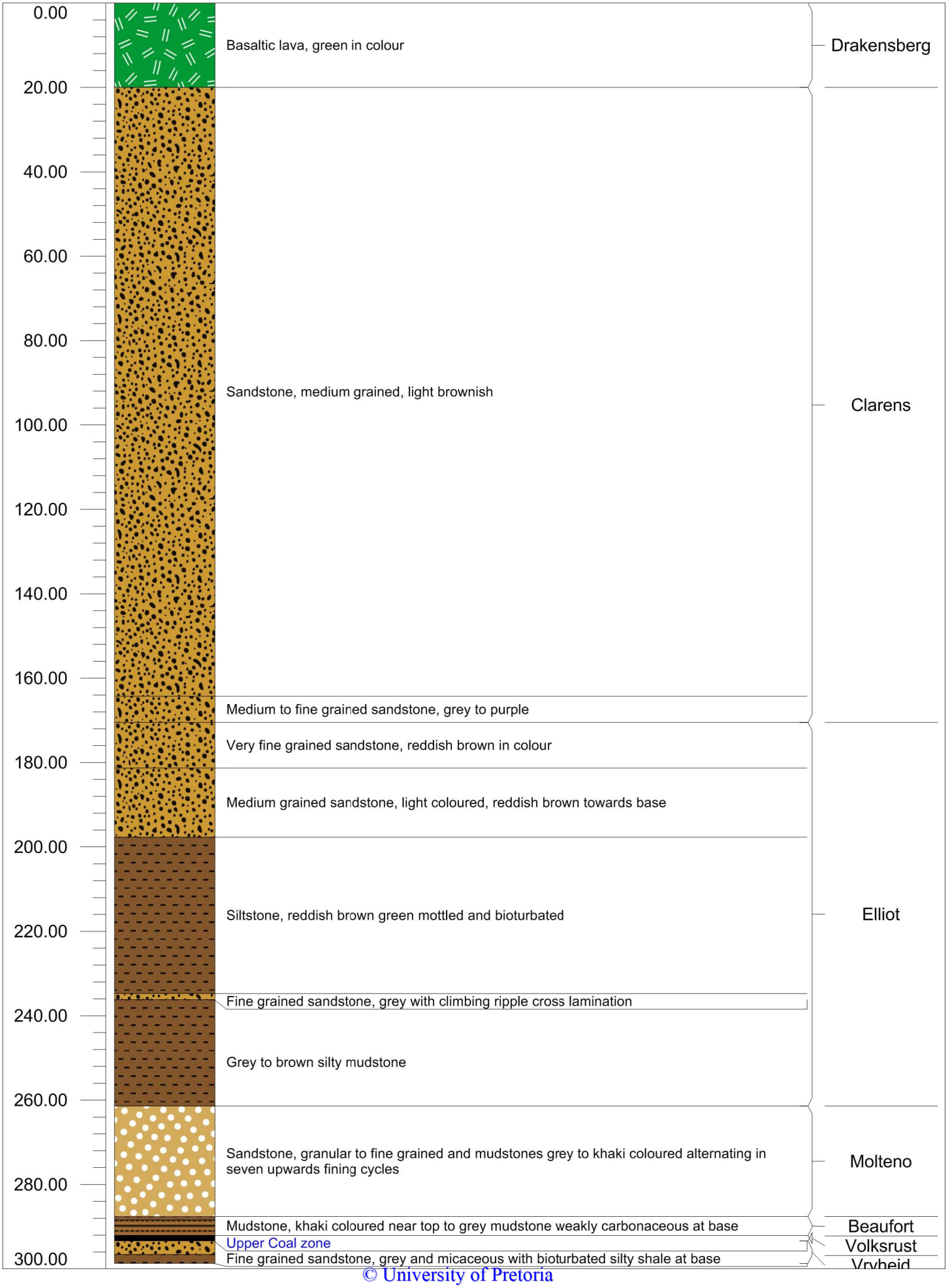

Area 6

Borehole: 3028659

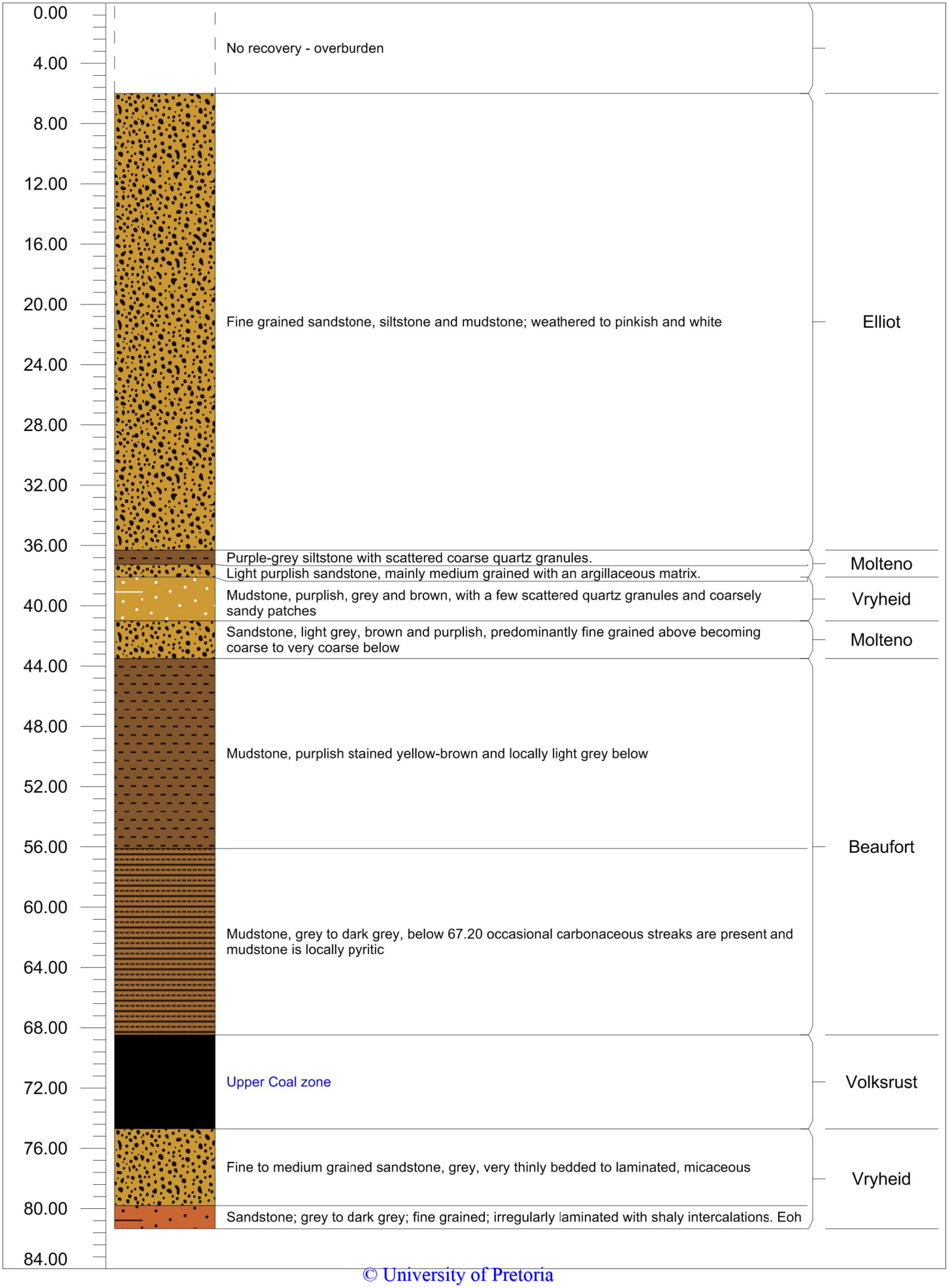

Area 7

Borehole: 3014405

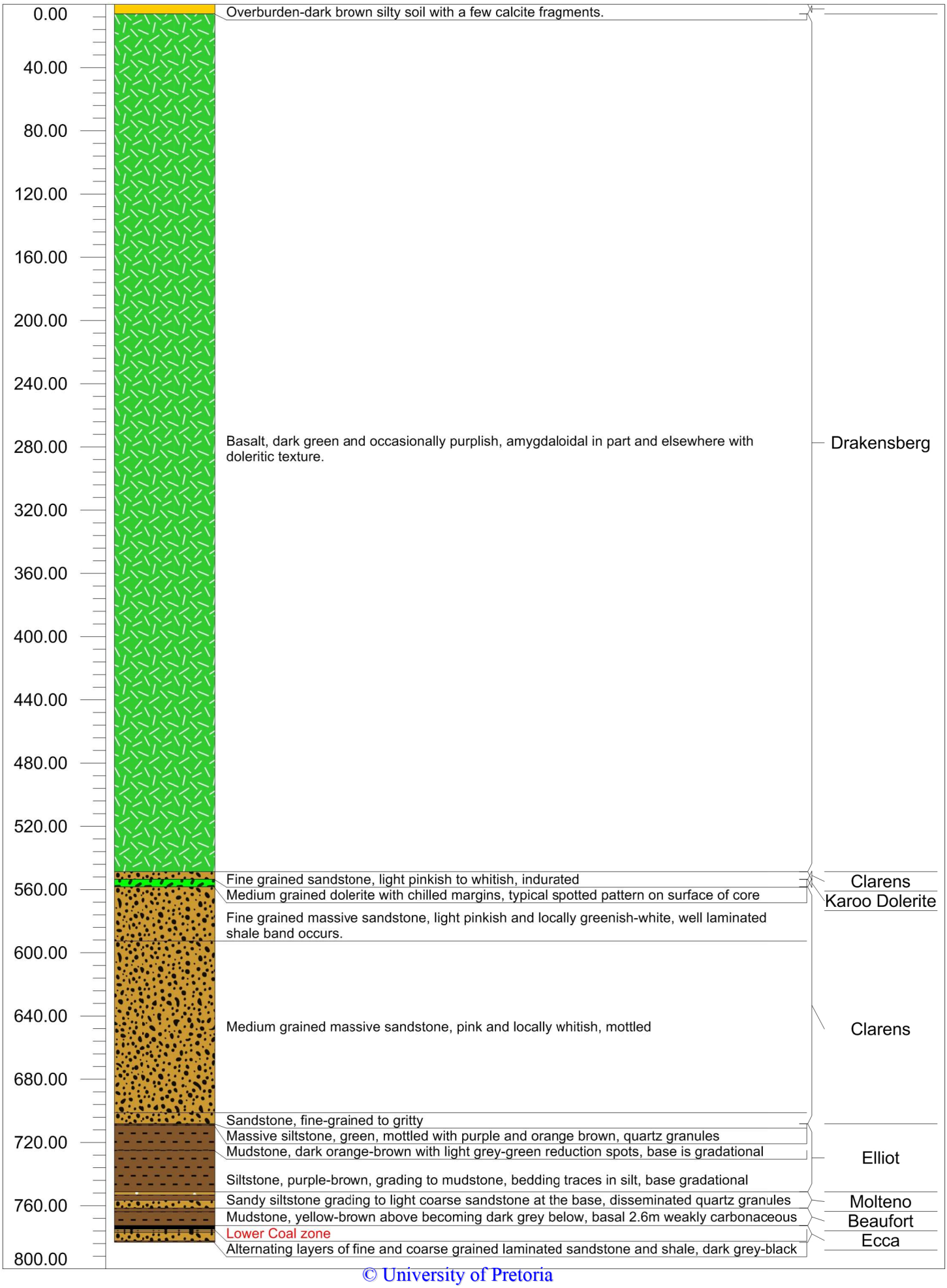

Area 7

Borehole: 3000201

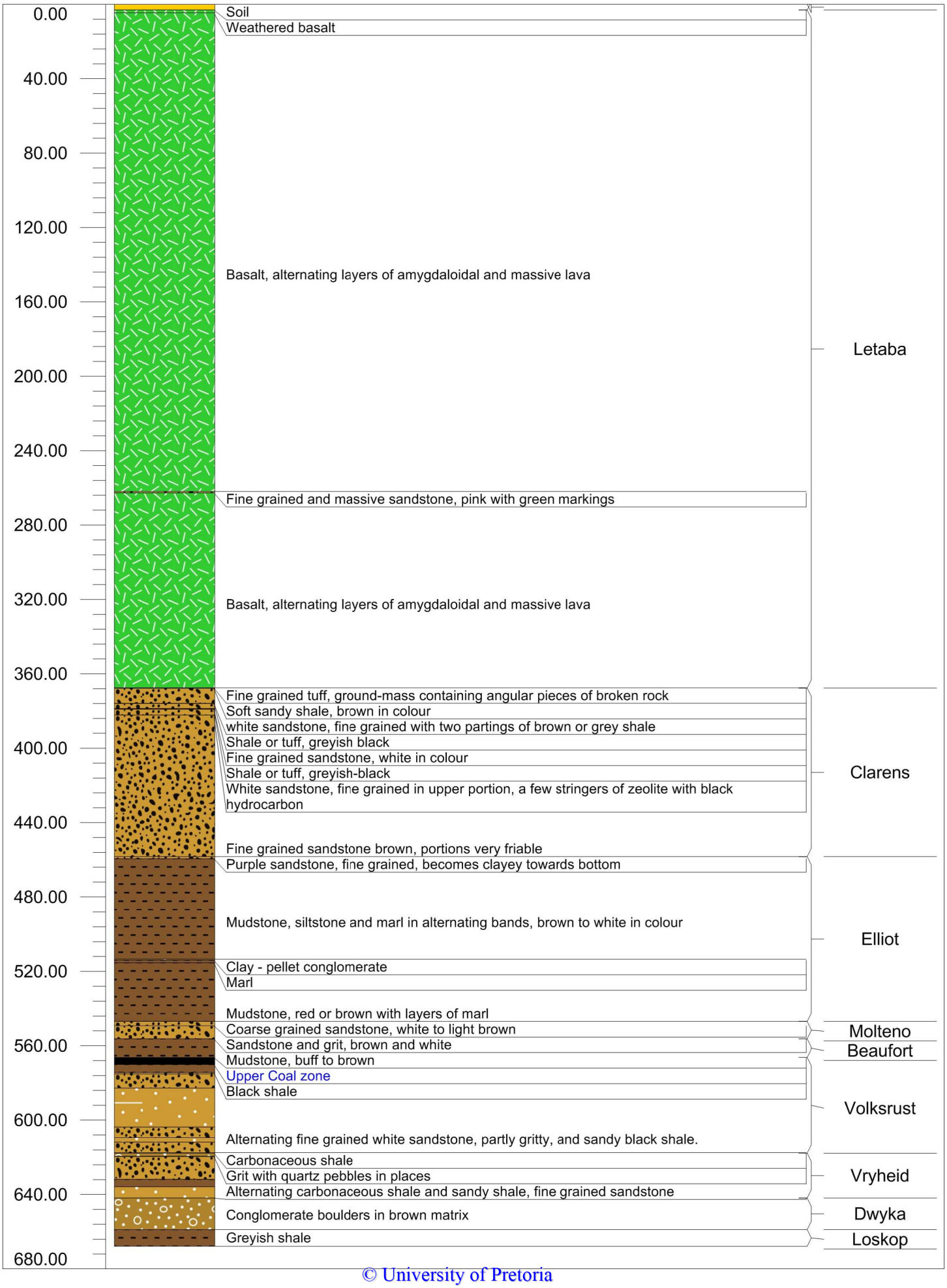

Area 7

Borehole: 3028808

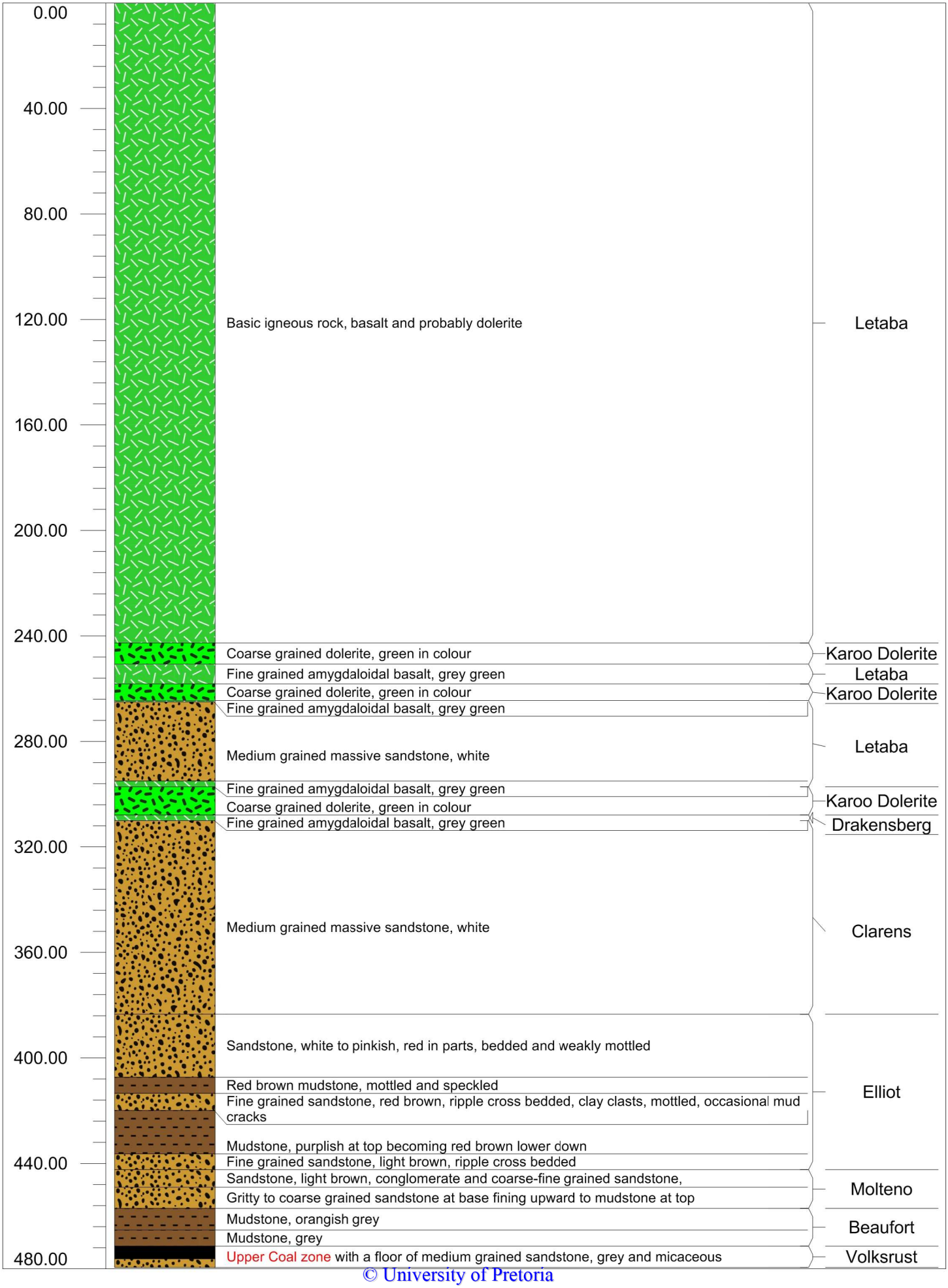

Area 7

Borehole: 3028815

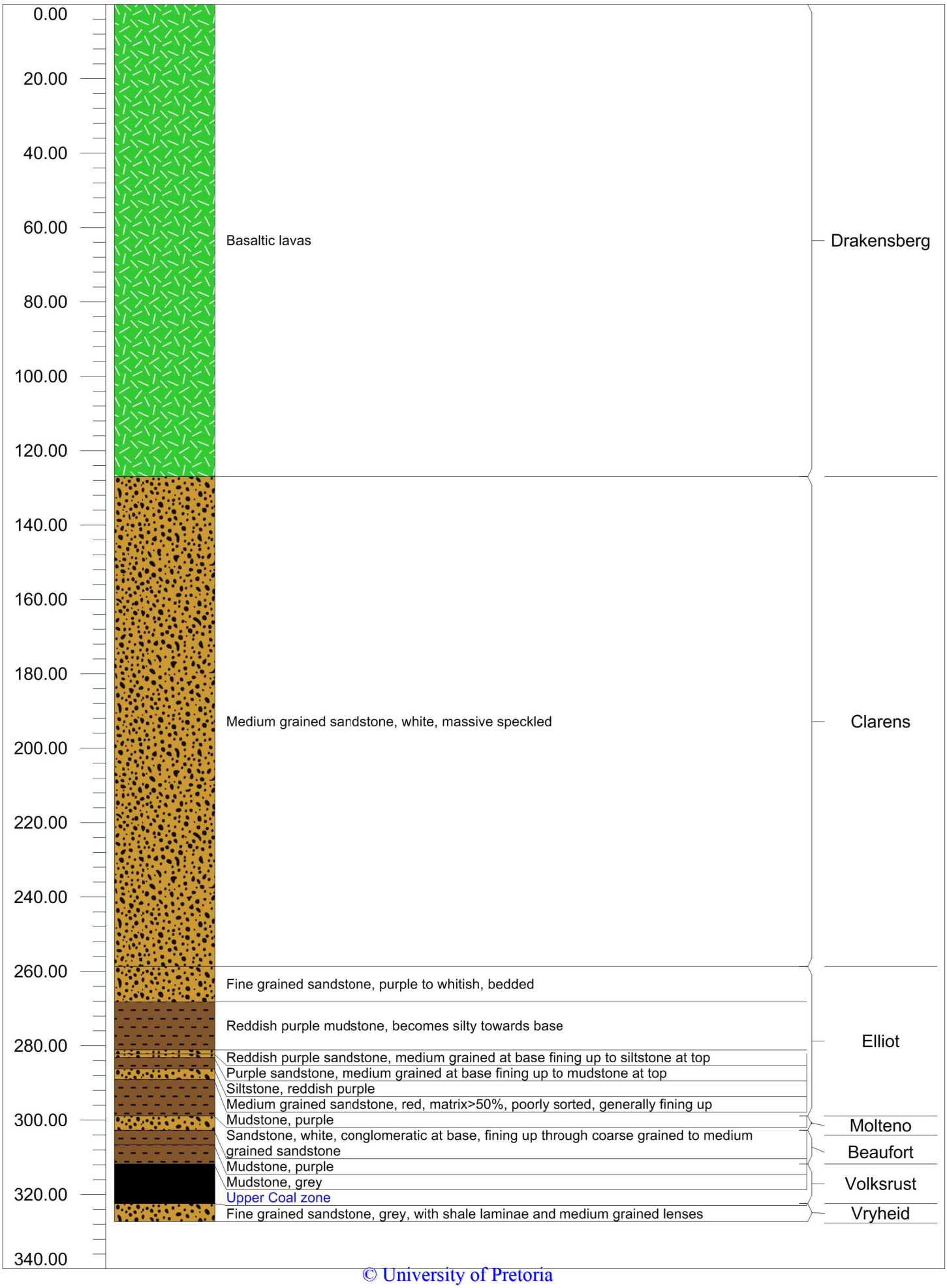

Area 7

Borehole: 3000183

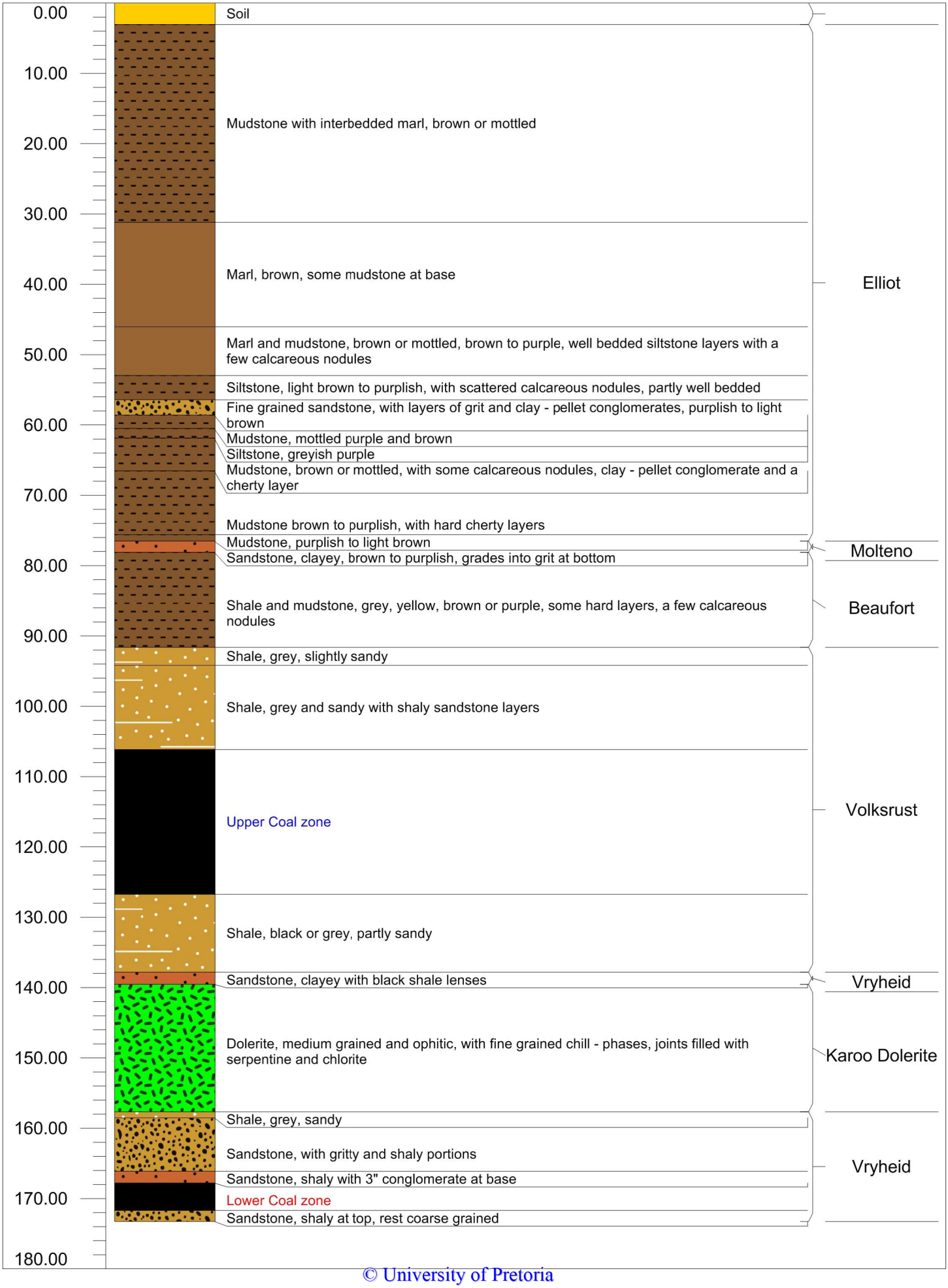

Area 1

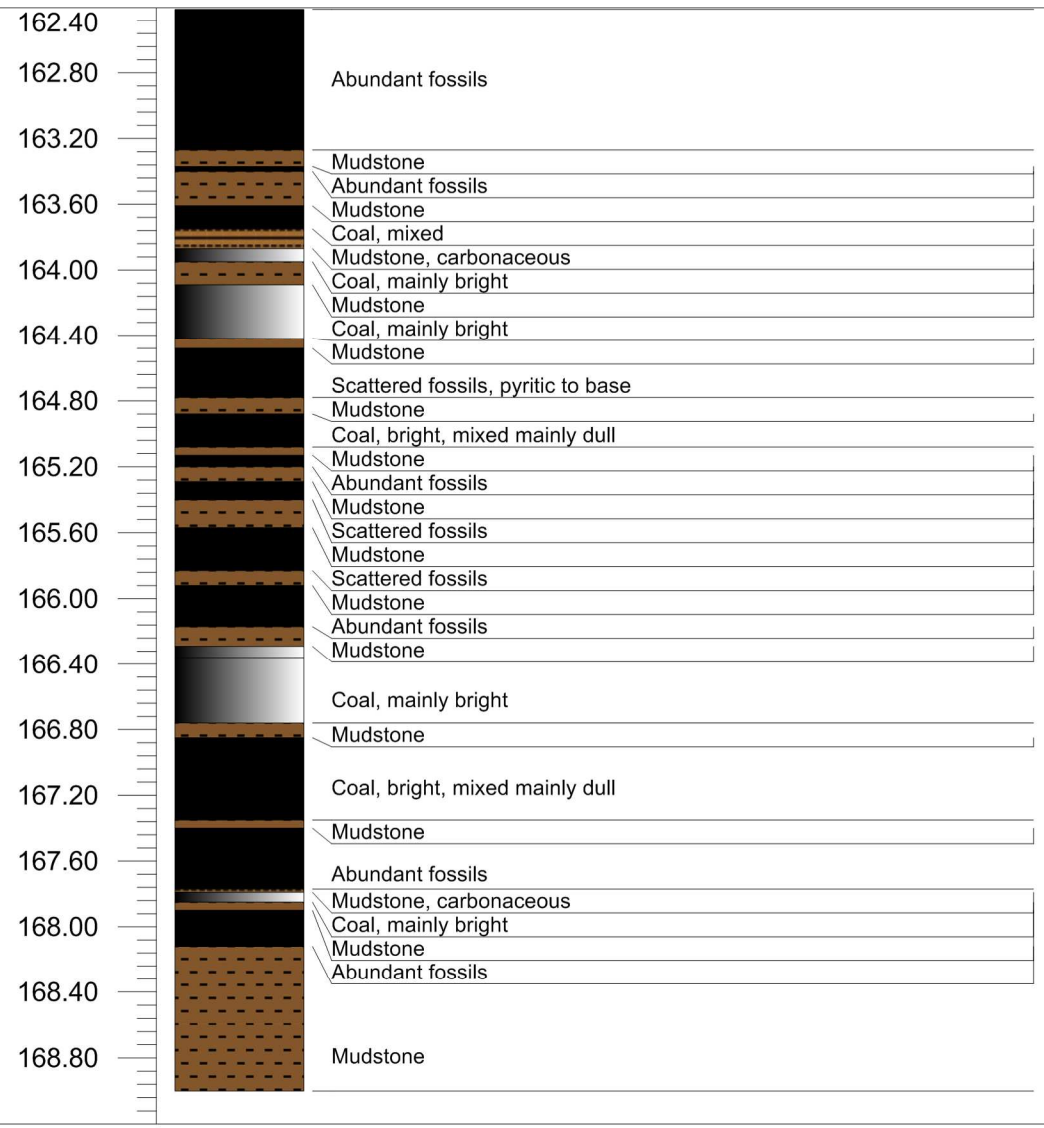

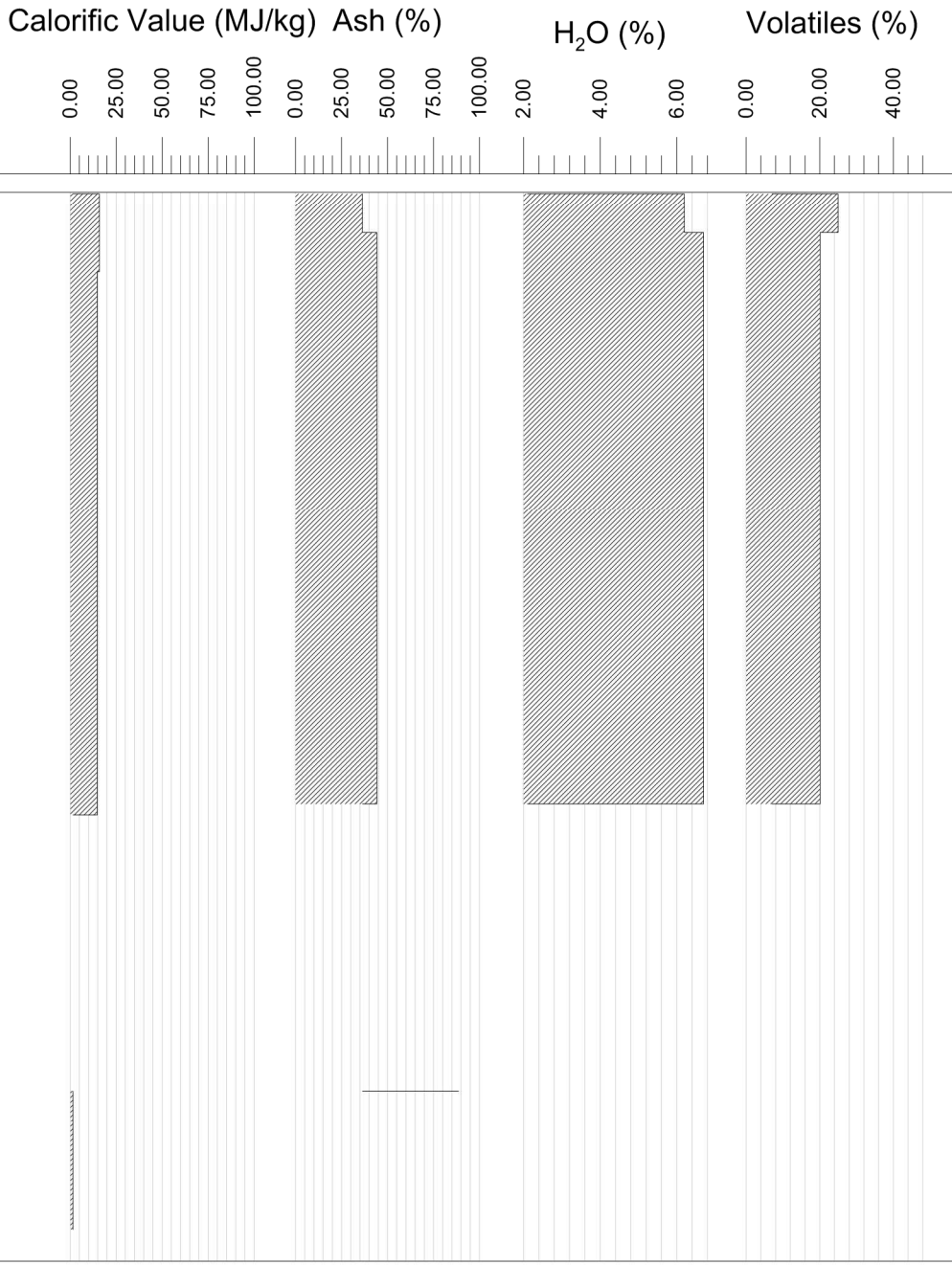

Coal Seam: Lower Coal Zone

Borehole: 1919834

Area 1

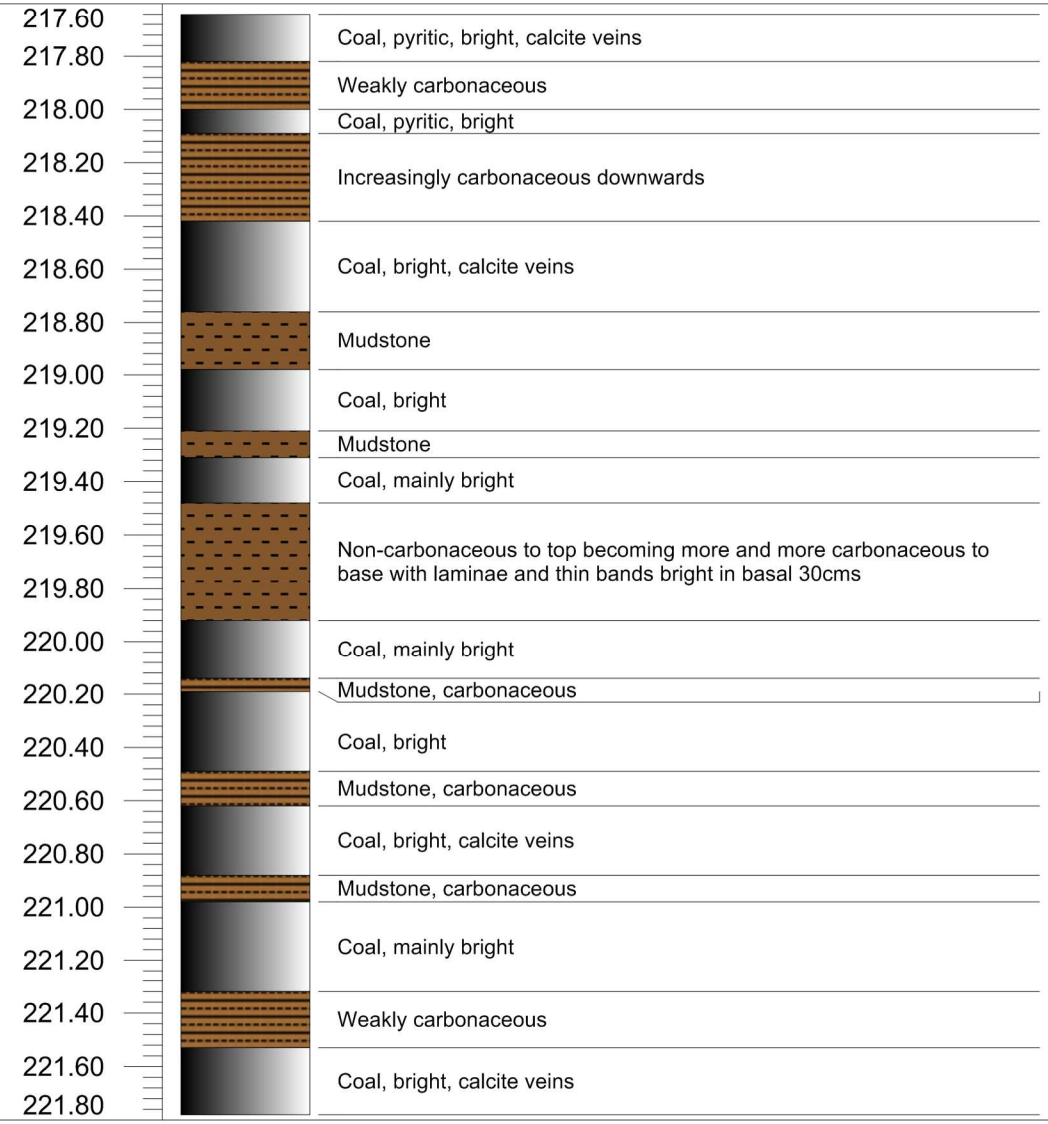

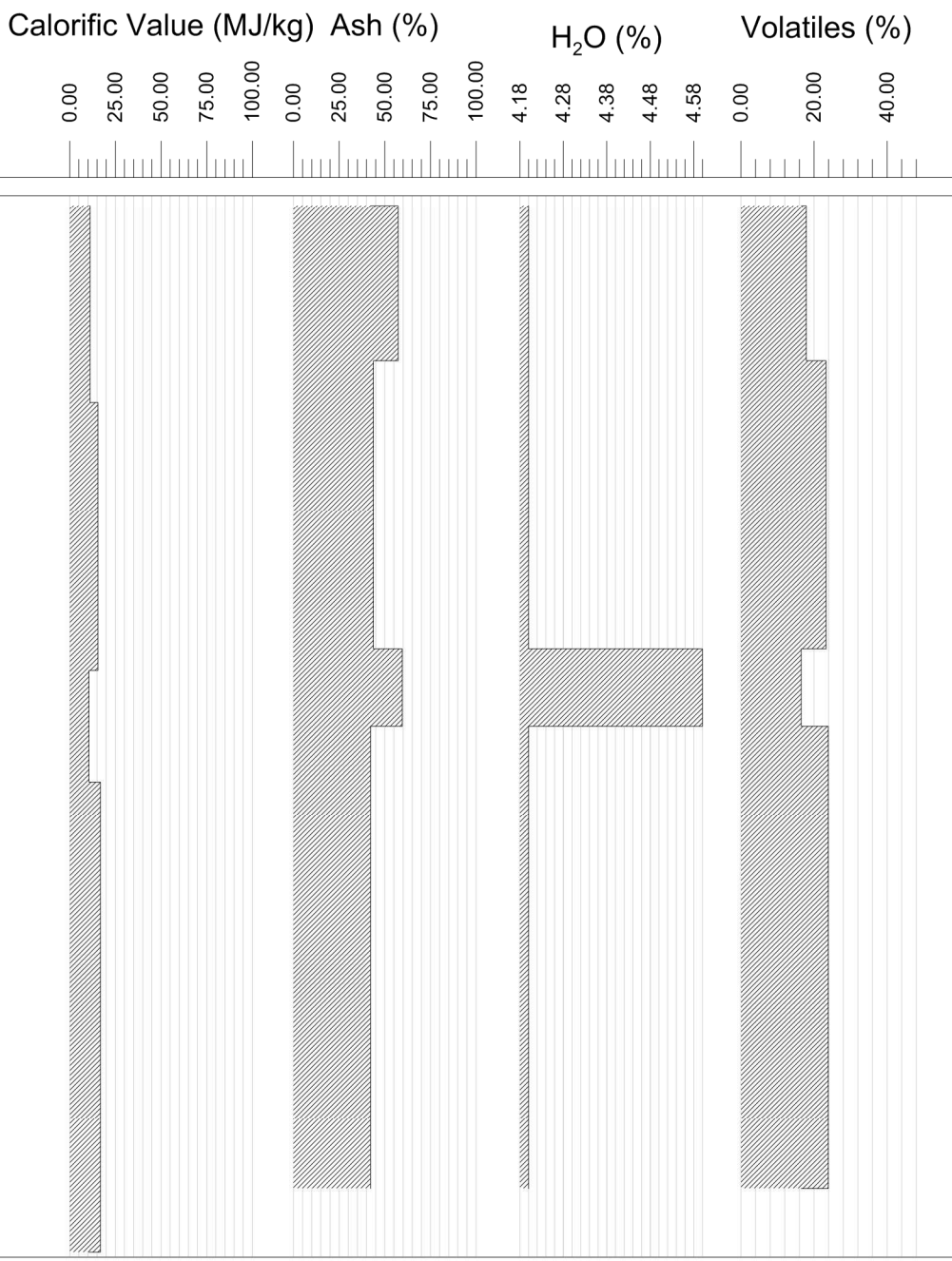

Coal Seam: Lower Coal Zone

Borehole: 1919761

Area 1

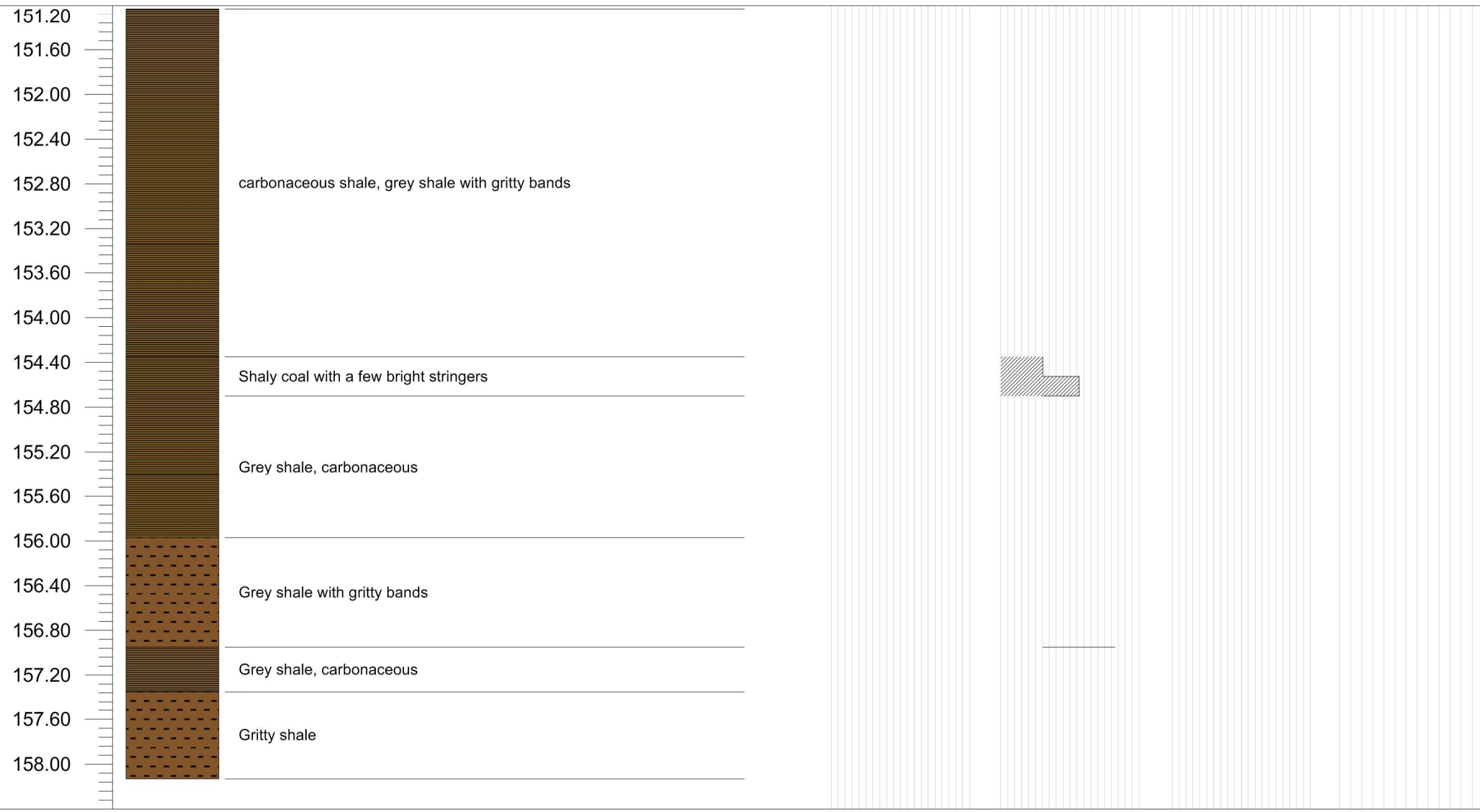

Coal Seam: Lower Coal Zone

Borehole:3028399

Area 1

Coal Seam: Upper Coal Zone

Borehole:3028399

Area 1

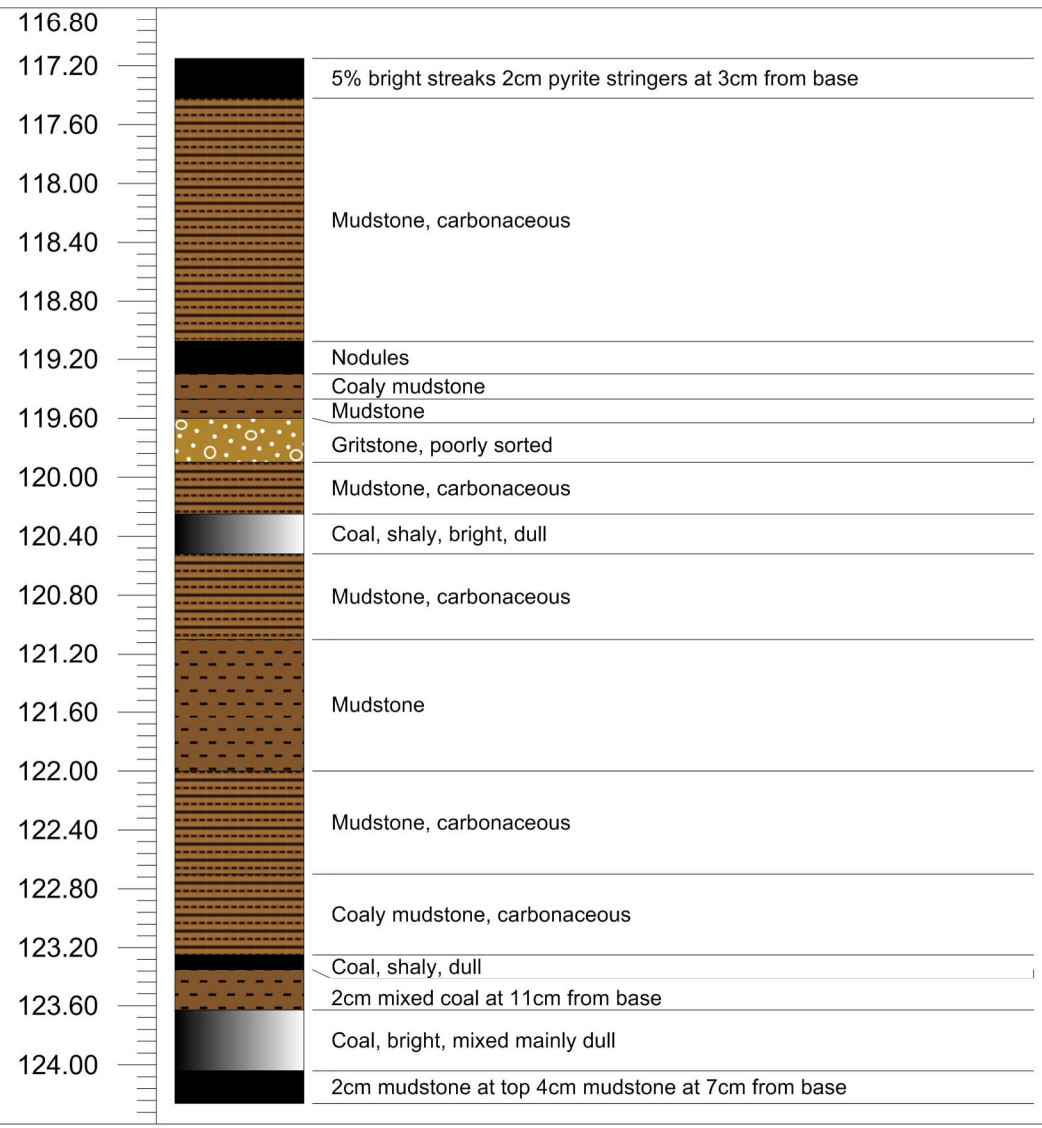

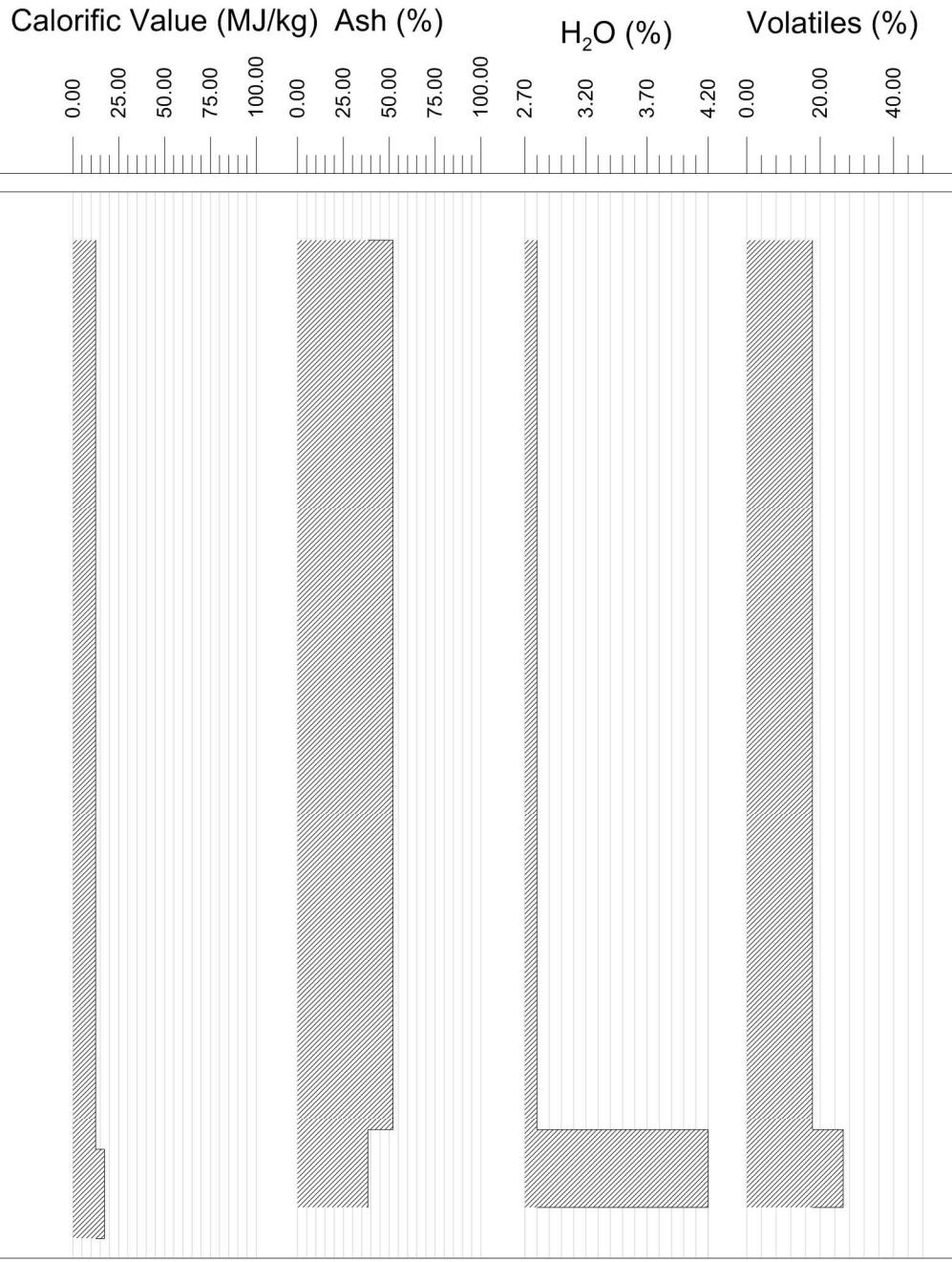

Coal Seam: Lower Coal Zone

Borehole: 1919455

Area 1

Coal Seam: Upper Coal Zone

Borehole: 1919455

Area 1

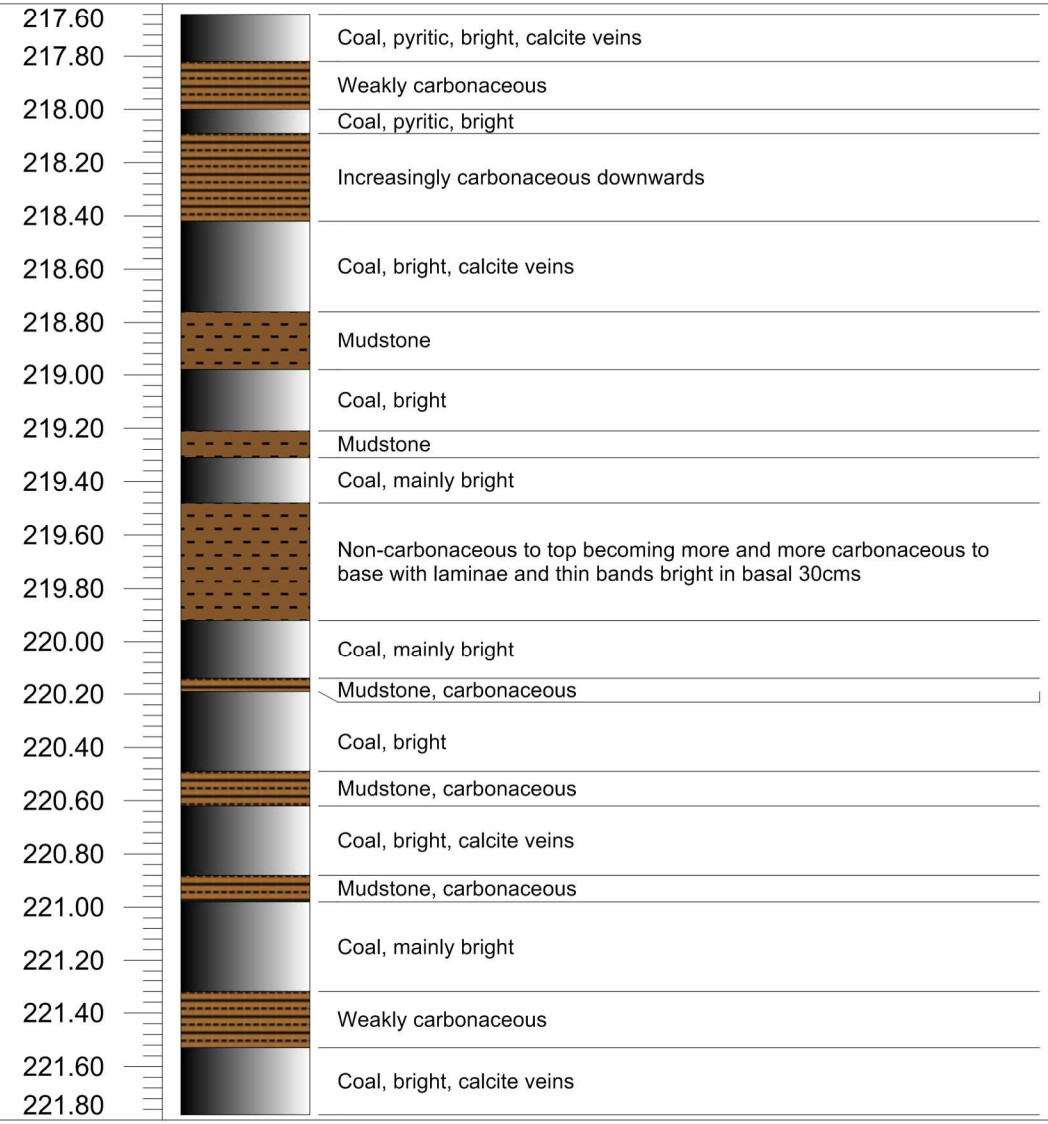

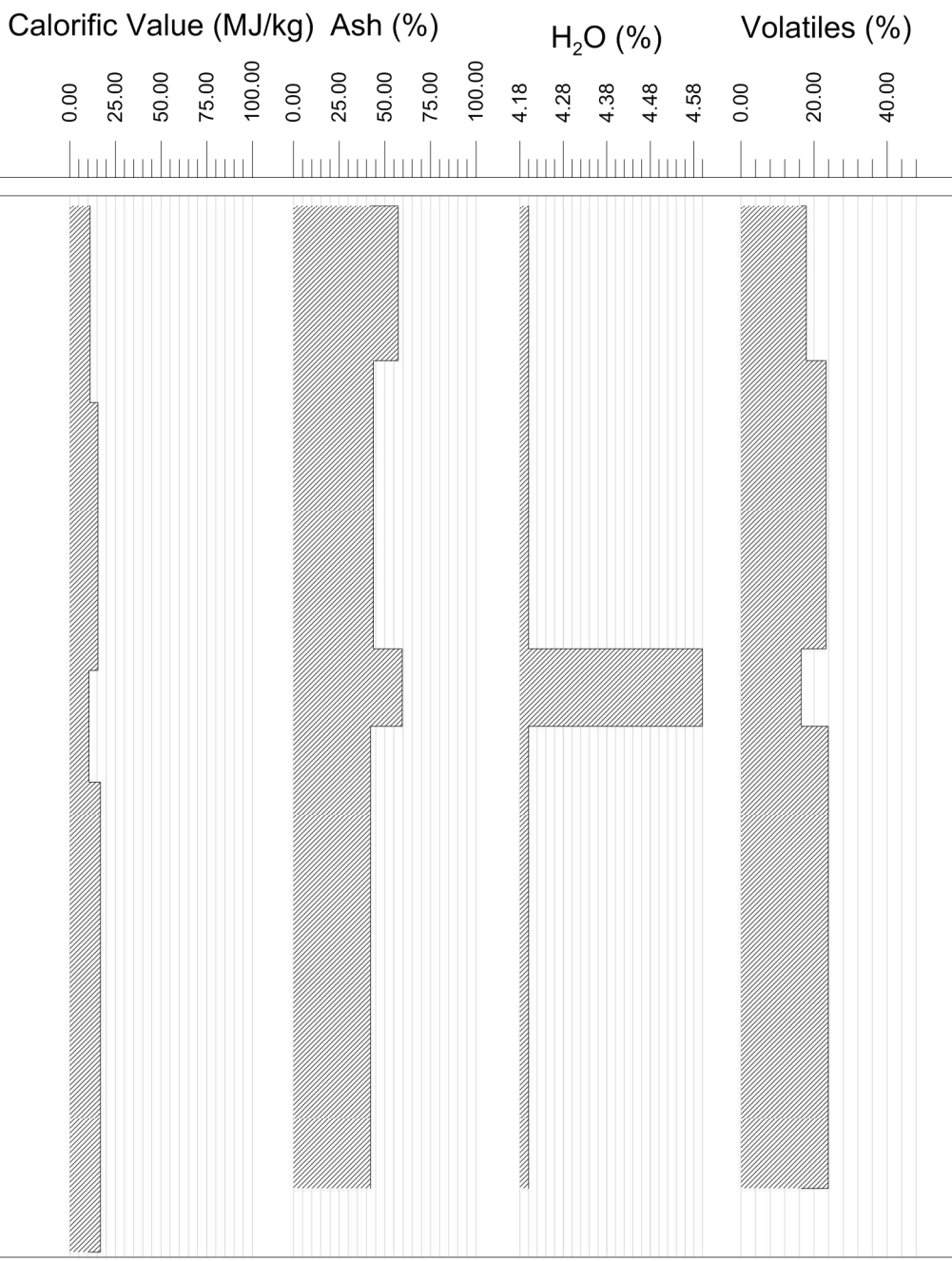

Coal Seam: Lower Coal Zone

Borehole: 1919761

Area 1

Coal Seam: Upper Coal Zone

Borehole:3028394

Area 2

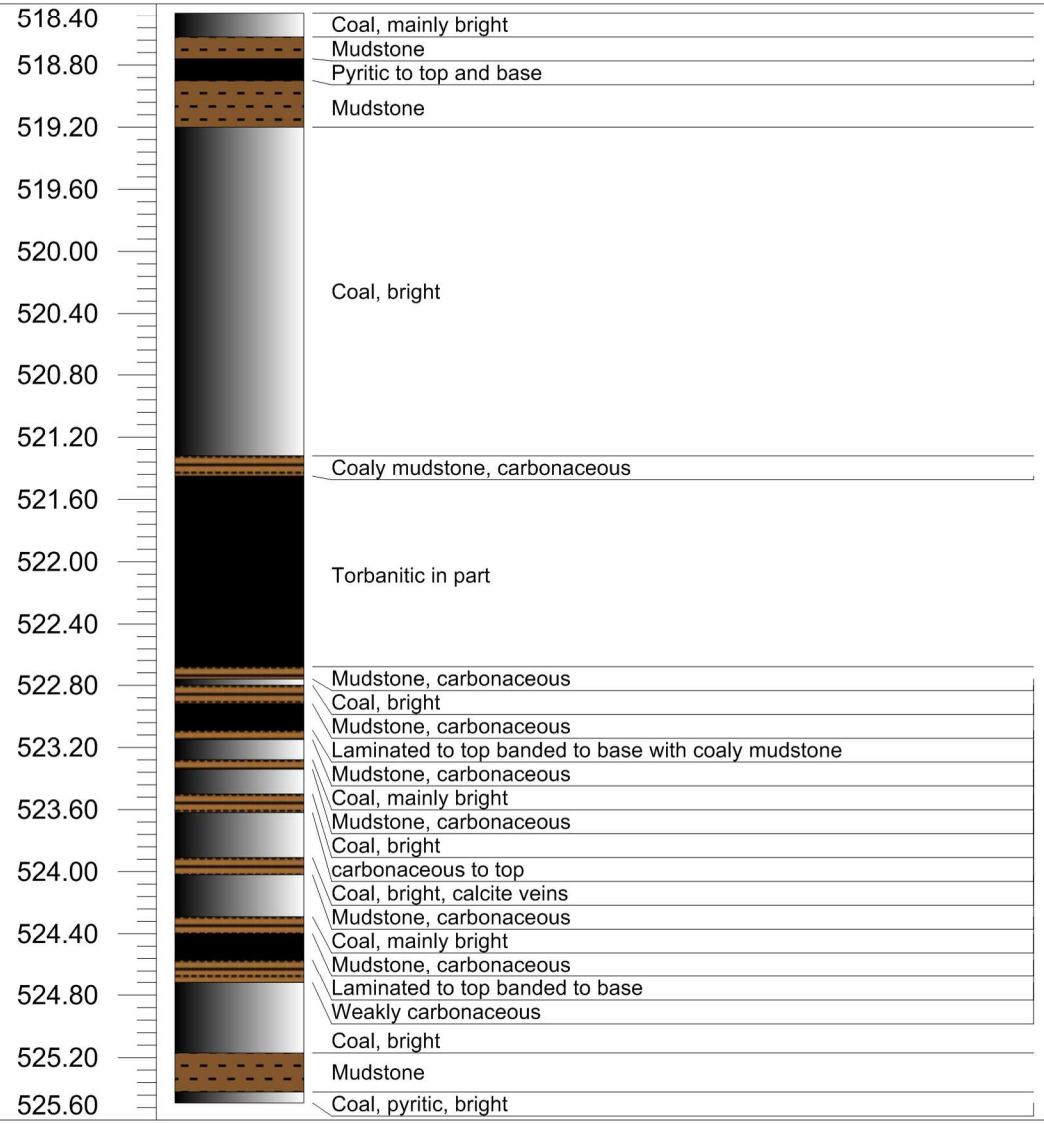

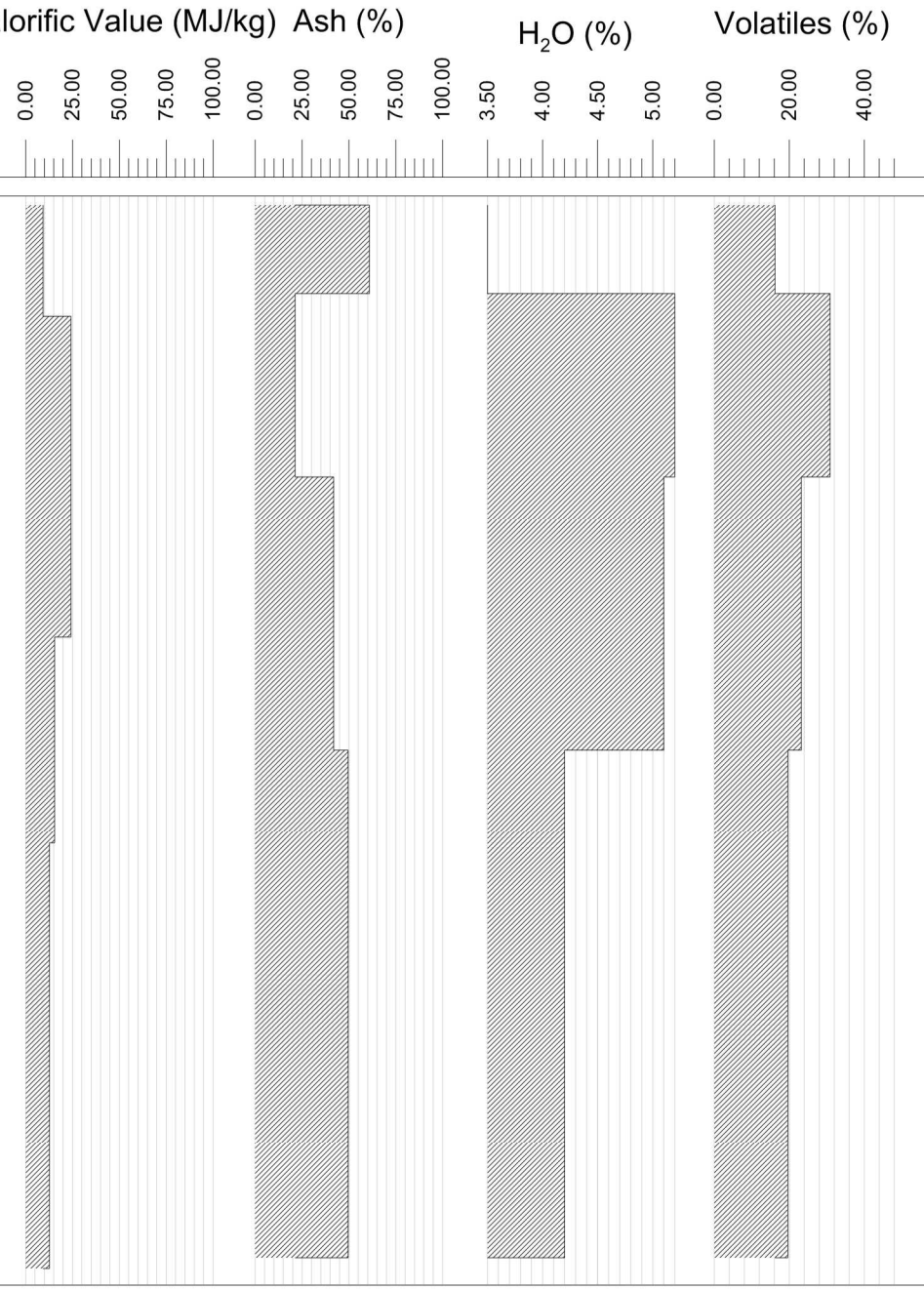

Coal Seam: Lower Coal Zone

Borehole: 1919754

Area 2

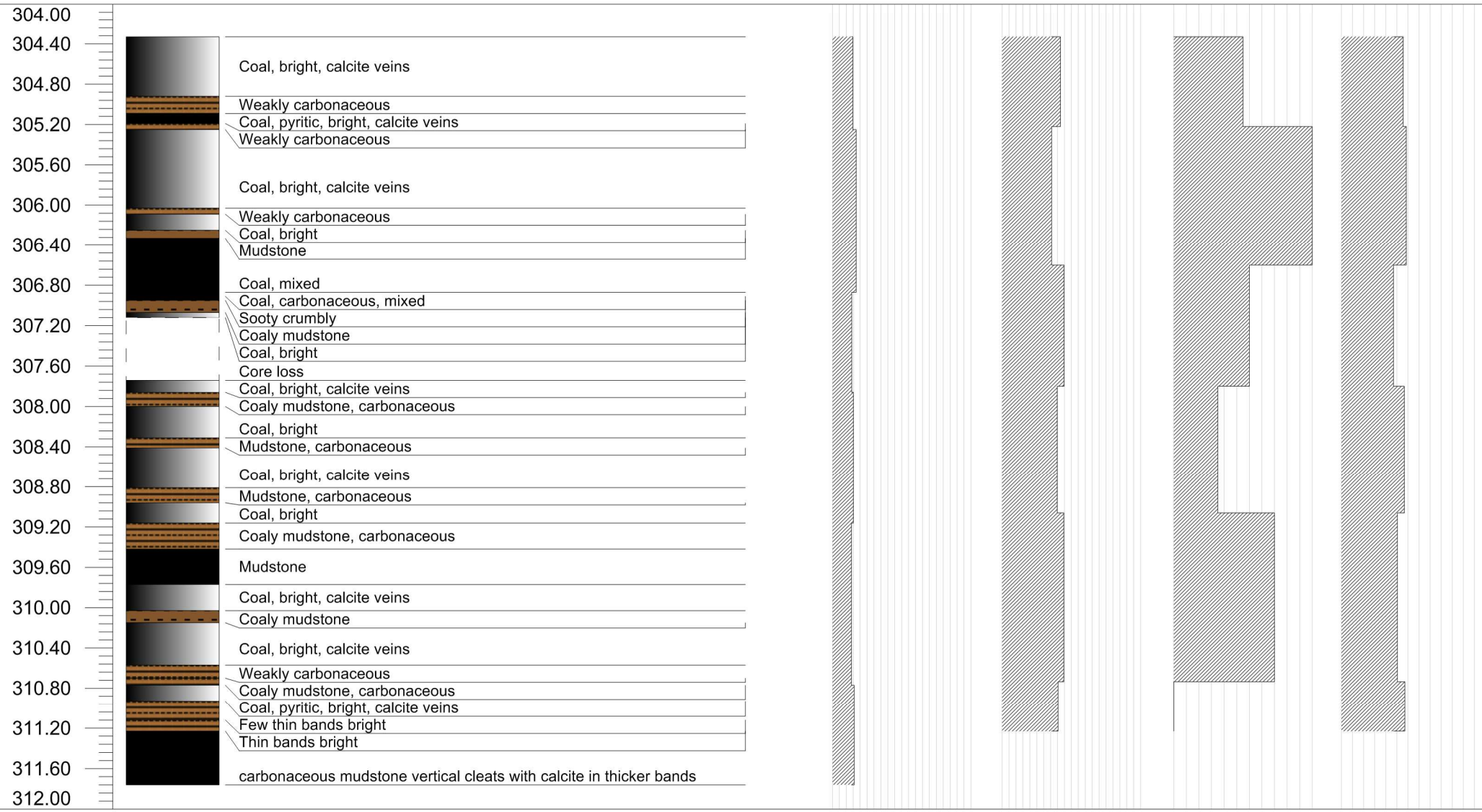

Coal Seam: Lower Coal Zone

Borehole: 1919571

Area 2

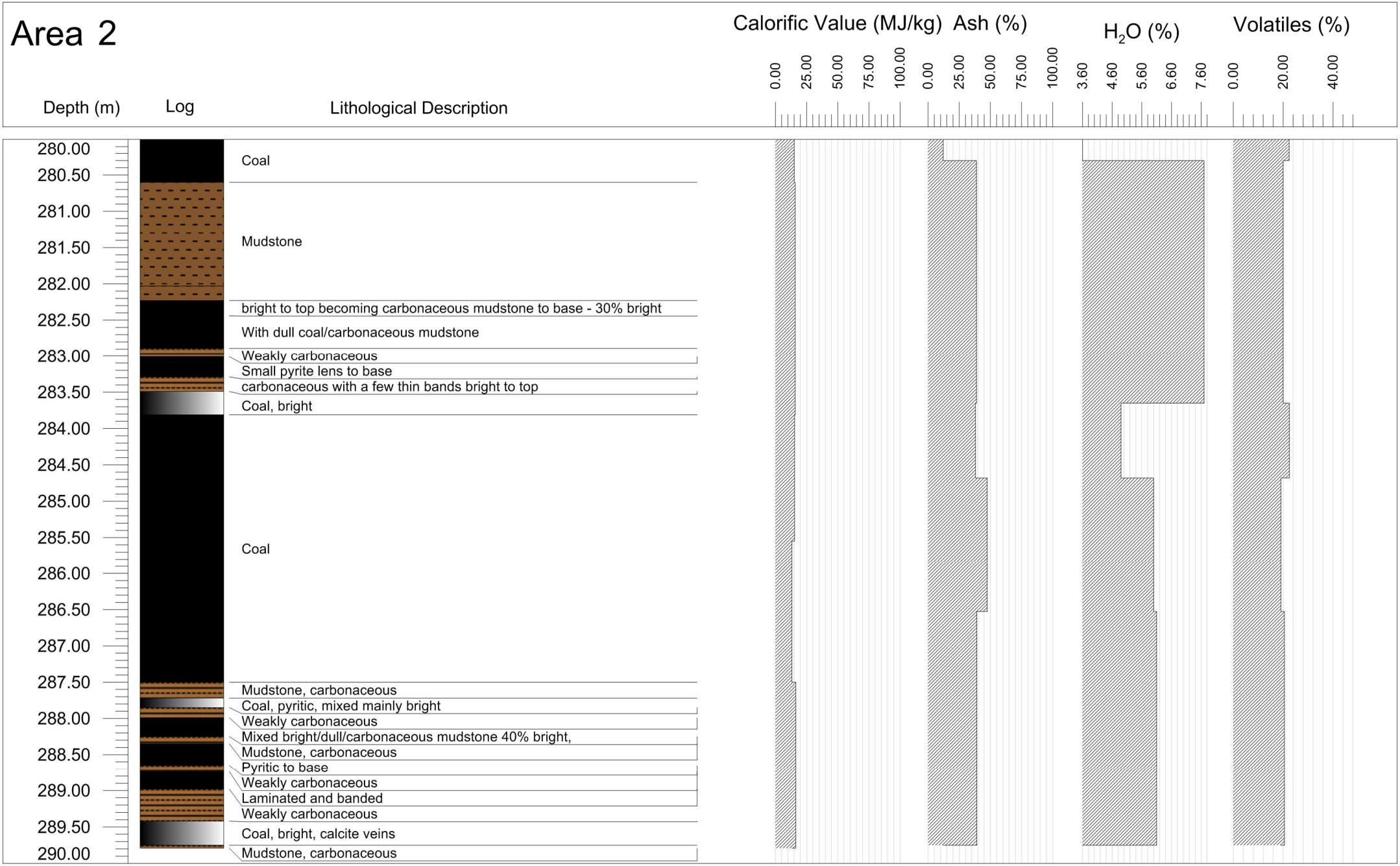

Coal Seam: Lower Coal Zone

Borehole: 1919651

Area 2

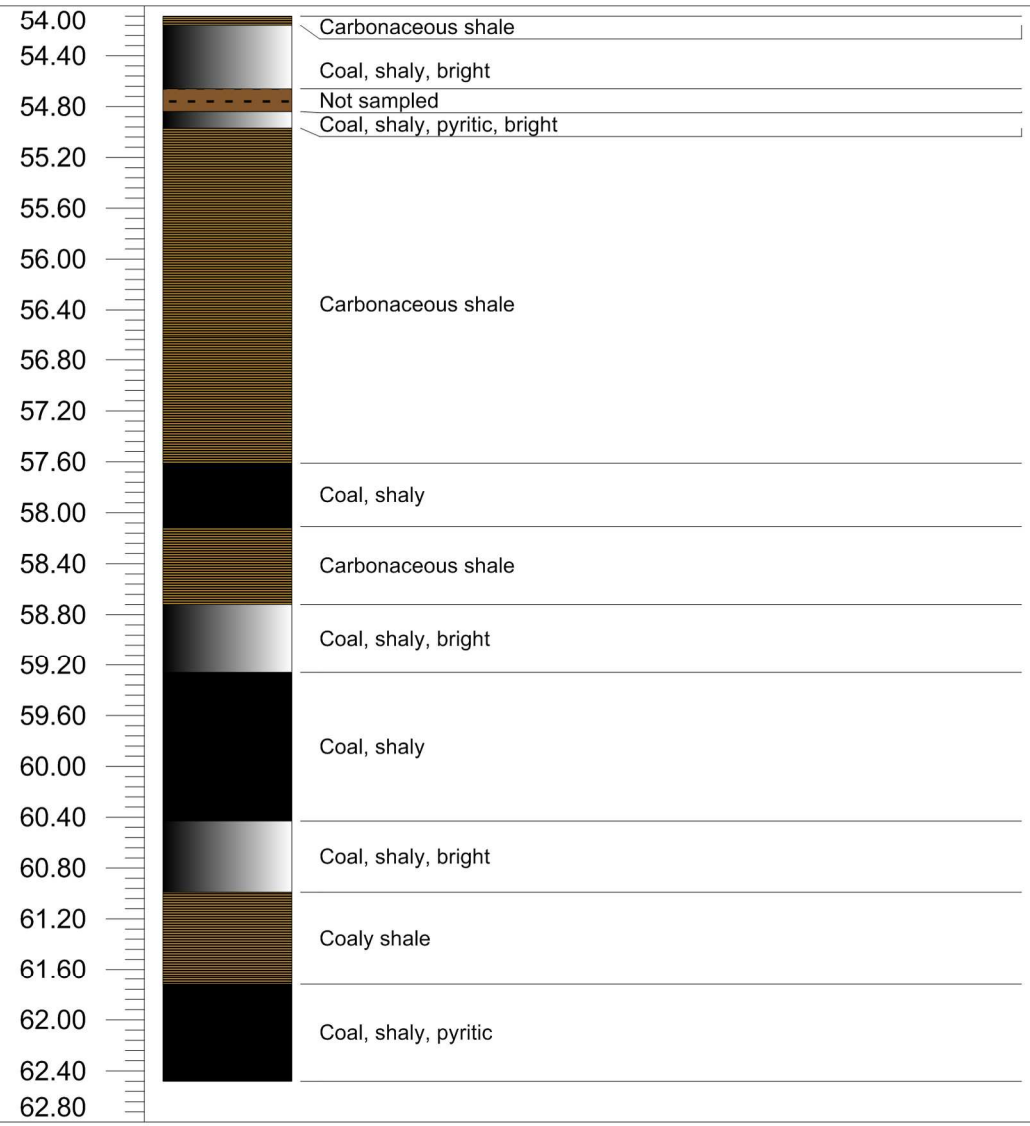

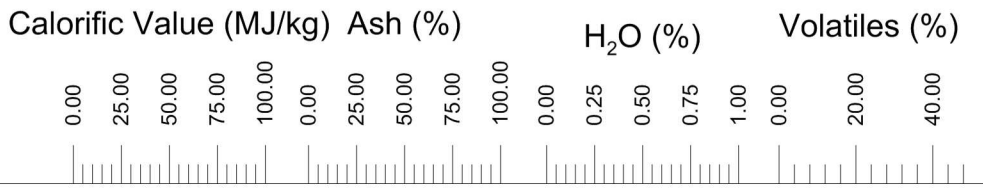

Coal Seam: Lower Coal Zone

Borehole: 1919595

Area 2

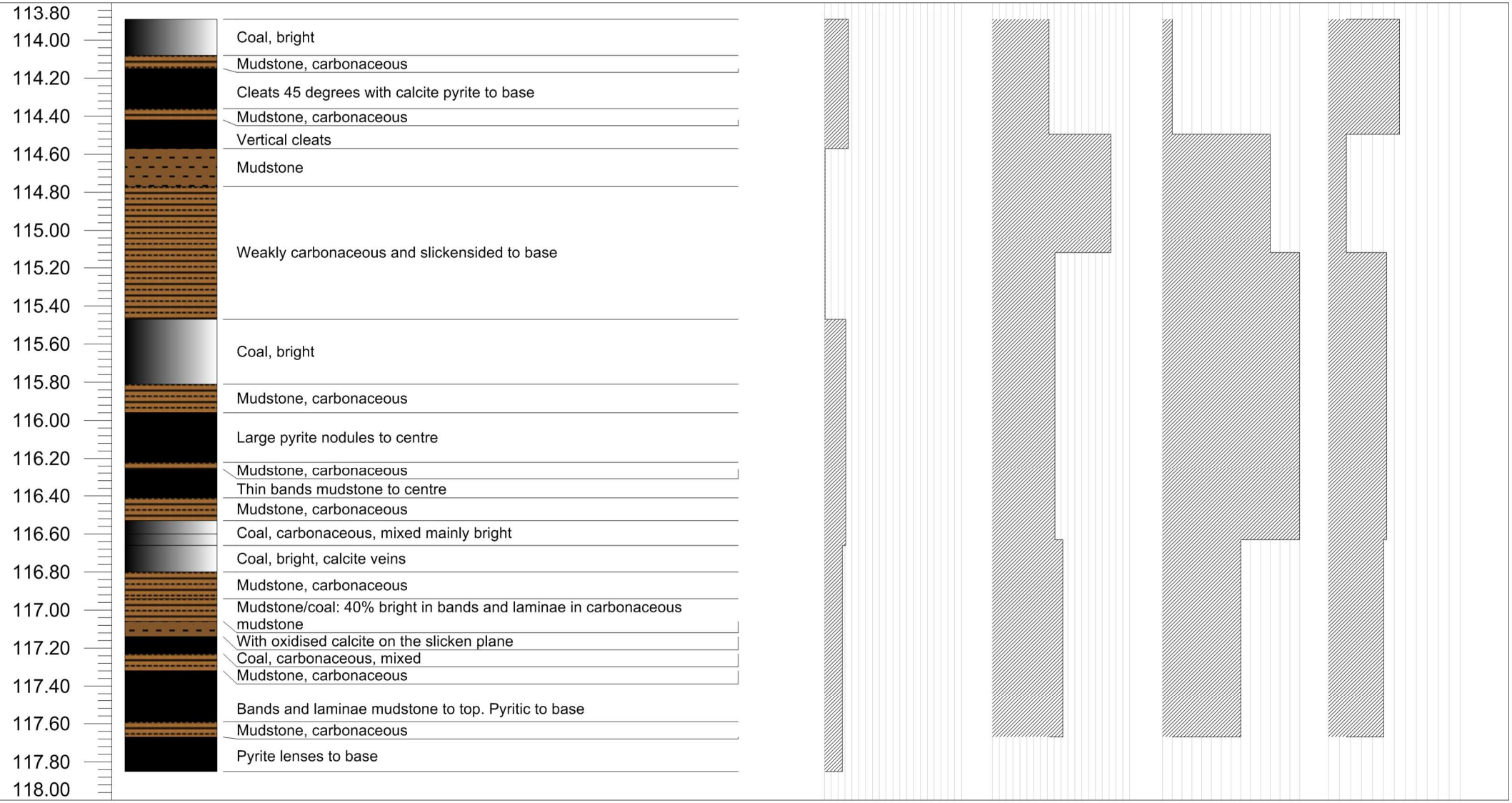

Coal Seam: Lower Coal Zone

Borehole: 1919563

Area 3

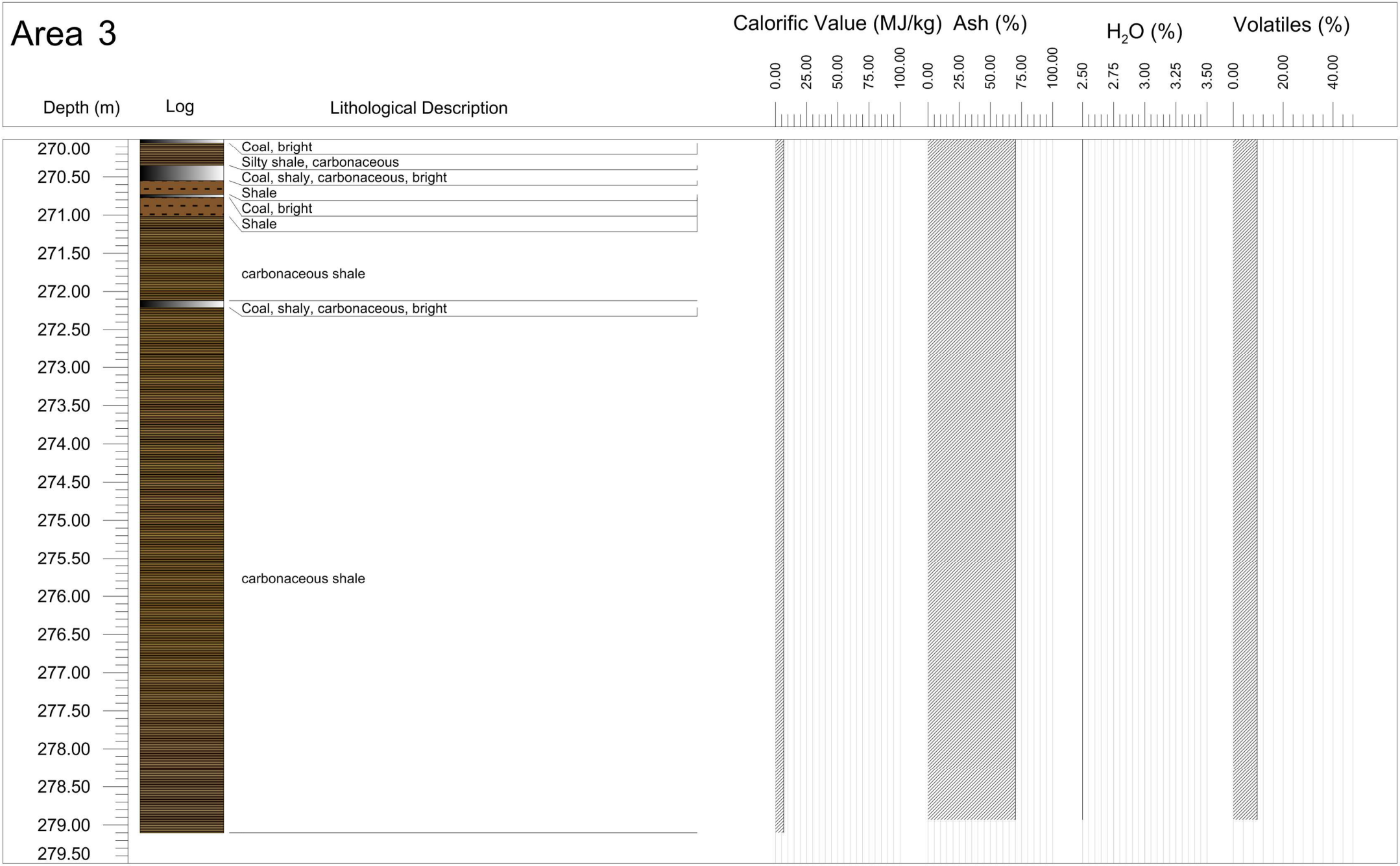

Coal Seam: Lower Coal Zone

Borehole: 1919552

Area 3

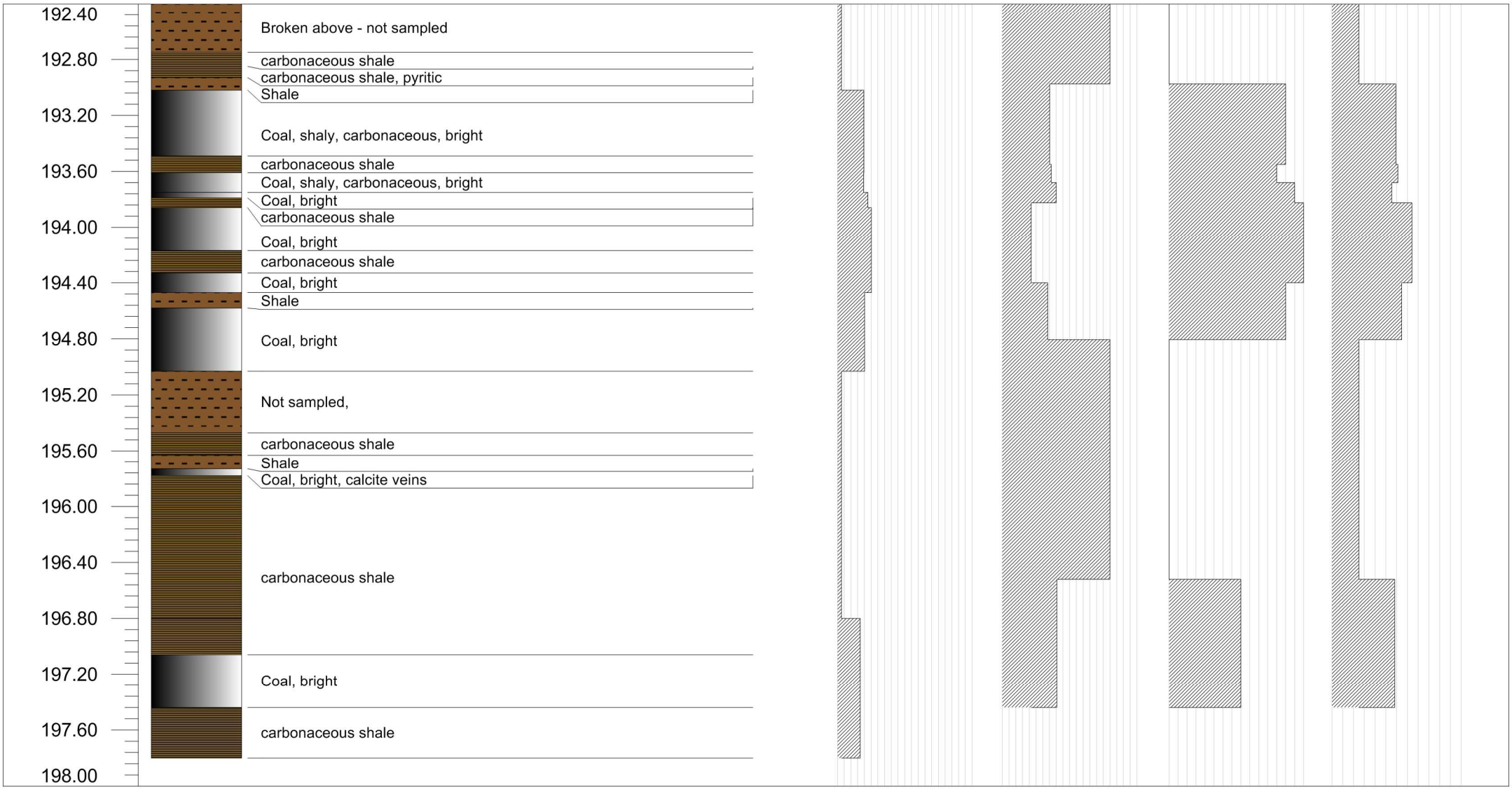

Coal Seam: Upper Coal Zone

Borehole: 1919552

Area 3

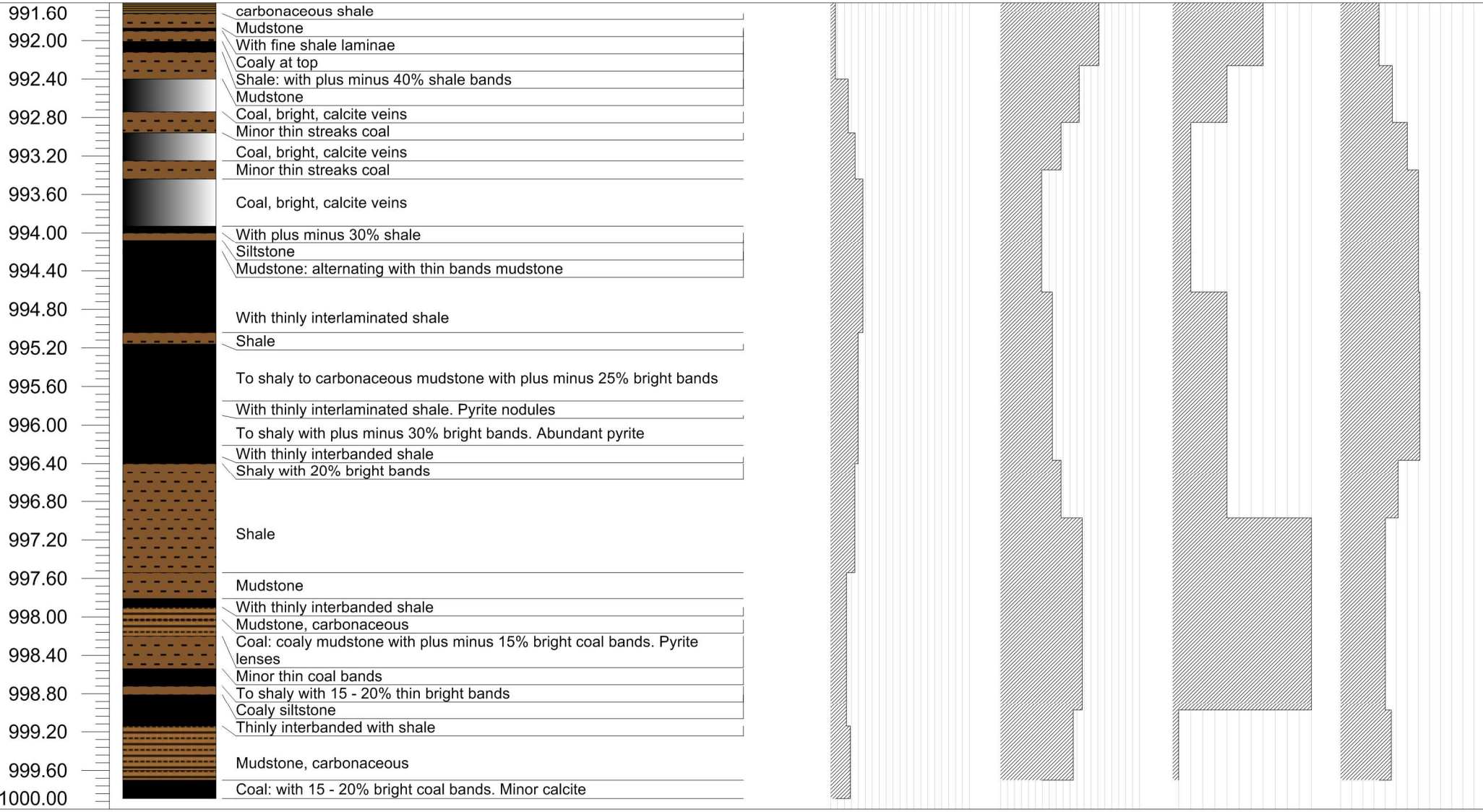

Coal Seam: Lower Coal Zone

Borehole: 1919483

Area 3

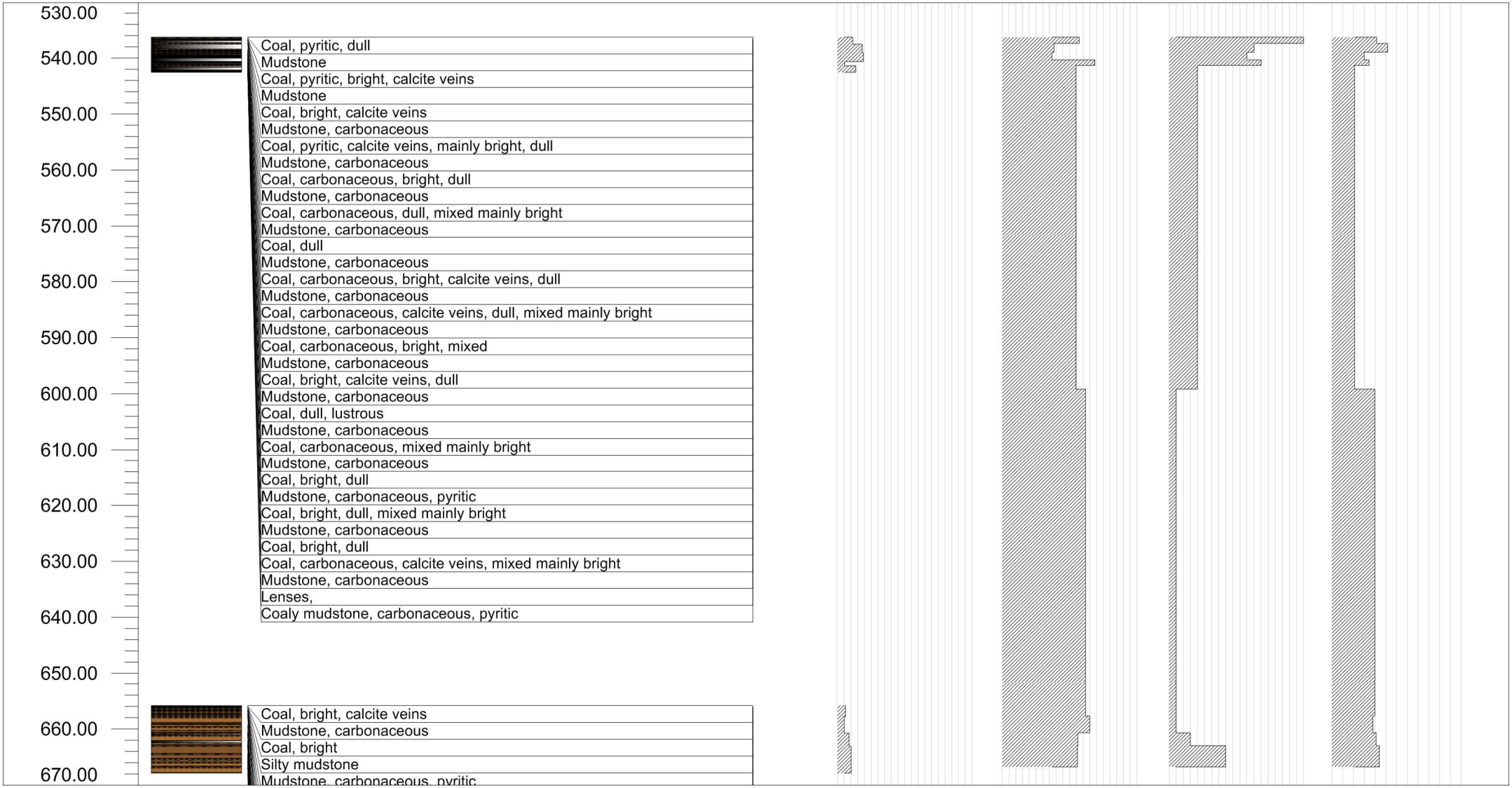

Coal Seam: Upper Coal Zone

Borehole: 1919567

Area 3

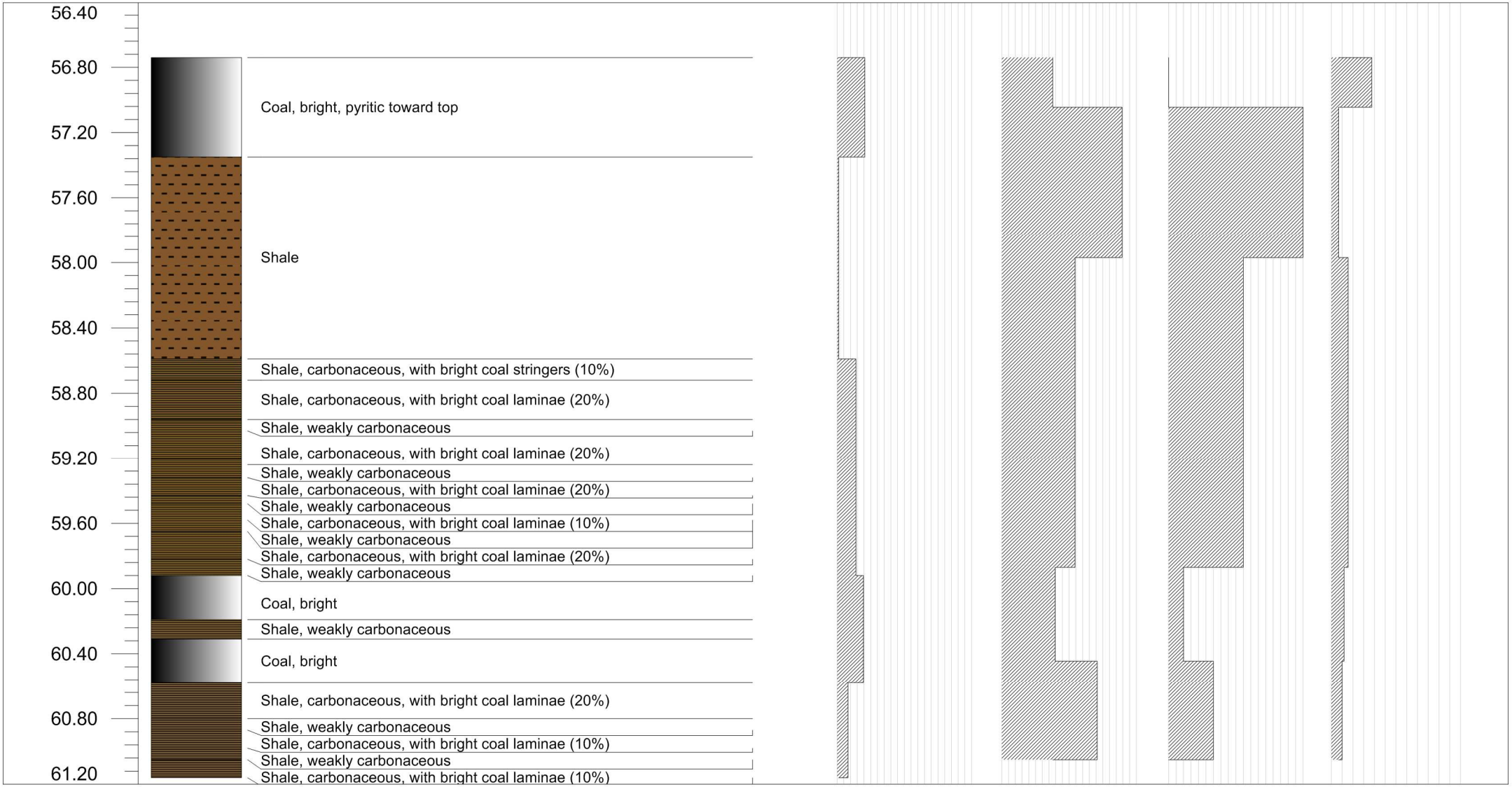

Coal Seam: Upper Coal Zone

Borehole:3028622

Area 4

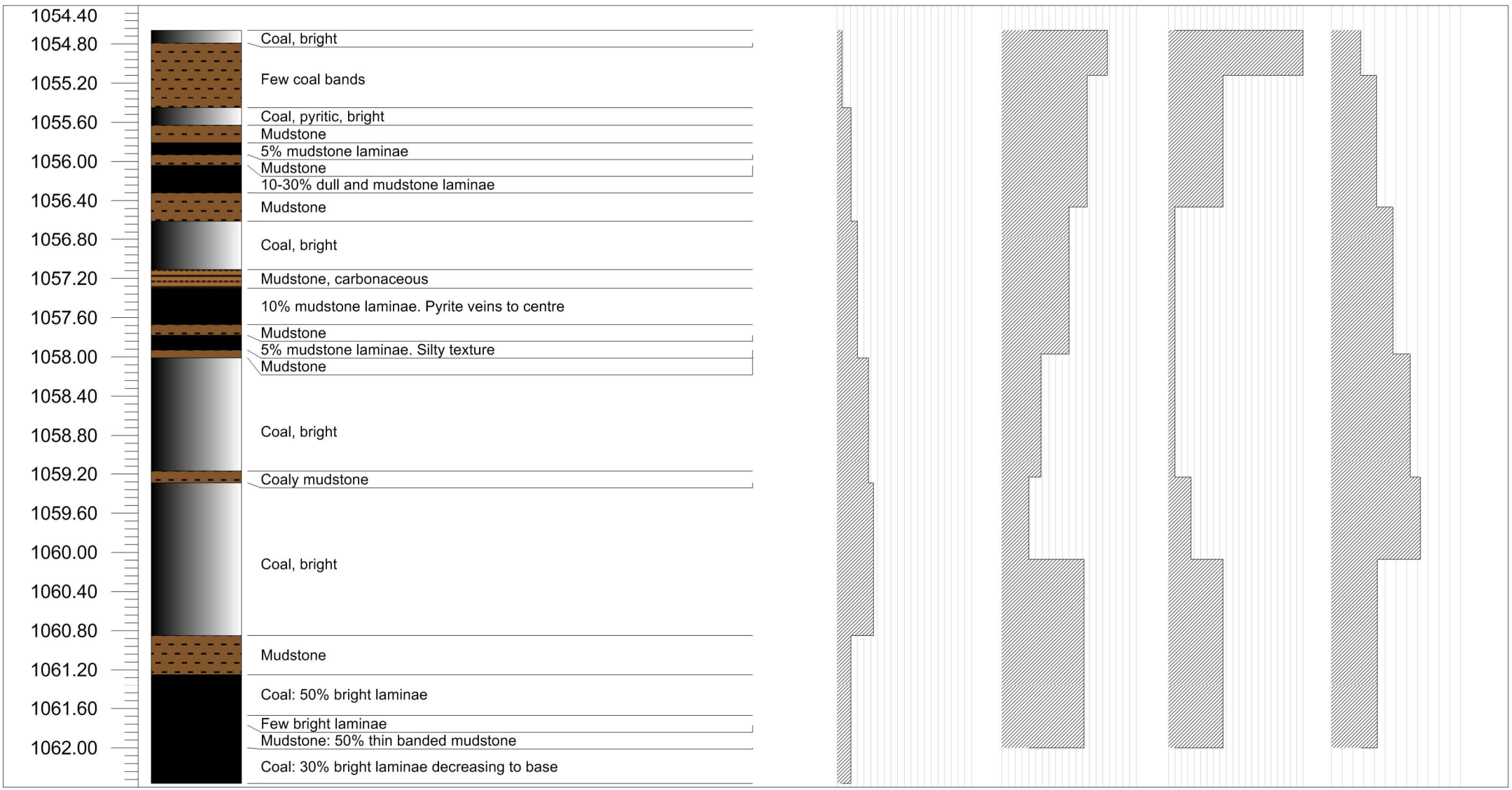

Coal Seam: Lower Coal Zone

Borehole: 1919545

Area 4

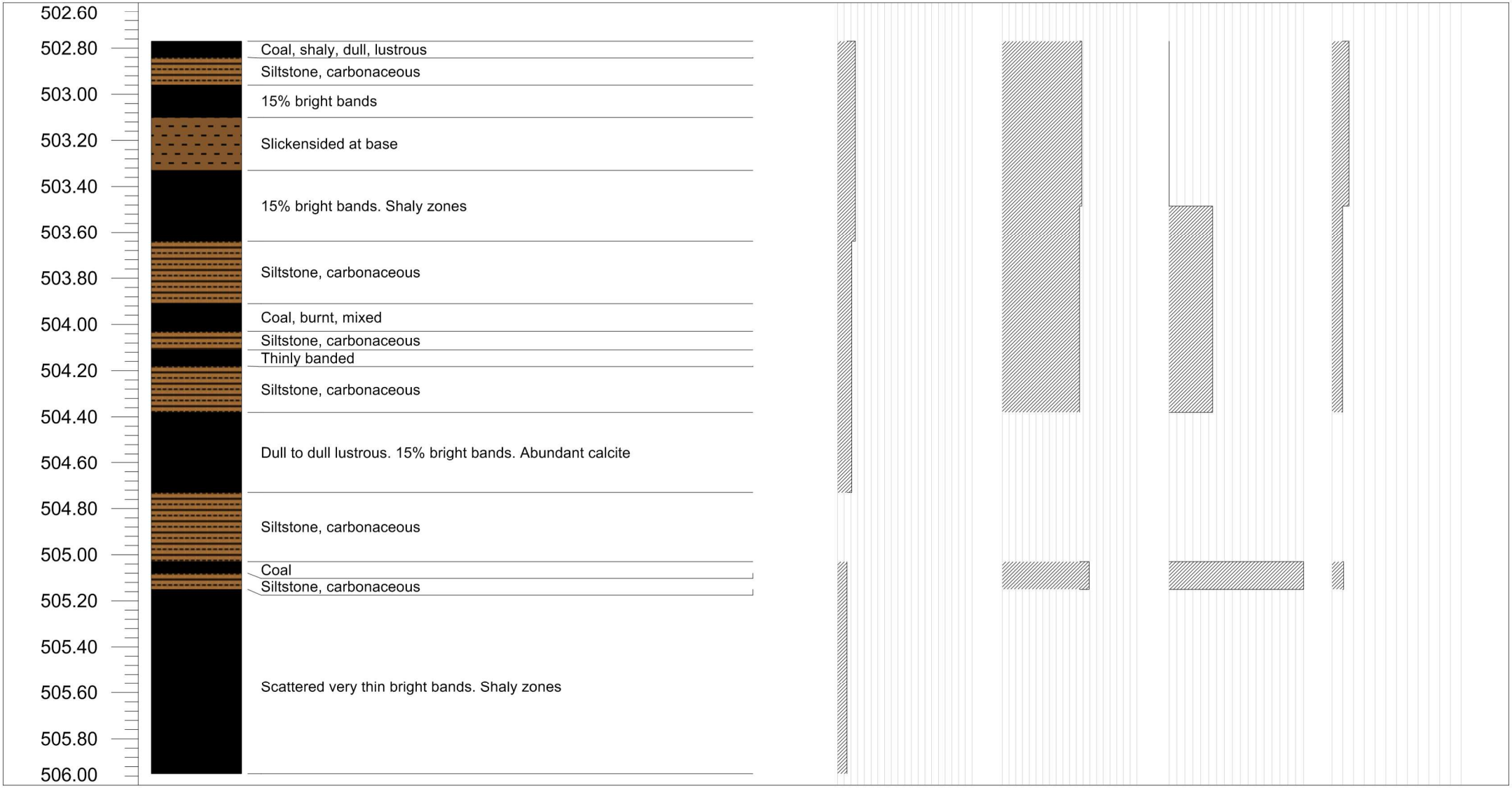

Coal Seam: Lower Coal Zone

Borehole: 1919509

Area 4

Coal Seam: Lower Coal Zone

Borehole:3026561

Area 4

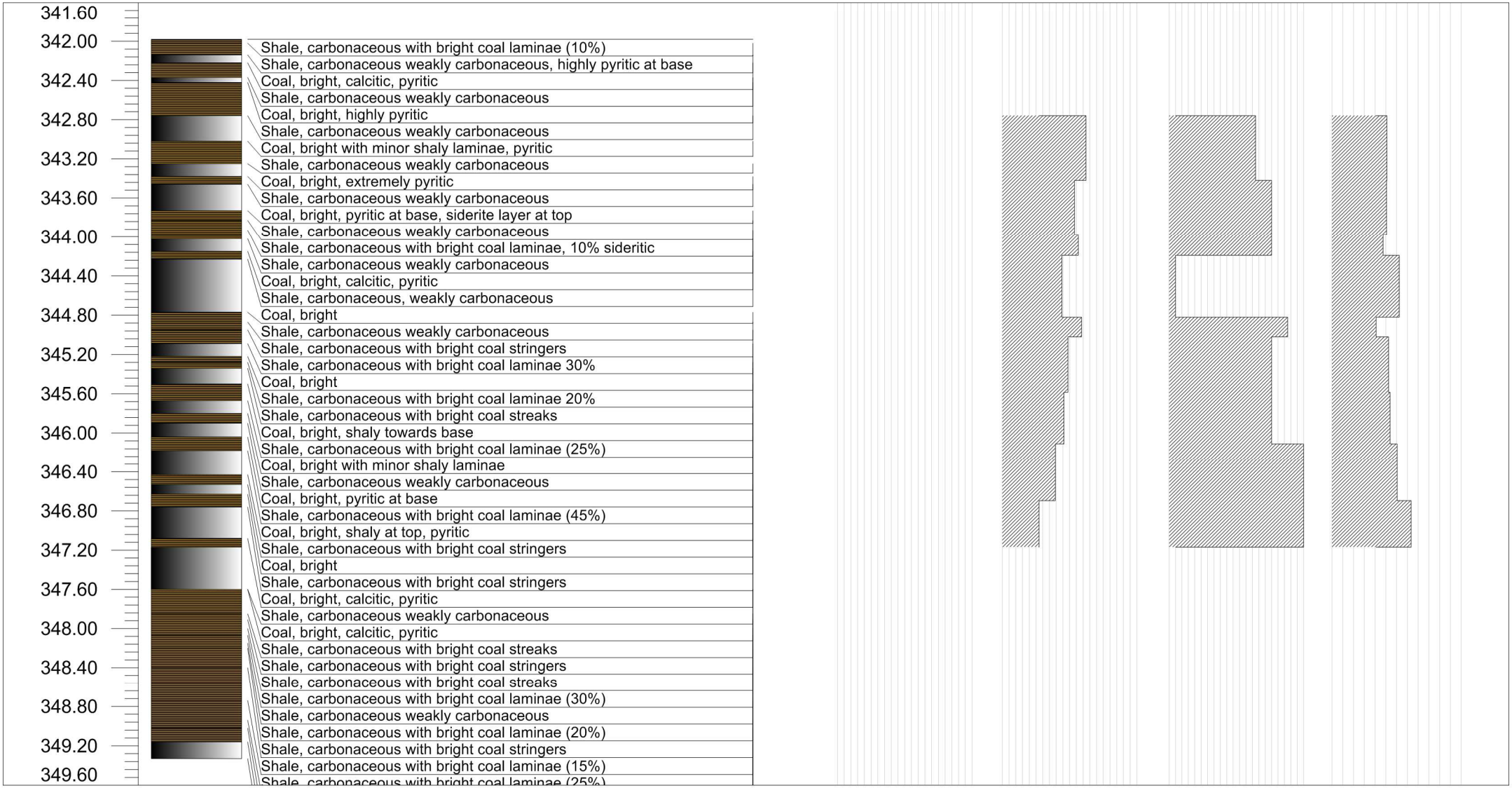

Coal Seam: Upper Coal Zone

Borehole:3026561

Area 4

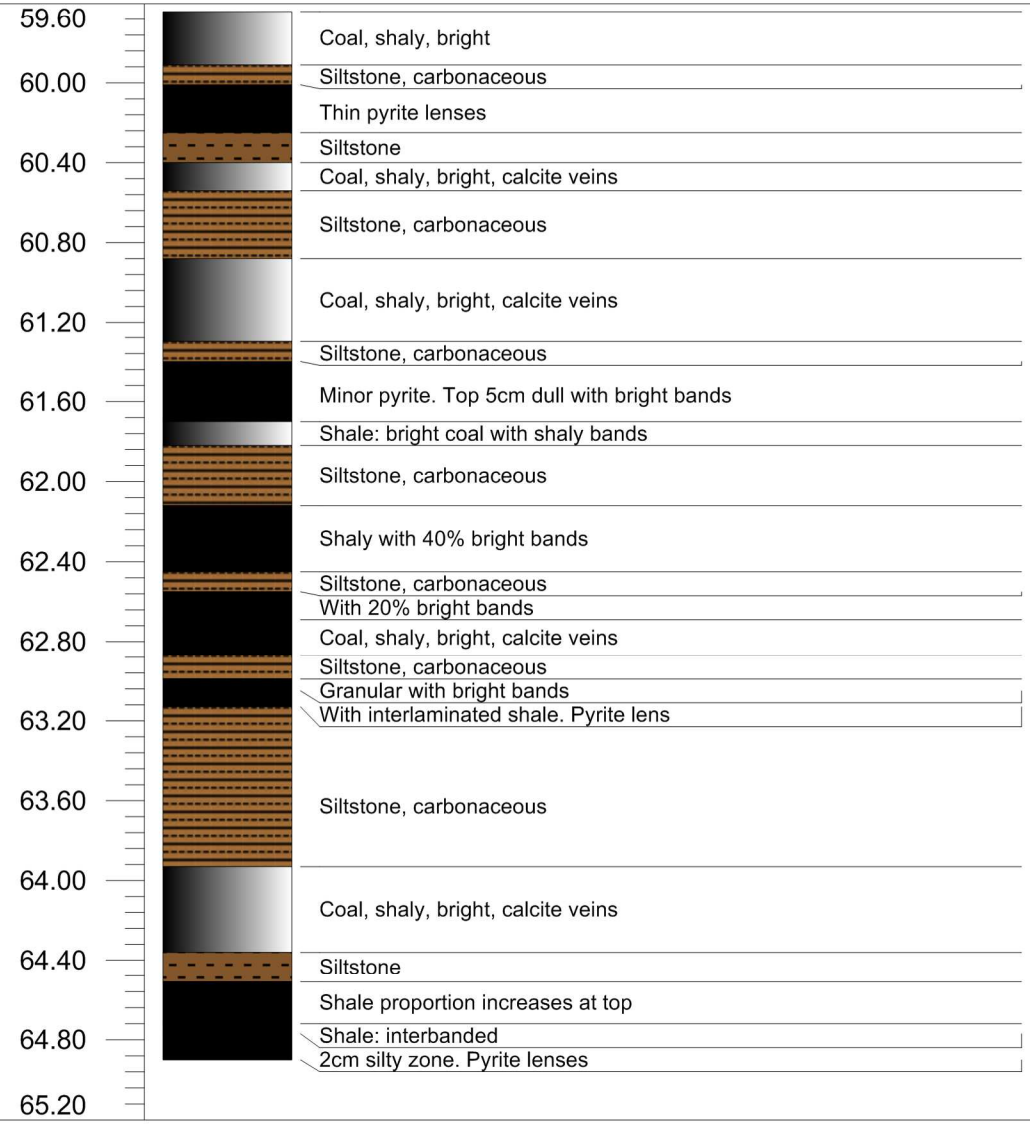

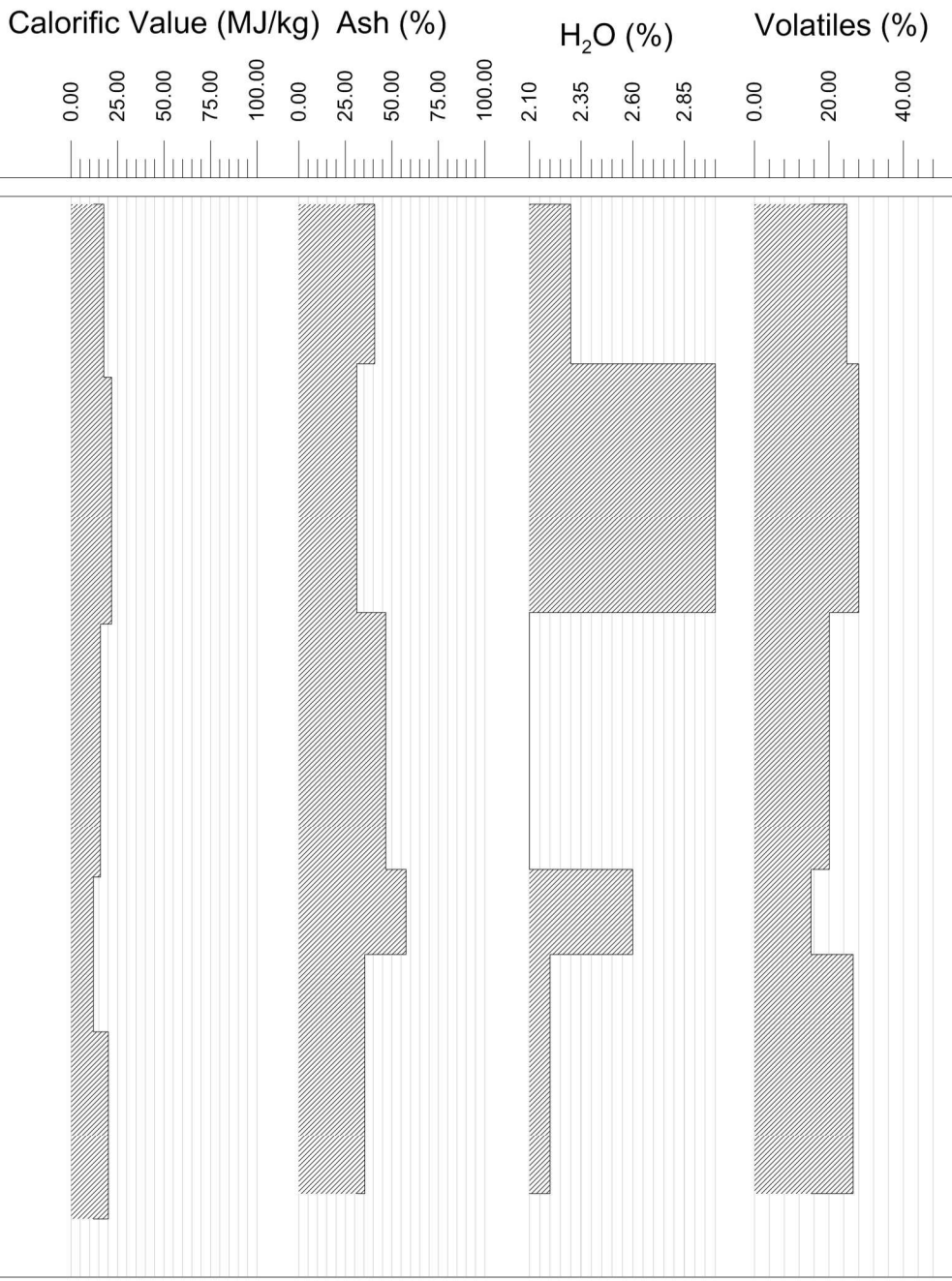

Coal Seam: Lower Coal Zone

Borehole: 1919503

Area 5

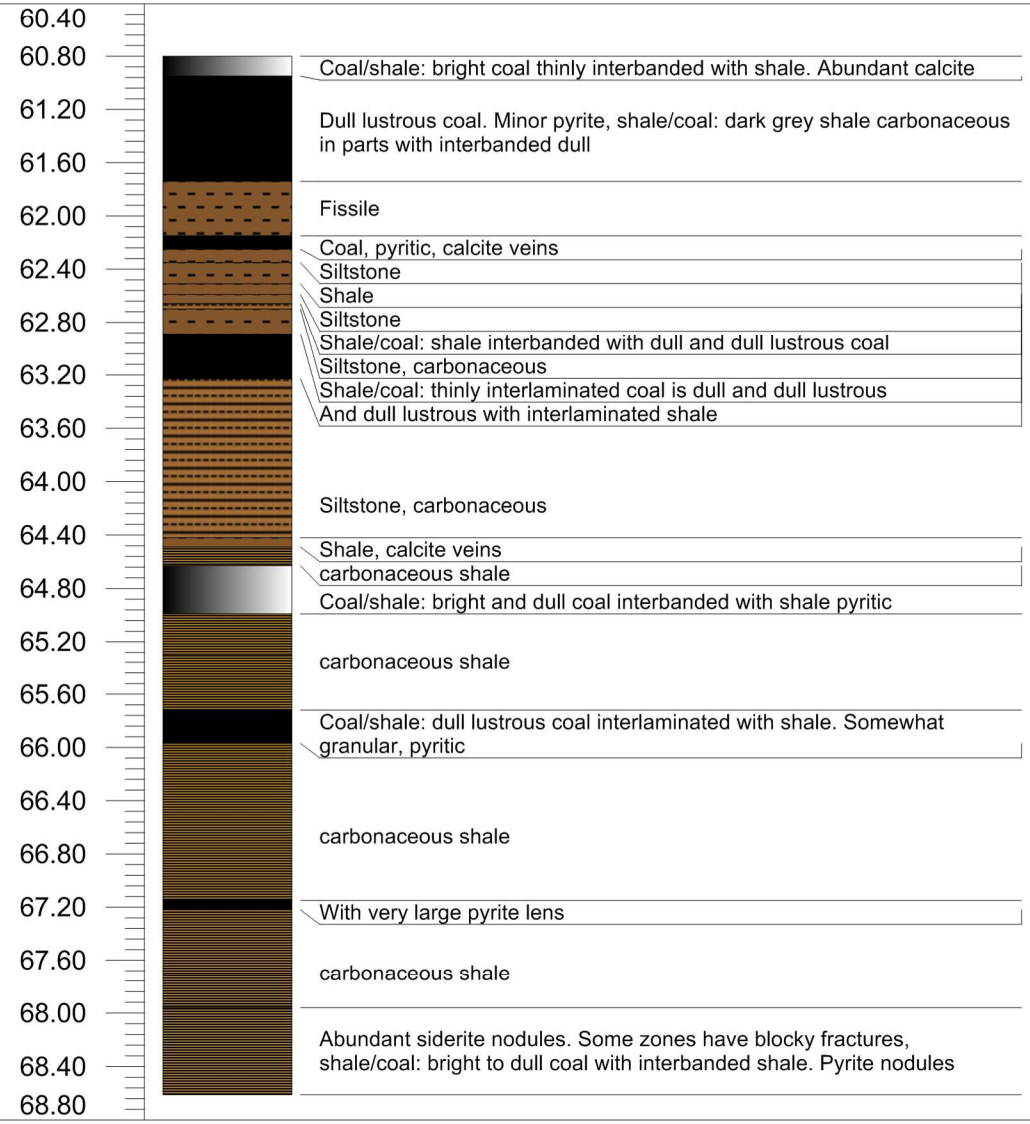

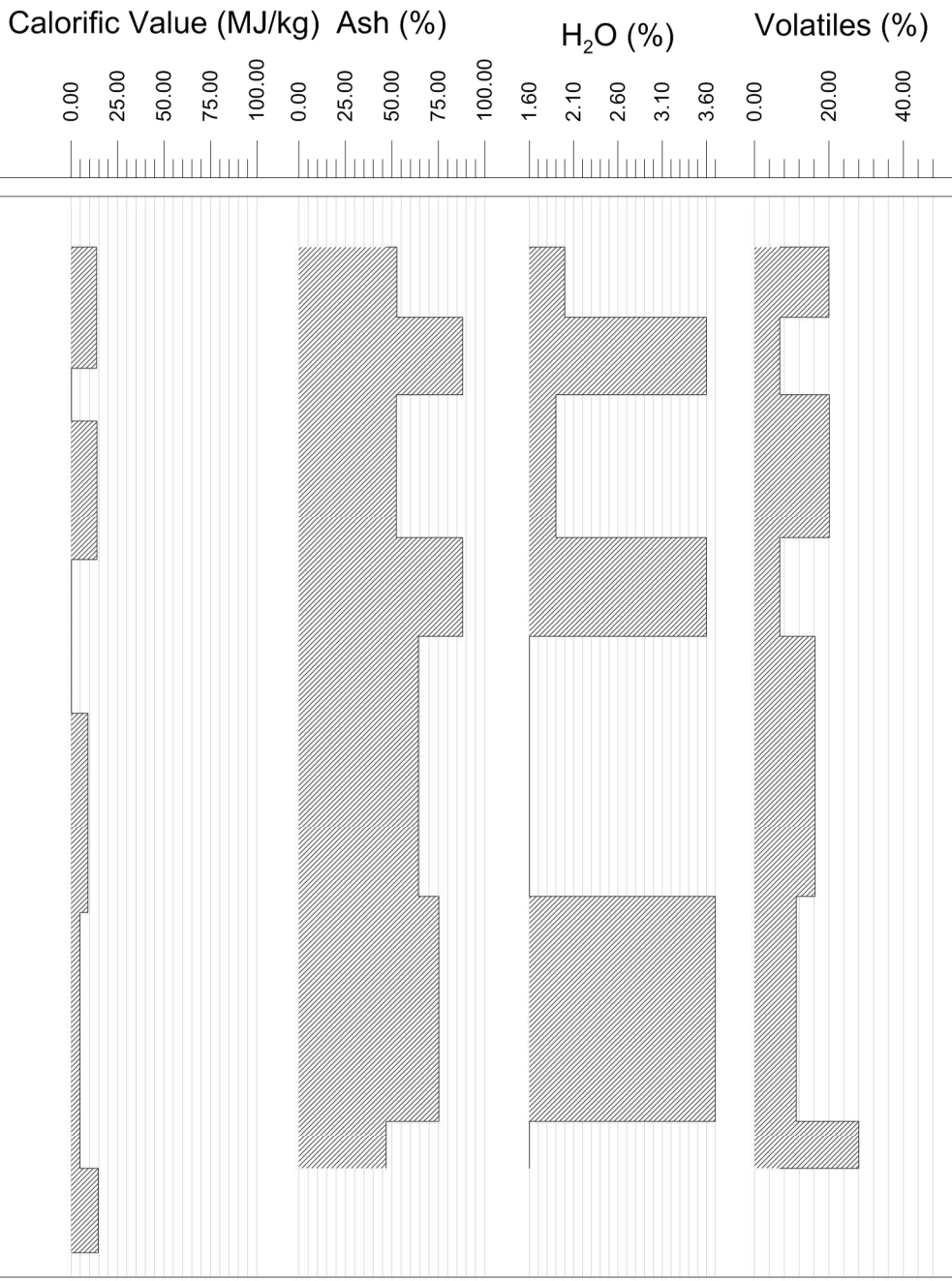

Coal Seam: Lower Coal Zone

Borehole: 1919351

Area 5

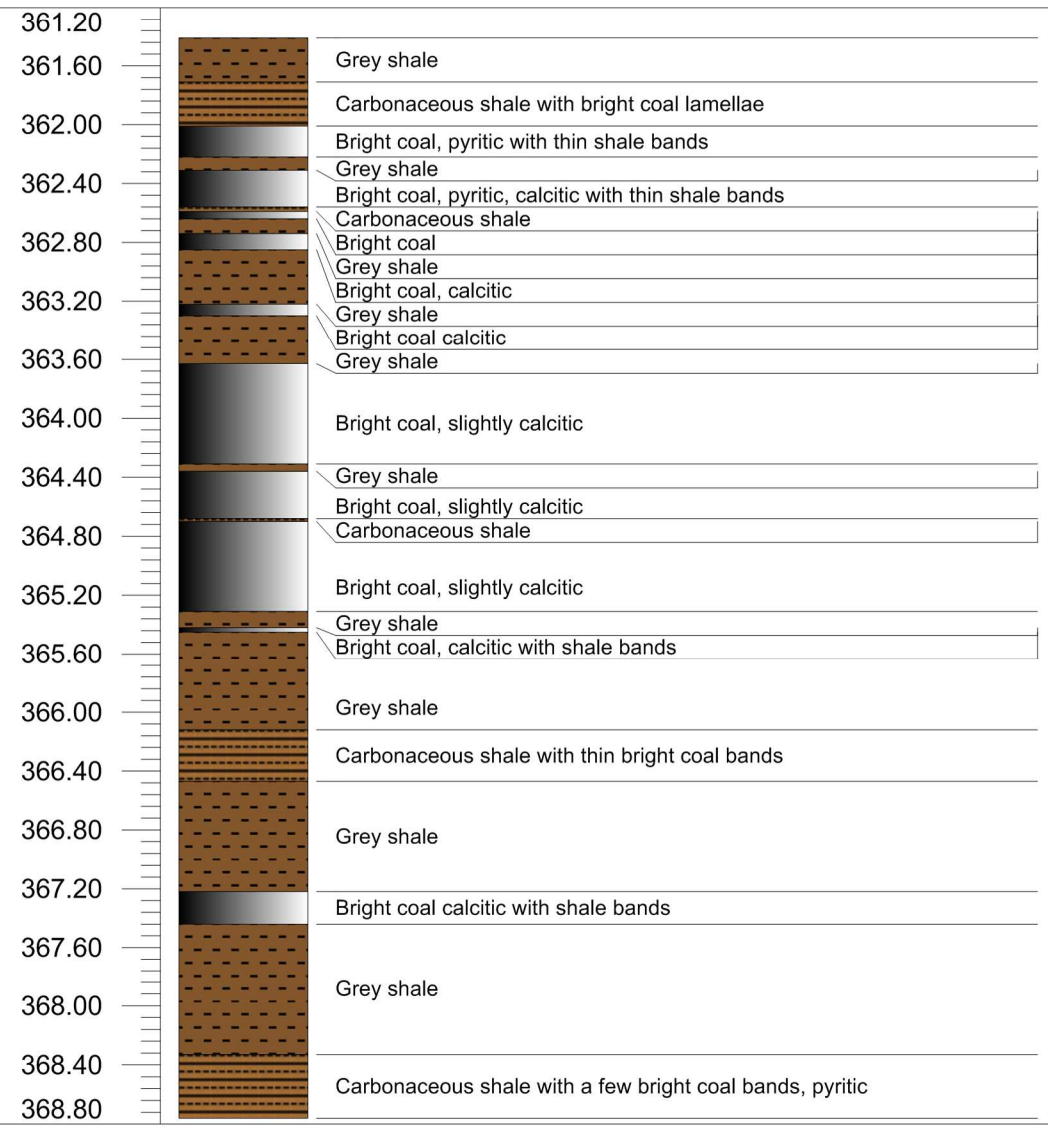

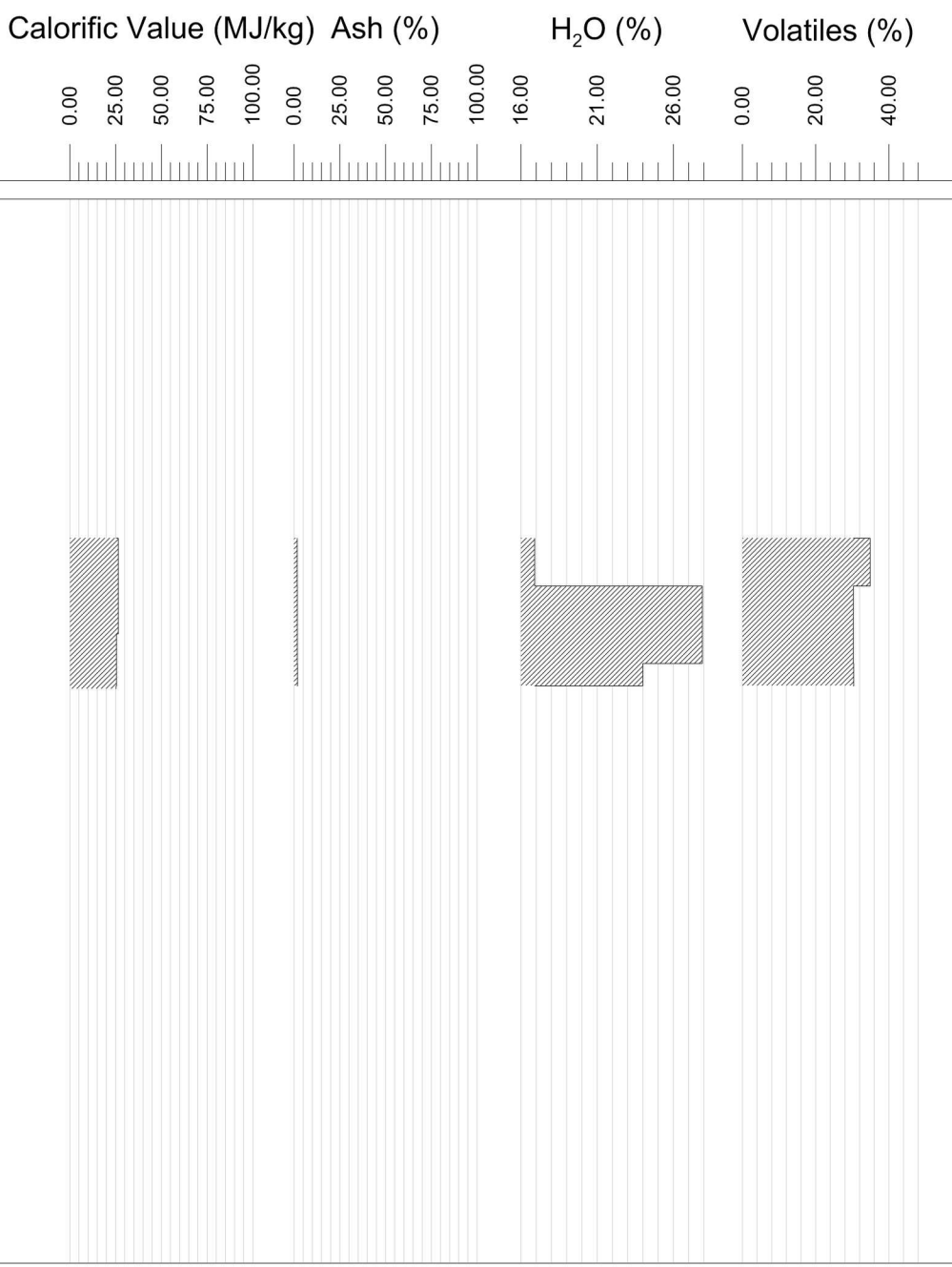

Coal Seam: Upper Coal Zone

Borehole:3026367

Area 5

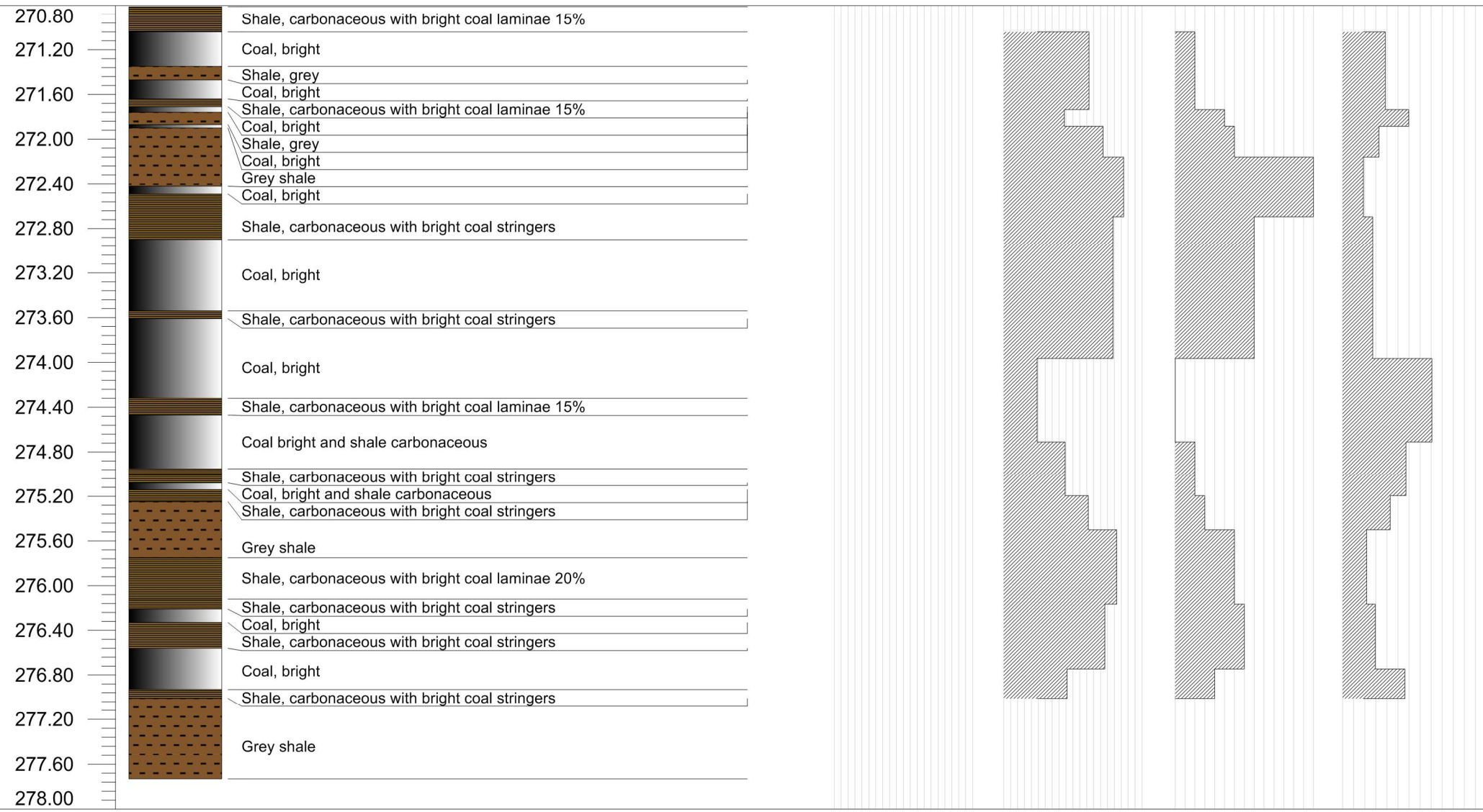

Coal Seam: Upper Coal Zone

Borehole:3028800

Area 5

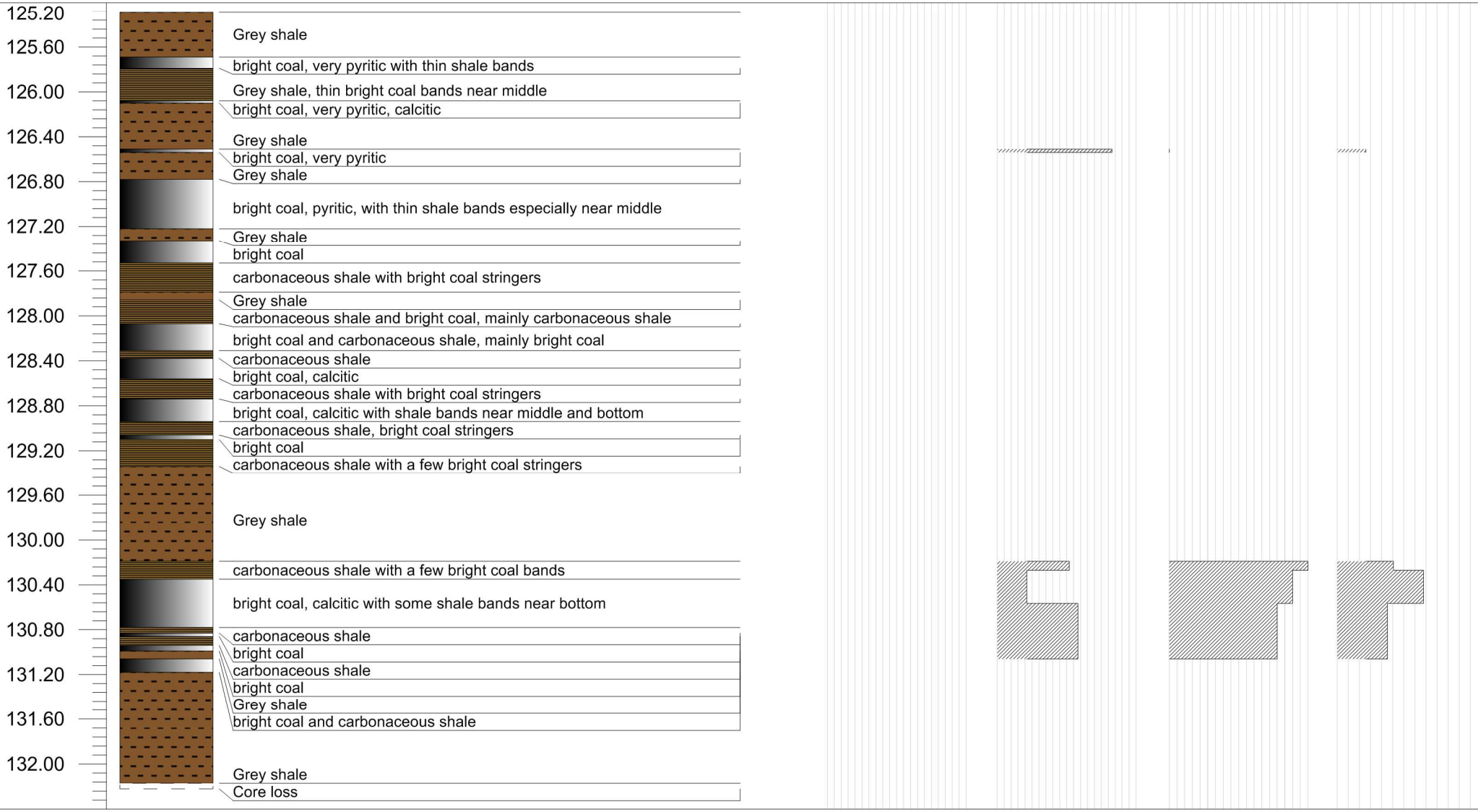

Coal Seam: Upper Coal Zone

Borehole:3028666

Area 5

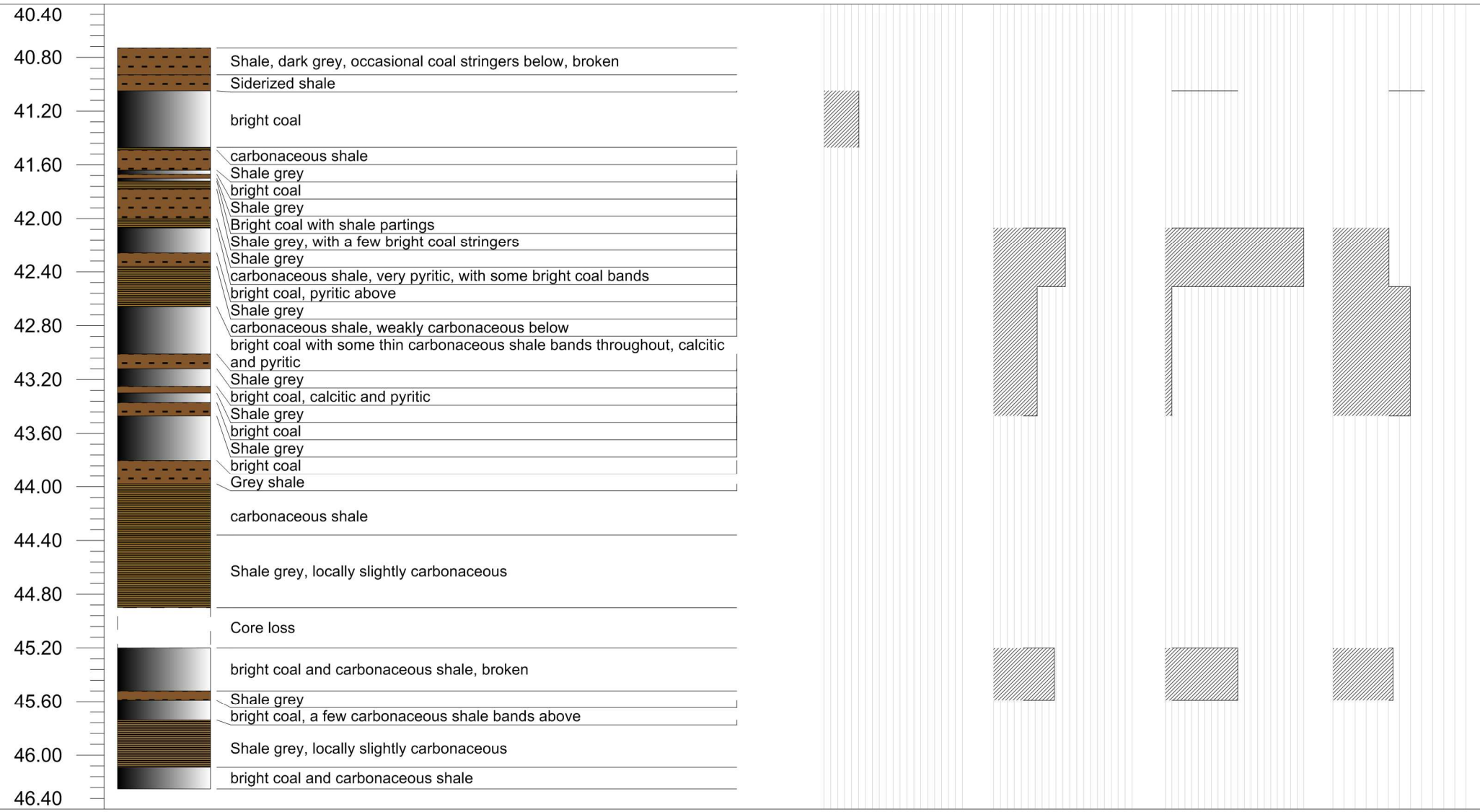

Coal Seam: Upper Coal Zone

Borehole:3028803

Area 6

Coal Seam: Lower Coal Zone

Borehole: 1919482

Area 6

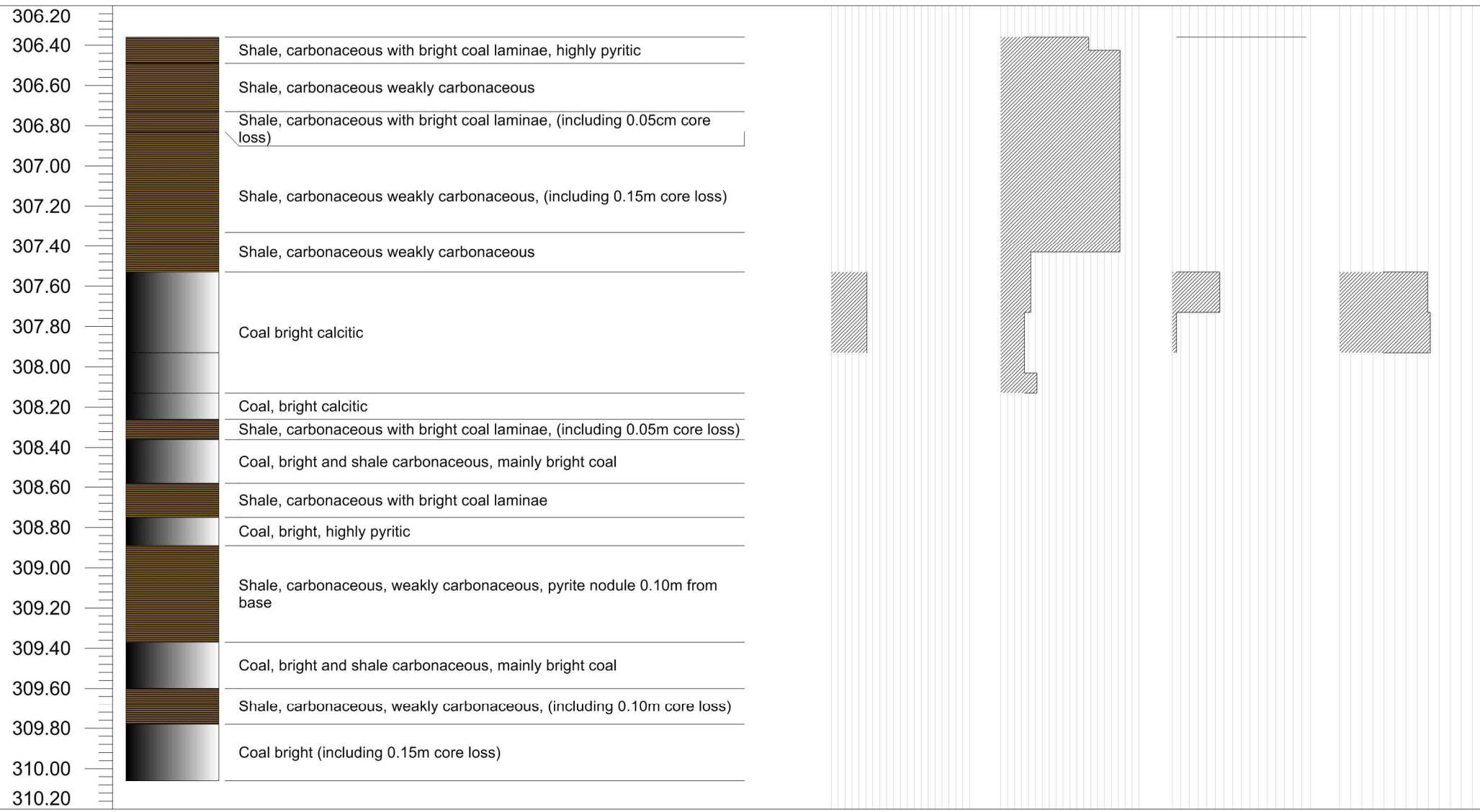

Coal Seam: Upper Coal Zone

Borehole:3027470

Area 6

Coal Seam: Upper Coal Zone

Borehole:3059424

Area 6

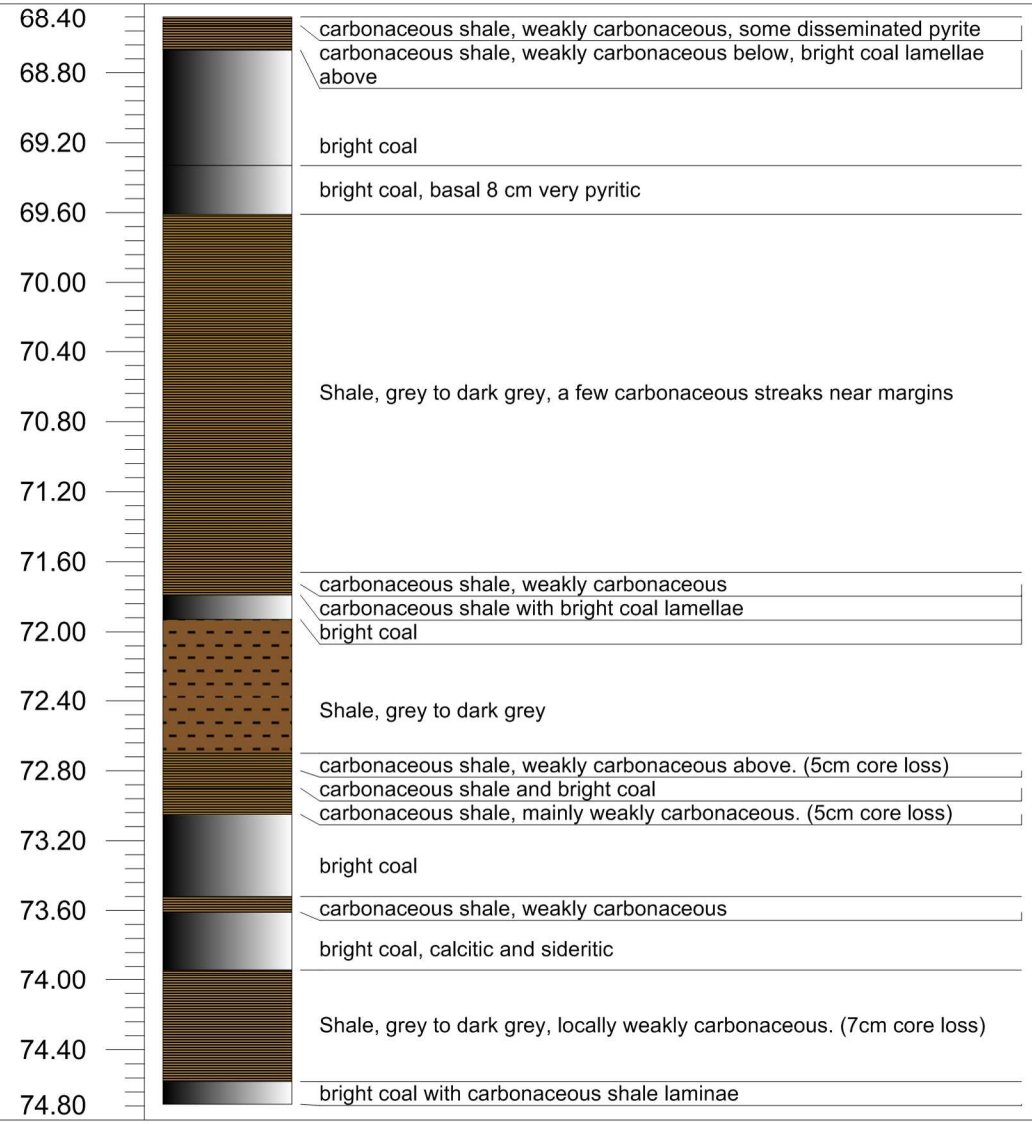

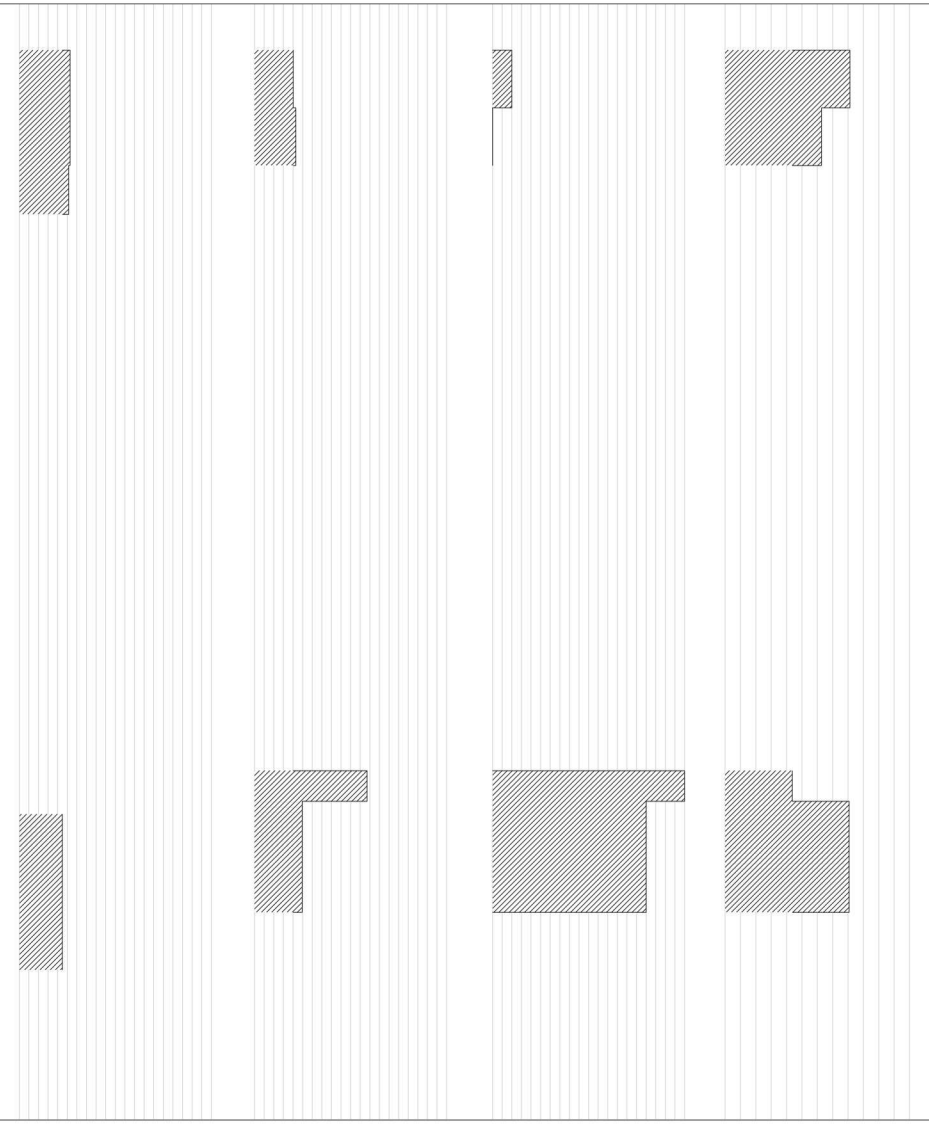

Coal Seam: Upper Coal Zone

Borehole:3028659

Area 7

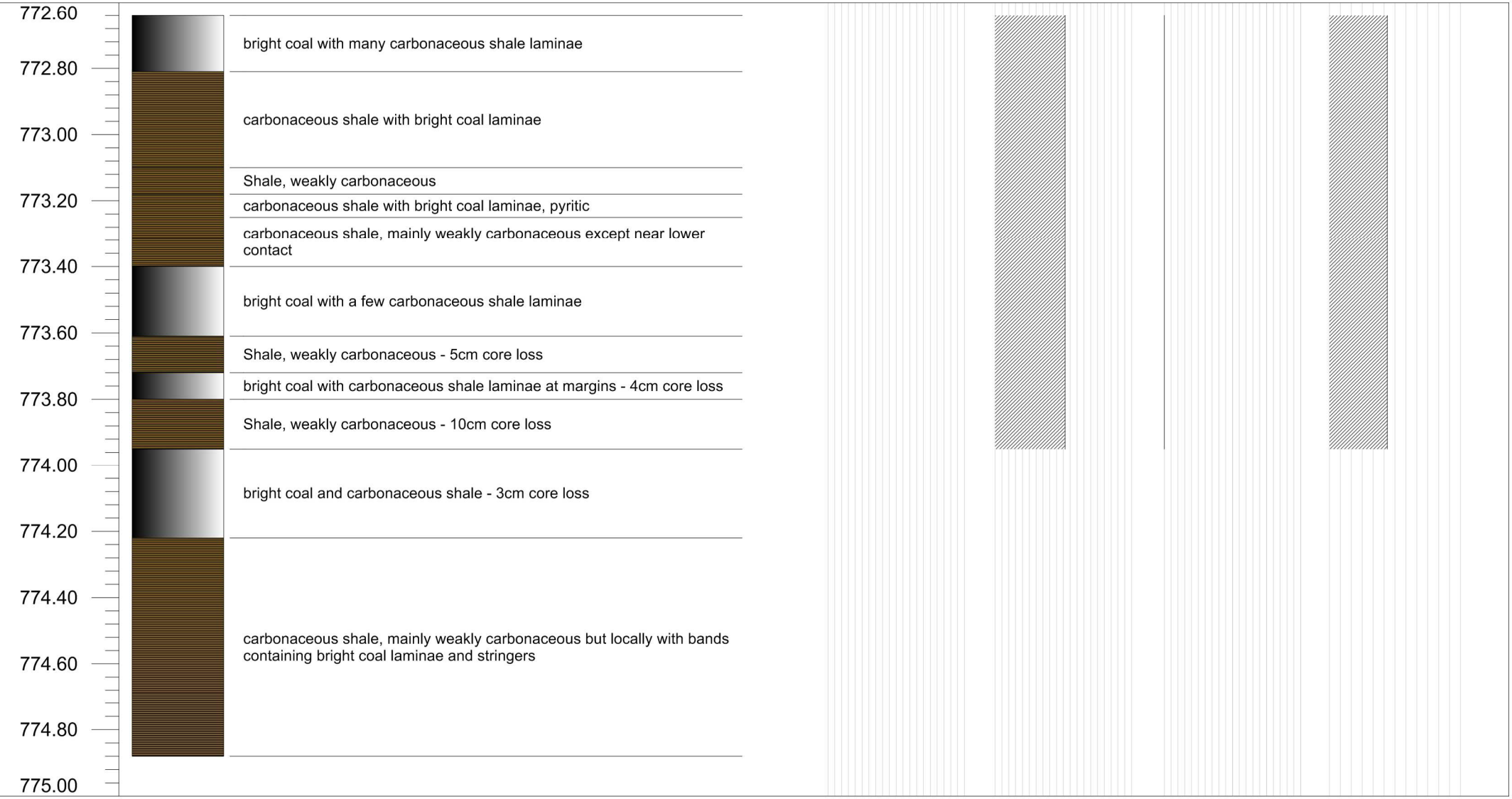

Coal Seam: Lower Coal Zone

Borehole:3014405

Area 7

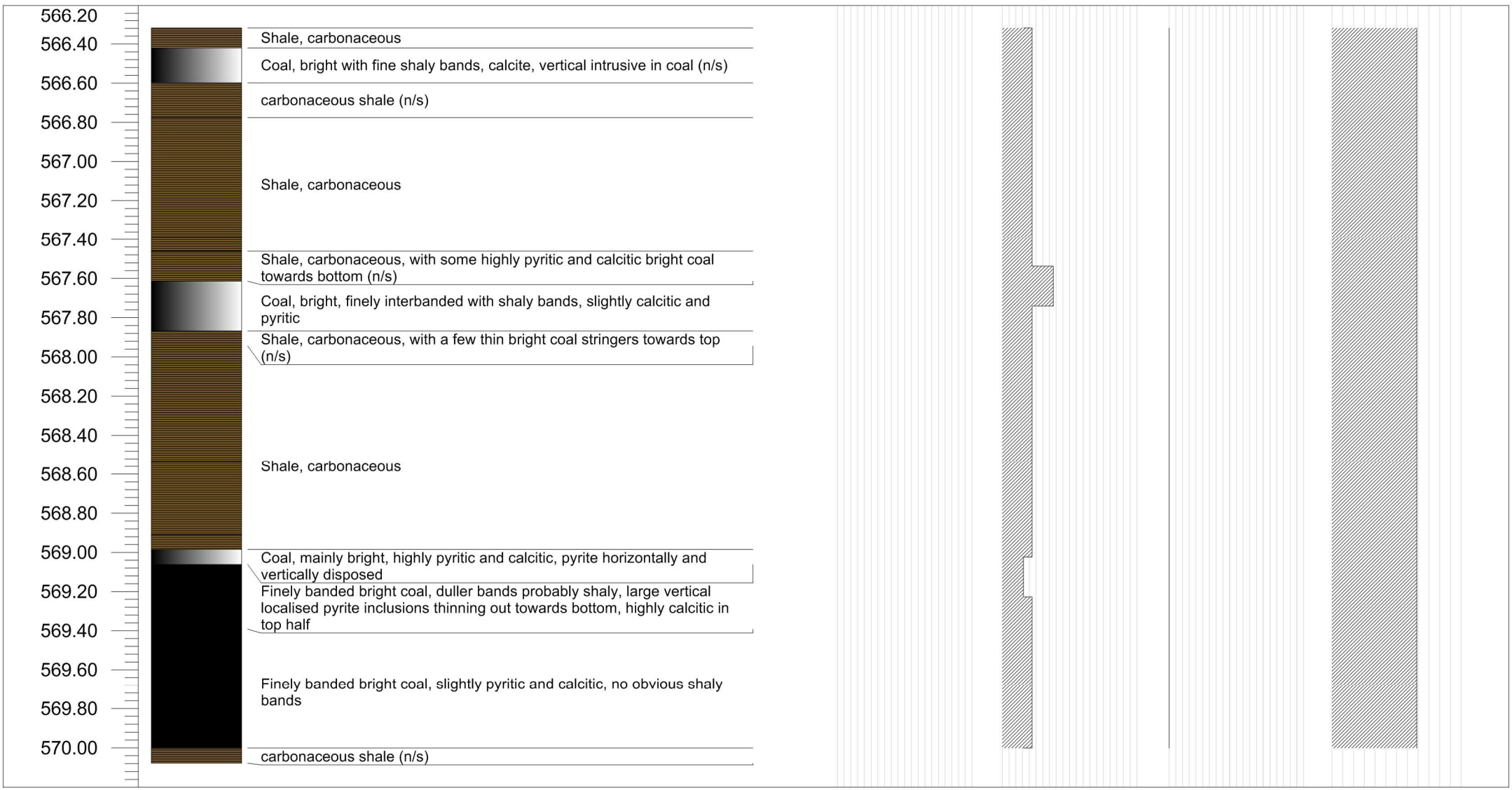

Coal Seam: Upper Coal Zone

Borehole:3000201

Area 7

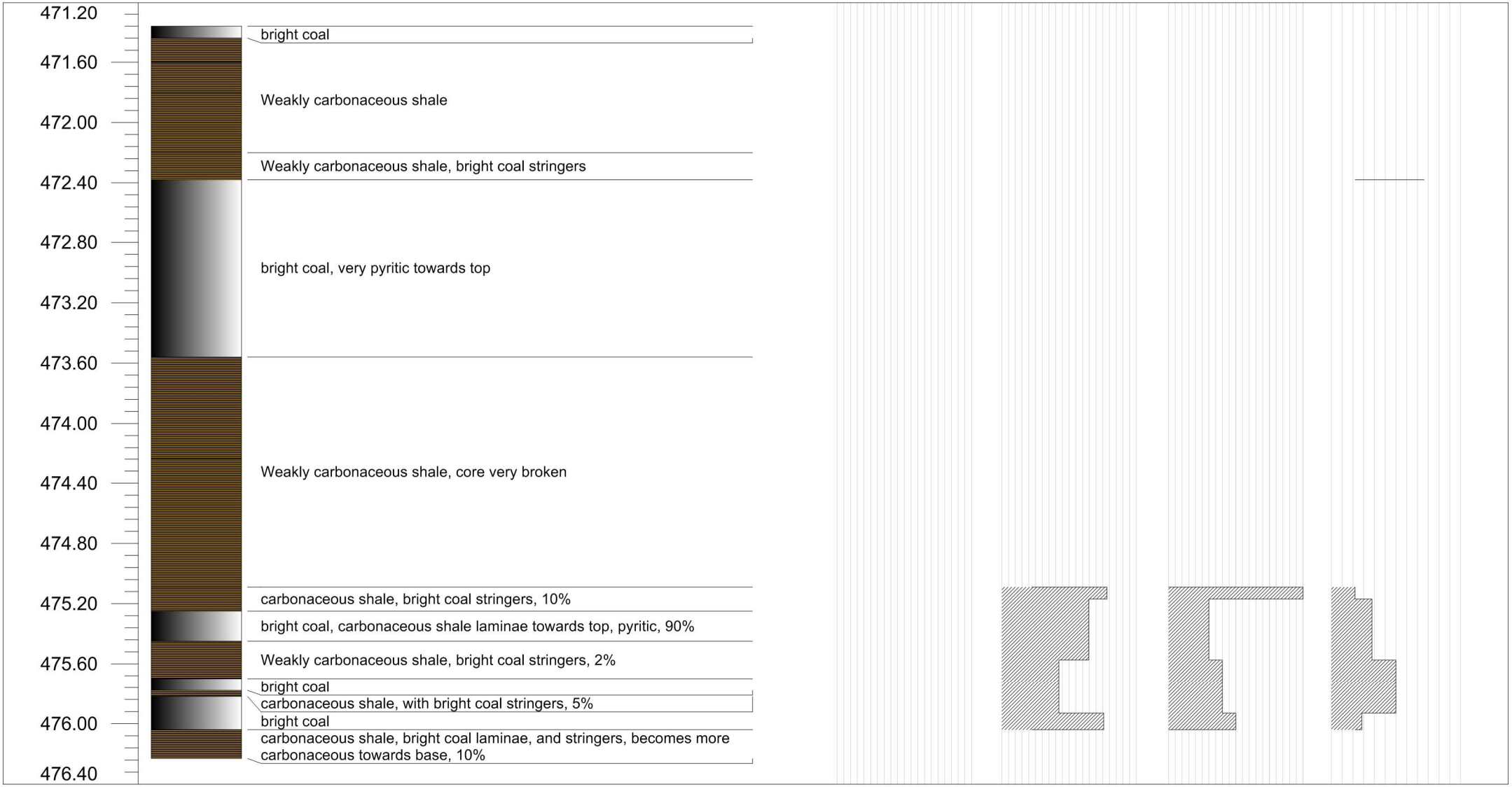

Coal Seam: Upper Coal Zone

Borehole:3028808

Area 7

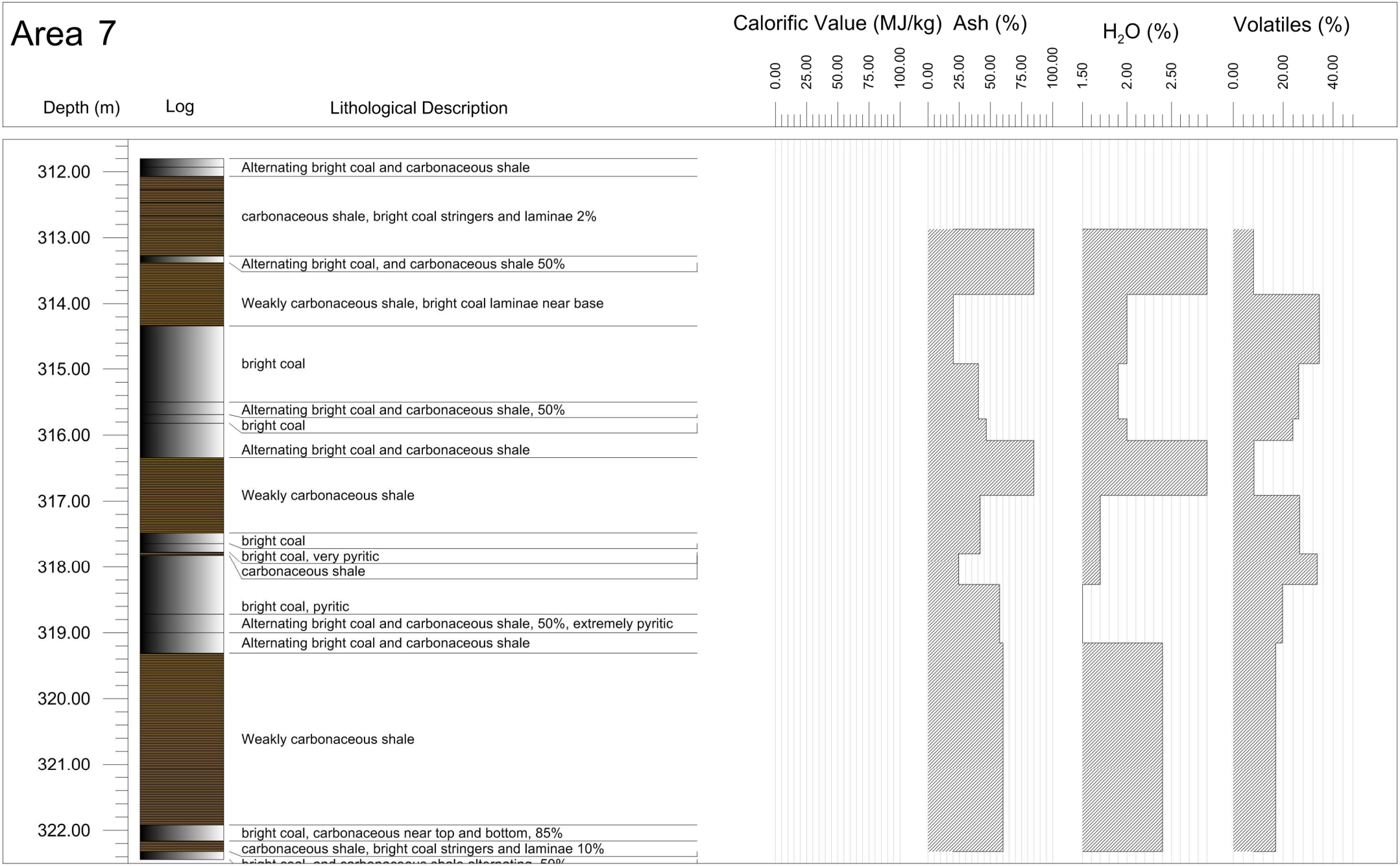

Coal Seam: Upper Coal Zone

Borehole:3028815

Area 7

Coal Seam: Lower Coal Zone

Borehole:3000183

Area 7

Coal Seam: Upper Coal Zone

Borehole:3000183